Kingston University London

Microbiology and Mechanisms of Oral Malodour

This thesis is being submitted in partial fulfilment for the degree of Doctor of Philosophy

by

Kelly Jane ROBERTSON

February 2020

Declaration

This thesis entitled ‘Microbiology and Mechanisms of Oral Malodour’ is based upon the work conducted in the Faculty of Science, Engineering and Computing at Kingston University London. All the work described here is the candidates own original work, unless otherwise acknowledged or referenced in the text. None of the work presented has been submitted for another degree at this, or any other university.

Acknowledgements

I would like to express my gratitude to all the people that helped me during my PhD. Firstly, my supervisory team: Prof. Declan Naughton, Dr Simon Gould and Dr David Bradshaw, they have provided guidance and allowed me freedom to experiment and follow the results and trends to advance my thesis. An extra shout out to Simon Gould who trained me in the arts of microbiology, in the lab and who gifted me with internships and opportunities to learn my trade during my undergraduate degree.

I would like to extend my thanks to BBSRC and GSK who generously funded this research which granted me the tools I needed as a PhD researcher.

A sincere thanks to the staff at Kingston University: Rosalind Percival for her knowledge and understanding extending to all post graduate researchers. Dr Ali Ryan for his support, knowledge and use of the biotech office, which greatly improved my standard of work. The people with whom I shared this office: Lucky, Milly and Ben. They challenged and supported me at every turn, and most importantly made every day a pleasure, for which I am grateful.

Finally, I would like to thank my friends and family. To name only a few, my parental team: Gali, Doug, Claer and Yael- you are an unrivalled support network, which I couldn't have done without. My brothers Ben and Jack are the best and always there to give me a push. And Sam, who's patience, encouragement and belief has inspired me from day one to the finish line and beyond. I couldn't have completed this thesis without all the people that believed in me along the way.

Lastly, I'd like to dedicate this work to my Sabba and Savta.

Abbreviations

BHI: Bran heart infusion

CFU: Colony forming units

CHX: Chlorhexidine

CSLM: Confocal scanning laser microscopy

DS: Dimethyl sulphide

DSF: Differential scanning fluorometry

DTT: Dithiothreitol

FISH: Fluorescent in situ hybridisation

GA: Gallic acid

GC-MS: Gas chromatography- mass spectrometry

H_2S: Hydrogen sulphide

HPLC: High performance liquid chromatography

IC50: Inhibitory concentration at 50%

IP: inhibitory panel

Kpg: Lysine gingipains

LPS: lipopolysaccharide

MGL: Methionine gamma lyase

Micro-CT: Micro computed tomography

MM: Methyl mercaptan

NA: Nicotinic acid

OD: optical density

PPB: parts per billion

PBS: Phosphate buffer saline

QPCR: Quantitive polymerase chain reaction

Rpga and Rpgb: arginine gingipains

SEM: Scanning electron microscopy

TEMED: Tetramethylethylenediamine

Trig: Trigonelline

VSC: Volatile sulphur compound

ZnAc: Zinc acetate

ZnCi: Zinc citrate

ZnCl: Zinc chloride

Table of Contents

List of figures

Dimethyl sulphide (ppb) taken at the time intervals represented by the x axis of the graphs. Error bars represent standard deviation (n=3).

4.2 1% Methionine solution incubated with oral bacteria over time (x axis). Data points exhibit the average result from the three and error bars display the standard deviation between the three experimental runs.

4.3 a, b, c Methionine solutions tested with Oral bacteria, Green tea and the combination of both described in the graph key. (a) Hydrogen sulphide, (b) Methyl mercaptan, (c) Dimethyl sulphide output (ppb) Errors represent standard deviation (n=3).

4.4 a, b, c Methionine solutions tested with Oral bacteria, Red wine and the combination of both- defined by the graph key. (a) Hydrogen sulphide, (b) Methyl mercaptan, (c) Dimethyl sulphide output (ppb) Error bars represent standard deviation (n=3).

4.5a Methionine solutions tested with Oral bacteria, Red wine (without alcohol) and the combination of both, these are the result of the hydrogen sulphide (ppb). Error bars represent ± SD (n=3)

4.6 a, b, c Methionine solutions tested with Oral bacteria, Garlic and the combination of both. (a) Hydrogen sulphide, (b) Methyl mercaptan, (c) Dimethyl sulphide output (ppb). Error bars represent ± SD (n=3)

4.7 a, b, c Methionine solutions tested with Oral bacteria, odourless garlic and the combination of both. (a) Hydrogen sulphide, (b) Methyl mercaptan, (c) Dimethyl sulphide output (ppb). Error bars represent ± SD (n=3)

4.8 a, b, c Methionine solutions tested with Oral bacteria, Zinc citrate and the combination of both. (a) Hydrogen sulphide, (b) Methyl mercaptan, (c) Dimethyl sulphide output (ppb). Error bars represent ± SD (n=3)

4.9 a, b, c Methionine solutions tested with Oral bacteria, instant coffee and the combination of both. (a) Hydrogen sulphide, (b) Methyl mercaptan, (c) Dimethyl sulphide output (ppb). Error bars represent ± SD (n=3).

4.10 a, b, c Methionine solutions tested with Oral bacteria, instant coffee and the combination of both. (a) Hydrogen sulphide, (b) Methyl mercaptan, (c) Dimethyl sulphide output (ppb). Error bars represent ± SD (n=3).

4.11 a, b, c Methionine solutions tested with Oral bacteria, zinc citrate, instant coffee and the combination of both. (a) Hydrogen sulphide, (b) Methyl mercaptan, (c) Dimethyl sulphide output (ppb). Error bars represent ± SD (n=3).

4.12 a, b, c Methionine solutions tested with Oral bacteria, zinc citrate, instant coffee and the combination of both. (a) Hydrogen sulphide, (b) Methyl mercaptan, (c) Dimethyl sulphide output (ppb). Error bars represent ± SD (n=3).

4.13 Taken from Toue *et al*., (2006) Diagram showing the basic intermediates between cysteine, methionine through the transmethylation and transulfuration pathways and methionine's products (H_2S, methanethiol (methyl mercaptan)) from the Transamination pathways.

Chapter 5

5.1 a, b, c Concentrations of gallic acid tested on lysed bacteria against increasing concentrations of methionine (x axis) Error bars represent ± SD

5.1 d Michaelis-Menten plot showing gallic acids' effect on hydrogen sulphide from methionine and lysed bacteria (Error bars represent ± SD)

5.1 e Graph showing the extrapolation of IC50 for gallic acid at 0.5% (5mg/ml) (33mM) Methionine.

5.2 a, b, c Concentrations of Zinc chloride tested on lysed bacteria against increasing concentrations of methionine (x axis) Error bars represent ± SD

5.2 d Michaelis-Menten plot showing Zinc chlorides' effect on hydrogen sulphide from methionine and lysed bacteria (Error bars represent ± SD)

5.2 e IC50 plot shows hydrogen sulphide producing activity (%) at 5mg/ml methionine with Zinc chloride increasing concentrations

5.3 a, b, c Concentrations of Zinc acetate tested on lysed bacteria against increasing concentrations of methionine (x axis) (Error bars represent ± SD)

5.3 d Michaelis-Menten plot showing Zinc acetates' effect on hydrogen sulphide from methionine and lysed bacteria (Error bars represent ± SD)

5.3 e IC50 plot shows hydrogen sulphide producing activity (%) at 5mg/ml methionine with Zinc acetate increasing concentrations

5.4 a, b, c Concentrations of Nicotinic acid tested on lysed bacteria against increasing concentrations of methionine (x axis) (Error bars represent ± SD)

5.4 d Michaelis-Menten plot showing Nicotinic acids' effect on hydrogen sulphide from methionine and lysed bacteria (Error bars represent ± SD)

5.4 e IC50 plot shows hydrogen sulphide producing activity (%) at 5 mg/ml methionine with nicotinic acid (NA) increasing concentrations

5.5 a, b, c Concentrations of Caffeine tested on lysed bacteria against increasing concentrations of methionine (x axis) (Error bars represent ± SD)

5.5 d Michaelis-Menten plot showing caffeine's' effect on hydrogen sulphide from methionine and lysed bacteria (Error bars represent ± SD)

5.5 e IC50 plot shows hydrogen sulphide producing activity (%) at 5 mg/ml methionine with caffeine increasing concentrations

5.6 a, b, c Concentrations of Trigonelline tested on lysed bacteria against increasing concentrations of methionine (x axis) (Error bars represent ± SD)

5.6 d Michaelis-Menten plot showing Trigonellines' effect on hydrogen sulphide from methionine and lysed bacteria (Error bars represent ± SD)

5.6 e IC50 plot shows hydrogen sulphide producing activity (%) at 5 mg/ml methionine with trigonelline at increasing concentrations

5.7 a, b, c Concentrations of Zinc citrate tested on lysed bacteria against increasing concentrations of methionine (x axis) (Error bars represent ± SD)

5.7 d Michaelis-Menten plot for Zinc citrate effect on hydrogen sulphide

5.7 e IC50 plot shows hydrogen sulphide producing activity (%) at 5 mg/ml methionine with zinc citrate at increasing concentrations

Chapter 6

6.1 a, b Visualisation of fluorescence from QPCR (DSF assay) using SYPRO orange as fluorescent detector for the unfolding of methionine gamma lyase. The blue line (with circles) represents the neat MGL with buffer

6.2 Extracted from Neisen, Burglund and Vedadi, (2007). This graph presents the reference plot for the DSF assay

6.3 SDS page gel electrophoresis image from GelDocTM XR+ (BIO-RAD)- a molecular imager. The right image shows the tested enzyme (with multiple bands) and to the left of it is a reference ladder.

6.4 Determination of unknown molecular weight using Rf (distance migrated (mm) X dye front (mm)) against log molecular weight.

6.5 Raw graph from HPLC excitation of methionine in buffer (NaAc) with a fluorescent detector of methionine (OPA) Column information (Sigma- Aldrich 59555- SUPELCOSIL LC-18-DB HPLC Column)

6.6 Raw HPLC graph of enzyme tested with Methionine (analysed at the 10-minute mark- Methionine concentrations) (sodium acetate, OPA, Methionine, MGL) (Sigma- Aldrich 59555- SUPELCOSIL LC-18-DB HPLC Column)

6.7 Raw HPLC graph analysed with Methionine + MGL + Zinc citrate (NaAc and OPA) (Sigma- Aldrich 59555- SUPELCOSIL LC-18-DB HPLC Column)

6.8 Methionine calibration curve using AUC mAU*S (Testing methionine concentrations (pmol/µl) in log)

6.9 Bar chart - methionine absorbance after addition of methionine gamma lyase and products for inhibition – Methionine alone is the control absorbance (log) of free methionine. Enzyme alone (shows methionine and enzyme measured together), and everything in between exhibits the abs of natural product added to enzyme and methionine (ZnCi- zinc citrate, Ga- Gallic acid, ZnCh- zinc chloride, CaF- caffeine, Na- Nicotinic acid)

6.10 Using a concentration gradient of Methionine concentrations up to 100µM a Michaelis-Menten plot has been constructed

6.11 Trigonelline IC50 graph showing % inhibition against methionine at 100µM and lysed bacteria on a log scale (x axis) of all three gasses (hydrogen sulphide- blue circles, methyl mercaptan- red triangles, dimethyl sulphide- purple squares) (2.0 log = 100 µM)

6.12 Gallic acid graph showing % inhibition on a log scale (x axis) of all three gasses (hydrogen sulphide- blue circles, methyl mercaptan- red triangles, dimethyl sulphide- purple squares) tested on 100µM methionine with oral bacteria

6.13 Zinc chloride graph showing % inhibition on a log scale (x axis) of all three gasses (hydrogen sulphide- blue circles, methyl mercaptan- red triangles, dimethyl sulphide- purple squares) tested on 100µM methionine with oral bacteria

6.14 Zinc chloride graph showing % inhibition on a log scale (x axis) of all three gasses (hydrogen sulphide- blue circles, methyl mercaptan- red triangles, dimethyl sulphide- purple squares) tested on 100µM methionine with oral bacteria

6.15 Docking (Autodock) MGL 5x2v chain D with Gallic acid- images rendered in pymol

6.16 Docking (Autodock) MGL 5x2v chain D with Trigonelline - images rendered in pymol

6.17 Gallic acid bound with methionine binding overlaid

6.18 Trigonelline bound with methionine binding overlaid

6.19 BLAST(NCBI) to find sequence alignment and conservation between 5x2v (MGL from *P.putida*) and other bacteria (*P.gingivalis, T.denticola, T.forsythia* (37% identical, 55% similar) , *V.ratti* (57% identical, 74% similar) and F.nucleatum (55% identical, 75% similar)

6.20 Visualisation of conserved and non-conserved regions of Methionine gamma lyase based on Bioedit results comapring *P.putida* (5X2V) to *P.gingivalis, T.denticola, T.forsythia, V.ratti* and *F.nucleatum*

Chapter 7

7.1 Development and bacterial aggregation in a biofilm. Image taken from a review article by Parashar *et al*., (2015)- shows the interspecies communications from early colonisers interactions and showing subsequent attachment and bonds created by late colonisers, creating an oral biofilm.

7.2 Confocal image showing the control growth of oral bacteria as a biofilm in the absence of any products. Stained with SYTO 9 and propidium iodine

7.3 Confocal image showing trigonelline incubated with oral biofilms and stained with the Live/dead procedure

7.4 Confocal image showing Zinc citrate incubated with an oral biofilm and stained using Live/Dead procedure.

7.5 Confocal image showing Zinc chloride incubated with an oral biofilm and stained using Live/Dead procedure.

7.6 Confocal image showing Gallic acid incubated with an oral biofilm and stained using Live/Dead procedure.

7.7 Hydrogen sulphide output from biofilms (pictured above), on top of each bar is the CFU/ml counted from the biofilm in the presence of the corresponding inhibitory product

Chapter 8

8.1 Adapted from Burnett and colleagues, (2011) and Maria Antonella sole (2014) (MSc project Kingston University). Demonstrates the sorbarod system set up.

8.2 Flow cell apparatus. Can be set up under a microscope and input and output tubes for media flow can be inserted into both ends.

List of tables

dependant and independent variables (ppb, concentrations of natural product/ substrate).

Chapter 6

Chapter 8

Abstract

Oral malodour is defined as bad breath originating from the oral cavity. Almost everyone will experience some degree of halitosis at least transiently for example in the morning or from food/ alcohol. Malodourous gases can also be indicative of more serious health conditions (e.g. diabetes) or of oral diseases such as gingivitis or periodontitis. The objective of this thesis was to investigate the microbiological contributors to oral malodour and identify the enzymatic mechanisms underlying malodour generation. In parallel, inhibitors were assessed to further characterise mechanisms as well as to identify the inhibitory potential of food extracts. Methods employed included using various bacterial strains, and using whole cell oral planktonic bacteria, lysed planktonic bacteria, methionine gamma lyase (MGL) solutions and complex oral biofilms. In this way 'real life' scenarios could be simulated together with identification of enzyme binding and kinetic characteristics.

These investigations showed that volatile sulphur compound (VSC) production is a direct product of bacterial enzyme metabolism. The addition of the amino acids: cysteine and methionine as promoters, provided data to reveal enzymatic reaction mechanisms, emitting over 1000 parts per billion (ppb) hydrogen sulphide. Crude extracts of foodstuffs such as teas and coffee produced a decrease in VSCs (chapter 3 and 4) resulting in 60-100% decrease in measured hydrogen sulphide. The components of these crude products were further purified to yield gallic acid, trigonelline and caffeine and these extracts assessed in chapter 5 on lysed bacteria which uncovered kinetic results indicative of enzyme inhibition (IC_{50}s ranging from 0.2- 0.7 mg/ml). The parameters were investigated in chapter 6 which verified action on MGL enzyme rate of reaction (IC_{50} range: 0.2- 1.6 µM). Finally, an oral biofilm model was used to evaluate the efficacy of a panel of inhibitory extracts. This assessment visually showed a top layer cell 'death' with a reduction in gases (by over 100 ppb) and a 1-log reduction in viable and culturable bacterial cells.

The results from this thesis suggest that a range of extracts of foodstuffs have potential as enzyme inhibitors and warrant further study with 'real life' biofilms. The products (gallic

acid, trigonelline, zinc citrate and zinc chloride) used in this thesis were effective in decreasing the gaseous release associated with oral malodour.

Chapter 1 Introduction

1.1 Halitosis in the oral cavity

Oral malodour (halitosis) mainly originates from the oral cavity, up to 50% of people in the developed world are thought to have a reoccurring issue with bad breath (Porter and Sculley 2006) although this statistic changes according to gender, age and lifestyle. This socially relevant disease can affect everyday life for all individuals and is of commercial importance.

Halitosis can be split into 3 categories with only 85% originating intraorally (e.g. periodontitis, gingivitis, xerostoma, insufficient oral hygiene), 10% originate in respiratory problems such as tonsillitis and bronchitis and 5% of halitosis being attributed to systemic diseases such as diabetic ketoacidosis, leukaemia or infection with *Helicobacter pylori* (Morita and Wang, 2001; Wei et al., 2019).

Measuring halitosis can be done organoleptically, where a clinician smells the oral cavity to detect the origin of halitosis, there are some cases where the patient will not have halitosis but perceive themselves to have chronic bad breath, this is referred to as halitophobia or pseudohalitosis and is not true halitosis. The root of this problem usually stems from mental health issues and is often diagnosed with other psychiatric issues such as obsessive-compulsive disorder (OCD) and social anxiety disorders (Mrizak *et al*., 2018). The organoleptic method using trained clinicians, at a specialist halitosis clinic (e.g in Leuven, Belgium) is the gold standard of halitosis detection. Quantification is ranked in numbers; 0: No malodour, 1: slight malodour, 2: clearly noticeable malodour, 3: strong malodour (Gufran *et al*., 2016). There is a new organoleptic based method proposed by Kim *et al.,* (2009), and reviewed against other methods in 2018 (Laleman *et al.,* 2018). This method includes the collection of breath in a gas tight syringe by negative pressure and expelling into a cup. This can then be smelled and scored away from the patient, the advantages of this include the removal of odour interference such as perfumes, increasing result reproducibility and assessment by more than one clinician away from the patient. Gasses

released from the oral cavity can also be quantified by gas chromatography, however, this is not recommended in a clinical setting and should be reserved for scientific studies.

1.2 The oral cavity

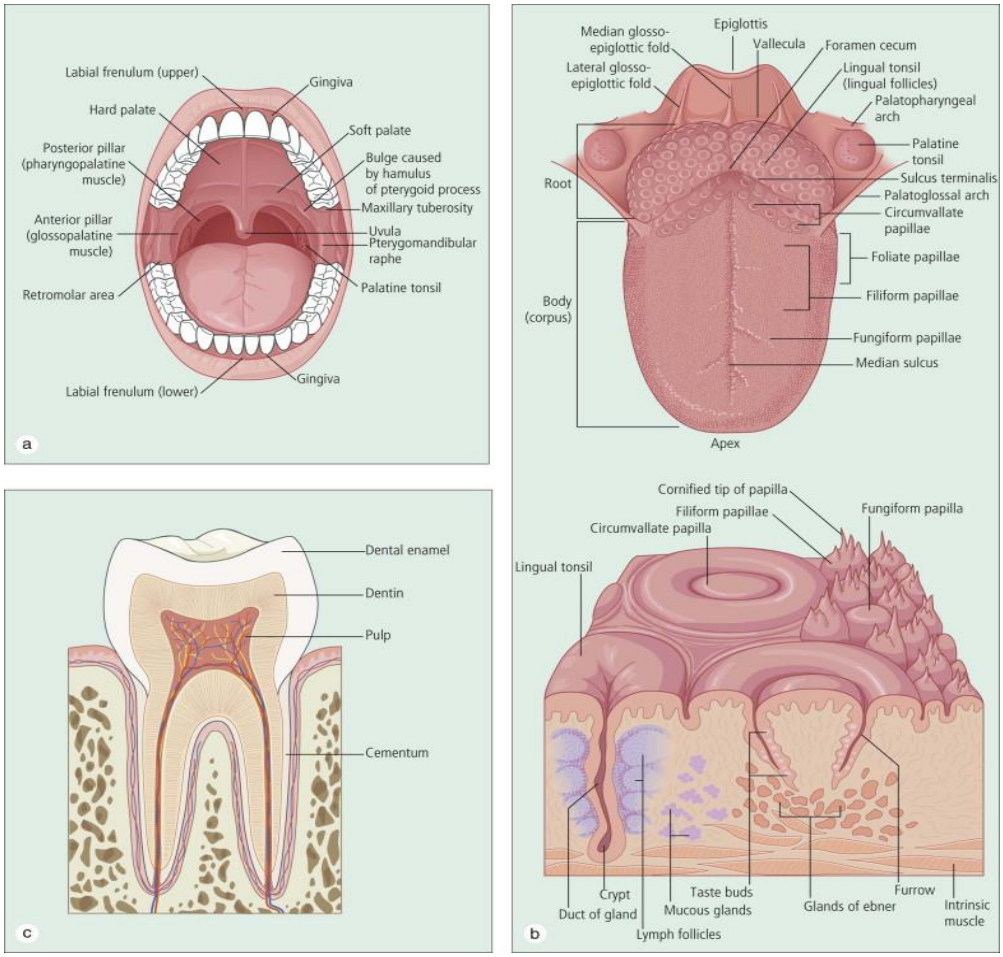

Figure 1.1 Areas in the oral cavity. Taken from Pediatric Dermatology (Fourth Edition) (Cohen, 2013).

As seen in Fig 1.1, there are many areas in the oral cavity subject to bacterial colonisation. The main areas of interest for studying bacteria involved in halitosis are the tongue, gingival crevice and teeth. The teeth offer a non-shedding surface for long lasting biofilms to thrive. The initial attachment occurs on the salivary pellicle coating each tooth, this pellicle allows specific bacterial binding (Palmer Jr, 2013). In the first 12 hours of colonisation, *Streptococcus spp*. colonisation makes up 25% of the total bacteria measured and is visualised by fluorescent in situ hybridisation (FISH) in a healthy oral cavity (Al-Ahmad *et al*., 2009). The gingival crevice is a deep area below the tooth margin that has relatively little oxygen available, this suits the facultative anaerobic bacteria that are able to colonise

these areas and affect immunological processes such as *P.gingivalis* which downregulates interleukin 8 (IL-8) from epithelia limiting the neutrophil migration to the periodontal pocket and protects all the species of bacteria residing there (Tang and Könönen, 2015). *Filifactor alocis* was detected near the soft tissue of subgingival plaque, mostly in unhealthy oral cavities, such as those with chronic periodontitis, its absence in the control groups class this bacterium as an indicator of pathogenic behaviour (Schlafer *et al.,* 2010). The tongue surface is covered in papillae which increases the surface area for harbouring bacterial species. The main species found on the tongue include *Fusobacteria, Actinobacteria* and *Proteobacteria* (Sun *et al.,* 2017), this research also determined the difference between microbial communities in a thin white tongue coating compared to a greasy white tongue coating. Whilst there were some difference between individuals, there were no major differences between the two groups suggesting tongue bacteria are relatively standardised among human beings.

1.2.1 Environments in the oral cavity

Changing environments within the oral cavity including pH, salivary flow and oxygen availability, allows for a multitude of bacteria with different properties to grow and thrive (aerobic, microaerophilic and anaerobic bacteria) (Paju and Scannapieco, 2007). The supra-gingival area and tongue both have soft surfaces which are coated with saliva as base for bacterial binding, these areas consist of a neutral/acidic pH over a range of oxygen availability. The tooth surface acquires a pellicle surface initiating bacterial adhesion, the pH is neutral with a low concentration of oxygen available, in this environment the metabolic activity of bacteria is mainly proteolytic (Takahashi, 2005). The oral microbiota protects the oral cavity against invading exogenous species by taking up sites of colonisation with resident microbes.

1.3 Bacterial involvement

The bacteria in the oral cavity which are involved in the process of malodour generation include *Fusobacterium nucleatum, Porphyromonas gingivals, Prevotella intermedia, Veillonella spp*. *and Treponema spp*. amongst others (Dewhirst *et al*., 2010). In fact, the oral cavity contains 700 species of bacteria including non-cultivable species (which can be detected and identified by 16s PCR, (Faveri *et al*., 2008) ranging in concentration from 10^8 -10^{14}. This is due to the exposure of the oral cavity to the outside environment (Hartley *et al.,* 1996; Guarner and Malagelada, 2003). The densest site of bacterial co-aggregation is formed on the surface of the dorsal posterior of the tongue (Lee *et al*., 2003), these bacteria organise into communities of multiple species co-inhabiting, and this is referred to as plaque or the oral biofilm (Kolenbrander *et al*., 2002).

When the health of a patient's oral cavity is compromised (e.g. through bad oral hygiene practices) a shift in the microbial composition can occur, a larger proportion of anaerobic Gram-negative bacteria assume their place as oppose to Gram-positive bacteria which tend to be aerobic and classed as early biofilm colonisers (Marsh, 2010)

Biofilm communities in the oral cavity are seldom single species, but are usually a mix, some complexes of bacteria are more destructive than others. In the worst-case oral cavity, a large proportion of three main periodontopathogens co-exist to form the red complex: *Porphyromonas gingivalis, Treponema denticola* and *Tannerella forsythia.* These are all gram-negative bacteria with high proteolytic activities.

1.3.1 The effect of *P.gingivalis* on oral health and immune system

P. gingivalis is a key periodontopathogen which can influence bacterial cell binding and virulence (Suzuki, Yoneda and Hirofuji, 2013). *P. gingivalis* expresses cysteine proteases on its cell membrane. These are called gingipains and there are two main types: arginine specific (RgpA, RgpB) and lysine specific (Kgp) (Gorman *et al.,* 2014). In a study by Bao *et al.,* (2014) a mixed biofilm was grown to determine the effects of *P.gingivalis* types and the results suggest that lysine gingipains increase the habitation of *T. forsythia* and that arginine specific proteases increase the aggregation of *T. denticola*. The inflammation

involved with this red complex of bacterial species at low levels can lead to periodontal bone loss (Hajishengallis *et al*., 2011). These gingipains have also recently been heavily implicated in Alzheimer's disease (Dominy *et al.,* 2019). The pharmaceutical company Cortexyme (2019) have proceeded with phase 2/3 clinical trial using COR388, a gingipain inhibitor for the treatment of Alzheimer's.

P. gingivalis can degrade C3 protein of the complement system via its gingipains, C3 cleavage results in c3a and c3b proteins that initiates pathogen destruction and inflammation (Janeway, 1999). The bacteria in a biofilm can uphold resistance to lysis by the complement system even without the gingipain proteins, indicating that the LPS (lipopolysaccharide) on the outer bacterial membrane of gram-negatives protects the bacteria residing in a biofilm. In combination with *P. gingivalis* which decreases serum bactericidal effects, the integrity of the biofilm is maintained. *T. forsythia* also expresses complement degrading protein in the form of karilysin which acts on various complement proteins inhibiting the lectin pathway (Hajishengallis *et al*., 2013). However, bacteria can also promote complement activation, for example, *P. gingivalis* recruits C5a proteins which seems counterproductive, but studies show that this is a manipulation of the complement systems communication with toll like receptor 2, which supresses the recruitment of macrophages and pro-inflammatory cytokines (Wang *et al*., 2010; Hajishengallis *et al*., 2011). *P. gingivalis* can also survive within macrophages, this may suggest a means of transportation by the hijacking of immune cells to travel and infect peripheral tissues (Hussain, Stover and Dupont, 2015). *P. gingivalis* is also implicated in cardiovascular disease and atherosclerosis. The protective high-density lipids (HDL) are oxidised and endocytosed by travelling infected macrophages to produce cholesterol, deposited in arterial walls (Kim *et al*., 2018).

Gingivitis, and the inflammatory pathways involved may be shared with and affect systemic systems, this can affect an array of diseases such as: rheumatoid arthritis, osteoporosis, type 2 diabetes, cardiovascular diseases, Alzheimer's disease and pneumonia (Buhlin *et al*., 2002; Kamer *et al*., 2008; Bingham and Moni, 2013; Holmstrup *et al*., 2017). The treatment of one ailment may have a knock-on effect controlling the other disease and therefore an

important link which warrants the study of associated mechanisms in more depth (e.g. COR388 clinical trials).

1.4 Foodstuffs

The most studied and causative foodstuff affecting dental caries (the process of causing demineralisation of enamel) is sugar. The oral bacteria can ferment sugars which rapidly decreases the pH in the oral cavity favouring acid tolerant bacterial species such as *Lactobacillus* and *Streptococcus spp*. These bacteria then create more acid via sugar metabolism which promotes the demineralisation of the enamel surface (Sheiham and James, 2015). Bacteria such as *Streptococcus mutans* also possess protective acid tolerating responses which allow survival in these acidic conditions such as altering membrane composition and metabolic activity (enhanced glycolytic activity) in acidic environments (Guo *et al*., 2015).

Dairy products can offer some protective value due to the calcium and phosphate protecting against decay (Wilson *et al*., 2009). In a study of the elderly, milk and calcium intake had an inverse relationship with the severity of periodontitis (Adegboye *et al*., 2012). Although calcium may be essential for tooth mineralisation, there is no specific mechanism attributing dairy intake to periodontitis control.

Phenols and polyphenols from fruits and teas and other phenolic compounds are implicated in the protection from cariogenic bacteria in the oral cavity, some of these effects have been attributed to activity on enzymes and oral tissues rather than a direct bactericidal effect (Petti and Scully, 2009). Some bacteriostatic effects are observed from compounds in coffee such as caffeic acid and trigonelline against *Streptococcus mutans* with a minimum inhibitory concentration (MIC) of 0.8 mg/ml. Coffee as a whole solution, does not exhibit the same inhibitory potential on the growth of oral bacteria due to amino acid and sugar molecules (Antonio *et al*., 2010).

1.5 Cysteine

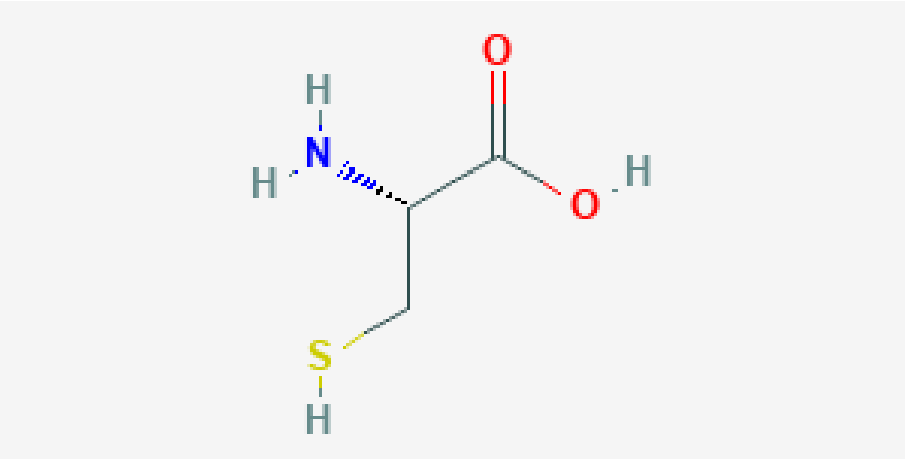

Figure 1.2 2D L-cysteine structure from PubChem

Cysteine and methionine are both sulphur containing amino acids, methionine is an essential amino acid whereas cysteine can be synthesised intracellularly from methionine (Ciborowski and Silberring, 2016). Cysteine is associated with the production of hydrogen sulphide from bacteria, there are various enzymes and pathways involved in this metabolic system. L-cysteine desulphydrase catalyses the αβ elimaination of cysteine to hydrogen sulphide, pyruvate and ammonia. In a study by Fukamachi *et al*., (2002) *F. nucleatum* produced the largest concentration of hydrogen sulphide from cysteine, compared to other sulphur containing amino acids, they also reported a high affinity to cysteine desulphydrase from L-cysteine (15.1 mmol min-1 mg-1 hydrogen sulphide production) and when the enzyme was purified from *F. nucleatum* there was an inability to react with other sulphur containing amino acids e.g. homocysteine. Chu *et al*., (1999) reported that the l-cysteine desulphydrase from *Treponema denticola* was able to reduce not only cysteine, but cystine and glutathione too to produce hydrogen sulphide, pyruvate and ammonia. Methionine gamma lyase from *F. nucleatum* was also involved in the production of hydrogen sulphide from cysteine but with a lower rate of reaction to that producing methyl mercaptan from methionine (Suwabe *et al*., 2011). Kleinberg and Codipilly, (2002) state that the amino acid that normally corresponds to the production of hydrogen sulphide is cysteine and suggest using a cysteine challenge of 6 mM for 30 seconds on bacterial sites to assess the effectiveness of novel inhibitors when considering real life inhibitory success.

The metabolism of cysteine by enzymes, which are present both in eukaryotes and bacterial cells, is key to the production of hydrogen sulphide (Matoba *et al*., 2017). Transulphuration enzymes are involved in this catalysis- cystathionine beta synthase (CBS) and cystathionine gamma lyase (CSE) which are also involved in the conversion from homocysteine to cysteine with a cystathionine intermediate (Carter and Morton, 2015).

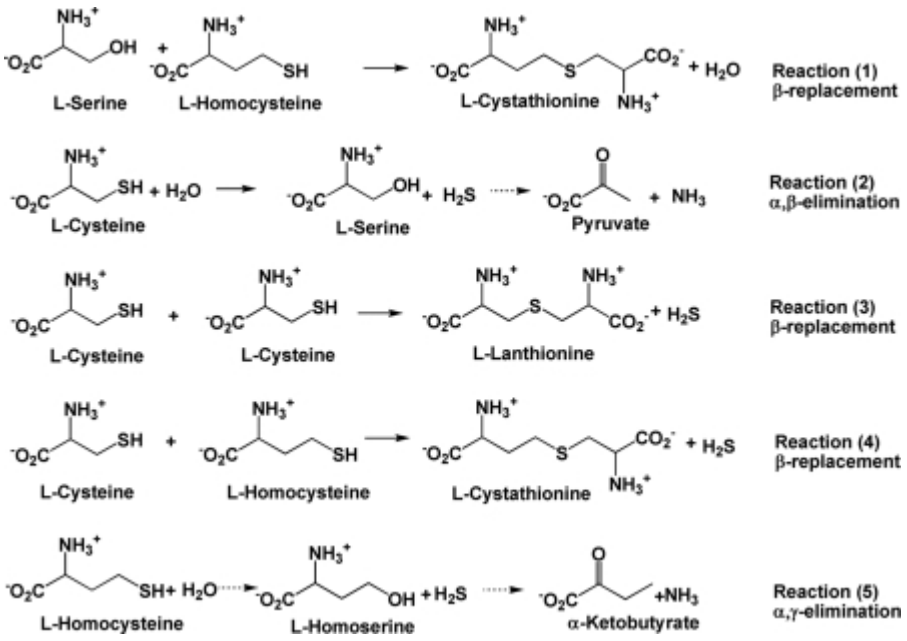

Figure 1.3 Reactions catalysed by Cystathionine Beta Synthase, extracted from article by Singh and colleagues (2009).

1.6 Methionine

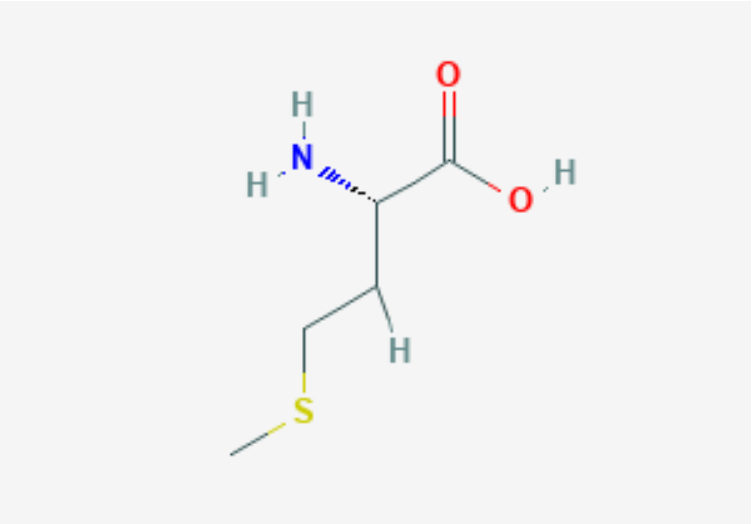

Figure 1.4 2D methionine structure from PubChem.

Methionine is an essential amino acid and is acquired through the diet. It is contained in foodstuffs such as nuts, meats and cheeses. Its structure consists of a methyl group covalently bonded to a sulphur atom; its conformation is key to its metabolism. In the oral cavity some bacteria have the enzyme necessary to catalyse the breakdown of methionine into methyl mercaptan, α-ketobutyrate and ammonia. This enzyme is methionine gamma lyase (MGL). The *mgl* gene encodes this enzyme, in an experiment using MGL deficient and a wild type strain of *P. gingivalis*, Yoshimura *et al*., (2000) concluded that this enzyme was responsible for the production of methyl mercaptan from methionine.

Methionine is a precursor for cysteine, therefore involved in hydrogen sulphide production indirectly. Essential methionine can be converted to homocysteine through a derivative of methionine -S-adenosylmethionine (SAM) and S-adenosyl homocysteine intermediates, using methyltransferases and S-adenosyl homocysteine hydrolase. From homocysteine, the enzymes cystathionine β synthase and cystathionine λ lyase with a cystathionine intermediate to irreversibly convert to cysteine. (Hullo *et al*., 2006; Brosnan *et al*., 2007)

The methionine gamma lyase enzyme makes a complex with methionine at the pyridoxal 5 phosphate co-enzyme which prompts the production of 3 intermediates (PLP methionine imine, PMP-αketomethionine imine, PMP-αβ dehydromethionine imine) to release the sulphur side chain in the form of methyl mercaptan (CH_3SH) (Sato *et al*., 2017).

1.7 Volatile Sulphur Compound Production

Volatile sulphur compounds (VSCs) are known to be the main malodorous compounds arising from bacterial putrefaction of salivary proteins and local debris. Primarily the volatile compounds associated with 90% of oral malodour are hydrogen sulphide and methyl mercaptan (Tonzetich, 1971) metabolised from cysteine and methionine. The increase in these volatile compounds has a role in the pathogenicity of inflammation leading to gum disease, producing VSCs as well as other by products which are toxic to the oral tissue (Ratcliff, 1999).

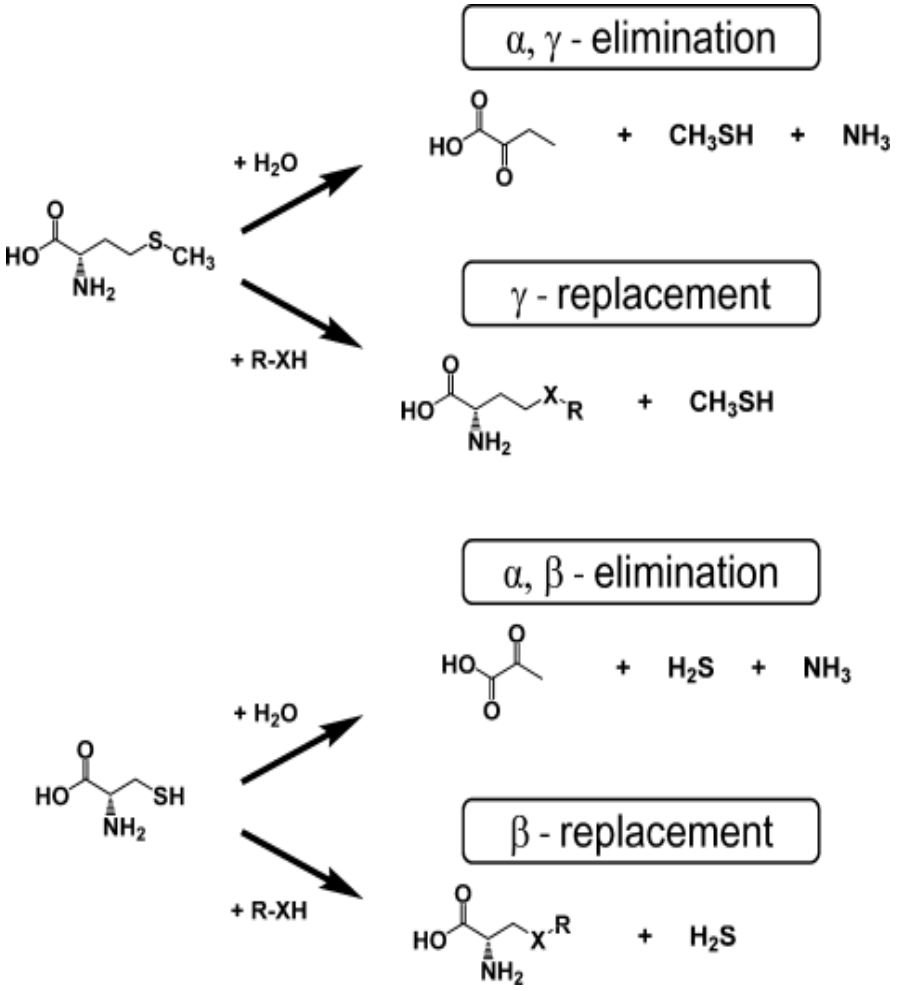

Figure 1.5 (Sato and Nozaki, 2009) The catalytic reactions that can arise from methionine gamma lyase (Top reaction shows the alpha gamma elimination (and gamma elimination) resulting mainly in methyl mercaptan. The bottom two reactions show the action of methionine gamma lyase on cysteine- alpha beta elimination and the beta replacement yielding hydrogen sulphide.

1.7.1 Volatile sulphur compounds (VSCs)

Hydrogen sulphide, methyl mercaptan and dimethyl sulphide are classed as odorous volatile sulphur compounds, the former two have the highest odour content and volatilise readily (Nakono, Yoshimura and Koga, 2002). Enzymes are heavily involved in the production of VSCs from amino acid and protein degradation.

1.7.2 Hydrogen Sulphide

Producing this substance is a common trait to many species of oral bacteria such as *Veilonella, Actinomyces* and *Prevotella* (Washio *et al*., 2005).

Hydrogen sulphide is a cytochrome c oxidase (COX) inhibitor, this enzyme is key in the ATP production of mitochondria via oxidative phosphorylation. This inhibition of aerobic metabolism could cause respiratory paralysis (Yaegaki, 2008). However, the role of hydrogen sulphide is complex as a biological mediator, and a product of bacterial metabolism. H_2S producing enzymes are available in most regulatory parts of the body, including smooth muscle, brain, gut and oral cavity. Early studies (1700's-1900's) implicated the toxicity of H_2S as a gas inhaled by sewage workers (Szabo, 2018), since there has been a surge in hydrogen sulphide studies e.g. as a neuromodulator in combination with nitric oxide to induce systemic vasodilatation through transient receptor potential channel A1 (TRPA1) opening allowing a calcium influx resulting in release of calcitonin gene-related peptide (Eberhardt *et al*., 2014). It is a direct regulator of blood pressure, as shown by a study in mice with deleted cytathionine gamma lyase gene and therefore decreased H_2S in the serum and heart, which produced mice expressing hypertension (Yang *et al*., 2008). The gas has been studied for its protective effects in neurons and inflammation. In neurons, the protective value of H_2S is evidenced by its upregulation of glutathione which prevents neuron oxytosis (Kimura and Kimura, 2004). On inflammation, H_2S can induce anti-apoptotic genes, by causing the sulfhydration of cysteine-38 p65 which creates a surge in Nf-kB gene activity, reducing hypersensitivity to cellular apoptosis by TNF-α (Sen *et al*., 2012).

H_2S is also a potential carcinogenic compound, it instigates DNA damage in fibroblast population such as HCF and HGEC (gingival epithelial cells) and can result in apoptosis, an early sign of cancer in these cells. The gas is also produced in the colon where it can migrate

in the blood stream to the liver, however this organ has detoxifying activity, as well as the colonic mucosa process of methylation and demethylation aiding the management of toxicity, this is necessary as the concentration of hydrogen sulphide produced in the colon is higher than in the periodontal pocket (Levitt *et al*., 1999).

1.7.3 Methyl mercaptan

Methyl mercaptan is known as methanethiol in some other literature. The sulphur in the methionine is catalysed to produce, through enzyme pathways, α keto acid, ammonia and the volatile compound (Yoshimura, Nakano and Koga, 2002). The odour threshold is higher than other volatile compounds contributing to oral malodour. In a study by Tangerman and Winkel (2007) the odour index (OI) is reported to be 53,300,000 OI compared to the 17,000,000 OI of hydrogen sulphide. An odour index is a ratio between the introduction of the sulphurous compound and the capacity to produce a recognisable response. Methyl mercaptan is predominantly produced by anaerobic Gram-negative bacteria in the oral cavity. Releasing methyl mercaptan in the periodontal pocket can increase the permeability of tissues by 66% implicating damage in the epithelial cells, which could, in part initiate or progress the onset of periodontitis (Johnson, Yaegaki and Tonzetich, 1996).

1.7.4 Dimethyl sulphide (DMS)

This gas is the third main volatile sulphur compound involved in bad breath odour. It is the only one of the VSCs which is stable in blood. In cases of blood-borne halitosis, DMS can travel from the gut to the lungs and depending on environmental factors can be exhaled in its gaseous form to create a perceived halitosis. (Harvey-Woodworth, 2013). In a study by Tangerman and Winkel, (2008) an elevated dimethyl sulphide output from mouth and nose air was observed for all 6 patients with extra-oral halitosis. Hydrogen sulphide and methyl mercaptan were the main intra oral halitosis contributors. Considering methyl mercaptans odour index, it can be described as the main source of foul-smelling breath in patients with genuine halitosis. Two moles of methyl mercaptan can also oxidise or react with methanol producing dimethyl sulphide (Kandalam *et al*., 2018).

1.7.5 Volatile Organic Compounds (VOC)

VOCs such as short-chain fatty acids (propionic and butyric acids), polyamines (cadaverine, putrescine) and phenyl compounds (indole, skatole) are also known to be present in oral malodour. Unlike VSCs, these compounds volatilise less readily and therefore their impact on halitosis may not be high in healthy individuals (van den Velde *et al*., 2009).

1.8 Oral biofilms

The definition of a biofilm is a group of microorganisms which adhere to the surface or each other and are embedded in an extracellular matrix known as the extracellular polymeric substance (EPS) (Marsh, 2004).

The constituency of a biofilm differs from planktonic bacterial cells by being a microhabitat which is hard to penetrate for chemical removal, up to 1500x more resistant than their planktonic counterparts (Saini *et al*., 2011), metabolic collaboration may be possible by the proximity of the cells as appose to liquid phase growth (Bradshaw, 1995). Hua Wei and Leiv Sigve Håvarstein (2012) state that fratricide within a biofilm is essential with initial quorum sensing to enhance virulence of the biofilm by exchanging DNA.

In plaque biofilms there is usually a change in species between healthy and diseased individuals shifting from gram positive predominant in a healthy oral cavity to gram negative bacteria which take over in diseased states, these are found in the heart of the biofilm in which they thrive free of oxygen due to their anaerobic nature. Both types of bacteria are present in every oral cavity and it is the balance between these bacteria which determine a healthy or diseased state (Patil, 2013). These gram negatives are proven to be the main source of VSC production, whereas the population of predominantly Gram-positive bacteria on the outer layers of the biofilm are involved with proteolytic activity (Sterer *et al*., 2009).

Biofilm formation starts with a pellicle which includes a thin layer of salivary glycoproteins adhering to the tooth surface (Bradshaw *et al*., 1997), this is vital for the composition of the later biofilm due to the introduction of a layer to build on for further adhesion (Li *et al*., 2004) The adhesion of bacteria to mature the biofilm starts by nonspecific interactions such as acid base interactions and electrostatic forces over a short distance, which is a trait common to all biofilms (Bos *et al*., 1999).

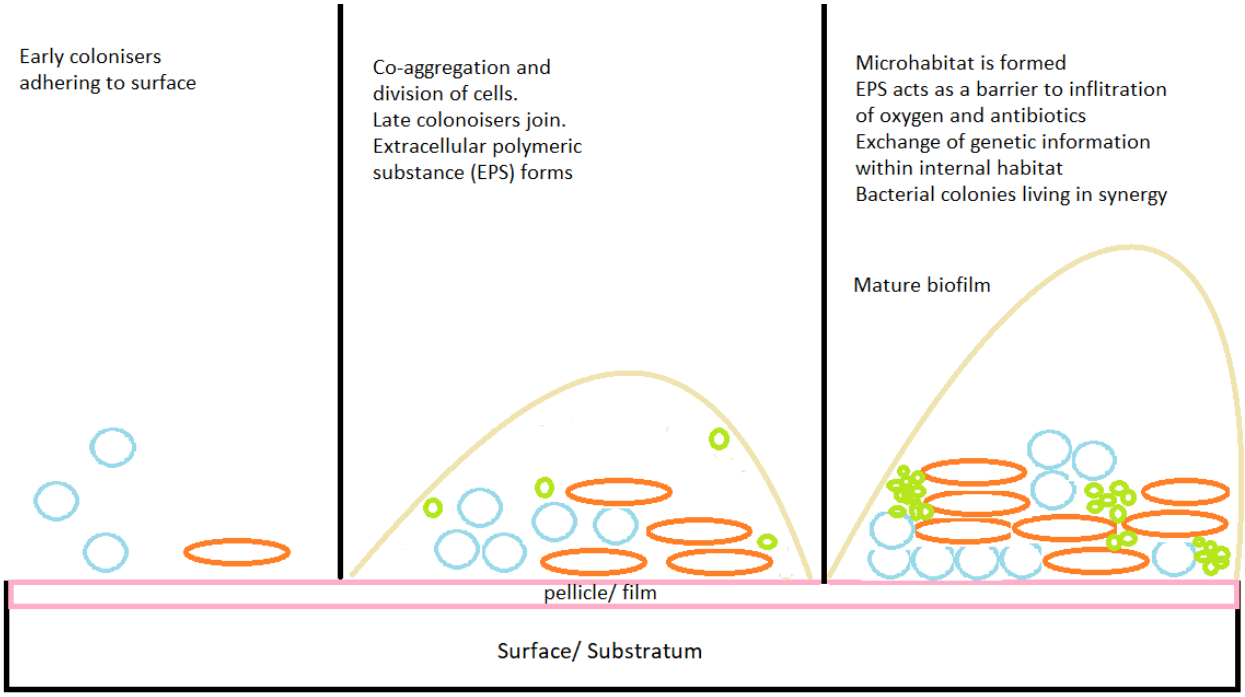

Figure 1.6 Information on the stages of biofilm development, adapted from (Bos et al., 1999; Hojo et al., 2009).

1.8.1 Biofilm colonisation

The early colonisers include *Streptococcus mitis* and *Actinomyces naeslundii*. Fusobacteria initiate the biofilm that is indicative of plaque by co-aggregation of other bacteria to create the anaerobic environment (Rickard *et al*., 2000). Specific interactions between bacteria have been noted, examples such as the CshA on *Streptococcus gordonii* can mediate co-aggregation of *Actinomyces* naeslundii and *Porphyromonas gingivalis* (periodontopathogen). Therefore, biofilm acquisition requires the presence of certain organisms on select surfaces. As an example of this, Periasamy and Kolenbrander (2009) grew *Porphyromonas giningivalis* in the presence of *Streptoccocus oralis*, this did not then flourish into a biofilm but with the addition of *Streptococcus gordonii* into the solution matrix, it did.

The biofilm exhibits complex cell to cell interactions. Duran-pinedo and colleagues (2014) tested the addition of *Porphyromonas gingivalis* to *Streptococcus mitis* and witnessed higher Streptococcus mitis cell death than the control viewed with LIVE/DEAD stain. The exact mechanism of death is not known but the authors witnessed a high level of the

transposase enzyme which may have a bearing, as well as other enzymes involved in controlled cell death. This acts as an example of the highly complex and controlled microhabitat maintenance.

Bacteria dispersal from the biofilm is inevitable to colonise a new site (Kaplan, 2010). There are multiple mechanisms behind this including enzyme action, where enzymes actively assist the degradation of the EPS to colonize new sites. For example *Aggregatibacter actinomycetecomitans* contain an enzyme called dispersin b which is able to break down Poly-β(1,6)-N-acetyl-D-glucosamine (PNAG). Chaignon *et al*., (2007) counted PNAG as an integral part of the EPS stability, hence the encasement and stability of the biofilm.

1.8.2 Biofilm nutrients

Saliva has key functions in the maintenance of oral health, its functions involve the protection against demineralisation, aids remineralisation, buffering and lubrication of the teeth. It is involved in taste and digestion and has an array of enzymes which work as an anti-bacterial, anti-fungal and anti-viral. (Amerongen and Veerman, 2002). Channels are made within the plaque composition which allow the exchange and transport of nutrients and oxygen (Robinsona *et al*., 2006) although some parts of the biofilm are not oxygenated which allow for anaerobic environments through the inner layers. It is the salivary proteins and glycoproteins which serve as the main nutritional source for early biofilms (Spratt and Pratten, 2003). Saliva can clear food and non-adherent bacterial cells much like the gingival crevicular fluid, however the pH of saliva at 6.75 is able to neutralise acid, a harmful by-product from the metabolism of oral bacteria (Marsh *et al*., 2009).

The gingival crevicular fluid (GCF) is yet another source of nutrition and can impact on the microbial environment. The glycoproteins and proteins in the GCF can ‘feed’ the bacteria for VSC production and plaque development leading to disease (usually stemming from bad oral health care) (Marsh *et al*., 2009).

The oral biofilm (dental plaque) on the dorsal posterior of the tongue is the main site of the bacterial accumulation that produces VSC’s (Scully and Greenman, 2011), therefore most

likely to be subject to *in vitro* testing of bacteria. The bacteria here can interact with desquamated epithelial cells and leukocytes retained in the papillary structure of the tongue as well as a consistent flow of saliva available for bacterial metabolism (Spencer *et al*., 2007; Yoshikawa *et al*., 2017).

1.9 Oral bacteria implicated in disease

An extensive study was published to determine the risk of coronary heart disease and associations with oral bacteria, this included 9760 people over 14 years. (DeStefano *et al*., 1993) The outcome showed a 25% increased risk of heart disease in cases of periodontitis. This association has been confirmed in the analysis of atherosclerotic plaque containing 23 oral bacteria such as *P.gingivalis, P. intermedia* and other gram negative species, however *Streptococcus sp*. is a gram positive species, and was also isolated from the plaque (Chhibber-Goel *et al*., 2016). The mortality rate of those with both cardiovascular disease and periodontitis is increased and this can be attributed to the effects of the immune system, the lesions seen in atherosclerosis contain macrophages and cholesterol, the virulence factors in *P.gingivalis* can release pro-inflammatory cytokines and recruit immune cells such as monocytes/macrophages, these inflammatory immune factors also initiate the changes in the endothelium, the artery will get congested leading to plaque formation (Serra e Silva Filho *et al*., 2014).

There is also a link between type-2 diabetes and periodontopathogens, a three-fold increase in bacteria such as *P.gingivalis* and *A.actinomycetemcomitan* were found in the biofilm of obese adolescents compared to normal weight controls (Zeigler *et al*., 2011). There is also a 10-fold increase in all bacteria tested in adults with type 2 diabetes compared to a no diabetes control implying an importance to the oral microflora although mechanisms of this are not classified. There is, however, a reverse in bacterial counts of Bifidobacteria between the two groups (10-fold lower in subjects with type 2 diabetes)- the author proposes that bifidobacteria may displace some pathogenic bacteria within the oral microbiome abating their invasiveness and inflammatory response (Shillitoe *et al*., 2012).

1.10 Enzymes

To this point, the implications of oral bacteria and their metabolic products has been discussed. As well as bacterial co-aggregation into micro-habitats- biofilms. All these functions are aided by enzyme involvement. This section aims to reveal some characteristics of enzymes in oral bacteria namely methionine gamma lyase, and look into its inhibitory potential and treatment options.

1.10.1 P5P co-enzyme

Pyridoxal-5'-phosphate (P5P) mediates both hydrogen sulphide production from cysteine and methanithiol from methionine. P5P is also known as a vitamer of vitamin B6 and this form binds its carbonyl group to the α-amino group on the amino acid reacting to cause a Schiff base (Caballero, Trugo and Finglas, 2003).

A study by Wolle *et al*., (2006) found that P5P can react directly with methionine but at a reduced rate compared to p5p catalysing the metabolism of amino acids. It is used as a co-enzyme to convert methionine to methyl mercaptan, alpha keto butyrate and ammonia. P5P is involved heavily in the intermediate's formation during methionine catalysis, it can react with lysine residues to facilitate the Schiff base, this is specific to lysine, verified by an increased dissociation (150-fold) with arginine as a mutant (Bertoldi *et al*., 2003). Taking a high dose of vitamin B6 can have adverse effects exhibiting the same clinical symptoms as B6 deficiency such as peripheral neuropathy (Hammond *et al*., 2013), this is due to the inactive form of pyridoxine which can inhibit the P5P co-factor (Vrolijk *et al*., 2017).

1.10.2 L-cysteine desulfhydrase / Cystalysin- hydrogen sulphide production

This enzyme has been recovered from oral bacteria such as *T. denticola* (Chu *et al*., 1999, Yano *et al*., 2009) and *P.intermedia* (Krupka *et al*., 2000). This enzyme has alpha beta elimination activity which assists the conversion of cysteine into hydrogen sulphide, ammonia and pyruvate. The active site of this enzyme, similar to Cystathionine γ lyase, tyrosine aminotransferase and Cystathionine β lyase, its residue is tyrosine which attaches to PLP, rather than tryptophan and phenylalanine found in other PLP dependant

aminotransferases (Krupka *et al*., 2000). The capacity to produce hydrogen sulphide from alpha beta elimination has also been separately characterised in other bacteria such as *F. nucleatum*. Fn1220 is homologous to *cdl* gene encoding cysteine desulfhydrase (Kezuka *et al*., 2012; Fukamachi *et al*., 2002) and is estimated to produce 87.6% of hydrogen sulphide from l-cysteine (Suwaybe *et al*., 2011). Interestingly the reaction that fn1220 catalyses is the beta replacement instead of the beta elimination of cysteine. The reaction produces hydrogen sulphide and lanthionine. The enzyme that carries out the beta elimination from F. nucleatum is fn0625 (Yoshida *et al*., 2010)- see Fig. 1.3.

1.10.3 Methionine γ lyase

This enzyme is encoded into the genome of many bacterial species found in the oral cavity such a *T.denticola, P. gingivalis* and *F. nucleatum*. It is responsible for catalysing the γ-elimination of l-methionine which is converted into methyl mercaptan (Suwaybe *et al*., 2011; Ito, Narise and Simura, 2008).

The enzyme is a tetramer that is divided into 2 catalytic dimers. (Kuznetsov *et al*., 2014) It is part of cystathionine synthase like family, this family of enzymes is known to aid the conversion of cysteine to its products which include hydrogen sulphide, therefore the similar structure of the active site to the cystathionine synthase like family suggests that many bacteria that produce H_2S also produce methyl mercaptan (Sun *et al*., 2008) This enzyme is encoded for by the *mgl* gene, this gene also has a role in the pathogenicity of the bacteria. In a study by Nakano, Yoshimura and Koga (2002) an MGL deficient strain of *P.gingivalis* was tested for virulence in a mouse model which significantly affected the rate of survival (7.7% survival rate with MGL gene, 36% survival with MGL deficient gene- 4 days post subcutaneous injection) . The gene in *F. nucleatum* which corresponds to the MGL gene has been named fn1419. Like the 'normal' MGL it has an affinity for cysteine, which is lower than its affinity for catalysing the reaction of methionine to methyl mercaptan. The methionine γ lyases tend to catalyse the alpha-beta elimination of cysteine at a lower rate to their catalysis of methionine through γ elimination (Suwaybe *et al.,* 2011).

The enzyme does not exist within mammalian cells and therefore an ideal therapeutic target for diseases/cells using methionine. This includes cancer where the cells rely on methionine for cell proliferation, as a therapeutic measure, MGL has been inserted into

recombinant proteins to assist the degradation of methionine, decreasing its abundance for use by cancerous cells.

In bacteria that contain the MGL enzyme, the degradation of methionine that produces volatile thiols keto acids and ammonia have advantages in the metabolism of bacteria. For example alpha-ketobutyrate is involved in ATP generation in anaerobic species- an environment rich in methionine can upregulate genes/enzymes for the catalysis of alpha-ketobutyrate (alpha- keto acid dehydrogenase) to propionyl-CoA involved in generating energy (ATP) (Cholet, Hénaut and Bonnarme, 2007). Methyl mercaptan can invade host cells by increasing bacterial pathogenicity leading to periodontitis (Sato and Nozaki, 2009). When the MGL active site binds methionine, a tyrosine residue removes a proton from the nitrogen terminal* and cysteine (110) thiol group promotes the proton relay. Next, p5p and methionine form a Schiff base due to the nucleophilic attack on the α-amino group of methionine and the C4 carbon of P5P. This forms an unstable intermediate which spontaneously coverts to a more stable intermediate. The next intermediate is made from the removal of a Cα proton from the initial intermediate, this is catalysed by Ɛ-amino lysine (205) from the p5p co-enzyme and is only possible due to the orientation of orbital and bonds.

The cleavage of Xδ-Cγ eliminates methyl mercaptan, once the X is protonated. The next intermediate before the release of alpha-ketobutyrate and ammonia are E and Z isomers (PMP-imine and PLP imine). Ɛ-amino lysin attacking C4 to replace Nα- regenerating p5p bound enzyme, 2-aminobut-2-enoate is produced, this product is unstable in water, therefore hydrolysed creating alpha keto butyrate. (Sato and Nozaki, 2009; Sato *et al*., 2017).

Figure 1.7 Methionine gamma lyase structure and active site produced with CCP4MG- This software allows the upload of a PDB file (2RFV) of the MGL protein. The active site is shown in pink Methionine gamma lyase from Citrobacter fruendii PDB code: 2RFV

Once the file is converted, the software allows manipulation of structure, colours and rotation. The original PDB file is in monomer form but its energetically stable form is as a tetramer; therefore, the image was rotated symmetrically on itself 3 times, creating an image representation of the entire enzyme structure.

Methionine gamma lyase comes from the family of p5p dependant enzymes- this can be categorised into fold types I-V. MGL has a fold type I, this is further subdivided into enzyme groups based on the N-terminals. MGL belongs to the cytathionine β lyase family.

MGL is present as a homotetramer with a weight of 200 kDa. It is made of two catalytic dimers and there are three main domains that make up the enzyme.

1. The N-terminal domain provides all the contact to other sub-units. A β strand is paired with the same residues on the other subunit to maintain stability of the enzyme.
2. P5P binding domain contains 7 β-pleated sheets and 8 α helixes found on either side of the β sheets. P5P is covalently bonded to Lys210 at α helix four.
3. C- terminal domain- residues 260-398. This terminus also contains β sheets with α helixes either side. There is no contact between this region and P5P binding domain.

MGL has slightly differing structures between bacteria, 37 can be found on protein data bank. Although there are features which are highly conserved, such as active site residues and α helix 16, there are also residues that are varied (hypervariant).
MGL catalyses the αλ elimination of methionine, the αλ- replacement and αβ- replacement reactions for methionine among other amino acids such as cysteine and homocysteine (Mamaeva *et al*., 2005; Kudou *et al*., 2007; Raboni *et al*., 2018)

1.10.4 Beta galactosidase

Beta galactosidase is a glycoside hydrolase enzyme which has been associated with aiding salivary putrefaction in the first step of oral malodour generation by oral biofilm. This initial deglycosylation is vital in the further degradation of proteins. In a study by Sterer *et al*., 2009 the use of confocal microscopy was utilized to determine the activity of the enzyme beta galactosidase. It was found that the activity was predominantly expressed from outer layer of the biofilm consisting of gram-positive bacteria. The deeper layers of the biofilm were associated with gram negative anaerobes which are involved in further catabolism in the production of malodorous compounds. The activity of beta galactosidase also correlates positively with oral malodour scores from a periodontally healthy group.

1.11 Enzyme inhibitors

Throughout the research, there are known small molecules that have an impact on oral bacteria. These target enzymes that would normally interact with amino acids. Their mechanism of inhibition is described in the table below. This thesis will additionally investigate the inhibitory action of novel products.

Table 1.1 Table of enzyme inhibitors associated with oral bacteria

Enzyme inhibitor	**Mechanism of action**
PAG- Propargylglycine	Inhibits methionine gamma lyase by trapping Tyr residue which blocks substrate release (Sun *et al.,* 2008)
TFM- Trifluoromethionine	Fluorinated methionine derivative shows inhibitory action by increasing survival in *P.ginvivalis* infected mice (Yoshimura, Nakano and Koga, 2002)
AVG- L- Aminoethoxyvinylglycine	Alphabeta unsaturated amino acid, makes a complex with PLP to inactivate the enzyme cystalysin (Krupka *et al.,* 2000)
Trifluoroalanine	Inhibits PLP dependant beta and gamma elimination reactions from transsulfuration pathways (CBS and cystathionine gamma lyase) in bacteria (Asimakopoulou *et al.,* 2013)
AOAA- aminooxyacetic acid	General aminotransferase inhibitor such as CBS and cystalysin and cystathionine gamma lyase (Asimakopoulou *et al*., 2013)
Myrsinoic acid B	From leaves of *myrisine seguinii lev*, inhibited methioninase- MGL production of 2-oxybutyrate from *P.gingivalis, T.denticola* and *F.nucleatum* (Ito, Narise and Shimura, 2008)

1.12 Harmful effects of harsh chemicals

There is a balance between achieving a high standard of oral health and using harmful chemicals to remove bacteria. Chlorhexidine (CHX) is considered the gold standard at reducing gingival plaque index and breath odour, however its adverse effects include an altering of taste perception and some reports of staining of the tooth surface, this is therefore not an acceptable healthcare product for daily use (Zanatta, Antoniazzi and Rösing, 2010).

Chlorhexidine mouthwash (0.2%) was tested against a herbal mouthwash which did not significantly differ in their results for breath odour after use, both having similar antibacterial effects (Mishra *et al*., 2016). The use of 2% CHX in hospitals left patients with an oral lesion which disappeared when CHX use stopped, 1% CHX was also ruled out due to intolerance noted in 4 hospitals (Plantinga *et al*., 2016). In an observational study, the widespread use of chlorhexidine for the non-critically ill in hospitals may be detrimental and increase mortality rate except in cases of mechanical ventilation where no correlation with mortality was observed (Deschepper *et al*., 2018). This is however, the gold standard for oral bacteria/ plaque index reduction due to its efficacy *in vitro*.

There is doubt surrounding the use of ethanol in mouthwash. There is no direct link to causing oral cancer however, ethanol can enhance the penetration of other substances into the oral mucosa, it can also increase salivary acetaldehyde due to ethanol oxidation in the oral cavity adding to the effects of bacterial metabolism (Lachenmeier, 2008).

In a study by Müller *et al*., (2017) the composition of mouthwash was reviewed, 20% ethanol failed to supress bacterial growth and moderate cytotoxic activity. There are various gaps in the research when investigating these products and conflicting assessments of effect, this may be due to different formulations, bacteria or patient selection. If herbal/natural products can reduce bacteria load and VSC production with no adverse effects, there would be no need for harsh chemicals in mouthwash/ toothpaste formulations.

Table 1.2 Examples of natural products as inhibitors of bacterial metabolism in the oral cavity

Enzyme inhibitors	**Function**	**Extra notes**
2% zinc citrate	Exhibited a larger effect than 0.75% solution (Brading *et al.,* 2003)	Most noteably used as anti-plaque, more potent than zinc sulphate (Sheng *et al.,* 2005)
Green Tea- epigallocatechin-3- gallate Black tea contains the responsible flavins contained in green tea as well- works when the leaves are chewed (Lee *et al.,* 2004)	*In vivo* as a significant effect against methyl mercatan (Lodhia *et al.,* 2007) Supresses in vitro growth of virulence factors in oral bacteria (Okamoto *et al.,* 2004)	Yasuda and Arakawa, 1995 proposed that reduction of oral malodour was due to egcg reacting with methyl mercaptan hydroxyl groups Xu *et al*., 2010 uncovers a different method by Supression of MGL gene of *P. gingivalis* W83 which encodes METase (a key enzyme in maloour) It also acts as an antimicrobial and bacteriostatic at sub MIC levels
Methyl Gallate and Gallic acid – Galla rhois	Proposed mechanism due to results of adhesion assay is the inhibition of *in vitro* adherence of *S. mutans* (Kang *et al.,* 2008)	Gallic acid also works as an antimicrobial – (Daglia *et al*.,2008)
Magnolia bark extract – contain magnolol and honokiol	Effective against oral bacteria- especially *P. ginigivalis* (effect same as chlorexidine gluconate) (Greenberg, Urnezis and Tian, 2007)	Low toxicity

1.13 Crude products and chemical composition

1.13.1 Coffee

Coffee originates from the dried seed of the fruit produced by a coffee genus tree commonly grown in South America and Africa and ingested daily by millions across the world (Arana *et al*., 2015). This is one of the key reasons for its wide study and it's use within this thesis as to understand its potential benefit to a multitude of oral diseases.
In its raw form, coffee has not been shown to have a potent inhibitory effect, although this could be attributed to the concentration of sucrose found in this extract (10.2mg/ml in C. arabica) which promotes the growth of certain bacteria. However, the chemical composition of coffee alters once roasted. The Malliard reaction occurs between reducing sugars and aldehyde groups, this browning process leaves less components such as chlorogenic acid (90% free chlorogenic acid lost), however Malliard reaction compounds can possess antioxidant activity and therefore the degree of roasting and type of bean have the biggest impact on eventual effectiveness (Liu and Kitts, 2011).

Coffee components have been shown to have bioactive effects, these extend from effects in the inhibition of angiogenesis, which is a required pathway in the metastasis of cancerous cells (Cardenas, Quesada and Medina, 2011), as well as antioxidant and free radical scavenging activities which are seen to be effective in both green and roasted coffee beans, with the melanoidins produced during the roasting process such as methylpyridium contributing to the antioxidant potentials of coffee. (Cämmerer and Kroh, 2006). The most commonly researched active components of coffee include caffeine, chlorogenic acid, trigonelline, (then the minor attributes: diterpenes: cafestol and kahweol).

There is no solid research implicating a role for caffeine in the control of halitosis, although sometimes mentioned in a negative light alongside tobacco and alcohol for causing transient extra-oral halitosis (Campisi *et al.,* 2010).

1.13.2 Trigonelline and Nicotinic acid

Trigonelline is one of the major components in coffee, it is a hormone which aids the growth of a plant as well as protecting against oxidative stress. During the Malliard reaction in coffee, (roasting process) 60-90% of trigonelline is demethylated, creating another bioactive compound- Nicotinic acid- otherwise known as vitamin B3 (Garg, 2016). It is also found in peas, oats and fenugreek (Tice, 1997) Trigonelline has an antiadhesive effect on *Streptococcus mutans*, as does nicotinic acid and whole coffee extract in a study by Daglia *et al*., (2002). It tests the extracts on saliva coated hydroxyapatite which adsorb to the host surface therefore preventing bacterial adhesion. Trigonelline is a good inhibitor of coffee adsorption with 75% inhibitory action percentage, however post-roasting nicotinic acid has an inhibitory action percentage of 36.6% which is a high considering it was present in very small concentrations in the coffee samples (Antonio *et al*., 2010).

Trigonelline and nicotinic acid has also been found to inhibit the invasion of cancerous cells in the liver without supressing the reactive oxidative species mediated (ROS-mediated) invasion (Hirakawa *et al*., 2005). In a study of cancer cells done on mice, trigonelline exhibits protective properties inhibiting the growth of cancerous colonocytes (Yoo and Allred, 2016). However, this protective effect of trigonelline on colon cells do not have a similar inhibitory effect on oestrogen dependant breast cancers, Allred *et al*., (2009) tested this on MCF-7 cells which continued to grow and proliferate.

Trigonelline along with other bioactive components in coffee such as caffeine were tested against coffee for antimicrobial activity of the whole and split chemical compositions using a disc diffusion method and observing the diameter clearance by each product on each bacteria, the results were as follows; Coffee extract (aqueous) (*C. freundii*: 8.8mm, *E.coli*: 8.1mm, *S. enterica*: 8.1mm), caffeine (*C. fruendii*: 7mm, *E. coli*: 8mm, *S. enterica*: 8.3mm), trigonelline (*C. fruendii*:7mm*, E. coli*: 8.1mm, *S. enterica*: 8.8mm), trigonelline and caffeine have a higher antibacterial effect on S. enterica than coffee extracts in full (Almeida *et al*., 2006).

Nicotinic acid with nicotinamide form niacin which is essential for regulation of nicotinamide adenine dinucleotide phosphate (NADP) reduction and oxidation reactions. A deficiency in niacin (Vit B3) can cause pellagra characterised by dermatitis (Magill and Hunter, 2013).

1.13.3 Red wine

Red wine has been suggested to have antihypertensive properties which, in moderate amounts protects against cardiovascular diseases associated with endothelial dysfunction. This is in part, is attributed to the polyphenols and antioxidant properties of red wine. There are many pathways in the human body which respond well to these components such as the Nitric oxide pathway (Diebolt, Bucher and Andriantsitohaina, 2001), and the AMP-activated kinase signalling pathways which can protect against cell death. (Saleem and Basha, 2010)

Red wine has a plethora of benefits associated with moderate intake such as decreasing lipid peroxidation, decreasing the release of proteases, inhibiting platelet aggregation and anti-inflammatory effects through the flavonoid's resveratrol and quercetin.

Wine also has antibacterial properties which, interestingly are associated with the smaller molecules of wine and the polyphenol free fractions such as acetic acid. In a study by Daglia *et al., (*2007) it was found that it was the combination of acids in wine such as acetic acid in combination with citric acid, lactic acid, succinic acid and malic acid which contribute to the antibacterial effect on *Streptococcus mutans*. It is important to note here that the wine has been dealcoholized so that the ethanol does not interfere with the bactericidal action.

1.13.4 Garlic

Garlic has been known as an antibacterial, it has also been described as antifungal and an antiviral and has been used since ancient times to treat and manage ailments. Allicin is the main studied component of garlic and is not present in raw garlic but its production is initiated by enzyme action once the garlic is crushed (Ankri and Mirelman, 1999). The Allicin reacts with thiol groups and therefore thiol containing enzymes such as cysteine proteases, a key group of enzymes in the development of halitosis notably the gingipains from *P.gingivalis* (arg- and lys- gingipains). The garlic at 57.1 w/v was able to inhibit these enzymes as well as inhibiting the growth of *P.gingivalis* and start 'killing' the organism

immediately after contact. This gives evidence that garlic should be considered in developing therapies for halitosis/ periodontitis (Bakri and Douglas, 2005).

1.13.5 Zinc studies

Zinc has been used in toothpaste formulations as an anti-plaque agent with no clinical side effects, there is some zinc present in saliva, however at 0.004mM is too low a concentration to have inhibitory effectiveness on plaque formation. Glycolysis of a mixed culture of plaque forming bacteria (suspended) could be shut down by 0.2-0.3mM zinc chloride but was not able to penetrate a multilayer biofilm (He, Pearce and Sissons, 2002).

Using a formulation with 2% Zinc citrate and 0.3% triclosan significantly reduced plaque formation 18 hours after use compared to a slurry containing 0.3% triclosan and 2% copolymer (Adams *et al*., 2003)

There are many forms in which zinc can be chemically prepared such as zinc citrate, zinc chloride, zinc acetate, zinc gluconate etc… Each have their own stability constants which determines how much free zinc ions can be dissociated in water. A high stability constant would mean less free zinc. However, Young, Jonski and Rolla (2002) concluded that there was no correlation between stability constants and anti-VSC effect. This phenomenon was explained by ions being present in the oral cavity (such as sulphide) which have a stronger affinity for the zinc ions than the attached ligands.

Most notable zinc salt used in commercial products is zinc citrate, it was shown to inhibit catabolism of peptides which applies more to anaerobic bacteria than aerobes, it has many targets and therefore many potential effects including the inhibition of *F.nucleatum* in producing reactive oxidase species (Sheng, Nguyen and Marquis, 2005).

1.13.6 Gallic acid

Gallic acid- 3,4,5-trihydroxybenzoic acid is a phenol abundant in certain berries, green tea, walnuts, apple peels, grapes, strawberries, mastika, lemons and in red and white wine (Lu *et al*., 2015). Gallic acid has been researched as a natural product extracted from plants for its anti-fungal (Nguyen *et al*., 2013), antioxidant, anti-cancer and anti-inflammatory effects (Kumar Singh and Patra, 2018; Saosoong and Ruangviriyachai, 2014)

Its anti-cancer effects include inducing apoptosis of cancerous cells by activating caspase 8. Cancer cells often have a mutation in the p53 gene or caspase signalling response (Bhouri *et al*., 2012). The antioxidant activity of gallic acid is based on its free radical scavenging activity and had some activity towards lipid peroxidation (Bhouri *et al*., 2010).

Gallic acid has a reported effect on oral bacteria with a 1mg/ml MIC on periodontal and cariogenic bacteria with no cytotoxic effect on cells. The proposed mechanism of action is by inhibiting metabolic oral enzymes in bacteria, but this interaction hasn't been updated in research since 2008 (Kang *et al*., 2008).

A recent paper describes that gallic acid significantly reduce hyphae formation and adherence of Candida albicans to oral epithelial cells after 24h. However, in this study, the acetone fraction of *Buchenavia tomentosa* – a tropical plant (which includes gallic acid) had a lower MIC and cytotoxicity values than gallic acid alone suggesting other chemicals in the mix are contributing to a larger anti-fungal effect (Teodoro *et al*., 2018).

1.14 Aims and objectives

The aims and objectives for this thesis were to investigate the mechanisms by which oral malodour is produced and inhibited. This involved the measurements of gasses and metabolic products from planktonic bacteria and a viable oral biofilm model. And enzymatic production of malodourous gasses from looking at the purified enzyme experimentally and computationally.

Products were employed throughout the thesis to investigate inhibitory effect of foodstuffs on oral malodour and bacterial metabolism, starting with crude products and filtering down to their chemical components called the inhibitory products/panel in current analysis.

Chapter 2 Methodology

2.1 Tongue Scrapings

Tongue scrapings were obtained from 50 people over the course of the project, ethics approved with signed consent forms and the study was approved by the Faculty of Science Engineering and Computing Research Ethics Committee of Kingston University, London. Using Whatman Omniswabs (Sigma- Aldrich) the tongue surface was rubbed up and down with ridges along the end of the swab providing high surface area, and immediately placed into 25 ml preservation broth in a 50 ml bottle containing: 4% brain heart infusion broth (BHI) (Oxoid, UK), 0.4% w/v peptone (Alfa Aesar, UK), 0.002% w/v DL-Dithiothreitol (VWR, UK), 10% w/v glycerol (Alfa Aesar, UK), and 0.00012% w/v haemin (Sigma- Aldrich). All the scraper tips were pooled together and mixed using a vortex on medium speed for 5 minutes, this ensures the bacteria transfers into the broth effectively. Aliquots of 1 ml of this broth was then transferred to 5 ml cryo-vial tubes (Nunc) and frozen at -20°C for 18 hours, they were then transferred to the -80°C freezer for storage. To retrieve and grow the bacteria from the freezer, a 1 ml aliquot was taken out and re suspended 10 ml preservation media broth to use once melted or inserted into 10 ml brain heart infusion broth to grow at 37°C overnight. If a solid culture was required, the sample of oral bacteria can also be thawed, followed by dipping a sterile cotton bud into the sample and streaking onto an agar plate of brain heart infusion (BHI) agar (Oxoid UK). This was incubated for 24 hours at 37°C. The solid culture allows for the mixed culture of oral bacteria to be viewed visually, and to test the viability and growth of the sample after being frozen at -80°C.

2.2 Standardising bacteria

The tongue scraping samples were grown overnight in the microaerophilic cabinet (gas mix in cabinet- 5%- Oxygen, 10%- Carbon dioxide and 85% - Nitrogen) at 37°C in 10 ml Brain heart infusion broth (Oxoid UK). This sample was then centrifuged at 3000g for 15 minutes, the broth was poured out carefully and replaced with 5 ml Phosphate Buffer Solution (PBS) (Thermofisher) using 1 ml at a time and vortexed to reincorporate the bacteria into

suspension. This process was repeated 3 times so that all remnants of the broth were removed. The final suspension was then made to an optical density of 0.4, 0.6 and 0.8 at 620 nm by diluting each sample in PBS. Each of these samples were then subject to serial dilutions in PBS up to $10^{-8.}$ A 10 µl drop of each dilution was placed onto brain heart infusion media. This was incubated under microaerophilic conditions (gas mix in cabinet- 5%- Oxygen, 10%- Carbon dioxide and 85% - Nitrogen) at 37 °C for 48 hours before counting the colonies. The colonies forming units/ml (CFU/ml) were determined and calculated based on the dilution factor. An optical density of 0.6 au at 620nm is equal to a CFU/ml of 1.0 X 10^8.

2.3 Crude product preparation

Black tea (PG tips- original black tea bag- 3 g each) and Green tea (Twinings pure green tea 100% green tea- 3 g each). Tea bags were placed in 100 ml boiling water and left to brew for 10 minutes. The solution was filter sterilized through a Millipore filter (0.45 nm) into a sterile falcon tube (SLS) ready to use and was made fresh per experiment.

Coffee- 1 g of instant Nescafe coffee was mixed with 100 ml of distilled water providing a 1% solution. This was mixed on a hotplate until all the coffee granules had dissolved (approx. 50 °C). This solution was filter sterilized into a sterile falcon tube (as described above).

Red wine (with and without alcohol)- Red wine (Shiraz 2014) was used in its pure form as a crude product inhibitor, however to de-alcoholise the wine, 100 ml was put into a beaker on a stirring hotplate (with a magnetic flea). The alcohol was boiled off at 100°C until the volume in the beaker reached half the original (50 ml), this boiling step will also affect the composition of chemicals within the wine.

Odourless garlic (Wilko Wellbeing)- The odourless garlic was bought in the form of 2 mg capsules. To extract this, the syringe was simply inserted into the capsule and the specified amount 0.5 ml taken out to be put straight into the headspace vial as a crude inhibitor.

Garlic- (softneck garlic from Waitrose) 70 g of garlic was blended into 35 ml of distilled water and left to stand for 10 minutes, this was then centrifuged at 3000 g for 10 minutes in an Amicon Ultra centrifuge tube (Sigma Aldrich) containing a 10 kDa membrane as a cut off. The supernatant was then extracted from the bottom of the tube and filter sterilized in 0.45nm millipore filter. The method taken from Bakri and Douglas (2005) who report a garlic extract of 57.1% (w/v).

2.3.1 Natural extracts and zinc products

Natural extracts and zinc compounds listed below are from Sigma Aldrich in powder form, these were made up to a concentration of 1% (w/v) in distilled water. The solutions were then filter sterilised through a Millipore filter into a sterile 50 ml falcon tube. These solutions are ready for use and were prepared fresh on the day of use.

Table 2.1 Purchased products (Sigma- Aldrich)

Product	**Assay purity and (molecular weight)**
Zinc citrate	97% (610.40)
Zinc acetate	98% (219.51)
Zinc chloride	97% (136.30)
Caffeine	Ph Eur testing spec. / anhydrous (194.19)
Nicotinic acid	99.5% (123.11)
Trigonelline	98.5% (173.60)
Gallic acid	98% (170.12)

2.4 Headspace model

The headspace model was used to determine gases that arose from bacteria catalysis of amino acids known to be broken down into volatile sulphur compounds (VSC's) notably hydrogen sulphide (H_2S), methyl mercaptan (MM) and dimethyl sulphide (DMS). The tongue scrapings in this method were placed into broth and grown overnight at 37°C and standardised to an absorbance of 0.6 at 620 nm according to above standardisation methodology (section 2.2).

The bacterial sample was kept on ice during the experimental procedure so that the viability of bacteria did not reduce whilst in the PBS. An aliquot of 0.5 ml of the bacterial preparation was added to each 10 ml screw top headspace vial (Sigma- Aldrich), added to this was 0.5 ml of the amino acid (L-cysteine/L-methionine) (Sigma- Aldrich) made with distilled water and filter sterilised through a Millipore filter. The concentration of amino acid is reconsidered in early experiments and tested along a spectrum of concentrations through the thesis (between 0.05% and 2%). The concentration used is specified along each experiment/ graph in the results. Lastly 0.5 ml of crude product (prepared according to method 2.3- crude product preparation) was inserted to the vial which is then immediately sealed (with screw cap) and incubated at 37°C. Separate vials with the same solutions were incubated for 0, 30, 60 and 120 minutes, following incubation, 1 ml of gas headspace was taken with 2.5 ml gas tight syringe (VWR) and mixed with 1 ml of lab air, this was inserted straight into the OralChroma using an SGE needle lock syringe (Sigma-Aldrich). The OralChroma measures the hydrogen sulphide, methyl mercaptan and dimethyl sulphide concentration for each vial, this is then plotted onto graphs (Chapter 4,5 and 6).

Controls: positive control vials (to measure the concentration of VSCs in the absence of crude products) consisted of 0.5 ml of amino acid 1-2% and 0.5 ml of the bacterial solution (0.6 a.u at 620nm) and 0.5 ml of PBS to bring the volume up to the same as vials containing crude product. Amino acid at 0.5 ml was incubated with 0.5 ml of crude product to check for interaction prior to the addition of bacteria into the sample as a negative control (not included in results).

2.5 Optimising cysteine as a substrate

Cysteine was used in the first few experiments, optimisation using a range of steps were tried using this amino acid due to the instability of results (see chapter 3). First a method to de-gas the water used to make the cysteine solution was attempted. A nitrogen supply tube () was inserted into the sterile water in an airtight cabinet, the cysteine powder was added 1% (w/v) (66mM), mixed and dissolved, the gasses were detected/measured on the oralchroma. This did not yield stable results; therefore, a second method was tried- the cysteine solution was made first and then the degassing took place using a nitrogen supply tube after the solution had been made. A third method was attempted using a sonicator, a beaker containing 1% (w/v) cysteine solution was placed in an ultrasonic bath for 30 minutes, this solution was then degassed using a helium supply tube (65 psi) to bubble through. When these steps did not provide consistent results on the oralchroma for use, methionine was taken forward due to its stability and lack of 'background noise' unlike those found with cysteine (See chapter 3 results).

2.6 Cell lysis

Several different cell lysis methods were used to determine the most effective lysis method on tongue scrapings (Method 2.2) to extract and expose enzymes- (namely methionine gamma lyase and L-cysteine desulphydrase).

Method 1: A lysosome solution from chicken egg white (10 mg/ml)- pre-made containing 25 mM sodium acetate and 50% glycerol (Sigma-Aldrich) was used. This aliquot (1 ml) was added to 9 ml of oral bacteria at 0.6 au at 620nm prepared from method 2.2. This was put in the shaking incubator at 100rpm at 37°C, for 10, 20, 30, 40, 50 minutes and 1 hour and then centrifuged (3000g for 10 mins at room temperature (20°C)) to remove the debris of the cell wall. This sample was swabbed onto nutrient agar in the incubator overnight at 37°C and to determine if viable cells were able to still grow. Any resulting colonies were gram stained (see method 2.6.1) which revealed that there were only gram-positive cells

left to lyse. Lysostaphin (2 mg/ml) (Sigma-Aldrich) was made to manufacturer's instructions and added to the solution of bacterial cells with lysosome. This resulted in the survival of gram positive bacterial cells.

Method 2- The 5 ml bacterial solution was sonicated for 10 minutes -which still produced growth when incubated for 24 hours at 37°C on nutrient agar.

Method 3 - CelLytic™ B kit (Sigma-Aldrich) was purchased which contains a cocktail of ingredients including protease inhibitor cocktail in DMSO solution, lysosome, 40 mM Trizma® -HCL (pH8) and Benzonase® Nuclease. 1ml of the cellytic B reagent was added to a pellet of prewashed bacteria (see bacteria standardisation 2.2) and 1 g of wet cell paste using 10 ml Cellytic reagent, 0.2 ml lysosome and 0.1 ml protease inhibitors. This was vortexed and gently shaken for 20 mins. The sample was then centrifuged (3000g for 10 minutes) to extract the supernatant, the supernatant showed no cell growth after incubation overnight on nutrient agar.

To test whether the enzymes were extracted, the headspace model was tested using whole bacteria, then using lysed bacteria which showed a much higher reaction rate from the conversion of substrate (methionine) into the products (hydrogen sulphide, methyl mercaptan and dimethyl sulphide).

2.6.1 Gram staining technique

A drop of water was first added onto a clear glass slide using an inoculation loop, then a small amount of the overnight culture was added to the water, before being allowed to air dry. This slide is then passed over a flame to fix the bacteria, the staining procedure starts with a flooding with crystal violet for 1 minute before washing off with distilled water. The slide was then flooded with grams iodine and left for 1 minute before washing off with distilled water. Decolouration step was achieved using acetone/alcohol (20:80) for 30 seconds and washing with distilled water. Finally, the slides were counterstained with carbol fuschin for 1 minute before washing with distilled water to finish the staining process. The slide can be viewed under a microscope (x100 oil immersion lens).

2.7 Follow up headspace model

This introduces a modified headspace model, introducing lysed bacteria to concentrations of methionine and natural products. Methionine was prepared to concentrations of 0.05, 0.1, 0.5, 1 and 2% in PBS/sterile distilled water. An aliquot of 0.5 ml of each of these concentrations were added to separate 10 ml headspace vials, 0.5ml of lysed bacteria (see method 2.2, and 2.6- method 3) added to each vial. An aliquot of 0.5ml of natural extracts (method 2.3.1) also made to a variety of concentrations (0.1,0.5, 1 and 5%) were added to the headspace vial (replaced by 0.5 ml PBS in the control samples). All samples were incubated for 10 minutes at 37°C before the gas is extracted (1 ml) with a syringe from the airtight system, mixed with 1 ml lab air and analysed on the oralchroma.

Table 2.2 *Combinations of methionine and product concentrations incubated with 0.5 ml of lysed bacterial solution*

Methionine concentration in vial (0.5ml)	**Natural product concentration in vial (0.5ml)**	**Methionine concentration in vial (0.5ml)**	**Natural product concentration in vial (0.5ml)**
0.05%	0% (control)	1%	0%
	0.1%		0.1%
	0.5%		0.5%
	1%		1%
	5%		5%
0.1%	0%	2%	0%
	0.1%		0.1%
	0.5%		0.5%
	1%		1%
	5%		5%
0.5%	0%		
	0.1%		
	0.5%		
	1%		
	5%		

2.7.1 The Oralchroma

The oralchroma is a Japanese made portable device for the measurements of VSC's, measuring 3 separate gasses- Hydrogen sulphide, Methyl mercaptan and Dimethyl sulphide using ambient air as a carrier gas. It is a sensitive apparatus which can differentiate gasses to allows the analysis of the nature of the halitosis e.g. extra/ intra oral (Tangerman and Winkel, 2008). The portable Gas chromatograph includes an injection port, which accepts 2ml of gas in a needle and syringe. 1ml of this gas should be lab air to dilute the sample, in some cases this provides the reader with measurable gas concentrations below the threshold limit, this is kept consistent throughout the thesis. The analysis of each sample takes 10 minutes, with a reset period.

2.8 Enzyme solution

The enzyme of choice to analyse the effect of an inhibitory panel on producers of oral malodour, was methionine gamma lyase. This enzyme was purchased and made for storage described below.

2.8.1 Preparing the enzyme solution

Methionine gamma lyase- the enzyme aiding catalysis of methionine in bacteria (see chapter 1.5) was bought from Sigma-Aldrich (EC 4.4.1.11) 1.45 mg lyophilised powder of was added to 1ml buffer (950 µL Tris-HCl 1M and 50 µL Glycerol). This was split into 25 µL aliquots into sterile Eppendorf tubes, this equated to 0.08 Units of enzyme present in each aliquot, these were then put into liquid nitrogen for a few seconds to flash freeze and stored at -80˚C.

2.8.2 Differential scanning fluorimetry on quantitative polymerase chain reaction

Differential scanning fluorimetry (DSF) essentially measures the fluorescence as a marker for the unfolding of a protein by adopting a dye which has an affinity for the hydrophobic

regions of the protein using quantitative polymerase chain reaction (QPCR) machine (Agilent technologies)

The protocol from nature (Niesen, Berglund and Vedadi, 2007) states an excitation wavelength of 492 nm and emission of 610 nm is required for Sypro orange dye ('Fluorescence gain upon the denaturing of lysosome'). The protocol is set up for RT-PCR scanning for approximately 1 hour at a temperature range of 25-95 ˚C to determine the temperature of protein unfolding.

A single aliquot of methionine gamma lyase was diluted through the experiment (1 µl:225 µl) by the addition of buffer and dye. Enzyme (3 µl) was added to 675 µl Tris buffer (1M) and 1µl SYPRO orange (Sigma- Aldrich) then mixed. This solution (19 µl) was pipetted into each well of a 96-well plate (ThermoFisher) to test the unfolding of that enzyme through QPCR temperature cycles. The plate was covered in an optical adhesive film for scanning under the QPCR fluorescence MX pro software.

2.8.3 SDS page- Gel electrophoresis

An aliquot of 0.08 units of Methionine gamma lyase (See method 2.8.1) was fully defrosted. A loading dye (Sucrose 40% w/v, Bromophenol blue 0.25% w/v and Dithiothreitol (DTT) 5 mg/mL) was added in the ratio 1:3 with the methionine gamma lyase sample and this was inserted into a heat block and denatured for 5 minutes at 95˚C. A gel was made using acrylamide:bis acrylamide (29:1) 12% v/v, SDS 0.125% w/v, ammonium persulphate 0.05% w/v, tetramethylethylenediamine (TEMED) 0.002% v/v, Tris HCl 390 mM) and a 6% w/v acrylamide stacking gel (acrylamide:bis acrylamide (29:1) 6% v/v, SDS 0.125% w/v, ammonium persulphate 0.05% w/v, TEMED 0.002% v/v and tris HCl 116.6mM) . A 1mm thick comb was used to make the wells for the protein sample. 10 µL of the sample was loaded into the wells alongside a ladder (EZ- RUN pre-stained protein marker (Fisher Scientific)). The gels were run in a MiniProtean Tetra system (BIO-RAD) with an SDS running buffer (Tris 0.25 M, Glycine 1.95 M and SDS 1% w/v) (National Diagnostics). The parameters for electrophoresis were set at 180V and run for 60 minutes.

Once the protein had run to the bottom of the gel after the hour, the gels were extracted and put in a stain of coomassie blue (0.0024% w/v), ethanol (50% v/v), acetic acid (10% v/v)

and water (40% v/v), this was stained in the shaking incubator (90rpm at room temperature) for 30 mins. Immediately after this step, the staining tin was washed out with water and a de-staining solution was added to the gel sheet (10% v/v ethanol, 10% v/v acetic acid and 80% v/v water). This was put back into the shaking incubator at 90rpm for 12 hours. The gels were viewed and captured using Molecular Imager GelDocTM XR+ (BIO-RAD).

2.9 High performance liquid chromatography (HPLC) analysis

Method by Sun and colleagues, (2005) was followed to for methionine quantification of the HPLC.

Initially a methionine calibration curve was constructed. Methionine concentrations of 5, 10, 25, 50 and 100 pmol/µl were measured and plotted to make this curve Figure 6.8. Methionine (10 ml) at each concentration was mixed with 30 µl acetonitrile. The vial for HPLC analysis contained 1 ml Sodium acetate (0.1M), 30 µl O-Phthalaldehyde (OPA) plus 70 µl of the methionine/ acetonitrile mix. Concentrations of methionine expressed in Area under the curve (mAU*S).

The methionine concentration for testing was 100 pmol/µl (10 ml/ with 30 µl acetonitrile), this was tested against the 25 µl of methionine gamma lyase (0.08 units) in a vial containing 1ml Sodium acetate (0.1M), 30 µl O-Phthalaldehyde (OPA) and 70µl of the methionine/ acetonitrile mix. This was followed by further adding 25 µl of 10 mM of Natural product to the mixture as above, including enzyme. These vials were put through the HPLC columns (sigma 58355-U and 59555) to define the enzyme binding capacity by methionine concentration measured through the column over 20 minutes.

Parameters of HPLC analysis

- Excitation: 350 nm, Emission: 450 nm
- The HPLC column in this method runs at a gradient of solution A and B over time:
  - Solution A- Tetrahydrofuran/ methanol/0.1M Sodium Acetate (5/95/900)
  - Solution B- Methanol.

- 0-5 min: 46% solution B, flow rate 1ml/min
- 5.1-10 min: 46-48% solution B, Flow rate 1ml/min
- 10.1-15 mins: 100% solution B, flow rate 2ml/min
- 15.1-20 min: 46% solution B, flow rate 2ml/min

- Sample loading volume 10 µl.

2.10 Bioinformatics

Protein docking for molecular analysis was undertaken using autodock 4 software. Each protein and ligand (inhibitory product) structures are acquired as files through protein data bank (PDB). The receptor of interest was methionine gamma lyase. There are many variations of this bacterial enzyme, for this thesis the 5X2V from *Pseudomonas putida* was chosen. This shows the crystal structure of wild type strain of methionine gamma lyase from a *Pseudomonas sp*. The file was open in notepad and water molecules removed (H_2O), the chains were also split by selecting the individual chains and saved as different files to leave one active site in each file. Files were then opened in autodock to edit.

Autodock options: (receptor preparation) Firstly, files required the addition of polar hydrogen bonds, then charges (which is completed by adding kollman charges). There is then the option to merge non-polar hydrogen which was selected. Secondly an 'autodock element' was added to atoms by editing individual atoms and assigning them an AD4 type. This edited PDB file should now be saved as a PDBQT file. These initial steps are options on the software to complete in order to commence with further analysis.

Search space preparation: This step is to set up the final interaction space. Once the receptor is saved as a PDBQT file, open a gridbox. Centre the gridbox on the atom most likely to interact with the Ligand e.g. LLP (active site co-factor in methionine gamma lyase). Set the spacing to 1 angstrom and formulate a gridbox around the area of study (active site).

Ligand preparation- Open the ligand PDB file (Gallic acid/ Trigonelline), select torsion tree and choose torsions (setting rotatable and non-rotatable bonds) as per their chemical composition, this can then be saved as a PDBQT file.

Two other files must be created (in notebook- Windows) for the docking calculations to take place:

1. Creating a configuration file including receptor and ligand file names and the gridbox set parameters
2. Create a docking.bat file, which should include all the autodock file name saved on the computer with '– configuration.txt', at the end followed by 'pause'.

All the files created should be put into a new folder together. Double clicking docking.bat should calculate binding affinities which will start as a pop up on the computer screen and save to the same file. This data can be visualised and analysed in autodock or Pymol by opening ligand-out.pdbqt file and the receptor pdbqt file.

Analysis on the 'Bioedit' software was conducted to consider alignment and conservation between sequences of methionine gamma lyase of other bacterial species. The FASTA (free online software) amino acid sequence from each bacterial species chosen was aligned to 5x2v (MGL of *P. putida*). The image created shows conservation areas between the bacterial species as dots (Fig. 6.19)

This sequence (algorithm) was loaded into a software called Chimera which loads the enzyme (MGL) including amino acid similarities created in bioedit, and colours the areas of conservation: maroon, low conservation: cyan, and mixed concentration: white (Fig 6.20).

2.11 Oral biofilms

2.11.1 Chamber slides- Biofilm growth

The oral bacteria described in section 2.2 was thawed and incubated in BHI broth (supplemented with 2% glucose) and prepared (see method 2.2) to achieve 10^8 CFU/ml, 500 µl of this was added to chambers (8 chamber slides in total). This is incubated at 37 °C for 24 hours (day 1) in a microaerophilic cabinet (gas mix in cabinet- 5%- Oxygen, 10%- Carbon dioxide and 85% - Nitrogen). The broth was removed with a pipette being careful not to dislodge the bacteria forming a biofilm, each chamber's broth was replaced with 500µl of fresh brain heart infusion broth with 2% glucose and immediately returned to 37 °C incubation. This change of fresh media step was repeated for day 2, 3 and 4. On the 5th day the broth was removed and replaced with 500 µl sterile water for a wash step and removing the debris. This process was repeated three times to remove any planktonic cells, leaving only the biofilm. Aliquot of 100µl of each product in the inhibitory panel (1%- caffeine, nicotinic acid, gallic acid, trigonelline, zinc chloride, zinc acetate and zinc citrate) were transferred to individual chambers and incubated at 37 °C for 10 minutes. The chambers were then washed out again with sterile water and stained with LIVE/DEAD stain (baclight- made to manufacturer's instructions). 100 µl of each dye was added to each chamber (3 µl of stock dye- Propidium iodide / SYTO 9 dye into 1ml sterile water) this was incubated for 20 minutes in a dark place at room temperature. The dyes were subsequently washed off with sterile water before using a confocal laser scanning microscopy (CLSM – Leica TCS SP2) using laser wavelengths between 450 nm and 650nm (adjusted per sample).

2.11.2 Analysing CFU/ml from biofilm growth

Another chamber slide treated in the same way as 2.11.1 until after the wash step with sterile water to remove debris and planktonic cells. At this stage, the biofilm was scraped of the bottom of the chamber slide into suspension (500µl sterile water) which was followed by a serial dilution step of 20 µl into 180µl in a 96 well plate up to 10^{-8}. These dilutions were plated (10 µl) onto brain heart infusion agar and grown for 24 and 48 hours at 37 °C in a microaerophilic cabinet before counting colonies to obtain a viable count (CFU/ml- colony forming units/ ml).

2.11.3 Analysing headspace gasses released from biofilms

Biofilms were grown in accordance to method 2.22.1, but in 10 ml headspace vials instead of the chamber slides. All steps were replicated, including all steps re-incubating the samples with broth and glucose and washing with sterile water. They are incubated with natural product in the same way but after 10 minutes of incubation, the sample headspace is injected out and inserted directly into the oralchroma, measuring the gasses (and gas inhibition) from a biofilm and the difference natural products makes to the gas produced from the biofilm.

To test the viability of growing the biofilm in the headspace bottle alongside the chamber slides, a crystal violet method was used to assess the bacteria adherence.

2.11.4 Crystal violet method for adherence

The oral bacteria grown from the tongue scrapings were prepared (see method 2.2). An aliquot of 0.5 ml of this suspension was inserted into a headspace vials, along with 1ml of brain heart infusion broth. The blank consisted of just the broth. These were incubated aerobically at 37 °C for 24, 48 and 72 hours, after incubation the broth was gently poured off the sample. Adhered cells were stained by addition of 220 µl of crystal violet (0.1%) for one minute then removed and exhaustively washed with distilled water. Bottles were then allowed to dry and 220 µl of decolouring solution (ethanol: acetone, 80:20%v/v) was added to each headspace vial for 15 minutes. The absorption of the eluted stain was then measured at 620nm on the spectrophotometer (Genevaux, 1996).

2.12 IC50 determination (Inhibitory concentration at 50%)

For the determination of IC_{50} the concentrations were decreased in keeping with enzyme activity assays (max 100µM). 10-100 µM of Methionine was prepared with sterile water, equal volumes (0.5ml) of Methionine was incubated with lysed bacteria (prepared as seen in methods 2.2 and 2.6- method 3) for 10 minutes in a headspace bottle with a silicon cap. The samples were then injected into the oralchroma and the gasses were measured at each concentration for preparation of a calibration curve as a Michaelis-Menten plot.

For the experiments containing natural products, 0.5ml of 100 µM of methionine was incubated with 0.5ml lysed bacteria (which includes the enzyme). This was tested with 0.5ml of 10-100 µM Natural products. The % activity was worked out from the control at 100 µM compared to the inhibitory effect increasing concentrations of natural products had on the original concentration and put into graph form (using graphpad) to extract IC50 values.

2.13 Sorbarod model

Sorbarod/ perfusion biofilm model is discussed in chapter 7 in detail. This apparatus was attempted multiple times during the course of this PhD and therefore, a brief methodology is stated here:

The Sorbarod apparatus includes marprene and silicon tubing which is initially set up to include the Sorbarod filter tip within and secured tightly with jubilee clips is autoclaved at 121°C for 15 minutes.

This is then inserted into the isothermic cabinet which is set at 37°C where it is left for 30 minutes, this allows for the temperature to equilibrate. Once this has occurred the tongue scrapings were thawed from the -80°C freezer, are re-suspended in 10ml of sterile inoculum media (4.1% w/v BHI, 0.05% w/v peptone, 0.000005% w/v haemin, 0.00083% w/v DTT in deionised water).

1 ml of above solution (re-suspended tongue scrapings) is taken up by a syringe and placed onto the filter (total of five). The inoculated filter is left with the cabinet sealed for two days to establish a biofilm. After the two days of inoculation, the media (4.1% w/v BHI, 0.05% w/v peptone, 0.000005% w/v haemin, 0.00083% w/v DTT in deionised water) and sterile air (lab air passed through a filter) are fed via peristaltic pumps through the Sorbarod and into waste effulent containers. The flow rate of the air was set to 36 rpm and media rate at 5.9 rpm. This runs for 18 hours before analysis.

2.13.1 Analytical methodology

The gas is extracted from a valve in the tubing underneath the sorbarod filter, mixed with 1ml of laboratory air and analysed in the oralchroma.

A sample of the effluent (100 µL) is taken and placed in 900 µL neutraliser (4% Tween 20 and 0.5% lecithin in Tryptone soya broth) (Oxoid, UK), for 10 minutes. Serial dilutions were carried out in Brain Heart infusion broth and 10 µL aliquots of up to 10^{-7} were plated onto

Colombia blood agar base (Oxoid, UK) supplemented with 5% v/v defibrinated horse blood. This is anaerobically incubated for 72 hours before being counted as colonies to attain CFU/ml. The filters are dissected into outer, middle and inner sections, these are prepared for confocal microscopy by placing the sections into 100 µL LIVE/DEAD BacLightTM stain which will be prepared according to the instructions given by the manufacturer. This will be ready to view under the confocal microscope (CSLM).

The Sorbarod method has been used and approved by GSK as a viable model in a paper by Burnett *et al*., (2011) and characterised within M.Res of Maria Antonella Sole from Kingston University (2015).

2.14 Enzyme assay (Methionine gamma lyase production of alpha keto butyrate)

This assay was taken from a method proposed by Foo, Terentis and Venkatachalam, (2016). Methionine was prepared at increasing concentrations in phosphate buffer saline (0.5mM, 1mM, 5mM, 10mM, 15mM, 20mM, 25mM, 30mM, 35mM, 40mM). 165µl of methionine at each concentration was added separately to a 96-well plate (Thermo Scientific™ 96-Well UV Microplate). 1.6µl from 15mM of natural products (zinc citrate, zinc chloride, trigonelline and gallic acid) was added pre-treating the wells/methionine with natural product. Aliquots of 1.6 µl Methionine gamma lyase solutions (preparation as in method 2.10) was added to each of these wells, plate were then placed in the spectrophotometer heated to 37°C, and the alpha-keto butyrate production was measured at 315nm at ten minutes (figure 6.22) and an alpha- keto butyrate control is produced at varying methionine concentrations over ten minutes, read at minute intervals (figure 6.21).

Chapter 3 The effect of cysteine on gas production by oral bacteria

3.1 Introduction

Halitosis is caused by the volatile sulphur compounds released from bacterial/enzymatic activity. The gasses released not only cause the halitosis but can be toxic to surrounding tissues, causing apoptosis in gingival epithelial cells and fibroblasts, this mechanism can progress the onset of periodontitis, presenting a detrimental circle of halitosis causing periodontitis and the periodontitis will, in turn, cause more halitosis. (Murata *et al*., 2008; Amou *et al*., 2013)

Cysteine is a naturally occurring amino acid in the oral cavity, it can be synthesised from methionine, therefore a non-essential amino acid in the diet (Ciborowski and Silberring, 2016). Enzymes contained in oral bacteria such as L-cysteine desulphydrase can catalyse the breakdown of cysteine releasing hydrogen sulphide, ammonia and pyruvate. In a study by Yoshida and colleagues, (2010) it was found that *Fusobacteria nucleatum*, (a main contributor to oral malodour residing on the tongue dorsum and gingival crevice) was able to produce hydrogen sulphide using two enzymes in two distinct ways. The first being beta elimination producing hydrogen sulphide alongside pyruvate and ammonia. The second is a beta-replacement mechanism producing hydrogen sulphide and lanthionine from cysteine.

The same bacteria are able to catalyse both cysteine and methionine into corresponding VSCs due to the presence of more than enzyme (Stephen *et al*., 2016). VSC's produced from the oral cavity are also theoretically able to react with each other. Dimethyl sulphide and hydrogen sulphide could react yielding methyl mercaptan:

$(CH_3)_2S + H_2S = 2\ CH_3SH$ (Alternative routes to methyl mercaptan from C1-compounds Christoph Rudolf Erwin Kaufmann). During this thesis, the oralchroma machine is used to measure VSCs, the threshold values to signify halitosis are mentioned below.

*Significance values in terms of halitosis:

- Hydrogen sulphide – 112 ppb
- Methyl mercaptan- 26 ppb
- Dimethyl sulphide- 18 ppb

3.1.1 Aims

The aims of this chapter are to assess the production of VSCs -hydrogen sulphide (H_2S), methyl mercaptan- (MM) and dimethyl sulphide (DMS) from the breakdown of cysteine by a mixed culture of pooled bacteria (method 2.1). The viability of using cysteine as a substrate will also be investigated.

3.2 Methods

Bacterial culture preparation from frozen (see method 2.2- standardising bacteria).

The Headspace model was employed by using a headspace vial (Sigma) which is sealed for contaminant free incubation and has a silicon cap in the top to extract gasses without introducing laboratory air or contaminants- See method 2.4.

In this chapter, it was attempted to optimise the use of cysteine as a substrate by degassing methods- See method section 2.5 and results in chapter 3 (and appendix 1).

3.3 Results

3.3.1 Preparing oral bacteria

Table 1 demonstrates the standardisation of bacterial concentrations used in reactions, based on colony forming units from specific optical densities. The bacterial optical density of 0.6 at 620 nm was needed to obtain 10^8 CFU/ml bacteria. This concentration was used for subsequent experiments, where the gas was measured with the addition of substrates.

Table 3.1. Represents the colony counts from serial dilutions performed onto nutrient agar plates from the corresponding bacterial optical density.

BACTERIAL OPTICAL DENSITY AT 620NM	**AVERAGE BACTERIAL COLONIES (CFU/ML)**
0.6	$4.35x10^8 \pm 3.12x10^8$
0.4	$3.85x10^7 \pm 5.36x10^7$
0.2	$4.26x10^6 \pm 2.21x10^7$

3.3.2 Cysteine with oral bacteria

Figure 3.1 shows the gas production level, when the oral bacteria were incubated with a 2% cysteine solution over 120 minutes. Demonstrating metabolic action producing gasses over time.

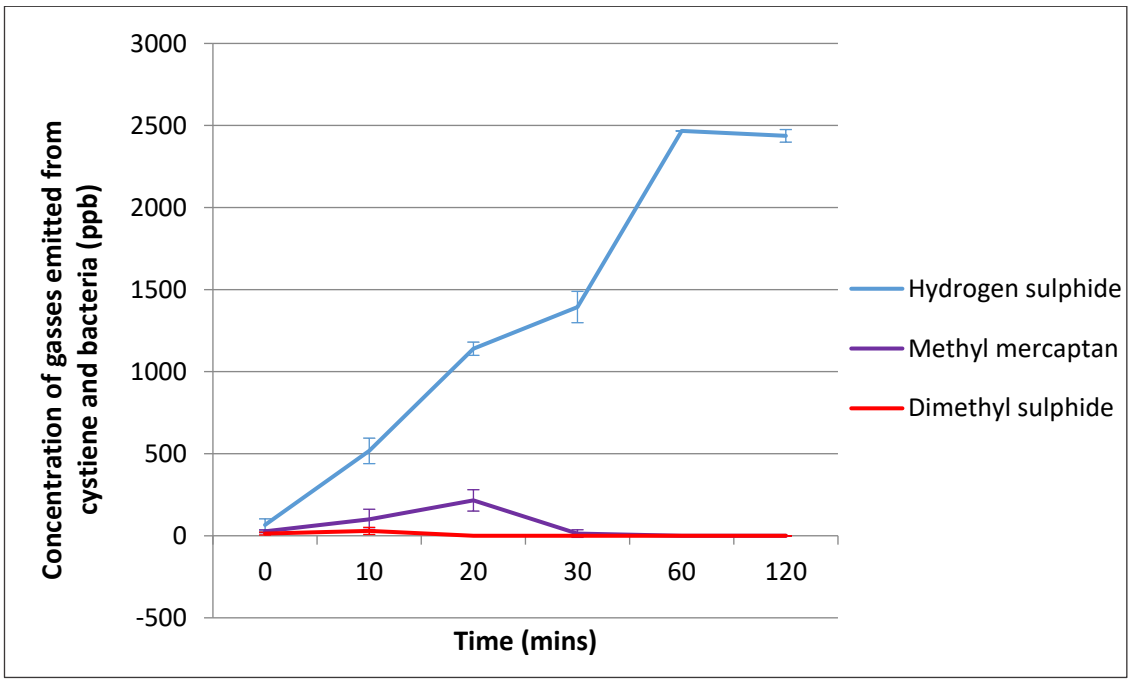

Figure 3.1. VSC production measured on the oralchroma from 2% Cysteine solution incubated with oral bacteria at 0.6 OD over time points (x axis), each data point is repeated in triplicate.

In Figure 3.1, there was a gradual increase in the concentration of hydrogen sulphide over time, to a max detection limit by 60 minutes. Methyl mercaptan concentrations initially rose to circa 215.6 ppb by 20 minutes, this then decreased to a non-detectable level by 30 minutes. Finally, dimethyl sulphide showed a slight rise by 10 mins and then to non-detectable levels by 20 mins.

These gasses were then tested with the addition of 2% zinc citrate (fig 3.2 a, b and c) to observe the effect of zinc citrate on cysteine and oral bacteria.

.

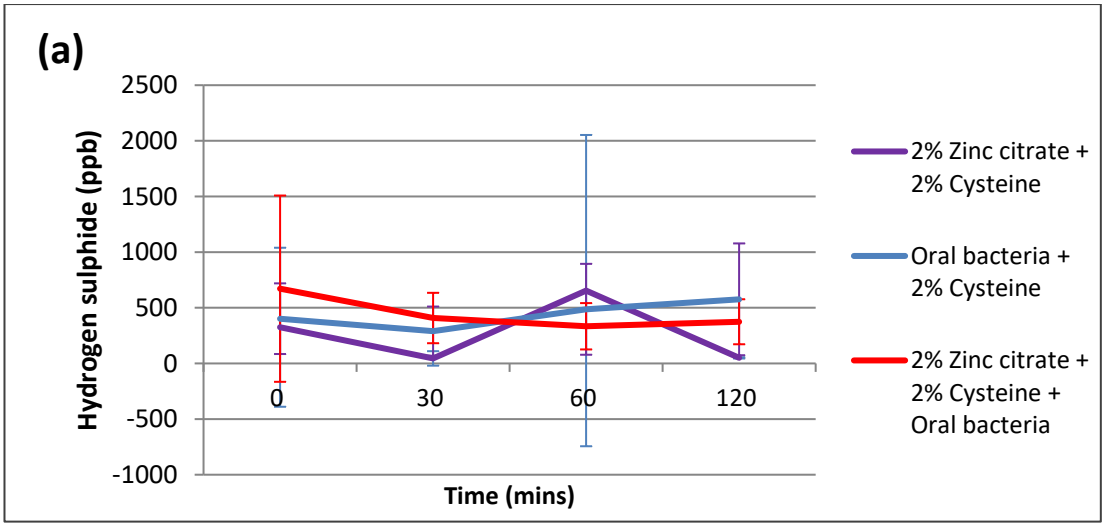

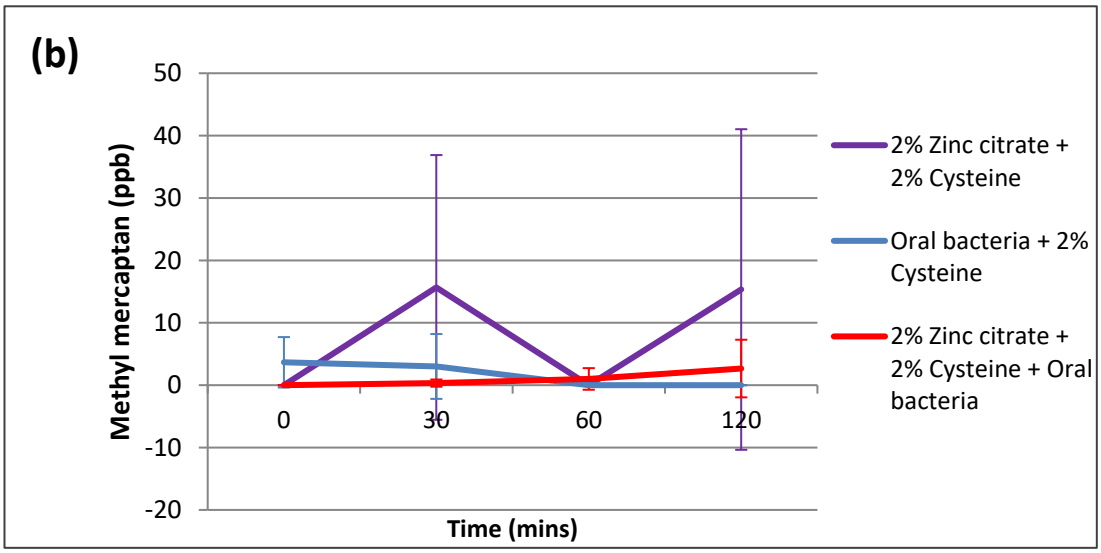

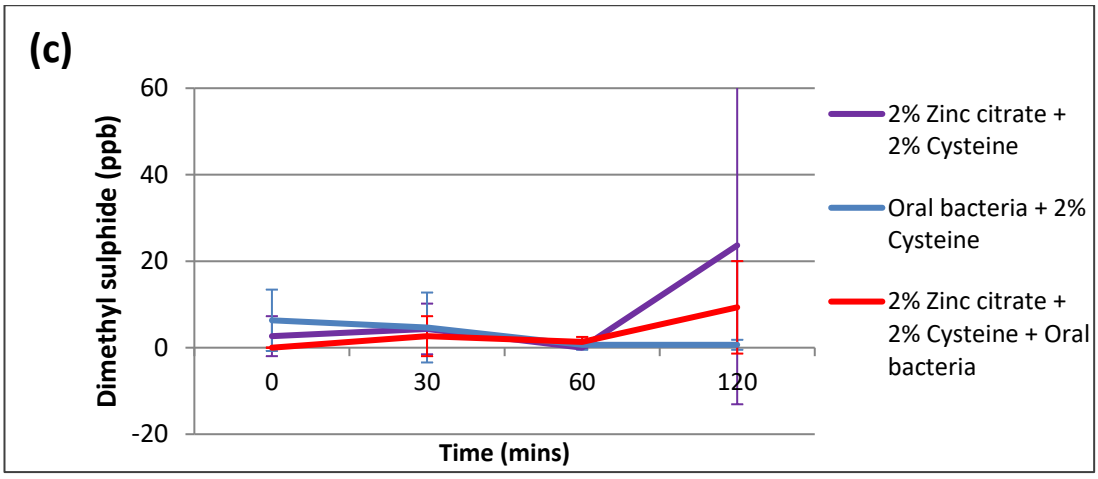

Figure 3.2. Graphs showing VSC production from (a) 2% zinc citrate + 2% cysteine as a negative control, (b) Oral bacteria at 0.6 OD + 2% cysteine used as a positive control and (c) 2% zinc citrate+ 2% cysteine + Oral bacteria as the test run.

In Figure 3.2, the error bars are highly variable especially the cysteine + oral bacteria positive control and the zinc + cysteine negative control (at 60 and 120 minutes- Fig 3.2a, 30 and 120 mins- Fig 3.2b and 120 mins- Fig 3.2c) indicating inconsistencies in the chemical reagents or the experimental procedure.

The control consisting of zinc citrate with cysteine released higher concentrations of all gasses (hydrogen sulphide at 30 minutes, methyl mercaptan at 30 and 120 minutes, dimethyl sulphide at 120 minutes) than the positive control.

The positive control reaches a maximum value of 576 ppb hydrogen sulphide concentration after 120 minutes of incubation, although this value is slightly higher than the output from the test sample of zinc, cysteine and oral bacteria (374 ppb), it is dramatically lower than 2437 ppb seen in Figure 3.1 after 120 minutes.

The controls were not behaving as expected, before testing each step in the experimental procedure for error, a different type of zinc (zinc chloride) was tested with cysteine and oral bacteria fig 3.3.

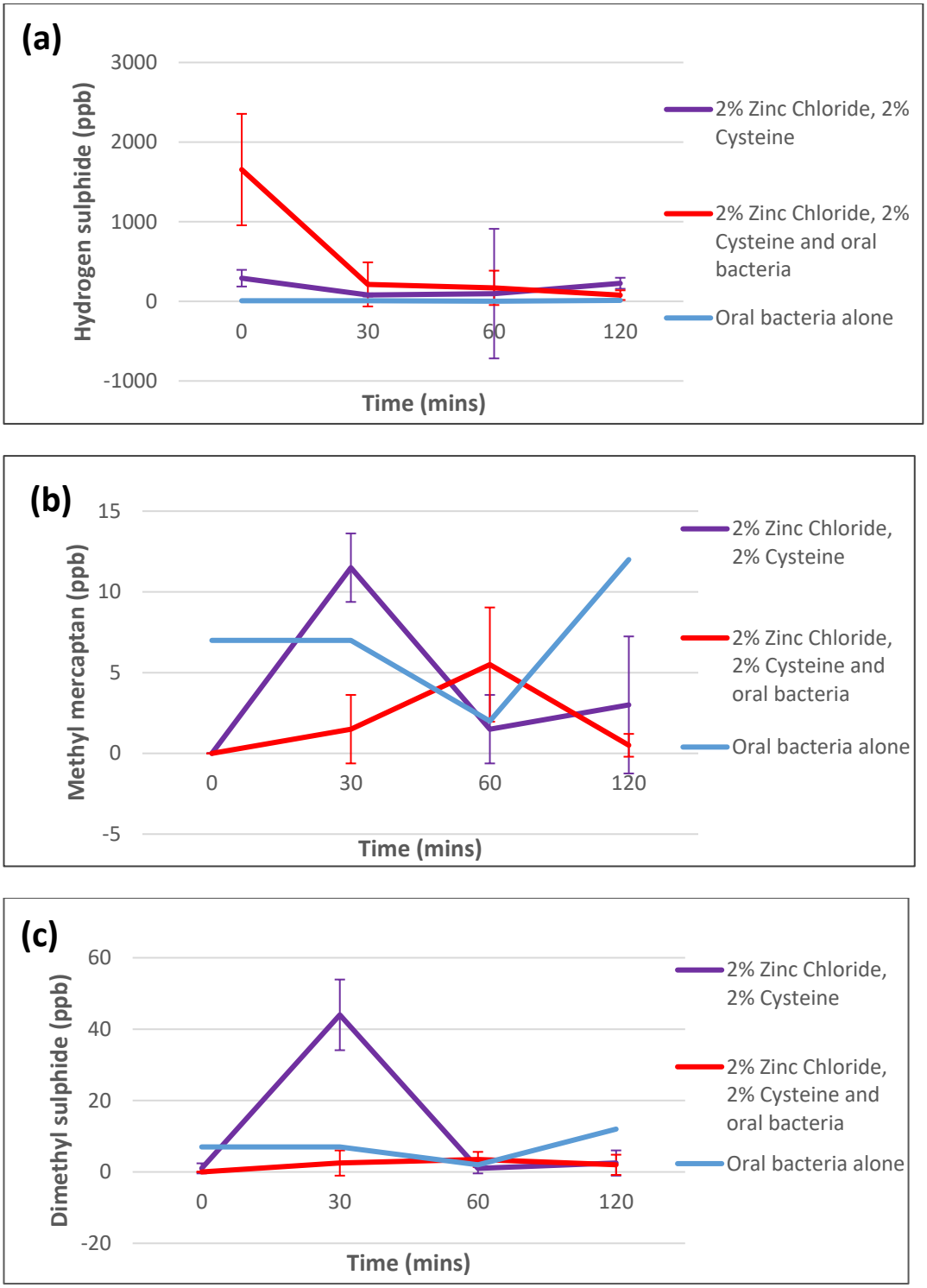

Figure 3.3 a,b,c. Graph showing VSC production from (a)2% zinc chloride+ 2% cysteine as a negative control, (b)Oral bacteria at 0.6 OD used as another negative control and (c)2% zinc chloride + 2% cysteine + Oral bacteria as the experimental run.

In figure 3.3 a, the combination of zinc chloride, oral bacteria and cysteine, show a peak hydrogen sulphide concentration of 1655 ppb (at 0 min) which then decreased to 213 ppb within 30 minutes. Concentrations of H_2S continue to decrease over time: by 44 ppb

between 30-60 minutes and by 91 ppb within the last hour (60-120 minutes). These values are above the positive control.

The results for methyl mercaptan are variable, the oral bacteria control ends up the highest value of the three solutions tested (12 ppb), but the irregularity of results made this problematic to decipher. The values (ppb) are also very low in terms of halitosis.

Interestingly, at 30 mins, the negative control of zinc chloride and cysteine produced a spike in methyl mercaptan (11.5 ppb) and dimethyl sulphide (44 ppb) which defies the trend of the graphs.

The data from figures 3.2 and 3.3 show that the controls did not behave as expected and so the validity of the test results were questionable, due to elevated H_2S in negative controls and the instability of results (ppb concentration) over time. Inconsistencies in results (positive controls) are seen between figures 3.1, 3.2 and 3.3. The oral bacteria and cysteine together show much lower values than previously seen in figure 3.1. The cysteine and zinc's together show an elevated hydrogen sulphide output, especially for a negative control. The varied values from these controls are too substantial to take on to further experiments without optimising the method. Therefore, an experiment was conducted where the concentration of hydrogen sulphide produced from cysteine was tested in the absence of any other reagent (Figure 3.4).

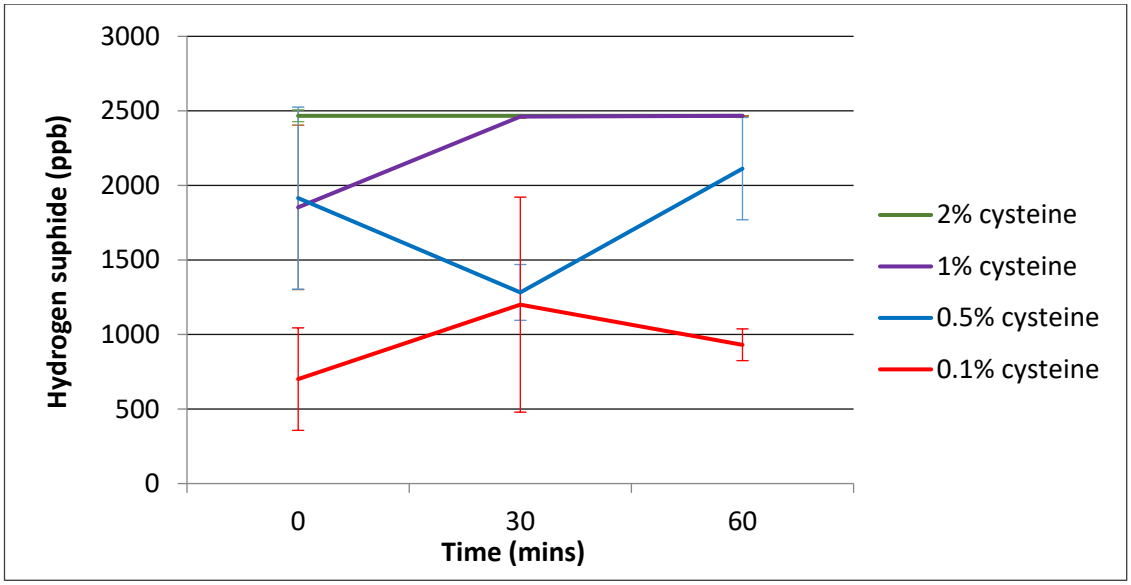

Figure 3.4 Hydrogen sulphide (ppb) measured from cysteine solutions alone at increasing concentrations. The time intervals reflected by the x axis of the graph; 0, 30 and 60 minutes. Standard deviation shown on data points

The results show that the concentration of hydrogen sulphide increases with increasing concentration of cysteine. However, the concentration is too high to be classified as 'background noise'.

The results at a lower concentration also seem to have a high degree of variability over the time. Surprisingly, the concentration of H_2S produced by 2% cysteine alone was much higher than the concentration detected in the presence of oral bacteria (2467 ppb vs 1429 ppb at 30 minutes). 2467ppb is also the limit of detection for the oralchroma, 2% cysteine reaches this at all time points, and 1% cysteine reach this point by 30 minutes and remains for the next 30 minutes.

A variety of techniques degassing techniques (degassed water via nitrogen, helium, and an ultrasonic bath) were employed to decrease the VSC's from cysteine alone (See chapter 2-Methods). All methods gave higher than expected VSC concentrations, the values obtained were too high to be classified as a negative control. (see appendix 1)

3.3.3 Testing the oralchroma compared to values from GC-MS

The oralchroma is a portable gas chromatograph, it could not be ruled out as a source of error. Therefore, hydrogen sulphide at known concentrations was tested on both the oralchroma and the GC-MS (gas chromatography- mass spectrometry) to compare results

and assess the error. Gas chromatography is a more reliable way of measuring specific gasses. The concentrations of hydrogen sulphide tested consisted of low (300 ppb), Medium (1000 ppb) and the highest detection limit of the oralchroma (2467 ppb).

Table 3.2. Hydrogen sulphide gas at known ppbs tested on the oralchroma

Oralchroma reading	**Known Hydrogen sulphide value (ppb)**		
	300	**1000**	**2467**
1	304	916	2467
2	277	1037	2467
Mean(±SD)	291 (±14.571)	976.5 (±85.559)	2467 (±0)

Table 3.2 shows that there is some variation within the oralchroma. At low concentrations of hydrogen sulphide, the average is within 9 ppb of the known gas concentration. At a medium output of hydrogen sulphide, the oralchroma has slightly more variation with a standard deviation of 85.559 ppb. The highest concentration is easily measured with no deviation from the true value by the oralchroma.

3.3.4 Testing amino acids

Table 3.3 Measurement of hydrogen sulphide with 1% cysteine and methionine added separately to the Gas Chromatography/Mass Spectrometer (GC/MS)

1% amino acids at time 0	**Hydrogen sulphide (ppb)**
Methionine	Undetectable
Cysteine	1194.96

The analysis of cysteine and methionine alone on GC-MS was to analyse the auto lysis of cysteine, compared to methionine, another sulphur containing amino acid.

The results in Table 3.3 show that even immediately after the preparation of the 1% cysteine solution in PBS, there is a considerable amount of H_2S present. This will interfere with results due to unreliable concentrations of hydrogen sulphide baseline from which any inhibition cannot then be reliably quantified. The results support earlier results in the

Kingston university laboratory. Cysteine is releasing a high concentration of hydrogen sulphide whilst methionine stays the more stable amino acid and doesn't break down in the presence of oxygen as easily.

3.4 Discussion

The bacteria in the oral cavity metabolise amino acids and release volatile sulphur compounds (VSC's). These VSC's namely hydrogen sulphide, methyl mercaptan and dimethyl sulphide are the foul-smelling gasses associated with halitosis, these arise from the catalysis of cysteine/methionine and other sulphur containing amino acids. 90% of oral malodour originates from the oral cavity, with the other 10% arising from extra oral origins such as diabetes and gastrointestinal tract diseases. (Washio *et al*., 2005).

The sulphur group from Cysteine is utilised by enzymes present in certain oral bacteria such *as Porphyromonas gingivalis, Citrobacter fruendii, Treponema denitcola* amongst other bacterial species (Sato and Nozaki, 2009). This was used initially in this thesis as a substrate to quantify the outlet of volatile sulphur gasses by reaction with whole bacteria over time. In the oral cavity, the metabolites formed from the cysteine catalysis aids the progression of pathogenesis by causing key changes in the oral environment: The ammonia can readily penetrate soft tissues in the oral cavity raising the pH over neutral. This can enhance the enzyme performance, increasing the rate of protein degradation and putrefaction leading to malodour (Kleinberg and Westbay, 1990).

In addition to VSC's causing malodour and the potential development of periodontal tissue diseases, hydrogen sulphide can down regulate cell cycle regulatory genes in squamous cell carcinoma cells, and therefore increase proliferation and cell cycle progression. (Ma, Bi and Wang, 2014). Hydrogen sulphide can cause changes to the enamel too, it can cause decay in the crystal structures and therefore contribute to dentin surface loss. (Hosoya *et al*., 2015).

The results from figure 3.1 shows the reaction between cysteine and oral bacteria over time, however, this is in the absence of a negative control. The hydrogen sulphide concentration rose over time, to the maximum of 2467 ppb- the oralchroma limit of

detection, then decreases very slightly (30 ppb) over the next hour, indicating that the reaction has reached its maximum velocity by 60 minutes.

Figures 3.2 and 3.3 show the reaction between cysteine, zinc products and bacteria, including controls of oral bacteria and cysteine (positive) and zinc products with cysteine (negative control). These graphs have shown the unreliability of the positive control containing cysteine. Firstly, compared to figure 3.1, the hydrogen sulphide concentration in figure 3.2 is much lower over time and unpredictable with large error bars-468 ppb at 60 minutes compared to 2467 ppb at 60 minutes from figure 3.1. Secondly, the positive control is often lower in VSC concentration than the negative control and test sample. This presents a problem with either the system or the substrate, in this case, the substrate-present in all reactions needed to be tested alone to rule out the auto breakdown of the cysteine.

Testing of cysteine as a substrate, as seen from Figure 3.4, cysteine releases a high level of hydrogen sulphide with a minimum of 700 ppb released by 0.1% cysteine at 0 minutes, with 1 and 2 % reaching the oralchroma limit of detection of 2467 ppb, this therefore presents a problem in using it to accurately measure its reaction with oral bacteria, and therefore with the introduction of a potential inhibitor. The reasoning behind the release of hydrogen sulphide has been theorised as the spontaneous oxidation of cysteine. This is a known phenomenon that occurs when the sulphur group of cysteine employs different bonds in its state of oxidation (McBean, 2017). Cysteine's changing forms can be a positive effect in the human metabolic system and protein signalling (Alcock, Perkins and Chalker, 2018), however a build-up of cystine in lysosomes can result in cystinosis and the onset of renal disease (Floege, Johnson and Feehally, 2010). For the current experiment, the change of form could lead to skewed results in an *in vitro* system. In bacterial species that require cysteine from the host such as *Legionella spp.* and *Neisseria gonorrhoea*, cannot usually utilise the oxidised cystine, this is expected to limit the growth and metabolism of bacteria (Ewann and Hoffman, 2006).

This oxidation process allows the release of intermediates as cysteine converts to cystine via its highly reactive thiol groups. The optimisation methods all included features to remove oxygen from the initial reaction such as a nitrogen supply during the mixing of autoclaved deionised water and cysteine, helium bath as described above and methods.

These attempts did not hugely decrease the VSC's released from the pure cysteine solution- see appendix 1.

The issues with cysteine brought to attention the importance of testing the amino acid for its stability before use with bacteria or the addition of inhibitors. This required a more sensitive and accurate measurement of the gasses that may be released from the amino acid on its own in solution (sterilised deionised water). This was achieved using Gas chromatography- Mass spectrometry (GC-MS)- and is ideal for measuring small volatile molecules that are less polar than water without derivatisation, due to the H-S bond having a smaller electronegativity difference than between H-O. Gas chromatography- Mass spectrometry (GC-MS) is a fast and sensitive technique capable of measuring analytes at low concentrations. The GC-MS is perfect for quantifying small volatile organic molecules with a high reproducibility of results. (Lynch, 2017)

Hydrogen sulphide can be measured sensitively on the GC-MS (Nair and Clarke, 2017) In a study by Stephen and colleagues, (2011) high VSC values were produced by the water and amino acids control, with cysteine producing 5 ppm, this could reflect the spontaneous breakdown of cysteine (seen in these results), although methionine also produces high values in the noted article. The amino acids could be reacting with other contaminants as the author does not state the base solution.

The concentration of cysteine tends to increase drastically over time therefore need to be measured instantly (Dong and DeBusk, 2009) this enforces the need to test cysteine at time 0 due to the oxidation process releasing higher than expected hydrogen sulphide. The oralchroma was tested against known hydrogen sulphide concentrations from a supply line (table 3.2)- these values are first verified on the GC-MS, then tested on the oralchroma to confirm a suitable limit of error to take back to the university for use in the analysis of volatile sulphur gasses. The biggest variability is at 1000 ppb with a standard deviation of 85. However, for this concentration 85 ppb is an acceptable error.

The GC-MS was also utilised to test amino acid stability (table 3.3). The production of hydrogen sulphide of the amino acids at 1% in PBS was tested. Cysteine produced 1194 ppb which is too high for a background hydrogen sulphide production, however, methionine also available for metabolism by bacteria in the oral cavity and releases VSCs when incubated with oral bacteria (Salako and Philip, 2011) (see introduction). Methionine was undetectable on the GC-MS when tested alone without bacteria. This gave the rationale to

continue experiments using methionine as the stable substrate for oral bacteria to produce gasses through enzymatic catalysis, and potential inhibition, assessed.

In conclusion, some amino acid substrates such as cysteine can be unpredictable and therefore problematic to use *in vitro* in a laboratory environment. In this chapter oral bacteria were tested alone as a negative control presenting viable data that did not react in the buffer solution to produce significant values of VSC's. But the addition of cysteine and zinc citrate proved sporadic results. Issues were investigated and the oxidation of cysteine seemed a viable mechanism of producing hydrogen sulphide in solution, skewing results. Methods seen in appendix 1, attempted to fix this problem such as nitrogen degassing, but eventually another amino acid native to the oral cavity was chosen as the substrate of research- methionine, with undetectable hydrogen sulphide measured from substrate alone (table 3.3).

Chapter 4 The effect of methionine on planktonic oral bacteria with the addition of crude products

4.1 Introduction

In this chapter, the ability of whole bacteria to break down methionine is assessed based on the measurements of volatile sulphur compound release (hydrogen sulphide, methyl mercaptan and dimethyl sulphide). Crude products (see chapter 2 for extraction methods) were added to the suspension, and their ability to inhibit the release of or neutralise the odorous gasses was investigated.

The initial products chosen were instant coffee, black tea, red wine and garlic. All of these have had literature published on potential effects against VSC concentration and oral bacteria (Almeida *et al*., 2012, Badhani, Sharma and Kakkar, 2015, Bakri and Douglas, 2005, Burguera-Pascu, Rodríguez-Archilla and Baca, 2007, Cueva *et al.,* 2012). The products chosen, have been shown to have multiple effects on cells they come into contact with including; anti-inflammatory, anti- adhesive and anti-viral properties. For example, caffeic acid, S-allyl cysteine, and uracil extracted from garlic can modulate Nuclear Factor -kappa-B cells (NF-kB) leading to an antioxidant effect (Kim *et al*., 2013). Free radical scavenging activities in coffee and tea also make these products antioxidants and multiple chemicals within the whole coffee have an anti-cancer effect such as trigonelline and gallic acid (Mojica *et al*., 2018). This chapter looks at crude products meaning all included compounds working in synergy to assess the effectiveness of these substances on oral malodour from prepared oral tongue scrapings.

A suspension containing whole cell, oral bacteria is representative of the bacterial interactions with products as they can occur in a human oral cavity, the reaction can be quantified and the inhibition by crude products assessed, this is used for the first stage in active product selection.

This chapter (4) will look at real time inhibitory effects on the outlet of malodorous gasses. Oral bacteria can bind to methionine, creating primarily methyl mercaptan, however hydrogen sulphide can be produced from methionine in a few ways. Firstly, the conversion of methionine to cysteine through enzyme intermediates e.g. S-adenosyl methionine,

cysteine can then be catalysed by oral enzymes to yield hydrogen sulphide (H_2S). Methyl mercaptan (MM) can also be directly oxidised to form H_2S via methyl mercaptan oxidase.

4.1.1 Aims

Methionine reacting with oral bacteria to assess level of hydrogen sulphide, methyl mercaptan and dimethyl sulphide released. Then adding 'inhibitory products' to reassess VSC gas production.

The following products were assessed: zinc citrate, black tea, coffee, green tea, red wine (with and without alcohol), odourless garlic, garlic, black tea + zinc citrate, coffee + zinc citrate. Their capability to inhibit VSCs produced from whole bacteria and methionine was also measured. These products are crude- meaning that each crude product has a chemical library making up a whole, apart from zinc citrate.

4.2 Methods

Method 2.2 standardising bacteria for use within the headspace system. Then the headspace method 2.4- was conducted over time (120 minutes) incubating headspace vials with 1.5ml (0.5ml of each product- methionine, oral bacteria and crude product)

Percentage changes are shown in tables 4.4-11.

4.3 Results

4.3.1 Methionine tested alone, and with planktonic bacteria

Initially methionine is tested on in a solution of PBS in the absence of bacterial suspensions. This is to assess the baseline reaction producing VSCs as a control before the addition of other products.

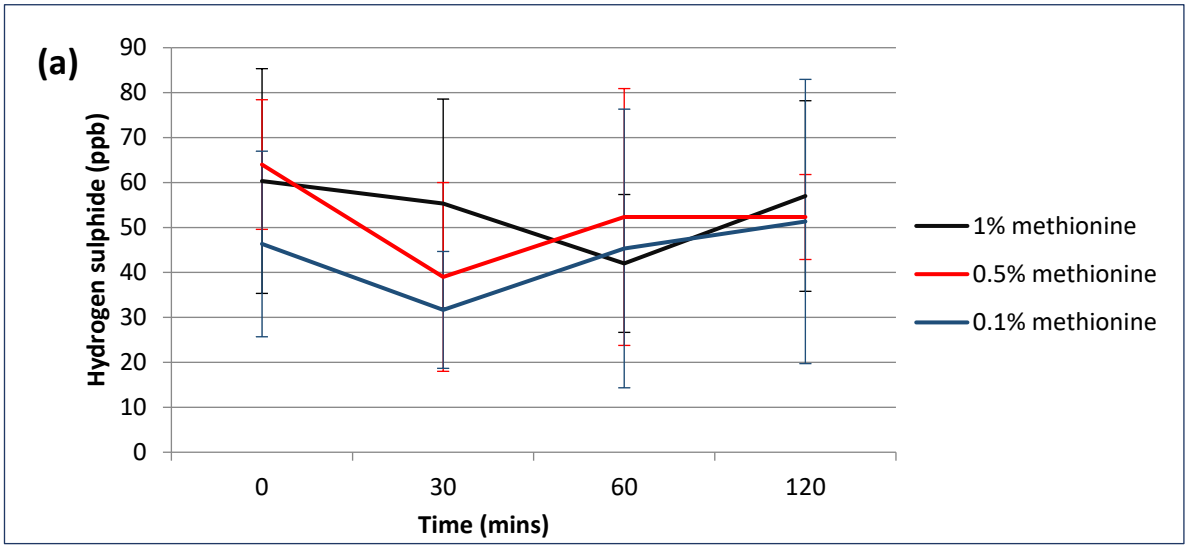

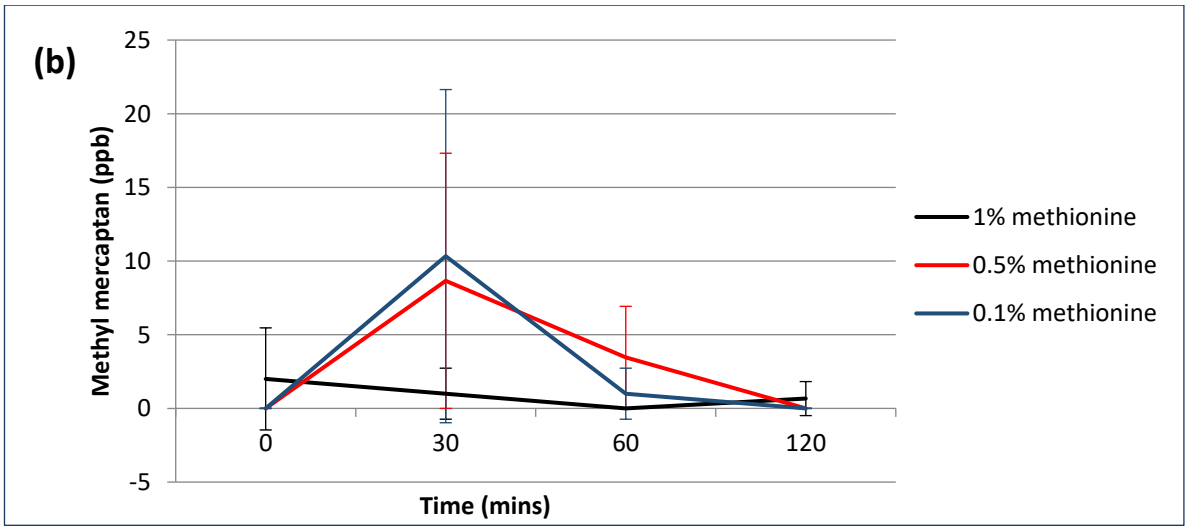

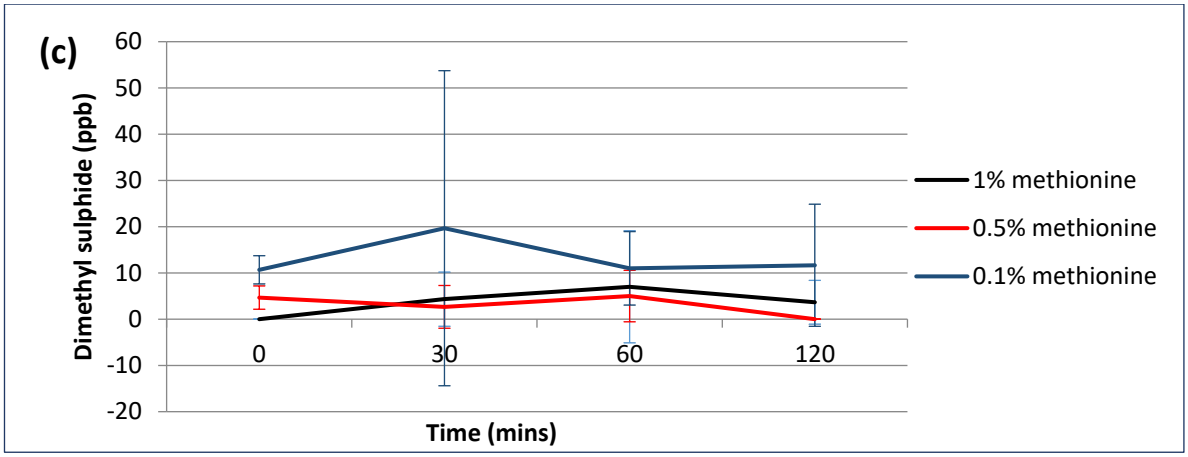

Figure 4.1. Methionine solutions at varying concentrations made in PBS and filter sterilised, tested to determine the background concentration of VSC gasses produced (a) Hydrogen sulphide, (b) Methyl Mercaptan and (c) Dimethyl sulphide concentrations (ppb) taken at the time intervals. Error bars show the standard deviation (n=3)

The results shown in Figure 4.1 (a), (b) and (c) represent a lower baseline 'background noise' than had been seen with cysteine tested on its own at increasing concentrations (Fig 3.4). The hydrogen sulphide (ppb) emitted does not surpass 64 ppb (by 0.5% Methionine at time 0), 0.1% and 0.5% methionine shows a dip in hydrogen sulphide concentrations after 30 minutes, the same dip occurs at 1% methionine at 60 minutes, all rising again to between 50 and 60 ppb by 120 minutes. Large error bars indicate variation within these results.

The methyl mercaptan does not exceed 10 ppb in Figure 4.1 (b) shown by 0.1% Methionine at 30 minutes and in Figure 4.1 (c) 0.1% methionine demonstrated the highest dimethyl sulphide concertation after 30 minutes at 20 ppb. Both these results have high error bars indicating the variation in results. However, 1% methionine presents a relatively stable line, with no huge spikes, producing low enough baseline gasses to add test reagents such as bacterial suspensions (fig 4.2) and crude products.

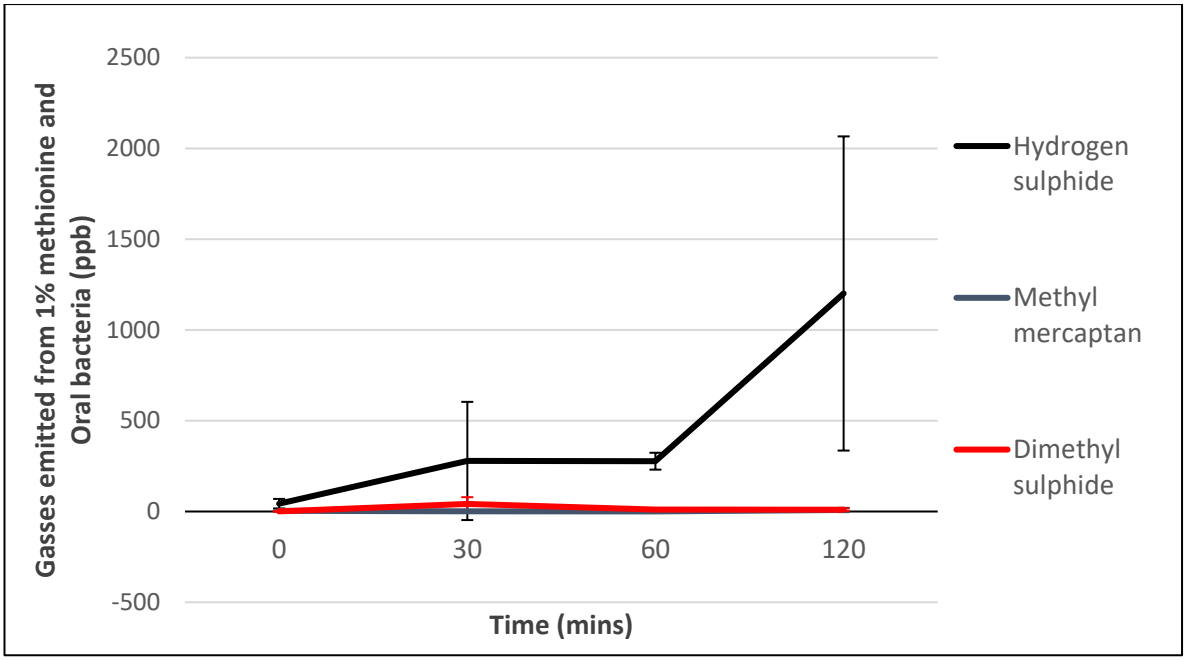

Figure 4.2. 1% Methionine solution with oral bacteria at 0.6 OD. Based on a triplicate where gas measurements were taken at time intervals and the data points exhibit the average result from the three and error bars display the standard deviation between the three experimental runs.

The reaction between methionine and oral planktonic bacteria shows a high concentration of hydrogen sulphide, large error bars indicate some variability.

Methyl mercaptan concentrations stay at very low concentrations in Figure 4.2 as does dimethyl sulphide apart from a slight rise to 41 ppb at 30 minutes. This indicates that the bacteria are metabolising methionine to produce hydrogen sulphide at a higher rate than these other gasses.

The conclusion from these experiments is that 1% methionine with the planktonic bacteria (Fig 4.2) produces a high level of hydrogen sulphide, alongside a very low background production (around 60 ppb) seen in Figure 4.1 (a). This was deemed as a viable model to test against plant extracts for a possible reduction in VSCs, namely, hydrogen sulphide.

4.3.2 The introduction of crude products to oral bacteria with methionine

The following figures will demonstrate the effect of VSC production when natural product (listed below) were added to oral bacteria and methionine.

Products used:

i) Green tea
ii) Red wine (with and without alcohol)
iii) Garlic
iv) Odourless garlic
v) Zinc citrate
vi) Instant coffee
vii) Black tea
viii) Zinc citrate + black tea
ix) Zinc citrate + coffee

i) Green tea

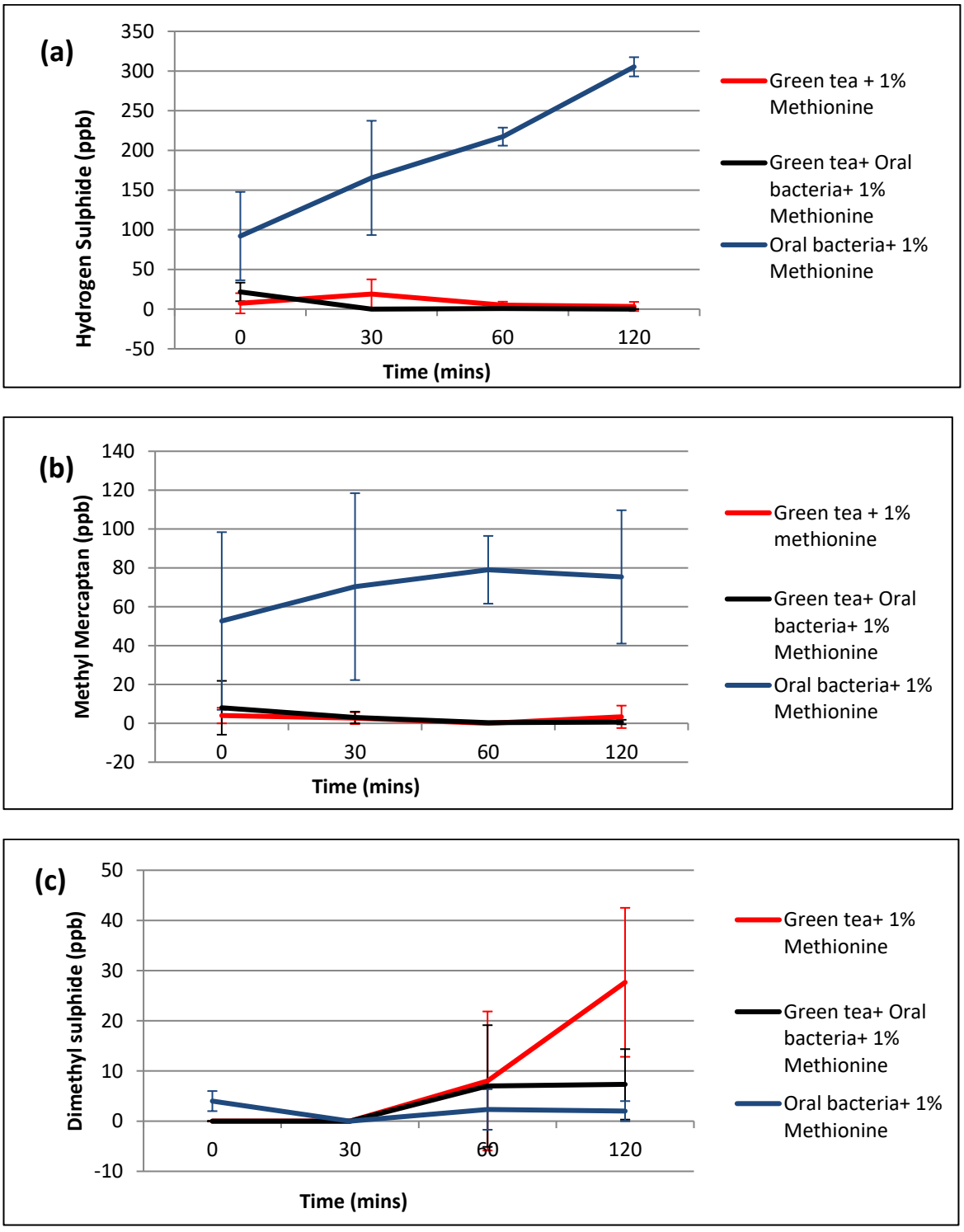

Figure 4.3 a, b, c. Methionine solutions tested with oral bacteria, green tea and the combination of both described in the graph key. (a) hydrogen sulphide, (b) methyl mercaptan, (c) dimethyl sulphide output (ppb).
Errors represent standard deviation (n=3).

In figure 4.3 (a), green tea and methionine produce a maximum of 25 ppb hydrogen sulphide at 30 minutes and then steadily decreases over the 120-minutes, indicating no prominent reaction production of H_2S (or any other VSC) from the negative control. Methionine and oral bacteria incubated together as the positive control steadily increase through all time points to 305 ppb. Green tea + oral bacteria + methionine presents a small rise in hydrogen sulphide when first incubated together but drops to 0 ppb by 30 minutes. Exhibiting a reduction of H_2S by green tea over all time points.

There is also a reduction in methyl mercaptan (Fig 4.3 (b)) when adding green tea to methionine and oral bacteria ranging from 50-80 ppb over all time points.

There is a low concentration of dimethyl sulphide produced through the whole experiment including the control of green tea and methionine 30 through to 120 minutes (figure 4.3 c) but one should consider the deviation in these results (error bars 12 ppb max).

ii) Red wine

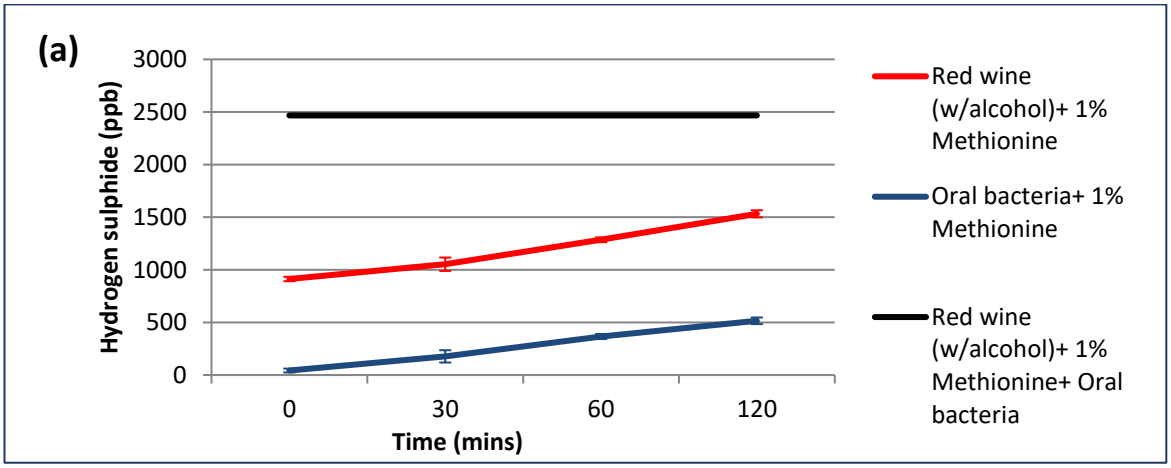

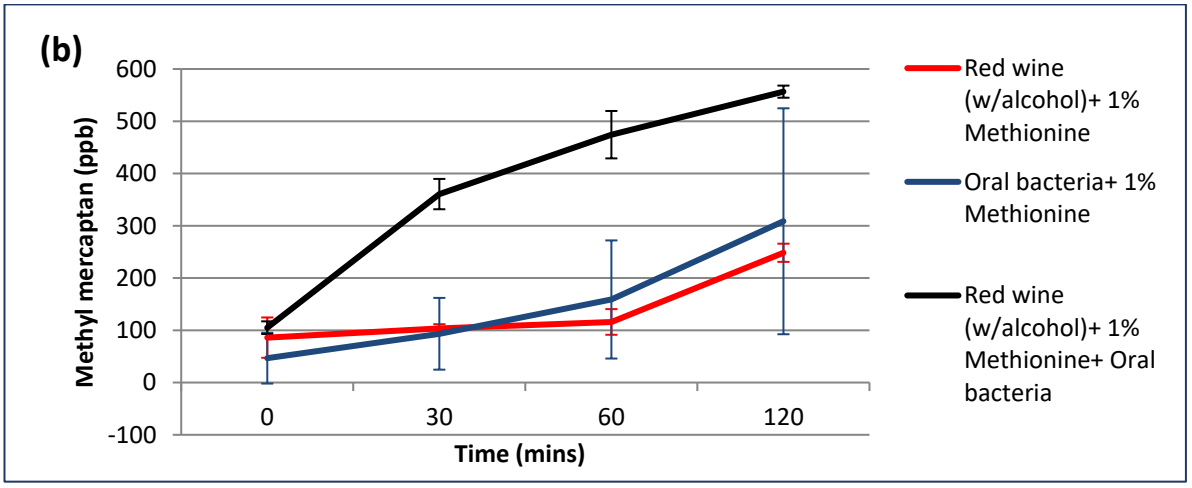

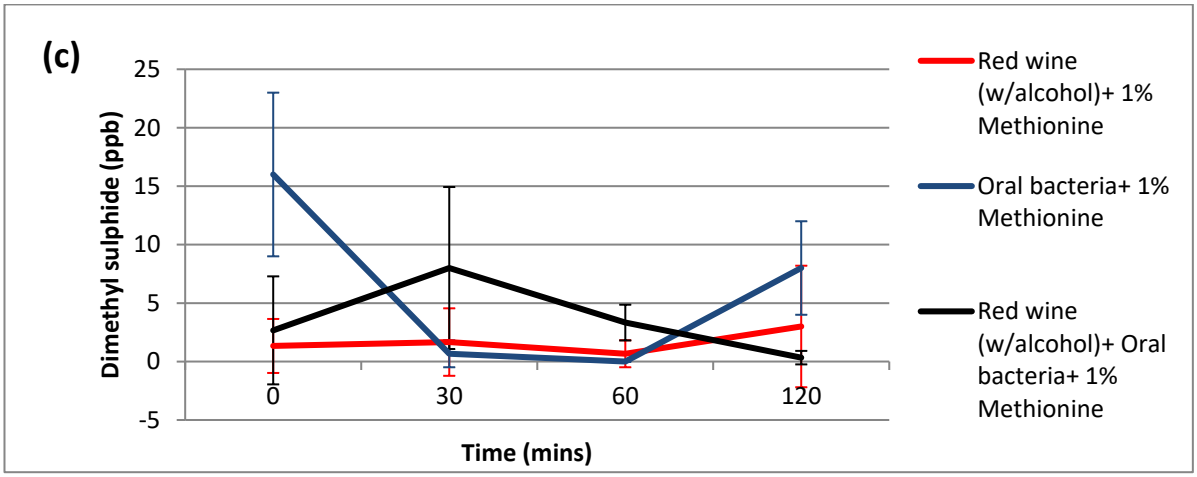

Figure 4.4. Methionine solutions tested with Oral bacteria, Red wine and the combination of both- defined by the graph key. (a) Hydrogen sulphide, (b) Methyl mercaptan, (c) Dimethyl sulphide output (ppb).
Error bars represent standard deviation (n=3).

Red wine + Oral bacteria + Methionine (Fig 4.4 (a)) incubated together reaches the oralchroma maximum detection limit from 0 to 120 minutes. This is the result of all three reagents being incubated together (Red wine, methionine and oral bacteria (black line)) and the reaction producing 2467 ppb H_2S. Red wine + Methionine (Fig 4.4 (a), red line) negative control reaches 1500 ppb which is significantly high for a negative control, and produces more H_2S than oral bacteria and methionine positive control (blue line), though this is over 1000 ppb lower than red wine, methionine and oral bacteria, as described above.

Red wine and methionine also produced an increased methyl mercaptan being produced (Fig 4.4 (b)) starting at 105 ppb and increasing to 360 ppb then by roughly 100 ppb for subsequent time points. The mixture of methionine+ oral bacteria+ red wine demonstrated a steady increase from 100 ppb at 0 minutes to 550 ppb at 120 minutes. Over the time there is a gradual rise in both the controls producing methyl mercaptan. There is no significant difference between the control of oral bacteria and methionine (blue line) and test reaction. In this experiment, there is no inhibitory effect of red wine on the methyl mercaptan produced by methionine and oral bacteria.

The dimethyl sulphide measurements show low and variable concentrations throughout the experiment which is evident in all combinations of reaction mixtures. Due to the unreliability and high degree of error in the controls in figure 4.4, red wine was not taken further in testing. Although it was theorised that the limiting factor may be the ethanol, therefore, in the next experiment, H_2S was quantified from dealcoholized red wine.

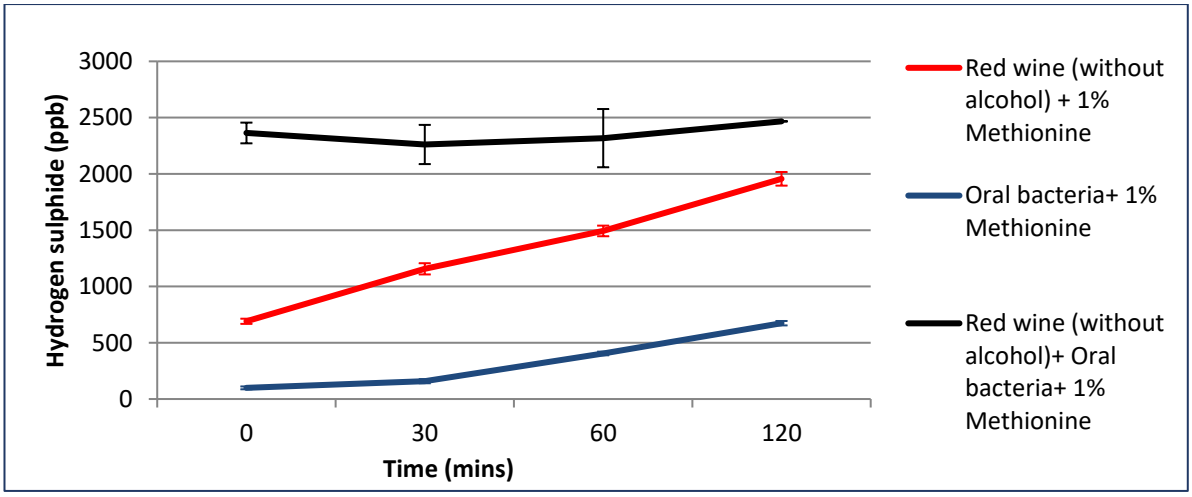

Figure 4.5. Methionine solutions tested with oral bacteria, red wine (without alcohol) and the combination of both, these are the result of the hydrogen sulphide (ppb).

Red wine without alcohol, methionine and oral bacteria (Fig 4.5) has a similar effect on hydrogen sulphide production as red wine with alcohol (Fig 4.4 (a)) where the concentration approaches the oralchroma maximum detection limit of 2467 ppb. This proves that there are other components in the red wine other than ethanol that can react with methionine and oral bacteria to result in a high concentration of hydrogen sulphide. The control of bacteria and methionine (blue line) gradually increased ending in 674 ppb. All solutions including red wine produced a minimum of 600 ppb higher hydrogen sulphide than no red wine.

iii) Garlic

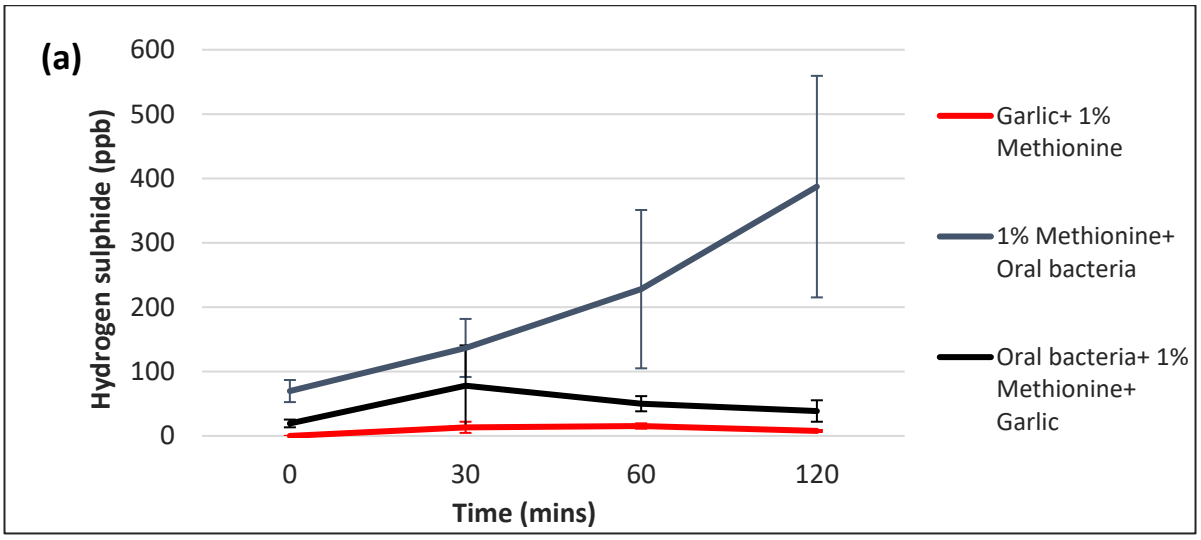

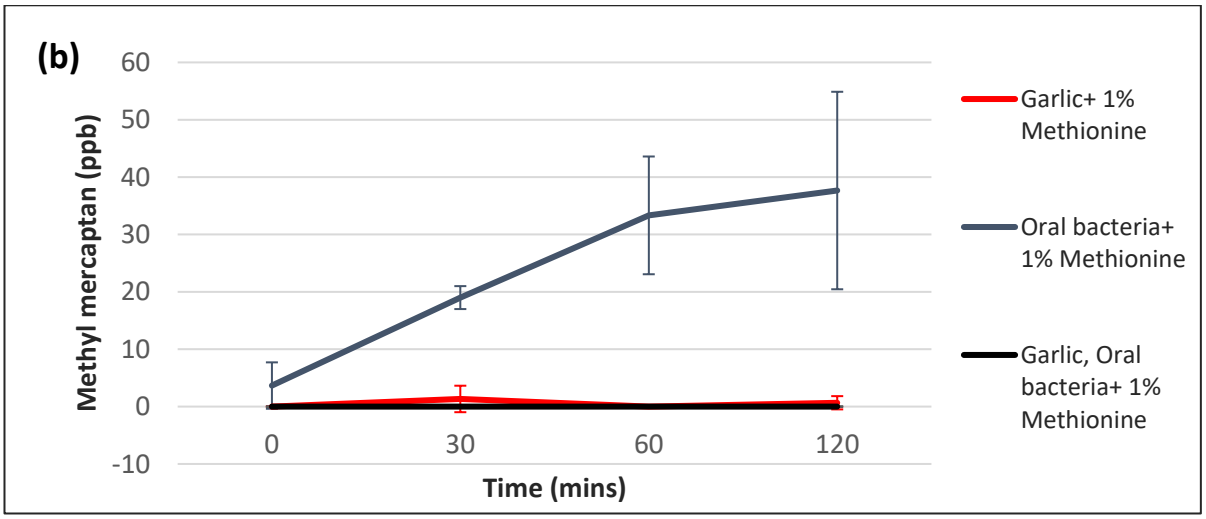

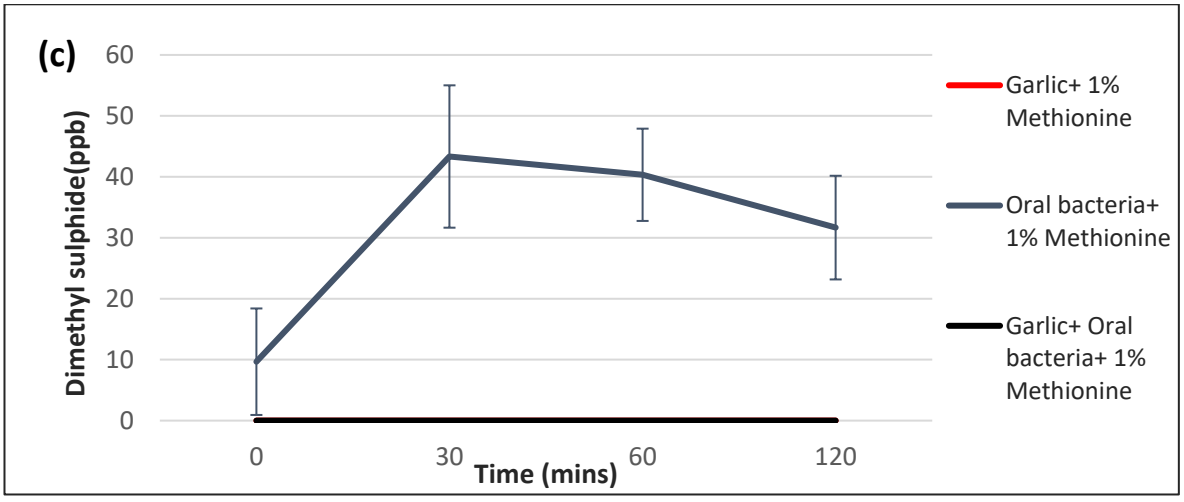

Figure 4.6. Methionine solutions tested with oral bacteria and garlic separately (red and blue line respectively) as controls. The black line represents methionine, oral bacteria and garlic incubated together (a) Hydrogen sulphide, (b) Methyl mercaptan, (c) Dimethyl sulphide output (ppb).

Garlic incubated with methionine did not react to produce a significant concentration of VSCs (Fig 4.6 (a), (b), (c), red line). Garlic is inhibitory when incubated with the methionine and oral bacteria compared to the rising control of oral bacteria and methionine. In Fig 4.6 (a), garlic demonstrated an inhibitor effect on hydrogen sulphide conc. of 70.8% over the 2-hour experiment (387 ppb vs. 38 ppb at 120 minutes).

The methyl mercaptan was inhibited by 100% when garlic, oral bacteria and methionine were all incubated together compared to the control of methionine and oral bacteria. The methionine + garlic control stays very low with small rises at 30 and 120 minutes (under 5 ppb) indicating no major reaction resulting in VSCs.

The control of methionine+ oral bacteria presented a rise in dimethyl sulphide concentrations up to 30 minutes then slowly drops from 42 ppb to 32 ppb over the next 90 minutes. There is no reaction between garlic + methionine or garlic + methionine + oral bacteria to produce dimethyl sulphide exhibiting inhibitory action of garlic on dimethyl sulphide production.

iv) Odourless garlic

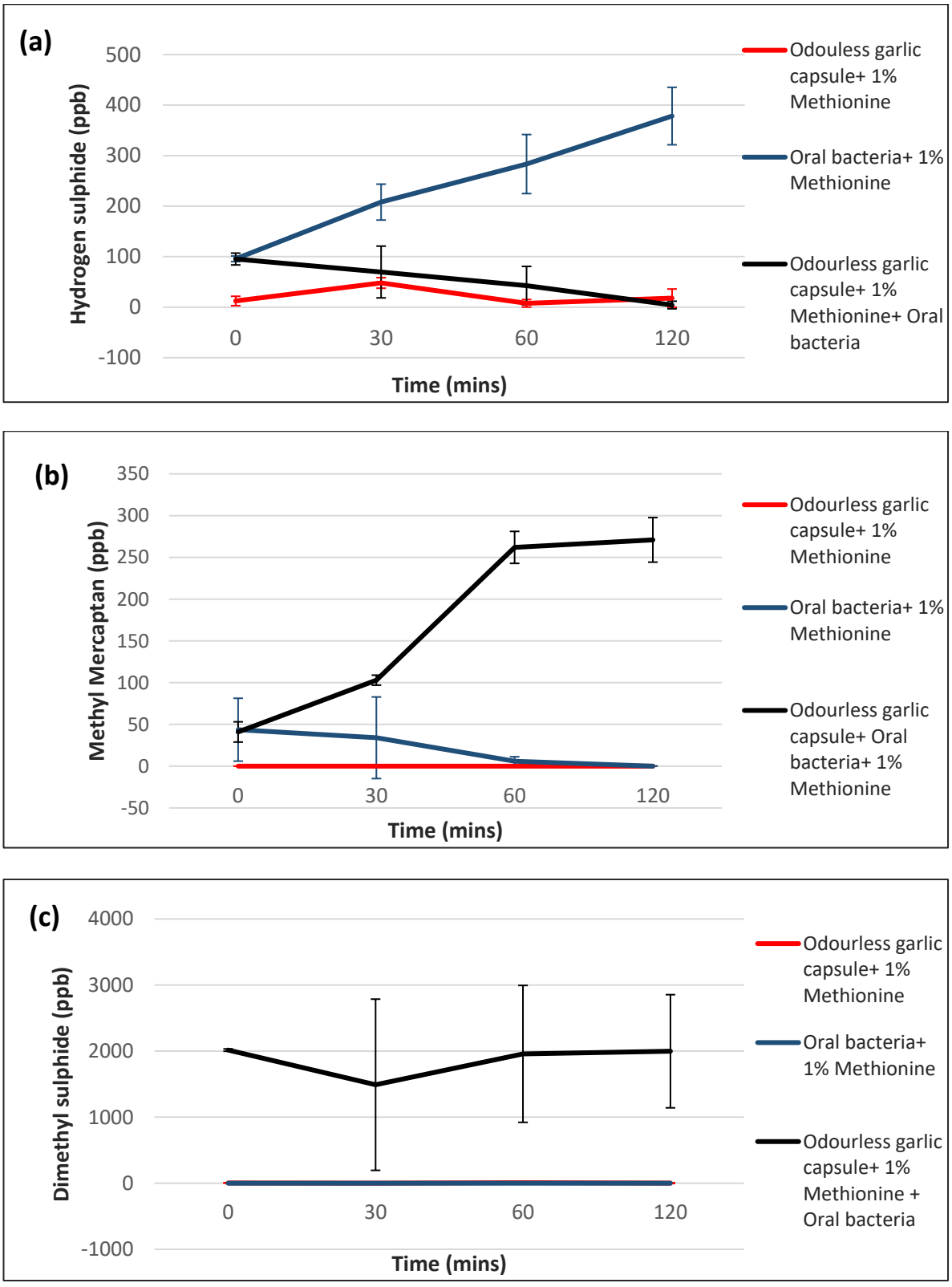

Figure 4.7 a-c. Methionine solutions tested with oral bacteria and odourless garlic separately (red and blue line respectively) as controls. The black line represents methionine, oral bacteria and odourless garlic incubated together (a) Hydrogen sulphide, (b) Methyl mercaptan, (c) Dimethyl sulphide output (ppb).

In figure 4.7 (a), the odourless garlic incubated with methionine and oral bacteria showed a steady decrease of hydrogen sulphide starting at 100 ppb at first contact then decreases. The control of oral bacteria and methionine also starts off at a similar point but continues to rise as expected. By 120 minutes the percentage inhibition of odourless garlic on hydrogen sulphide is 98.9%.

In figure 4.7 (b), methyl mercaptan concentrations rise steadily when methionine + oral bacteria + odourless garlic are incubated together; this rises to 271 ppb above the control which steadily decreases to 0 ppb by 60 minutes. There is no reaction that produces methyl mercaptan between odourless garlic and methionine.

Figure 4.7 (c) shows no reaction between methionine and odourless garlic to produce dimethyl sulphide, however, the oral bacteria added to this reaction mixture raises the dimethyl sulphide result to 2000 ppb, nearing the oralchroma limit of detection, presenting a VSC producing reaction to produce dimethyl sulphide (and methyl mercaptan) shown by the black line and the blue line on figure 4.7 (b) and (c).

v) Zinc citrate

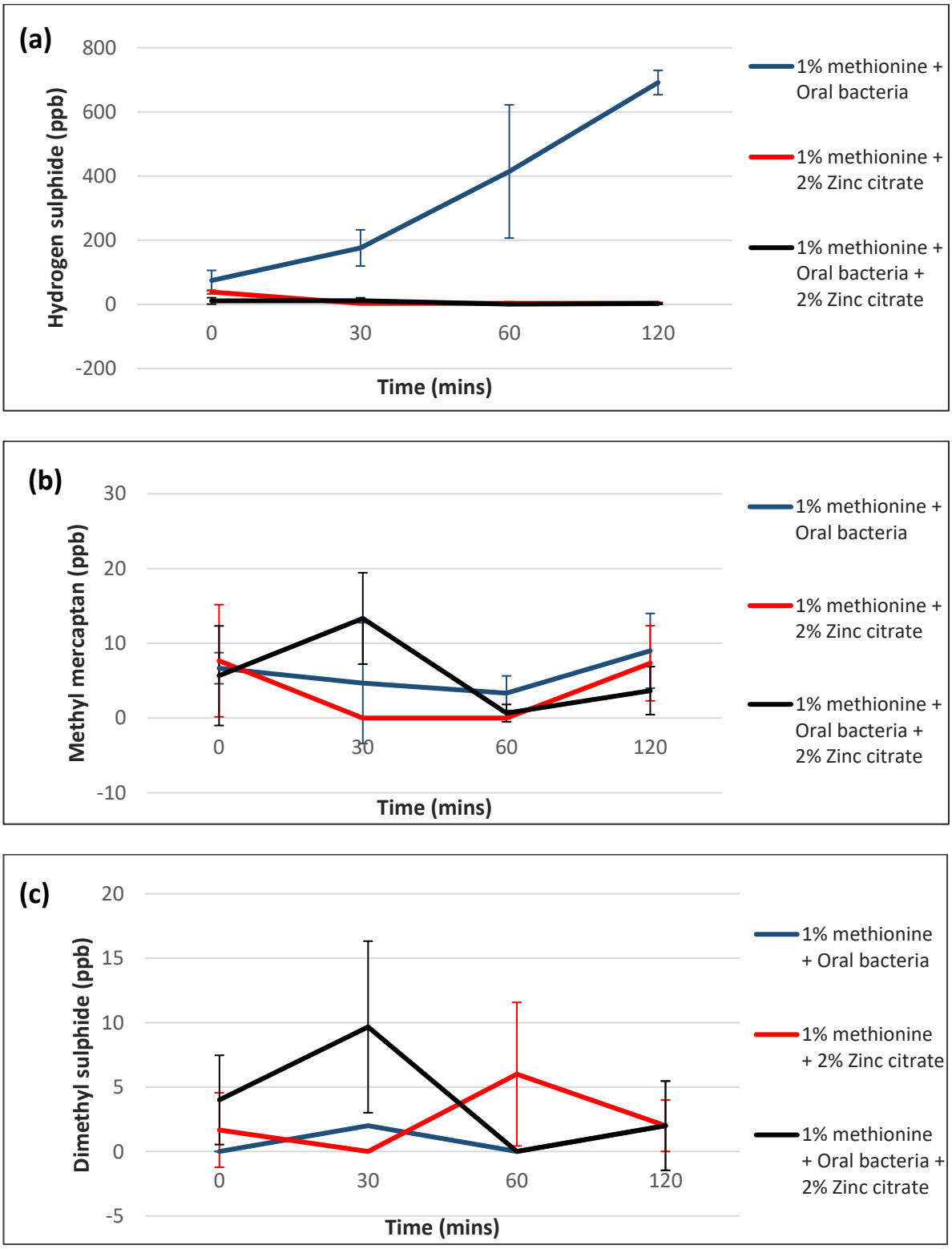

Figure 4.8 a-c. Methionine solutions tested with oral bacteria and zinc citrate separately (red and blue line respectively) as controls. The black line represents methionine, oral bacteria and zinc citrate incubated together (a) Hydrogen sulphide, (b) Methyl mercaptan, (c) Dimethyl sulphide output (ppb).

Methionine and oral bacteria controls display a graduated increase to a final hydrogen sulphide concentration of 692 ppb (figure 4.8 (a)). Zinc citrate when added to the bacteria and methionine decreases hydrogen sulphide concentrations. The highest concentration at 0 minutes is 11.3 ppb and decreases to 0 ppb for the rest of the time points. The methionine incubated with the zinc citrate shows a similar trend, behaving as expected.

In figure 4.8 (b), the addition of zinc citrate to oral bacteria and methionine the methyl mercaptan concentrations were variable, but still low and insignificant in terms of the halitosis threshold.

In figure 4.8 (c), dimethyl sulphide concentrations emitted from methionine and oral bacteria start at 0 ppb and stays very low. This is too low to get a measure of dimethyl sulphide inhibited by zinc citrate. The combination of methionine, oral bacteria, zinc citrate, the dimethyl sulphide demonstrated a higher level than the positive control and peaks at 30 minutes at 9.67 ppb before decreasing to 0 ppb in the next 30 minutes. There is a reaction between methionine and zinc citrate which peaks at 60 minutes (6 ppb) but with high error and continues to decrease in the next hour.

vi) Instant coffee

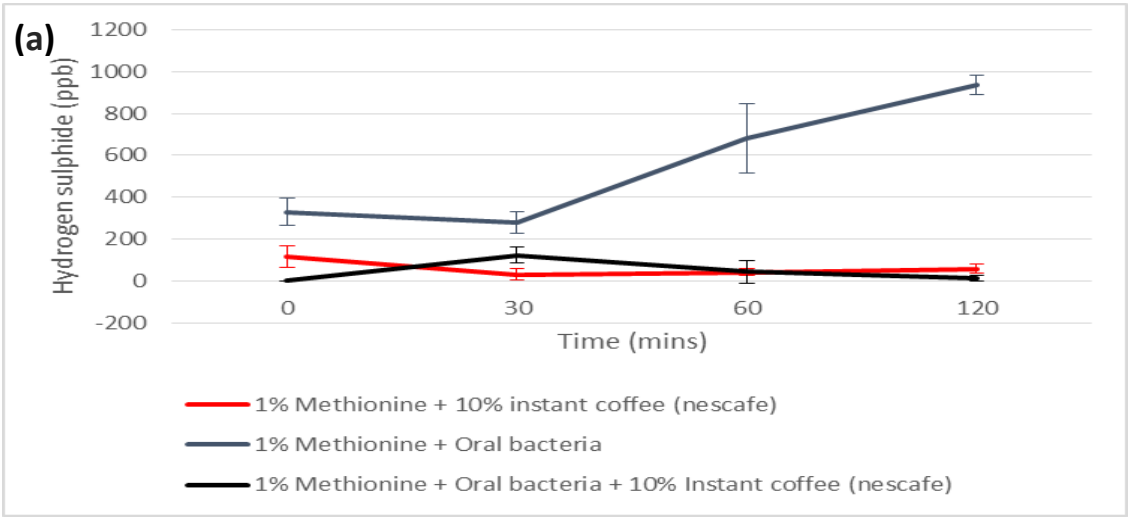

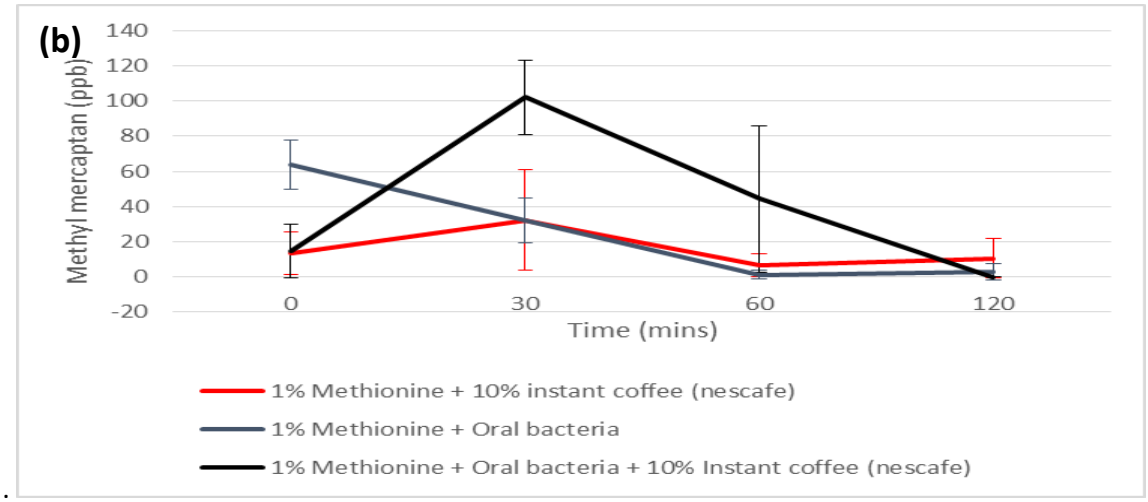

.

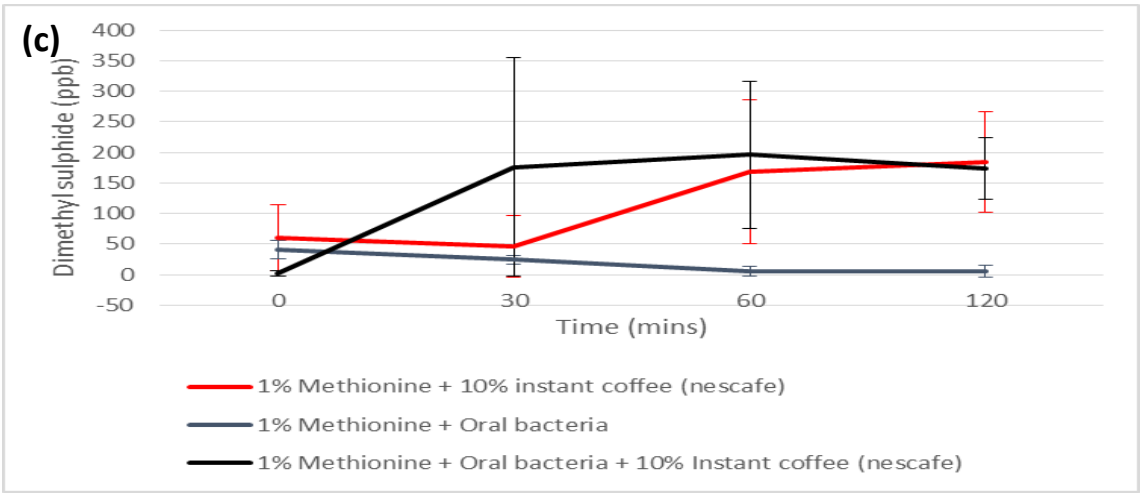

Figure 4.9 a-c. Methionine solutions tested with oral bacteria and instant coffee separately (red and blue line respectively) as controls. The black line represents methionine, oral bacteria and instant coffee incubated together (a) Hydrogen sulphide, (b) Methyl mercaptan, (c) Dimethyl sulphide output (ppb).

The methionine + oral bacteria control in figure 4.9 (a) produces a rising concentration of hydrogen sulphide through the experiment. Methionine + oral bacteria + instant coffee incubated together showed production of hydrogen sulphide rising at 30 minutes but to less of an extent compared to the control therefore exhibiting inhibition. After 30 minutes the hydrogen sulphide from this test reaction gradually decreases. The instant coffee reacts with the methionine to release hydrogen sulphide from 0 minutes, it then decreases in the next 30 minutes and stays low.

Methyl mercaptan concentrations in the test group of all three components incubated together rise to 101.3 ppb by 30 minutes from 16 ppb at 0 minutes then decreases over the next 90 minutes to 0 ppb. Values are higher than the positive control of methionine with oral bacteria except for time 0, therefore inhibition of the methyl mercaptan gas cannot be quantified as inhibitory. Similarly, the reaction of methionine and instant coffee incubation rises to peak at 30 minutes at 30 ppb and stays low, however by the end of the 120 minutes this negative control shows the highest concentration of methyl mercaptan at 10 ppb (figure 4.9 (b)).

The methionine and bacteria controls in Figure 4.9(c) exhibit dimethyl sulphide concentrations that peak at 0 minutes (38.67 ppb) and slowly fall over the course of the experiment. The overall effect of the instant coffee on dimethyl sulphide cannot be quantified due to the negative control (Instant coffee with methionine) producing more dimethyl sulphide at the end point of the reaction.

vii) Black tea

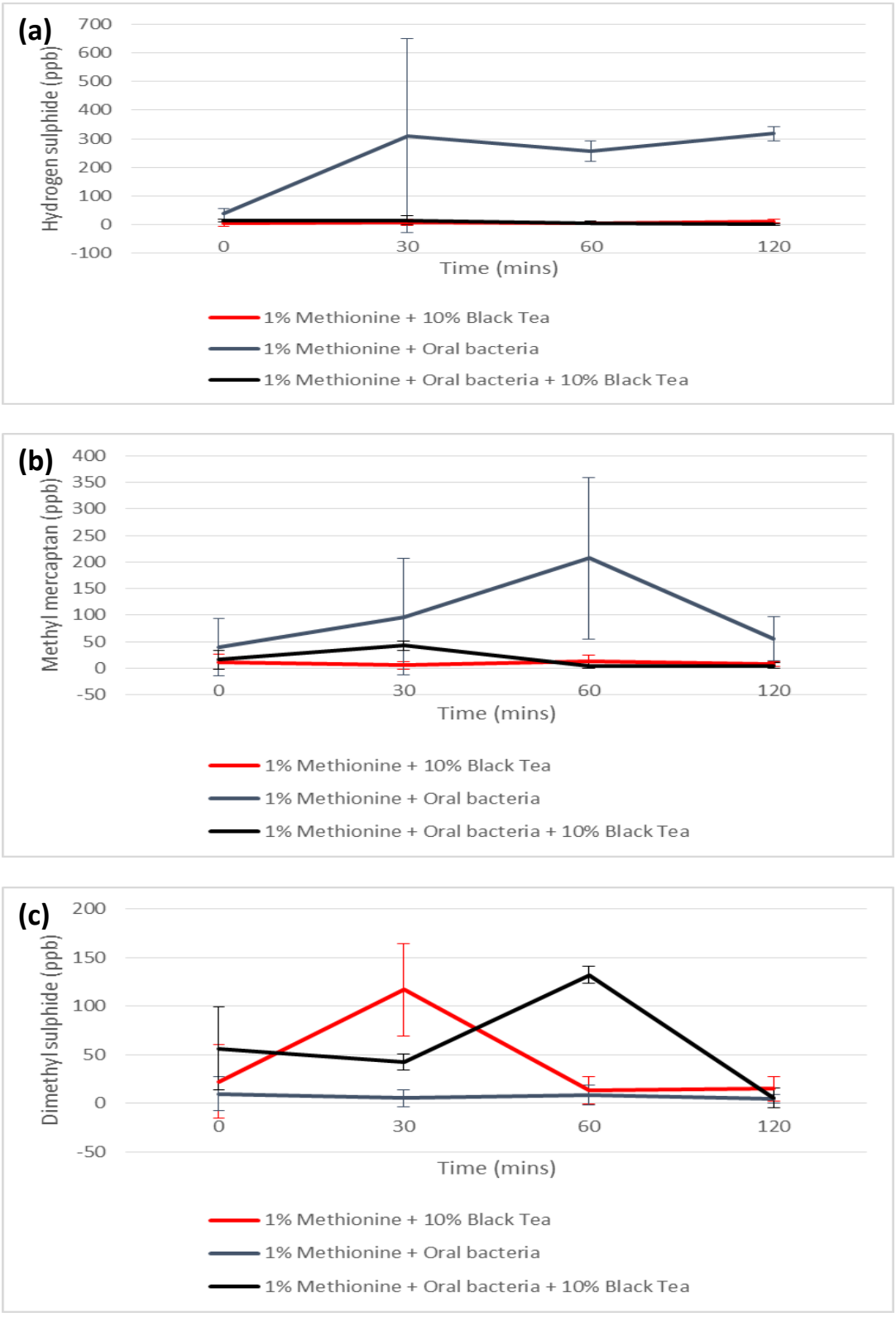

Figure 4.10 a-c. Methionine solutions tested with oral bacteria and black tea separately (red and blue line respectively) as controls. The black line represents methionine, oral bacteria and black tea incubated together (a) Hydrogen sulphide, (b) Methyl mercaptan, (c) Dimethyl sulphide output (ppb).

Methionine incubated with bacteria show rising concentrations of hydrogen sulphide to 30 minutes (with high error) which then slightly decreases over the next 30 minutes and a slight increase again to 120 minutes ending at a peak of just over 300 ppb, where the error decreased from 30 minutes. The black tea inhibits the hydrogen sulphide emissions from methionine and oral bacteria which ends at 0 ppb at 120 minutes with a percentage change from the control of 99.9%. The Methionine does not significantly interact with the black tea to produce hydrogen sulphide with small rises at both 0 and 120 minutes

In Figure 4.10 (b), Methionine and bacteria incubated together exhibit a slow rise in methyl mercaptan production between 0 and 60 minutes to 210 ppb, then a decrease to 51 ppb at 120 minutes. The black tea incubated with methionine and oral bacteria is lower than the control exhibiting inhibition but rises in methyl mercaptan is witnessed in the first 30 minutes followed by a decrease to 0ppb by 120 minutes. Methionine and black tea incubated together does not show a high level of a methyl mercaptan production with values staying consistently low.

Dimethyl sulphide emissions from the oral bacteria and methionine control stay low through the experiment and black tea added to the mix makes the dimethyl sulphide concentrations rise to peak at 60 minutes then commences to drop in the next hour. The methionine interacts with the black tea in a similar way where there is a peak (at 30 minutes) and falls by 60 minutes, there is then a small rise in the next hour of incubation.

The results of black tea on hydrogen sulphide concentrations from methionine and oral bacteria above warrants further investigation into potential synergies. Ideally, this would be put together once the mechanism of action is established to complement each-other and should be tested in the same experiment as testing the components alone. However, some preliminary experiments are shown below (fig 4.11 and 4.12) where the synergies are analysed using the headspace method consistent with the rest of this chapter.

viii) Zinc citrate + black tea

The potential synergistic interaction between the addition of zinc citrate to the crude natural was also investigated to evaluate their effect at reducing VSC production.

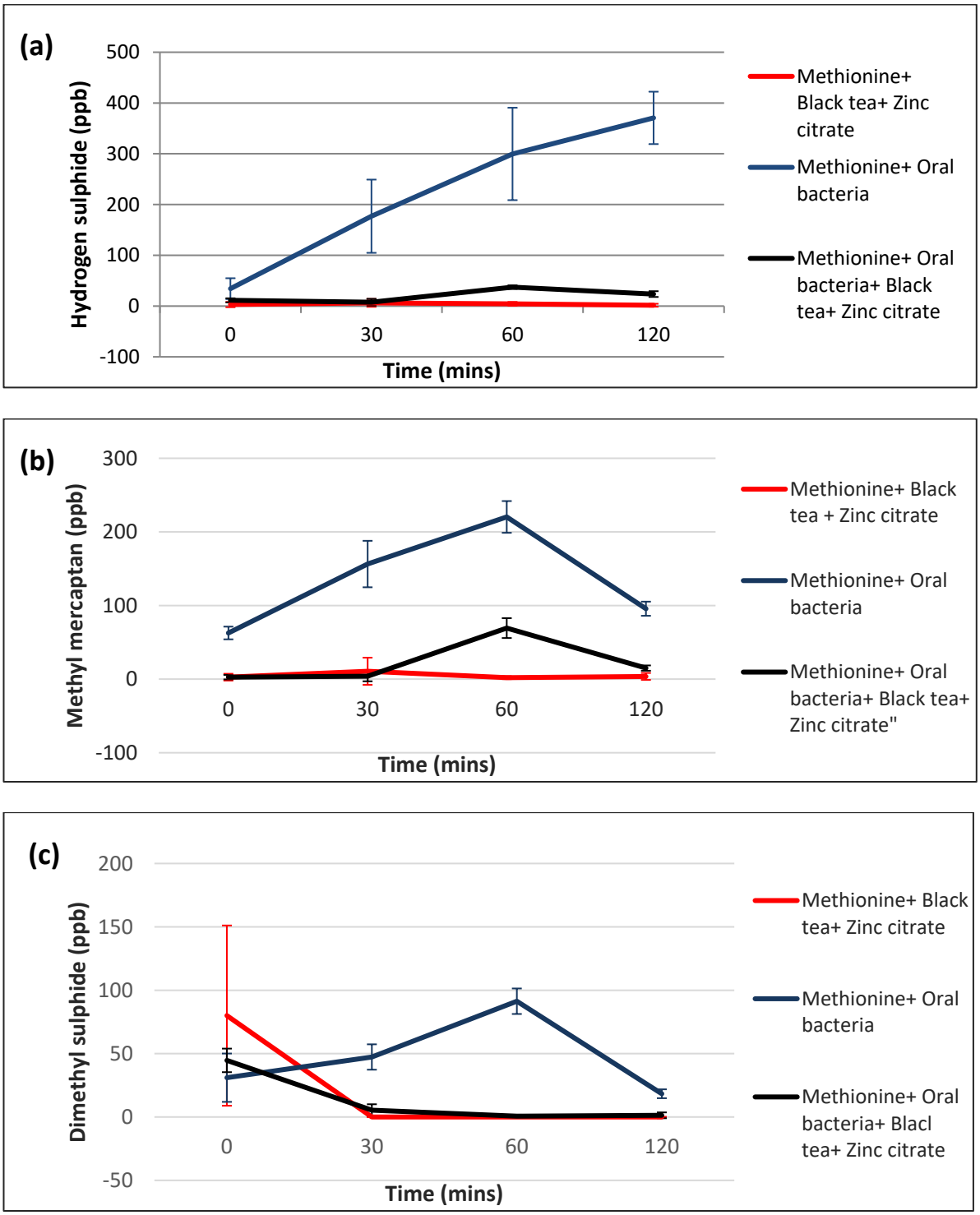

Figure 4.11 a-c. Methionine solutions tested with oral bacteria, black tea and zinc citrate separately (red and blue line respectively) as controls. The black line represents methionine, oral bacteria, black tea and zinc citrate incubated together (a) Hydrogen sulphide, (b) Methyl mercaptan, (c) Dimethyl sulphide output (ppb).

Methionine and oral bacteria incubated together in figure 4.11 (a) produce a steady increase in hydrogen sulphide concentrations. The inhibition of zinc citrate in combination with black tea is less than the inhibition of each of these products alone (measured in separate experiments- fig 4.10 and 4.8), however, is still showing inhibition of hydrogen sulphide emissions with a rise at 60 minutes (under 50 ppb) and 262 ppb lower than the positive control of oral bacteria and methionine (blue line). Zinc citrate+ black tea + methionine incubated together (negative control, red line) does not have a significant interaction producing hydrogen sulphide.

The methionine and bacteria control produce steady rising methyl mercaptan concentrations but decreases from 220 ppb to 93 ppb in the last hour of the experimental procedure. There is a small reaction at 60 minutes that produces some methyl mercaptan from the test of methionine, oral bacteria and zinc citrate+ black tea but not at a significant concentration in terms of halitosis and lower than the positive control (oral bacteria and methionine). The reaction between zinc citrate + black tea and methionine does not produce any methyl mercaptan apart from a small rise to 10 ppb at 30 minutes.

The dimethyl sulphide concentrations released from methionine and oral bacteria increase to 86 ppb at 60 minutes and then fall to 19.67 ppb in the next 60 minutes. The reaction between methionine, zinc citrate and black tea starts at a similar point but decreases as the positive control increases, exhibiting some inhibitory effect on dimethyl sulphide concentrations. The negative control starts with the highest concentration but falls after 30 minutes to the lowest concentration showing variation over time.

ix) Zinc citrate + coffee

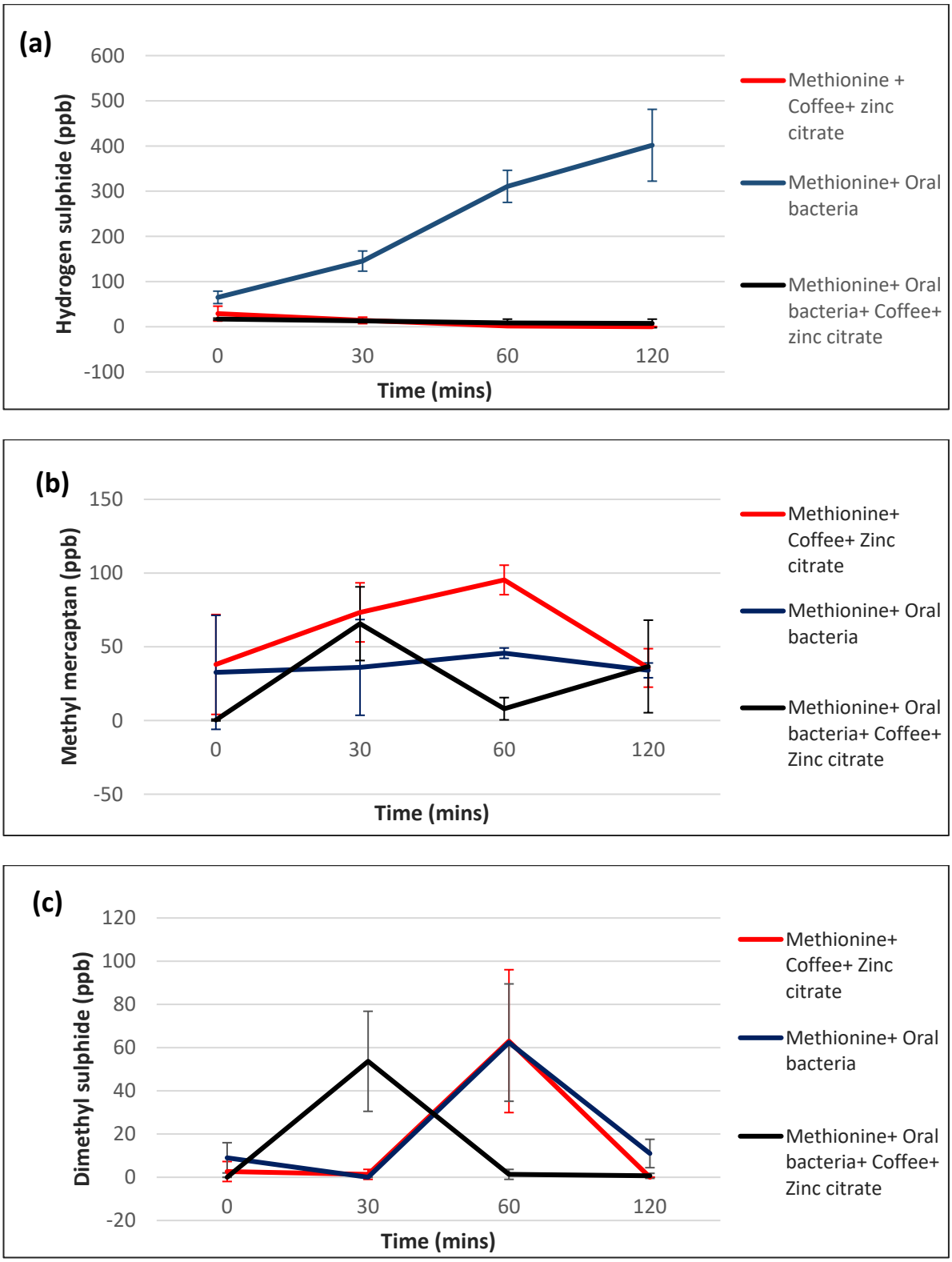

Figure 4.12 a-c. Methionine solutions tested with oral bacteria coffee and zinc citrate separately (red and blue line respectively) as controls. The black line represents methionine, oral bacteria, coffee and zinc citrate incubated together (a) Hydrogen sulphide, (b) Methyl mercaptan, (c) Dimethyl sulphide output (ppb).

The methionine and oral bacteria control show hydrogen sulphide ppb concentrations rising steadily as expected from 65 ppb to 401 ppb over 120 minutes, and the other two reactions (methionine with zinc citrate+ coffee and the test subject of methionine, oral bacteria, zinc citrate + coffee) barely deviates from 0.

When examining methyl mercaptan fig 4.12 (b), the negative control rises to a peak of 94 ppb at 60 minutes, this is higher than the positive control and test solution through the 120 minutes, indicating a reaction between methionine and these two products together (zinc citrate and coffee). The results for the test solutions bounces around variably peaking at 30 minutes and 120 minutes, in both instances rising above the methyl mercaptan ppb in the positive control of methionine with oral bacteria.

For the dimethyl sulphide output the positive and negative controls follow the same trend peaking at 62.3 ppb after 60 minutes and decreasing the next 60 minutes. However, the test solution of all reagents incubated together have an inverse trend, peaking at 30 minutes rising above the controls then decreasing by 60 minutes and stays low in the next 60 minutes.

4.3.3 Percentage changes between methionine and oral bacteria to the addition of crude product

The tables below represent the percentage change between the positive control in the graphs above (figures 4.3 - 4.12) to the test solution of methionine, oral bacteria and crude product, also shown on the graphs. The aim of manipulating that data was to compare and categorise the crude products by their inhibitory action on gas release.

Tables 4.1-4.8 correspond to percentage change between control (methionine and oral bacteria) and test (methionine, oral bacteria and crude products) for each time point.

4.1	**Black Tea**							
Percentage change between Methionine + Oral bacteria AND Methionine + Oral bacteria + Black tea								
Mins	**Hydrogen sulphide % Change**		**Mins**	**Methyl mercaptan % change**		**Mins**	**Dimethyl sulphide % change**	
0	60.345	▼	0	59.663	▼	0	55.881	▼
30	94.742	▼	30	56.014	▼	30	95.441	▼
60	94.659	▼	60	97.584	▼	60	36.587	▼
120	99.58	▼	120	91.667	▼	120	68.893	▼

4.2	**Garlic**							
Percentage change between Methionine + Oral bacteria AND Methionine + Oral bacteria + Garlic (57.1%w/v)- 2004								
Mins	**Hydrogen sulphide % Change**		**Mins**	**Methyl mercaptan % change**		**Mins**	**Dimethyl sulphide % change**	
0	72.249	▼	0	100	▼	0	100	▼
30	42.927	▼	30	100	▼	30	100	▼
60	78.07	▼	60	100	▼	60	100	▼
120	90.017	▼	120	100	▼	120	100	▼

4.3	Zinc citrate + Black tea							
Percentage change between Methionine + Oral bacteria AND Methionine + Oral bacteria + Black tea+ Zinc citrate								
Mins	Hydrogen sulphide % Change		Mins	Methyl mercaptan % change		Mins	Dimethyl sulphide % change	
0	67.087	▼	0	95.746	▼	0	44.084	▲
30	95.669	▼	30	97.441	▼	30	88.733	▼
60	87.542	▼	60	68.533	▼	60	99.271	▼
120	93.615	▼	120	84.32	▼	120	92.728	▼

4.4	Zinc citrate							
Percentage change between Methionine + Oral bacteria AND Methionine + Oral bacteria + Zinc citrate								
Mins	Hydrogen sulphide % Change		Mins	Methyl mercaptan % change		Mins	Dimethyl sulphide % change	
0	85.651	▼	0	15.001	▼	0	0	
30	93.561	▼	30	100+	▲	30	100+	▲
60	99.839	▼	60	80.018	▼	60	0	
120	99.663	▼	120	50.007	▼	120	0	

4.5	Green tea							
Percentage change between Methionine + Oral bacteria AND Methionine + Oral bacteria + Green tea								
Mins	Hydrogen sulphide % Change		Mins	Methyl mercaptan % change		Mins	Dimethyl sulphide % change	
0	76.45	▼	0	84.809	▼	0	100	▼
30	100	▼	30	95.735	▼	30	0	
60	99.694	▼	60	99.578	▼	60	100+	▲
120	100	▼	120	99.116	▼	120	100+	▲

4.6	Black coffee							
Percentage change between Methionine + Oral bacteria AND Methionine + Oral bacteria + Black coffee								
Mins	Hydrogen sulphide % Change		Mins	Methyl mercaptan % change		Mins	Dimethyl sulphide % change	
0	100	▼	0	76.964	▼	0	-93.549	▼
30	55.47	▼	30	100+	▲	30	100+	▲
60	93.643	▼	60	100+	▲	60	100+	▲
120	98.507	▼	120	-100	▼	120	100+	▲

4.7	Zinc citrate + Coffee							
Percentage change between Methionine + Oral bacteria AND Methionine + Oral bacteria + Coffee+ Zinc citrate								
Mins	Hydrogen sulphide % Change		Mins	Methyl mercaptan % change		Mins	Dimethyl sulphide % change	
0	73.846	▼	0	98.981	▼	0	100	▼
30	91.055	▼	30	82.405	▲	30	0	
60	97.317	▼	60	82.481	▼	60	97.861	▼
120	98.174	▼	120	7.841	▲	120	93.945	▼

4.8	Odorless garlic							
Percentage change between Methionine + Oral bacteria AND Methionine + Oral bacteria + Odourless garlic (2mg)								
Mins	Hydrogen sulphide % change		Mins	Methyl mercaptan % change		Mins	Dimethyl sulphide % change	
0	0.35%	▼	0	-5.712	▼	0	100	▲
30	66.50%	▲	30	100+	▲	30	100	▲
60	84.90%	▲	60	100+	▲	60	100	▲
120	98.90%	▲	120	100	▲	120	100	▲

The result from these tables is a percentage analysis completed on the graphs presented in chapter 4 (figure 4.3-4.12). The analysis has been done to show a percentage change

between the positive control of oral bacteria and methionine and the test reaction mixture with added crude products at each time point. Below in table 4.9, products are categorised into gasses they inhibit to simply analyse the products that show potential in VSC reduction from oral bacteria.

Table 4.9. Evaluation of gas inhibition by reviewing tables 4.1-4.8.

Only hydrogen sulphide inhibition	**Inhibition of both hydrogen sulphide and methyl mercaptan**	**Inhibition of hydrogen sulphide, methyl mercaptan and dimethyl sulphide**	**No inhibition on VSCs**
Zinc citrate	Odourless garlic	Garlic	Red wine with alcohol
Instant coffee	Black tea	Black tea + Zinc citrate	Red wine without alcohol
Instant coffee+ Zinc citrate	Green tea		

The products that seem to inhibit all VSC gasses released are Garlic and black tea+ citrate, the combination of black tea and zinc citrate increases the inhibition of methyl mercaptan and dimethyl sulphide concentrations, however zinc citrate and black tea are more prolific inhibitors of hydrogen sulphide alone rather than in combination. Garlic inhibits methyl mercaptan and dimethyl sulphide to 100% at all time points. It is also inhibitory to hydrogen sulphide concentrations but not to the same extent (42-90%).

The red wine assessed was ruled out of further testing and manipulation of results due to the promoting effect to VSC gasses it provided during experimentation (fig 4.4). Whilst odourless garlic is in the inhibitory column for hydrogen sulphide and methyl mercaptan, however, this was only at time point 0 and by 0.35 and 5.7% respectively- therefore not a true contender in potential inhibition of bacterial gas production. Black coffee shows H_2S inhibition ranging from 50%-100%, with some time points (0,120) showing a decrease in methyl mercaptan % concentration showing enough promise to take onto further analysis in chapter 5.

4.4 Discussion

From figure 4.1 It is evident that methionine is not as variable as cysteine seen in chapter 3. Looking at 1% methionine across all three gasses seems the most stable in terms of error and reproducibility. The concentrations of gasses produced remain below the baseline acceptable for a negative control (significance halitosis values*) and gives a solid starting point. Therefore, all subsequent experiments used 1% methionine concentration. In this chapter, oral bacteria from pooled tongue scrapings (method 2.2) were assessed with the addition of methionine, and an array of crude products to quantify their ability to inhibit VSC production from the reaction of bacterial enzymes and amino acid.

Methyl mercaptan concentrations throughout this chapter stay at lower than expected concentrations (figure 4.2) as does dimethyl sulphide apart from a slight rise to 41 ppb at 30 minutes. These are lower than expected as methyl mercaptan is the first gas expected to rise from the addition of oral bacteria with methionine. A higher level is expected as the enzymes from oral bacteria such as methionine gamma lyase (MGL) are more prolific producers of methyl mercaptan (Fukamachi *et al*., 2005).

The conclusion from these experiments is that the methionine with the viable bacteria (Fig 4.2) produces a high level of hydrogen sulphide using 1% methionine, with a very low background production (around 60 ppb) seen in figure 4.1 a,b and c. Although the production of methyl mercaptan and dimethyl sulphide are at insignificant values in term of halitosis, the oral bacteria are also capable of producing hydrogen sulphide from methionine which provides gas ppb values in the range of halitosis. This is therefore a viable model to use for testing against plant extracts, natural products and an inhibitory panel for a possible reduction in hydrogen sulphide production. Bacteria, such as *Veilonella spp*, which is one of the most abundant producers of H_2S (Wahsio *et al.,* 2014) containing methionine degrading enzymes (Kegg pathway for *Veillonella parvula*).

The nutrients in the oral cavity include crevicular fluid, saliva, degenerated cells and amino acids such as methionine available for enzyme catalysis (Kolenbrander *et al*., 2002). Methionine is used as a substrate by bacterial enzymes in the oral cavity which catalyse the production of sulphurous thiols. Methionine gamma lyase (MGL, sometimes seen as METase) a bacterial enzyme can catalyse the alpha- beta (αβ) or alpha- gamma (αγ)

elimination reactions of methionine, homocysteine, cysteine and S-adenosylmethionine producing both hydrogen sulphide and methyl mercaptan (secondary metabolites; alpha keto-butyrate, ammonia, pyruvate). Some methionine can also be converted to cysteine which would subsequently increase hydrogen sulphide output. Methionine can convert to homocysteine via the reverse transulphuration pathway catalysed by S-adenosyl methionine (SAM) followed by cystathionine intermediates leading to the production of cysteine (fig 4.13), which bacterial enzymes such as cysteine desulphydrase utilises to produce more hydrogen sulphide. The cystathionine intermediate is also able to react with homocysteine to produce hydrogen sulphide (Christersson *et al*., 1992; Yoshida *et al*., 2009).

Methyl mercaptan with oxygen and water, catalysed by methyl mercaptan oxidase can react to produce formaldehyde, hydrogen peroxide and hydrogen sulphide (Tangerman, 2009).

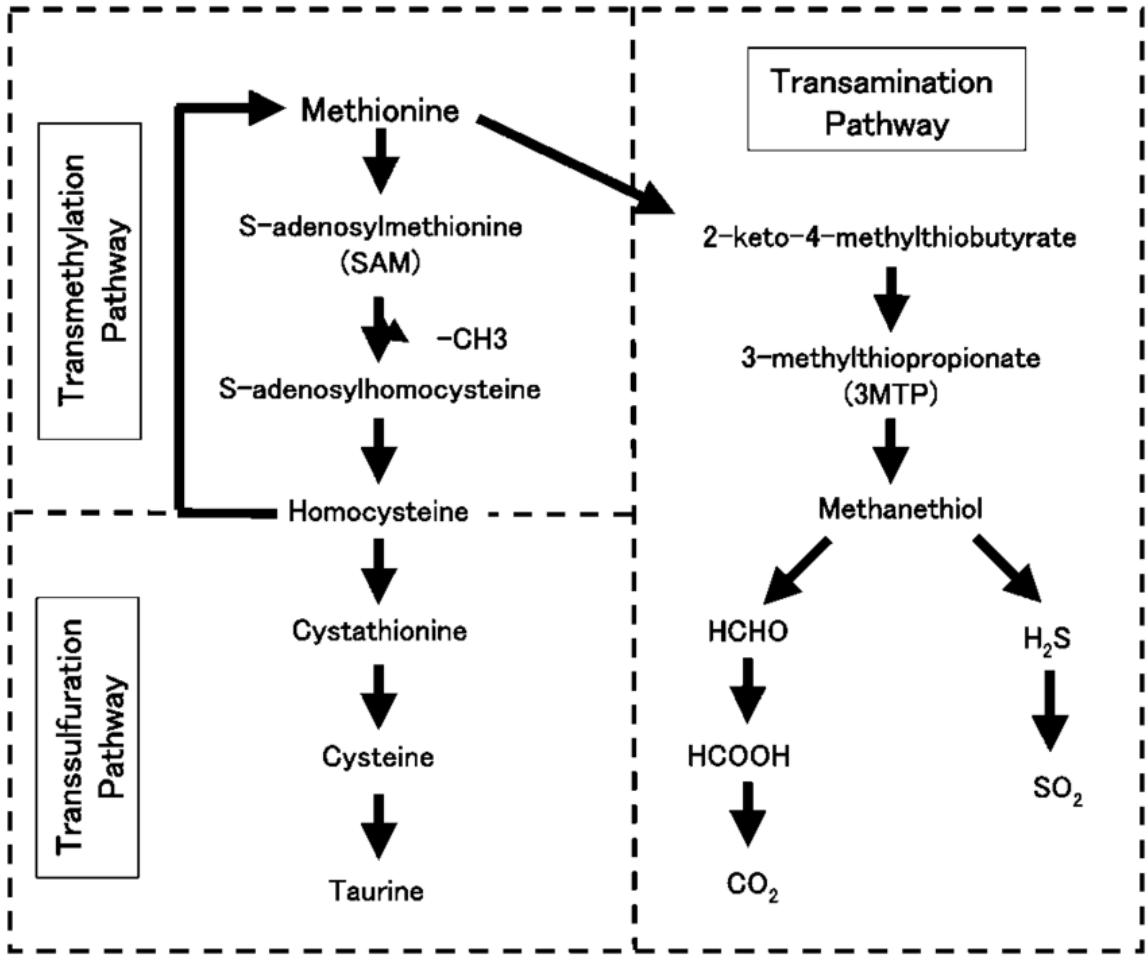

Figure 4.13 Taken from Toue et al., (2006) Diagram showing the basic intermediates between cysteine, methionine through the transmethylation and transulfuration pathways and methionine's products (H_2S, methanethiol (methyl mercaptan)) from the Transamination pathways.

In a study by Basic and colleagues (2015) the method for producing hydrogen sulphide from two distinct methods were investigated- bismuth salt precipitation and methylene blue formation. The results from this suggest there are multiple mechanisms used by bacteria to produce hydrogen sulphide. The difference in hydrogen sulphide production can also be seen between strains of the same bacteria as shown by the differing kinetic results from *F. nucleatum* using cytoplasmic and membrane bound proteins (Yoshida *et al*., 2011). This study concluded that more investigation was required to analyse the hydrogen sulphide production mechanisms/ capabilities in the oral cavity.

H_2S is also the gas produced most readily in current experiments from the batch of tongue scrapings collected and their bacterial compositions, therefore the main bulk of assessment

in chapters 4 and 5 follow the impact on hydrogen sulphide production with the addition of product.

4.4.1 Crude product and methionine analysis

In this current study "crude products" are referred to as each product that was available in shops and supermarkets, unaltered, with all its bioactive components intact, mimicking the effect of everyday solutions on malodourous VSCs.

The results from crude product analysis were analysed in percentage change tables (4.1-4.8) and simplified in terms of gasses inhibited in table 4.9. In the current study it was shown that garlic extract was able to inhibit all three gasses: 90% of hydrogen sulphide and 100% decrease for methyl mercaptan and dimethyl sulphide. In a study by Bakri and Douglas (2005) shown that garlic extract (prepared in the same way as in this thesis) had a killing effect on *P. gingivalis* organisms immediately after incubation, but also had an inhibitory effect on the proteases from this bacteria using BANA hydrolysing and Azcoll hydrolysing assays, conferring with the current research that shows garlic can decrease oral bacteria's ability to produce or release gaseous metabolites over time, once its mechanism is defined (gas neutralising/ antimicrobial/ enzyme inhibition) it can be utilized for potential therapeutic applications. In this current study, however, odourless garlic capsules did not have the same desired effect, only demonstrating a very small inhibitory effects on hydrogen sulphide and methyl mercaptan at time 0. Gasses production was then seen increased through the rest of the time points.

Zinc citrate used in this current study decreased hydrogen sulphide by 99.8%, similar to a study by Burnett and colleagues (2011) that reduced hydrogen sulphide to near 99%. This is attributed to the reaction between zinc ions to thiol groups inhibiting the volatilization of hydrogen sulphide, therefore exhibits gas neutralisation rather than enzyme inhibition. This can be further supported by this research showing that zinc citrate only inhibits the production of hydrogen sulphide and not the other gasses (methyl mercaptan and dimethyl sulphide) through all time points.

Green tea drastically decreased hydrogen sulphide and methyl mercaptan values between 76.45% and 100% *in vitro.* In a study by Rassameemasmaung, Phusudsawang and Sangalungkarn (2013), green tea was given to patients suffering from gingivitis. This study

tested over a 4 week period in which oral rinsing with green tea continued to reduce VSC concentrations from patients *in vivo*, both current and this research imply therapeutic effects of green tea against oral malodour in vitro and in vivo, long term and short term.

Red wine has many chemicals in its composition, and these are made up of phenolic compounds, acids and ethanol. These components can have both beneficial and detrimental effects on the oral microbiome. Ethanol is associated with an increased adherence of S*treptococcus mutan*s associated with the development of caries, in a study performed on rats (Kantorski *et al*., 2007). The red wine graphs in results (Fig 4.4) shows an increase in gas production when incubated with bacteria and methionine (maximum ppb reached- 2467ppb), compared the positive control of just bacteria and methionine and the negative control (red wine and methionine -1532 ppb). Interesting to note that the negative control produces more hydrogen sulphide than the positive, this may indicate a reaction between a product in the wine (or multiple products) and methionine which creates hydrogen sulphide and methyl mercaptan, although heightened by the addition of oral bacteria. *In vivo*, alcohol can reduce the flow rate of saliva and decreasing natural antibacterials' and other proteins such as amylases found in saliva (Enberg *et al*., 2001). Generally, ethanol research exhibits more negative outcomes than positive such as cytological alterations (Reis *et al.,* 2006) and bacterial cell destruction. However, the naturally occurring products within wine have been shown to have a positive effect such as activation of antioxidant chemicals and decreased apoptosis by fibroblasts, and malodour control from epigallocatechin and gallic acid content (Markoski *et al*., 2016). Therefore, the red wine was dealcoholized (boiling to 50% volume decrease) and tested, which produced a similar effect to red wine with alcohol, reacting with methionine to a larger extent than with bacteria and reacting with both together to achieve a maximum hydrogen sulphide ppb, which deems this product unsuitable for the management of malodorous products from oral bacteria.

Black coffee has various effects given its plethora of natural products within the solution; however, these are subject to change during roasting due to the malliard reaction. Products such as caffeine and chlorogenic acid are reduced, whereas trigonelline is methylated into nicotinic acid, with different properties (Budryn *et al*., 2009), Coffee is still a good source of caffeine and other bioactive ingredients and will change based on roasting and brewing process e.g. water temperature/ pressure/ coffee bean type (Beder-Belkhiri *et al*., 2018).

Coffee has been analysed in terms of oral health. One of the main virulence factors *S. mutans* possesses is the ability to adhere to the pellicle surface of the tooth. Medium roasted coffee in a study by Namboodiripad (2009) suggests that there are greater anti-adhesive properties than in other types of coffee, even though some of the bioactive ingredients are decreased in concentration by heat application. The antibacterial effects of coffee against *S. mutans* has been tested too and it was found that the higher the degree of roasting the lower the inhibitory effect, however, increased inhibition was apparent with additions of the individual bioactive ingredients in coffee, such as trigonelline (Almeida *et al*., 2012). In the current chapter, black coffee (instant) as a crude product extract, was able to decrease the hydrogen sulphide measured, but an increase in the other gasses (methyl mercaptan and dimethyl sulphide) was observed.

Some interaction and synergies were observed from the combination of zinc with tea and coffee e.g Black tea enhancing zinc's action against methyl mercaptan, this is most likely a gas neutralisation effect along with enzyme inhibition- this will be investigated in the coming chapters.

Conclusion- Methionine able to synthesise hydrogen sulphide, methyl mercaptan and dimethyl sulphide through a variety of enzymes, intermediates and mechanisms. In this chapter (4) the mechanism of enzyme inhibition cannot be fully studied due to availability of the enzyme within the cell wall (Kuznetsov *et al*., 2014). When the enzyme is readily available in solution, (chapter 5 and 6) kinetics and bioinformatics can display potential rates and interactions between oral bacterial enzymes and natural component/product.

The addition of crude products to whole oral bacteria into the corresponding reaction was analysed. The assessments made in this chapter act as a selection of crude products proving potential to take on to further experiments which could reveal which natural components within the crude products interact with bacterial enzymes to inhibit the release of VSCs, or perhaps the mechanism is gas inhibition, which (Sheng, Nguyen and Marquis, (2005) and others in literature have theorised is the case with zinc products.

The crude products that did work in this chapter such as garlic, zinc citrate and teas have been taken on to the next chapter where natural components from these crude extracts are selected to assess their potential enzymatic activity.

Chapter 5 The effects of methionine on lysed oral bacteria, with the addition of natural products

5.1 Introduction

Within bacteria there are a plethora of enzymes ready to catalyse nutrients such as amino acids into metabolites. Extracting proteins/ enzymes from the cell via lysis techniques is crucial to further study on enzyme kinetics, structure and function (Shehadul *et al*., 2017). Therefore, in this chapter the cell was lysed to allow amino acids and natural products direct access to the enzyme.

There are various methods used to lyse bacterial cells (some of which are attempted in this chapter). Mechanical cell lysis techniques including; French press, sonication, homogenisation, bead-milling and freeze thaw (Bury *et al*., 2001; Mohd Arshad, Amid and Othman, 2015), these techniques break open the cell to release the cytoplasmic contents into solution. Chemical cell lysis aims to cleave the bacterial cell wall. Lysozyme from hen egg white, probably the most used chemical for cell lysis cleaves the polysaccharide chains to release the cytoplasmic contents (Salazar and Asenjo, 2007). Other chemicals such as lysostaphin have a more specific method of cleaving the peptidoglycan cell wall in gram positive bacteria through pentaglycine bridges (mostly staphylococcus species) (Brooks and Jefferson, 2012).

In the current study a mix of 20 mM Tris-HCl, pH 7.5, and CelLytic™ B, a mild non-ionic detergent (Sigma-Aldrich) was used to lyse bacterial cells. This solution was mixed with lysozyme to create a lysis solution which was effective without the need for mechanical disruption. The use of lysed bacteria to study the enzymes in bacteria is an established method, examples of enzymes that have been studied this way include; Methionine gamma lyase (MGL)- (Err-Cheng *et al*., 2005), Cystathionine gamma/beta lyase (Steegborn *et al*., 1999) and B-galactosidase (Wolf, 2002).

5.1.1 Aims

Having tested inhibition of gas production with whole bacteria, it was decided to also explore the behaviour of the cellular components after lysis, to determine whether this

would affect the inhibitory action of the products used (inhibitory panel) with direct access to enzyme binding.

Inhibitory panel: Gallic acid, Zinc chloride, Zinc acetate, Zinc citrate, Nicotinic acid, Trigonelline and caffeine.

5.2 Methods

Method 2.6 Bacterial cell lysis- The working solution to lyse cells was called cellytic b (a premade solution from Sigma Aldrich) method outlined in 2.6.

Gram staining described in method- 2.6.1

2.7 Follow up (modified) headspace model was used. This involved a range of methionine concentrations tested with a lysed, oral bacteria mix and a range of natural product concentrations (replaced by PBS in the positive controls).

Enzyme kinetics were conducted on the headspace data acquired. The data was manipulated to create Michalis-Menten plots on graphpad- shown by graph (d) in figure 5.1 to 5.7, from which Vmax and Km values could also be obtained (appendix 3).

An alternative graph was used plotting the % activity against the natural product concentration extrapolating an Inhibitory concentration at 50% (IC50) shown by graph (e) in figures 5.1 to 5.7.

5.3 Results

5.3.1 Bacterial lysis

A few methods of lysing the bacteria were employed – see method 2.6 for example sonication and the use of chemical mix (lysostaphin and lysozyme). To initially assess the lysis technique, the growth on plates was inspected.

When using both sonication and lysozyme mixture on oral bacteria, the supernatant was grown on agar from which gram-positive bacteria could still be isolated- meaning these cells were still viable. When lysostaphin was tried, viable bacteria still grew, there was a mixed culture of Gram positive and negative bacteria when Gram stained. These techniques did not suffice in lysing the mixed culture of oral bacteria.

The only method that passed this initial screening was a commercial preparation cellytic b showing no growth of bacterial cells on agar. This working solution was compared to whole bacteria with methionine on the oralchroma looking at release of gasses caused by enzyme catalysis. This was to ensure a larger reaction occurred with the free availability of enzyme binding.

Table 5.1. Hydrogen sulphide (H2S) measurements (ppb) from oralchroma analysis of lysed and non-lysed bacterial cells in a solution of PBS and 0.1% Methionine

Time (mins)	0	30	60	120
Lysed (H2S)	207	126	364	292
Non lysed (H2S)	12	27	34	99
Time (mins)	0	30	60	120
Lysed (MM)	69	98	119	68
Non lysed (MM)	30	47	51	18
Time (mins)	0	30	60	120
Lysed (DS)	44	51	84	21
Non lysed (DS)	0	2	16	4

Table 5.1 represents the testing of oral bacteria in 2 different forms (lysed and whole cell) to observe differences over a prolonged period of 2 hours (292 ppb H_2S from lysed vs. 99 ppb from H_2S emitted from whole cell with methionine). The lysed bacteria have an

increased rate of reaction due to the availability of enzymes for a more immediate and larger reaction. The lysed bacteria prepared with cellytic b were taken forward for further testing of interactions with methionine and natural products.

5.3.2 Testing natural products on lysed bacteria

In this section methionine was tested with a range of natural products. These natural products are components that make up the crude products in the previous section, here they are tested for their individual effects on oral bacteria lysate. This is done by analysing the VSCs by using the headspace model. Each dot on the graph denotes a concentration of natural product in solution with a concentration of methionine, plus lysed oral bacteria. From these experiments, Michaelis-Menten plots were used to determine IC_{50} (inhibitory concentration) of the natural product at 0.5% methionine.

i) Gallic acid

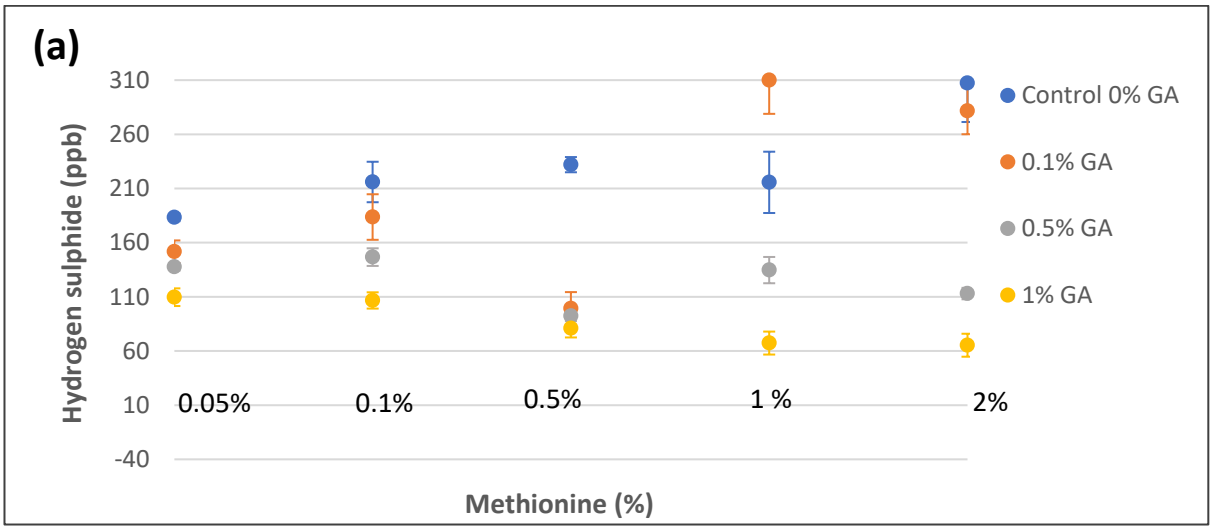

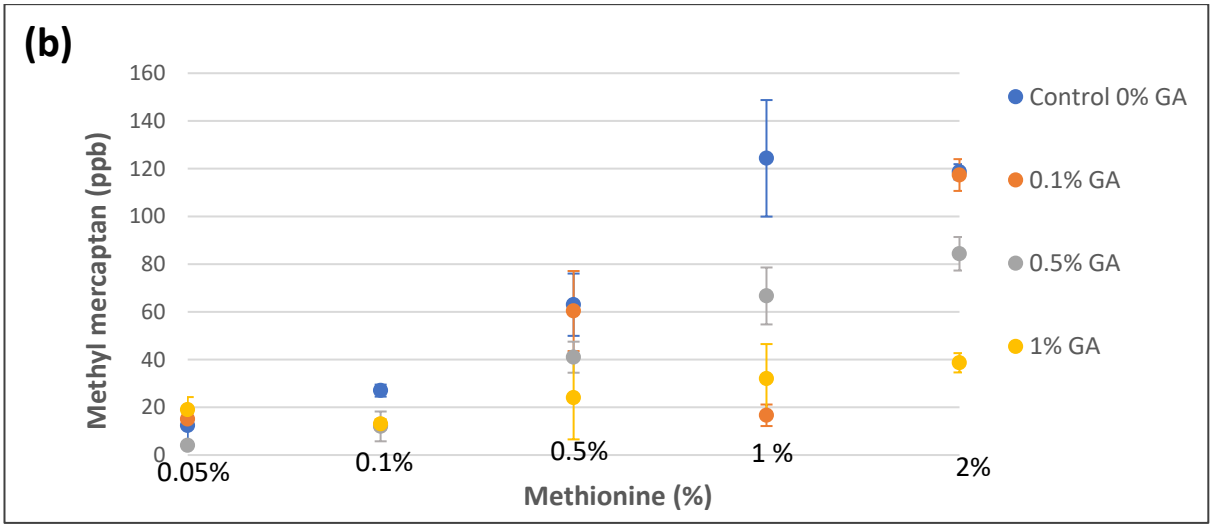

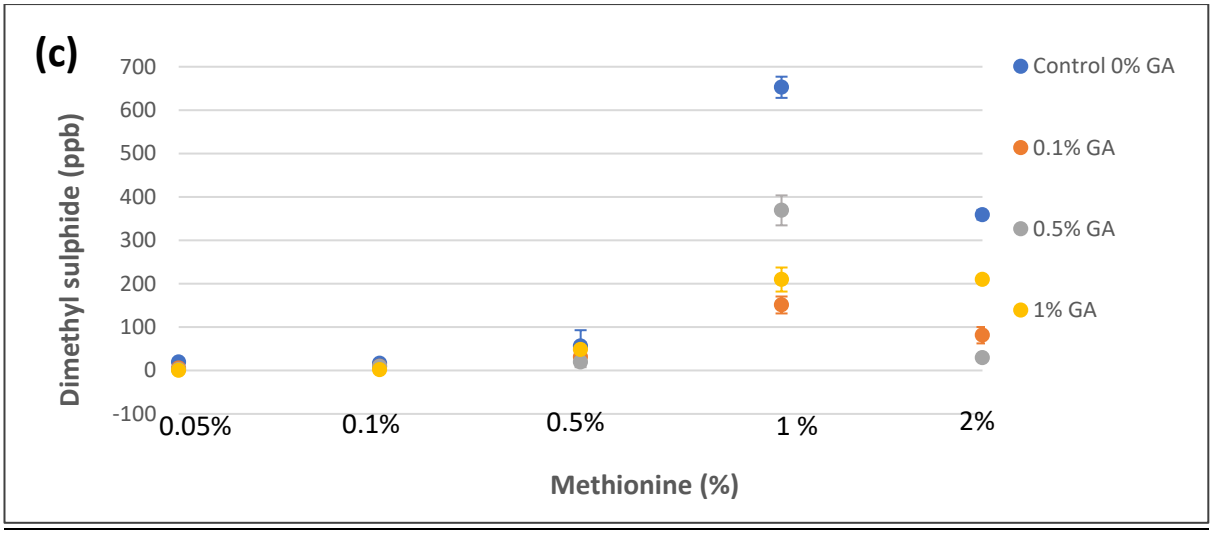

Figure 5.1 a, b, c. Concentrations of gallic acid (GA) tested on lysed bacteria, with increasing concentrations of methionine (x axis) Error bars represent ± SD

Gallic acid vs. Lysed bacteria- Figure 5.1a (H_2S)

As the concentration of methionine increased the production of hydrogen sulphide also increased in the control of methionine and lysed bacteria, as expected. In the control sample, with a methionine concentration of 0.05% the concentration of hydrogen sulphide was recorded at 183 ppb. The addition of increasing levels of gallic acid resulted in a gradual decrease in hydrogen sulphide concentrations from 151.667 ppb to 109.667 ppb. However, the combination of 1% methionine and 0.1% gallic acid, resulted in hydrogen sulphide levels resulted were greater than the control (310 ppb vs 215.667 ppb), indicating a reaction between gallic acid and methionine at this concentration.

There are two interesting trends, the 0.5% and 1% gallic acid inhibition stays relatively stable across all concentrations of methionine with a slight downward trend towards the higher concentration of gallic acid, exhibiting the inhibition more hydrogen sulphide. The second point of interest is that 0.1% Gallic acid has little effect on the H_2S towards the higher concentrations of methionine.

Gallic acid vs. lysed bacteria- figure 5.1b (Methyl mercaptan- MM)

Low levels of hydrogen sulphide are detected for the solutions containing 0.05% methionine. At 0.1% Methionine the control value was 27 ppb for methyl mercaptan and all solutions containing gallic acid decrease this by 14-15 ppb. At 0.5% methionine, there is an expected distribution of results with the highest concentration of inhibitor producing

the lowest concentration of methyl mercaptan and the lowest concentration of inhibitor (0.1% GA) is closest to control, however, it is only 3 ppb lower than the control.

The solutions tested with 1% methionine shows 0.1% Gallic acid has the largest inhibitory percentage (86.5%), followed by 1% (74.2%). At 2% methionine the reactions containing 0.1% gallic acid is shown to be inconsistent where it rises again to 1 ppb short of the control value. 1% Gallic acid has the strongest inhibitory effect on methyl mercaptan production at this high methionine concentration.

Gallic acid vs. lysed bacteria- figure 5.1c (Dimethyl sulphide- DMS)

The control of 0.05% methionine gave a reading of 19.667 ppb which is too low to carry any significance in terms of halitosis. At 0.1% Methionine there is a gradient decrease according to gallic acid concentrations however, the control is 3 ppb lower compared to the reading of 0.05% methionine. There is a drastic change by 1% methionine where the control shoots up to 652 ppb, however the highest concentration of gallic acid did not inhibit the most dimethyl sulphide. 0.1% gallic acid is the most effective at decreasing dimethyl sulphide here at 151 ppb. The control values of dimethyl sulphide ppb drops by 293 ppb between 1 and 2% Methionine, however all solutions containing gallic acid still have an inhibitory effect on dimethyl sulphide outlet (0.5% gallic acid most effective).

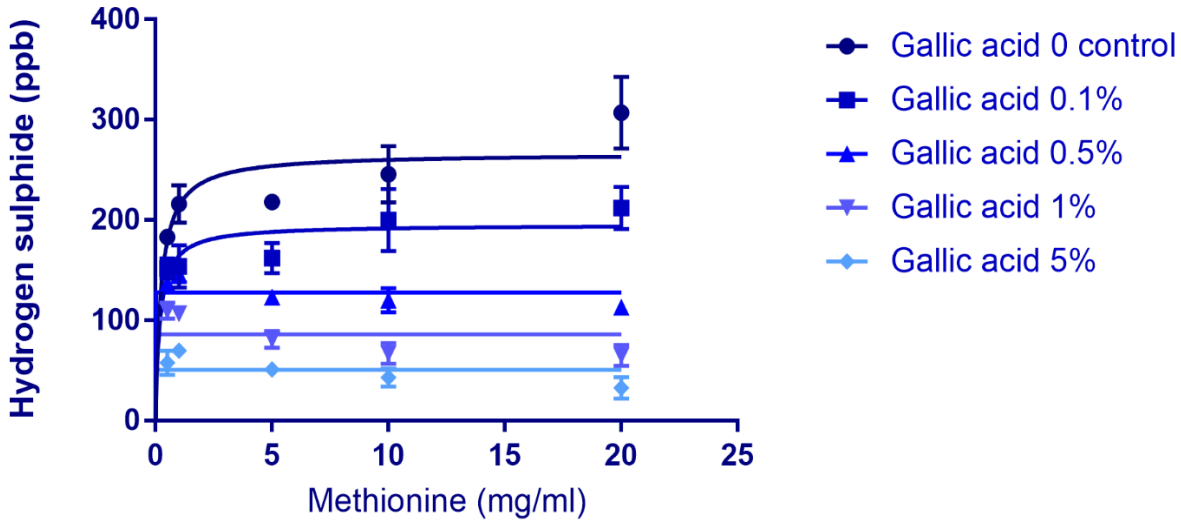

Figure 5.1 d. Michaelis-Menten plot showing gallic acids' effect on hydrogen sulphide from methionine and lysed bacteria (Error bars represent ± SD)

Figure 5.1.d shows a Michaelis-Menten plot of the data in figure 5.1a. (with the addition of 5% gallic acid). From this figure (5.1d) it can be seen that, as the concentration of gallic acid increases, the level of hydrogen sulphide decreases. The highest concentration (5%) gallic acid inhibits H_2S by the largest proportion compared to the control. This trend continues showing that a lower concentration of gallic acid in solution produces higher concentrations of H_2S. This plot was used to extrapolate the Km and Vmax data (table 5.2).

IC50 for Gallic acid using 0.5% (33mM) methionine

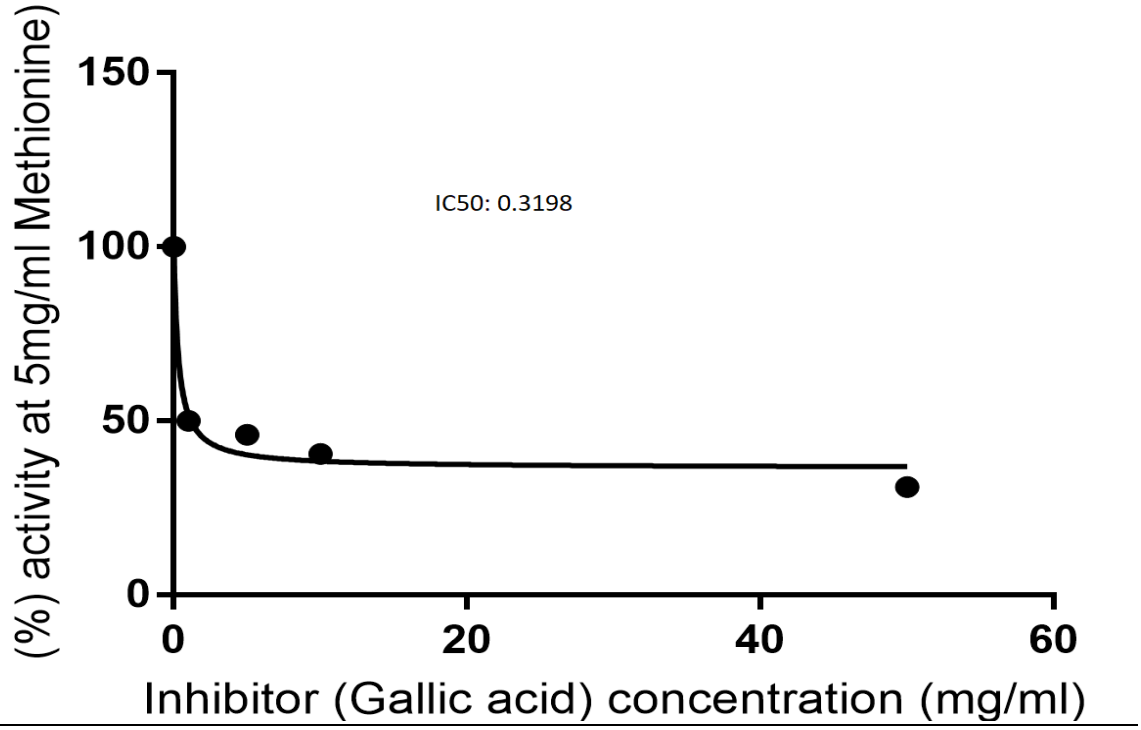

5.1 e. Graph showing the extrapolation of IC50 for gallic acid at 0.5% (5mg/ml) (33mM) Methionine.

This graph looks at the hydrogen sulphide percentage inhibitory activity at gallic acid concentrations. From this, an IC_{50} value is extrapolated and assigned to the natural product- 0.32 mg/ml. This is the concentration of gallic acid necessary to inhibit 50% of hydrogen sulphide released by the activity of methionine (at 5 mg/ml) and lysed bacteria. Whilst this value is low (0.32 mg/ml), the plateau that follows suggests gallic acid in all concentrations inhibits 50% hydrogen sulphide measured from bacterial metabolism of methionine.

ii) Zinc Chloride

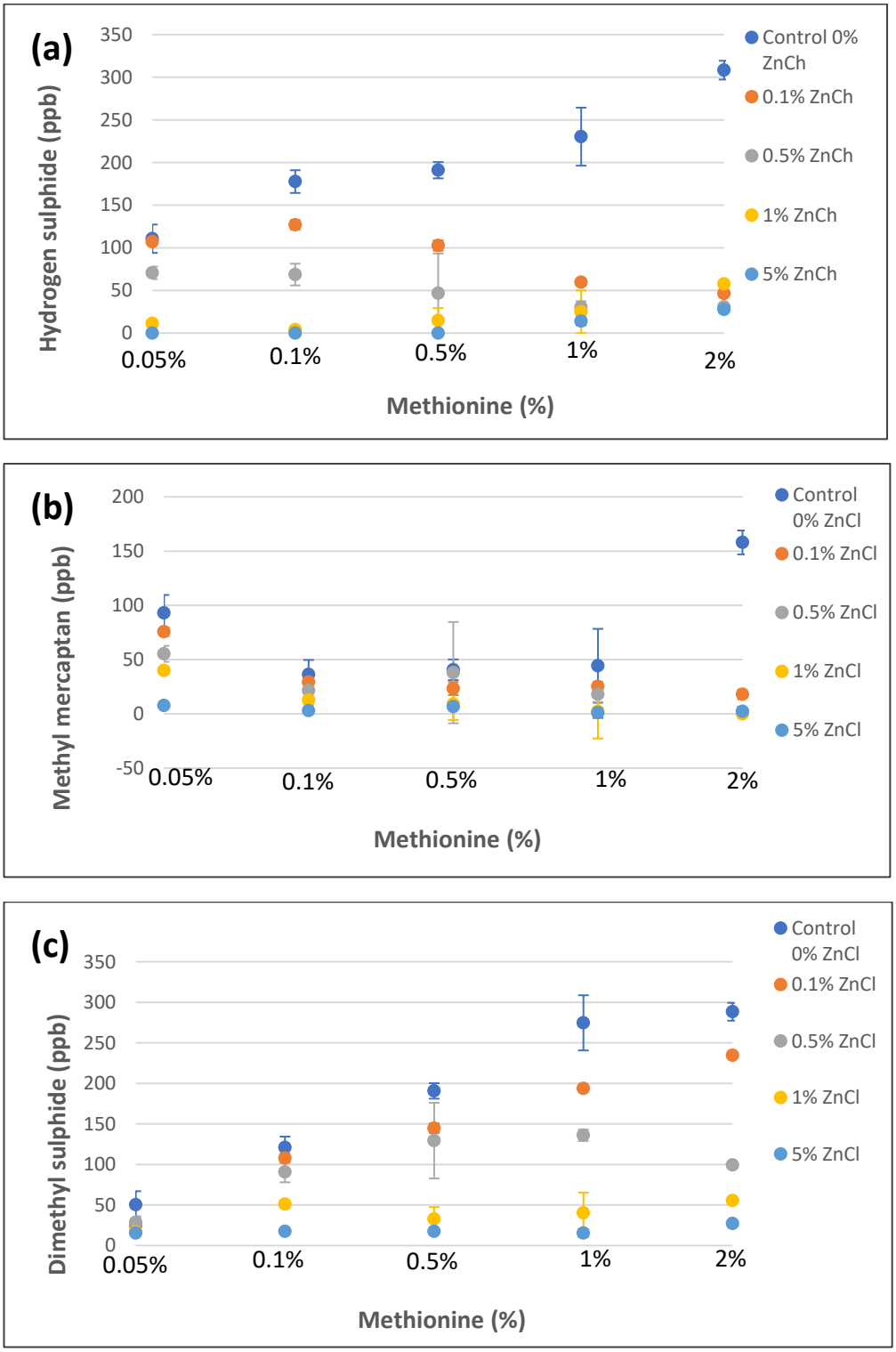

Figure 5.2 a, b, c. Concentrations of Zinc chloride (ZnCl) tested on lysed bacteria with increasing concentrations of methionine (x axis) Error bars represent ± SD

Zinc chloride vs. lysed bacteria- Figure 5.2a (H_2S)

There is a trend wise decrease in hydrogen sulphide ppb when adding increasing concentrations of zinc chloride and as the methionine concentration increases the control values increase. At 0.05% Methionine there is only a 3 ppb difference between the control and 0.1% Zinc chloride. From 1% to 2% methionine, the control ppb increases but this is not mirrored through the addition of zinc chloride which inhibits the solution as well at both methionine concentrations. 0.1% zinc chloride with 1% Methionine (and lysed bacteria) exhibits 59 ppb of hydrogen sulphide (control :230 ppb) but at 2% methionine, 0.1% zinc chloride shows 46 ppb hydrogen sulphide while the control increased to 308 ppb.

Zinc chloride vs. lysed bacteria- figure 5.2b (MM)

The control at 0.05% methionine is 93 ppb, however, as the methionine concentration increases the methyl mercaptan emitted from the control decreases (not the usual trend) up to 0.5% methionine where the methyl mercaptan ppb increases to 2% (158 ppb).

All reactions with zinc chloride in, produce lower methyl mercaptan ppb measurements than the control. At 0.5% methionine, 0.5% zinc chloride inhibits the least methionine only deviating from the control by 2 ppb. 2% Methionine exhibits an increase in methyl mercaptan released from the control, at this methionine concentration the minimum inhibition is from the 0.1% Zinc chloride addition at 88.6% inhibition and the maximum inhibitory concentration being 1% Zinc chloride which reduces methyl mercaptan ppb to 0 (100% inhibition)

Zinc chloride vs. lysed bacteria- figure 5.2c (DMS)

The control of methionine + lysed bacteria shows higher dimethyl sulphide ppb (50.333) than the solutions containing zinc chloride at 0.05% methionine. The maximum inhibition is from the solution containing 5% ZnCl with 69.5% inhibition. There is a graduated decrease at 0.1% methionine, 5% inhibiting the most dimethyl sulphide (85.6%). This gradient is followed through all concentrations of methionine. At 2% methionine the minimum inhibition from 0.1% ZnCl is 18.6% and maximum comes from the solution containing 5% ZnCl (90.6% dimethyl sulphide decrease compared to control).

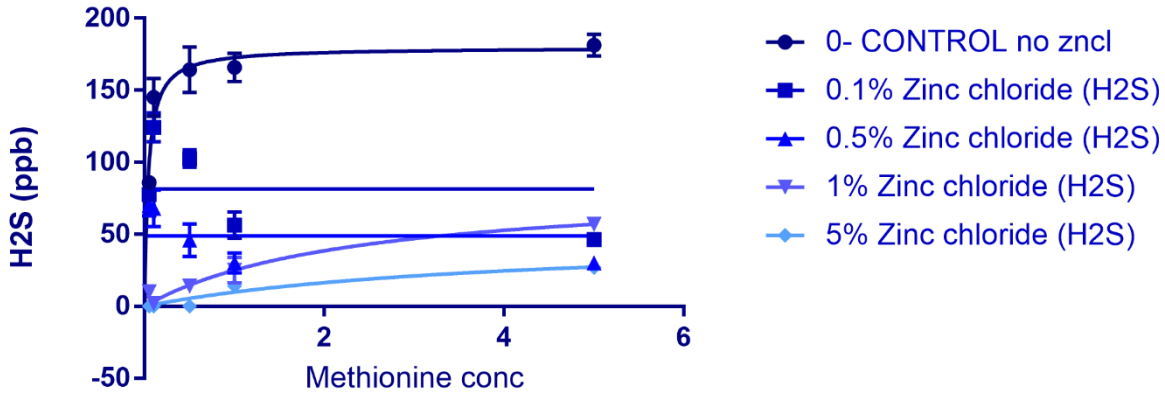

Figure 5.2d. Michaelis-Menten plot showing Zinc chlorides' effect on hydrogen sulphide from methionine and lysed bacteria (Error bars represent ± SD)

The trends in this plot are are variable, reflected in the results, for example 0.1% Zinc chloride is the closest line to the control, however, the points do not sit on this line of best fit and vary between the control values and 0.5% zinc chloride inhibition. 1% zinc chloride starts with very low hydrogen sulphide output but the hydrogen sulphide producing activity increases over methionine concentrations and 1% zinc chloride inhibits less than 0.5% zinc chloride at 20 mg/ml methionine.

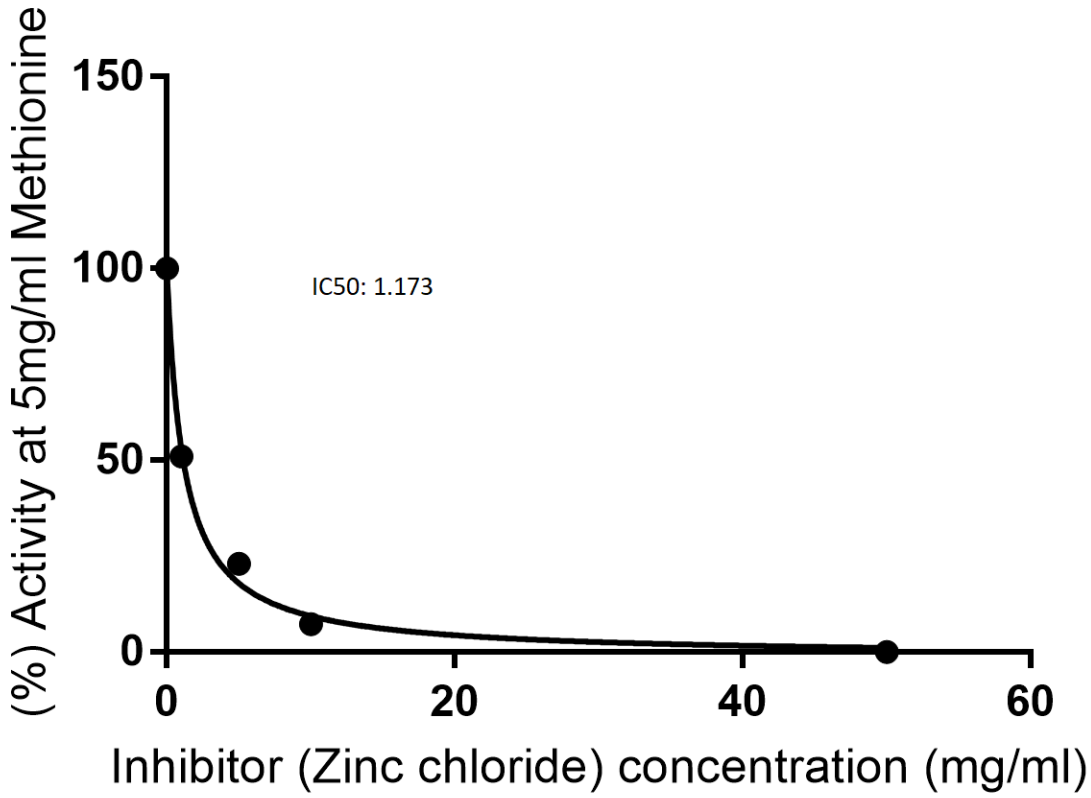

5.2 e. IC50 plot shows hydrogen sulphide producing activity (%) at 5mg/ml methionine with Zinc chloride increasing concentrations

The IC50 value is 1.17 mg/ml, indicating that this concentration of zinc chloride will inhibit 50% hydrogen sulphide being released/measured. 5 and 10 mg/ml zinc chloride reduce hydrogen sulphide output (% methionine activity) respectively. This plot shows that 40-50 mg/ml zinc chloride will inhibit all hydrogen sulphide released from 33mM methionine + lysed bacteria.

iii) Zinc Acetate

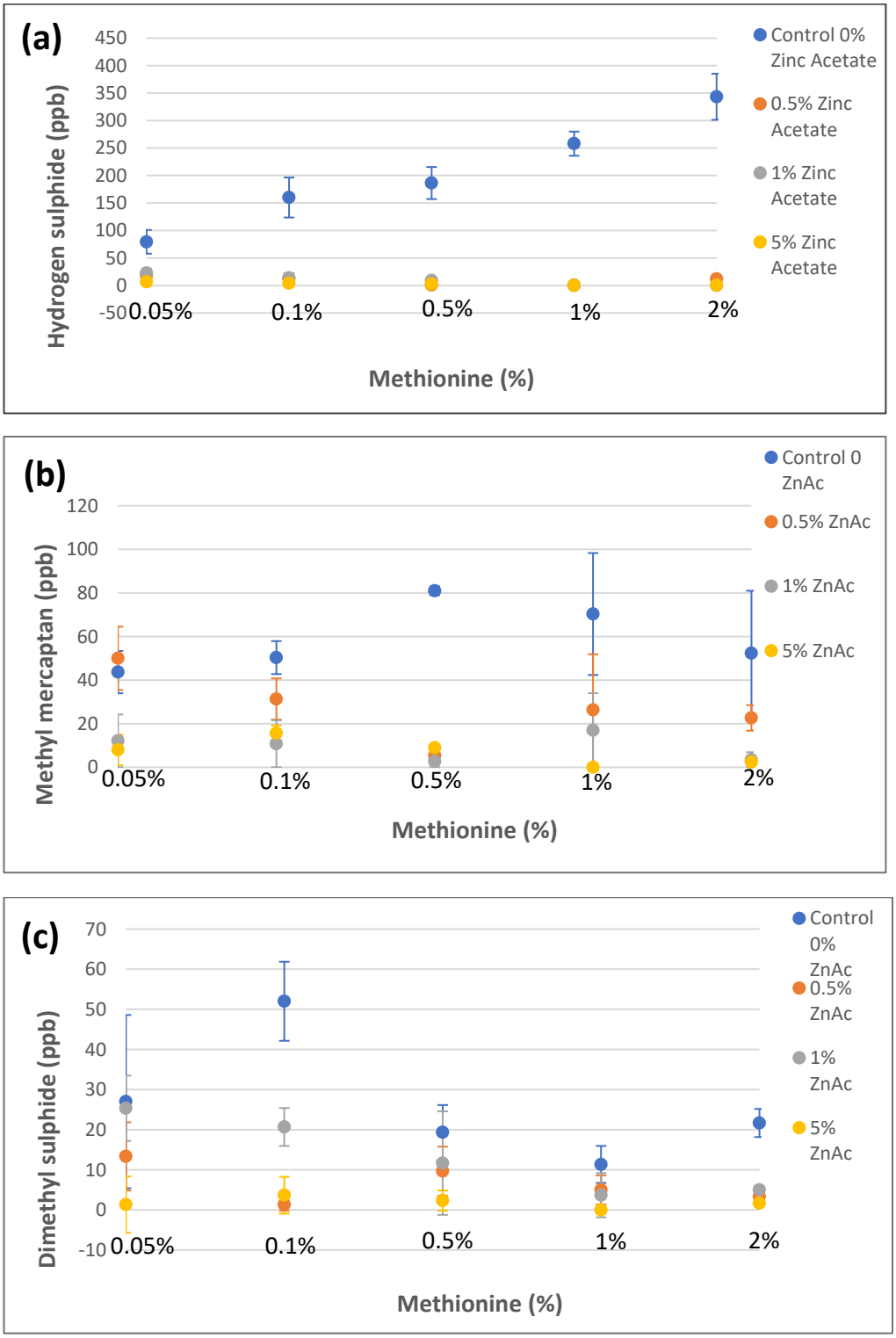

Figure 5.3 a, b, c. Concentrations of Zinc acetate tested on lysed bacteria with increasing concentrations of methionine (x axis) (Error bars represent ± SD)

Zinc acetate vs. lysed bacteria- figure 5.3a (H_2S)

Through increasing concentrations of methionine tested, the control (with lysed bacteria only) increases according to expected trend. All concentrations of zinc acetate tested with the control decreased the hydrogen sulphide output significantly (around 0 ppb). The highest hydrogen sulphide output seen by a solution containing zinc acetate is at 0.05% methionine and 1% zinc acetate which produces 12.333 ppb H_2S. This is insignificant in terms of halitosis.

Zinc acetate vs. lysed bacteria- figure 5.3b (MM)

The control values of methionine and lysed bacteria rise with the rise of methionine concentrations until 0.5% (81 ppb) and decreases for the next two concentrations to 51 ppb at 2% Methionine.

0.5% Zinc acetate incubated with 0.05% methionine and lysed bacteria is 6.7 ppb higher than the control but decreases through the experiment, edging closer in values to the other zinc acetate concentrations of inhibition for methyl mercaptan ending at 21 ppb.

Zinc acetate vs. lysed bacteria- figure 5.3c (DMS)

Control dimethyl sulphide concentrations peak at 0.1% Methionine (51 ppb), then decreases until 1% methionine but increases by 10.3 ppb with 2% methionine. The control values remain higher than the addition of zinc acetate additions through all methionine concentrations (the whole experiment), however, the addition of 1% zinc acetate at 0.05% methionine is only 1.7 ppb lower than the control. 1% Zinc acetate continues to be the least inhibiting concentration of zinc acetate for dimethyl sulphide output.

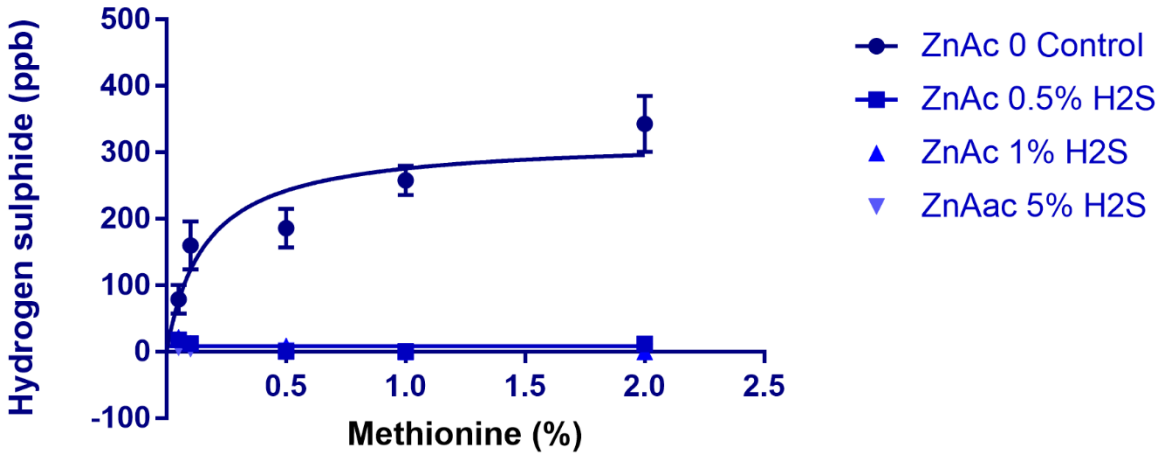

5.3 d. Michaelis-Menten plot showing Zinc acetates' effect on hydrogen sulphide from methionine and lysed bacteria (Error bars represent ± SD)

This graph shows the control increase throughout the experiment and reaching a plateau, zinc acetate decreases hydrogen sulphide to 0 ppb at all concentrations tested. This illustrates a vast reduction of hydrogen sulphide from lysed bacteria and methionine with the addition of zinc acetate at every concentration, attributed to gas neutralisation or enzyme inhibition (see discussion).

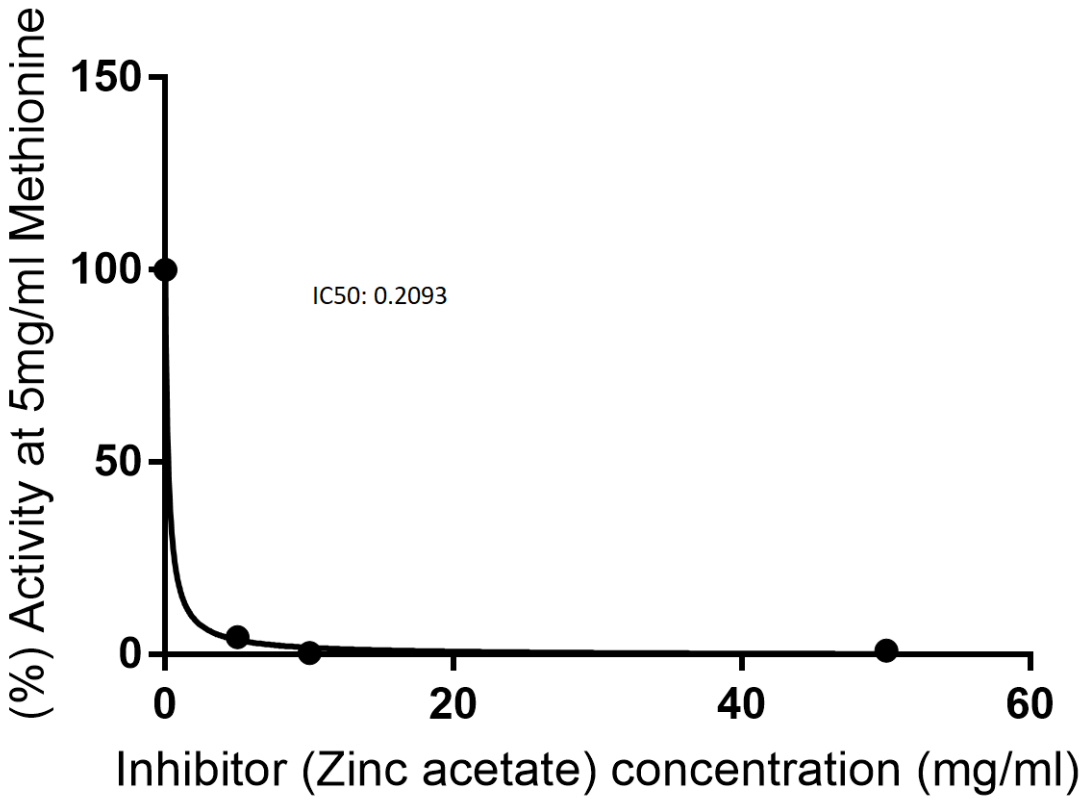

5.3 e IC50 plot shows hydrogen sulphide producing activity (%) at 5mg/ml methionine with Zinc acetate increasing concentrations

This low IC50 (0.2) is expected as 0.5 – 5% zinc acetate inhibited most of the hydrogen sulphide production/ measurements from methionine and lysed bacteria (Fig 5.3 a, d). By 10 mg/ml zinc acetate, no hydrogen sulphide is released shown by 0% methionine activity on graph 5.3 e.

iv) Nicotinic acid

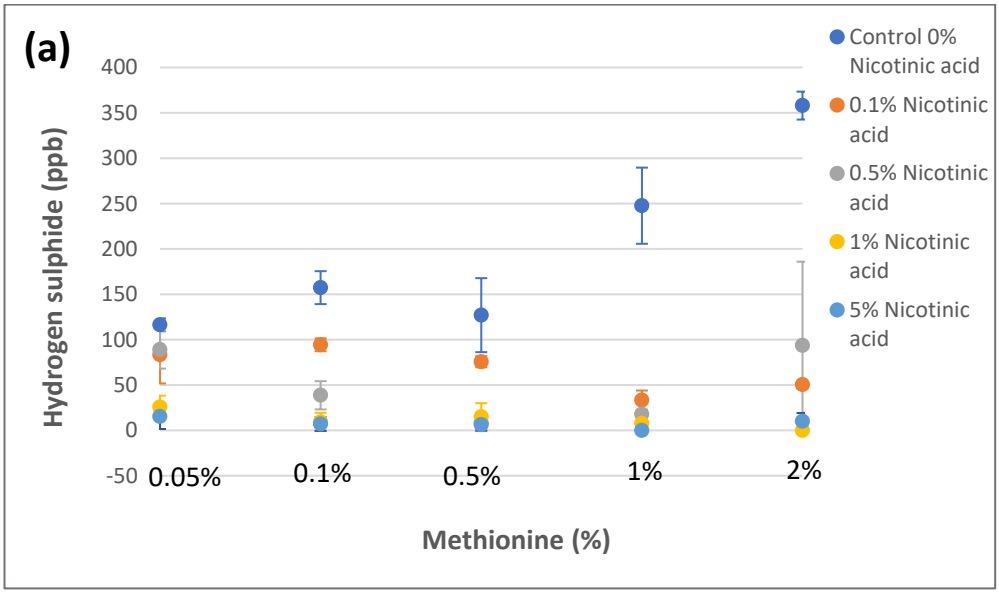

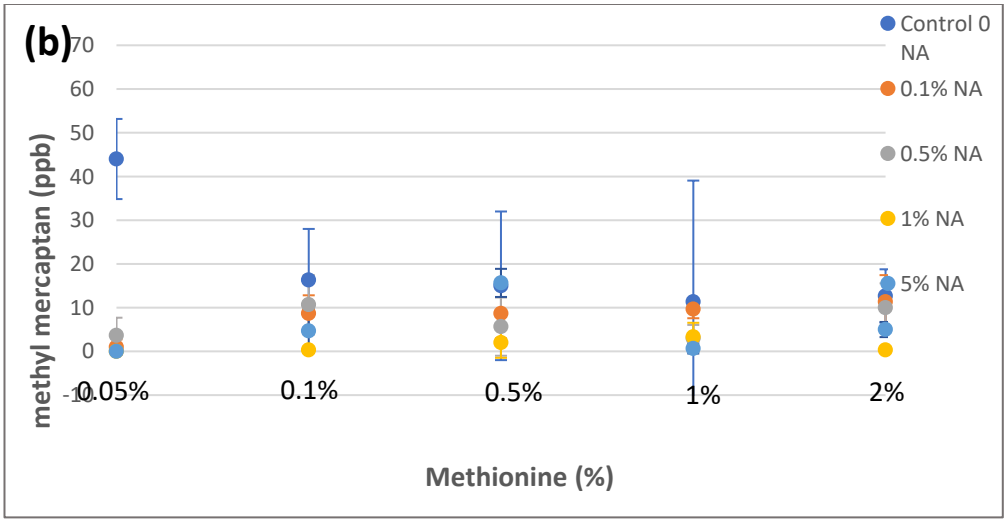

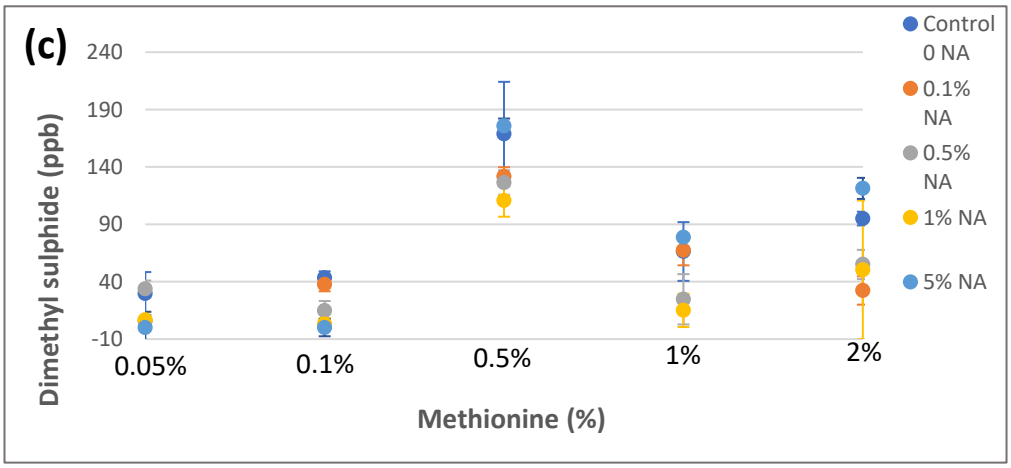

Figure 5.4 a, b, c. Concentrations of Nicotinic acid tested on lysed bacteria against increasing concentrations of methionine (x axis) (Error bars represent ± SD)

Nicotinic acid vs. Lysed bacteria- figure 5.4a (H_2S)

Methionine at 0.05% shows an expected decrease of hydrogen sulphide in accordance to increasing nicotinic acid concentrations (except 0.5% nicotinic acid, which produced 6 ppb more hydrogen sulphide than 0.1% nicotinic acid). A similar picture is seen throughout methionine concentrations. However, at 2% methionine, 0.5% nicotinic acid inhibits the least hydrogen sulphide, still 265 ppb below the control- but with high degree of error (50 ppb).

Nicotinic acid vs. Lysed bacteria- figure 5.4b (MM)

All concentrations of nicotinic acid decrease the methyl mercaptan released by the control. From 0.05% methionine to 0.1% the control ppb of methyl mercaptan from methionine and lysed bacteria decreases, this is not the expected trend for a positive control (this may partly be explained by a high degree of error seen by large error bars). Solutions containing nicotinic acid still decrease the methyl mercaptan output. Nicotinic acid at 1% tested with lysed bacteria and 2% methionine shows the largest reduction in ppb.

Nicotinic acid vs. Lysed bacteria- figure 5.4c (DMS)

Nicotinic acid at 5% is the most inhibitory concentration to dimethyl sulphide release at 0.05% methionine as is expected. However, 0.5% nicotinic acid is unexpectedly above the control value (methionine 0.05% + lysed bacteria). At 0.1% methionine there is a decrease in order of nicotinic acid concentrations, except 0.5% methionine, where solution containing 5% nicotinic acid is 7 ppb higher than the control. At 1% methionine, 5% NA is still producing more dimethyl sulphide than the control and 0.1% NA is higher than control by 1 ppb, however 0.5% NA inhibits the control by 62.8% and 1% NA by 77.3%.

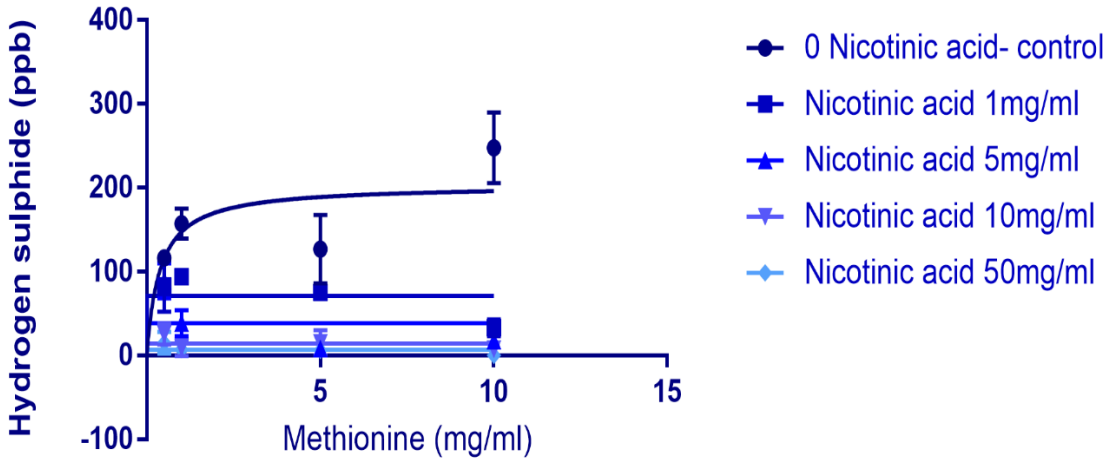

5.4 d. Michaelis-Menten plot showing Nicotinic acids' effect on hydrogen sulphide from methionine and lysed bacteria (Error bars represent ± SD)

Nicotinic acid at all concentrations lowers the hydrogen sulphide ppb as the solution with 0% nicotinic acid rises (with a slight dip at 5mg/ml methionine). 50 and 10 mg/ml nicotinic acid in the solution decreases the control to the largest extent, respectively, followed by 5 mg/ml and 1 mg/ml which do not increase past 90 ppb.

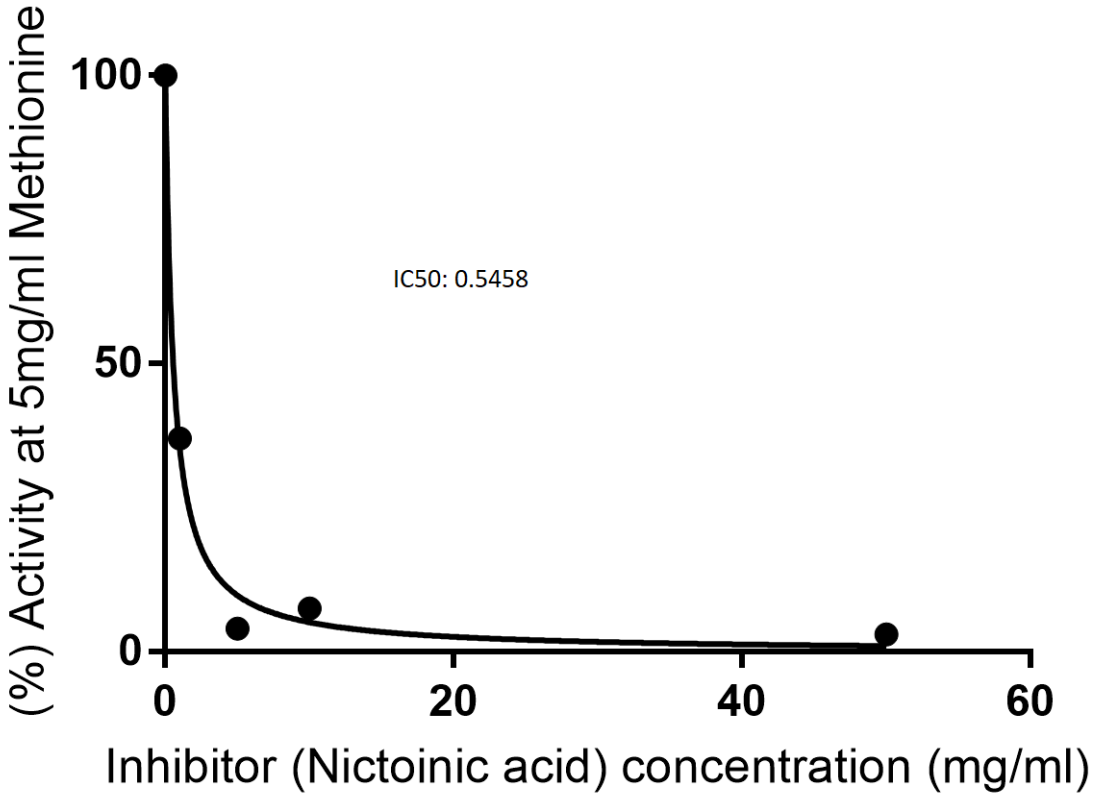

5.4 e. IC50 plot shows hydrogen sulphide producing activity (%) at 5 mg/ml methionine with nicotinic acid (NA) increasing concentrations

Nicotinic acid displays an IC50 of 0.55 mg/ml, there is a decrease towards 0 for the next point (5 mg/ml) but this is not captured by the line of best fit as 10 mg/ml shows a slight increase in methionine activity producing hydrogen sulphide. The line plateaus and percentage methionine activity slowly decreases to 0 with increasing concentrations of nicotinic acid.

v) Caffeine

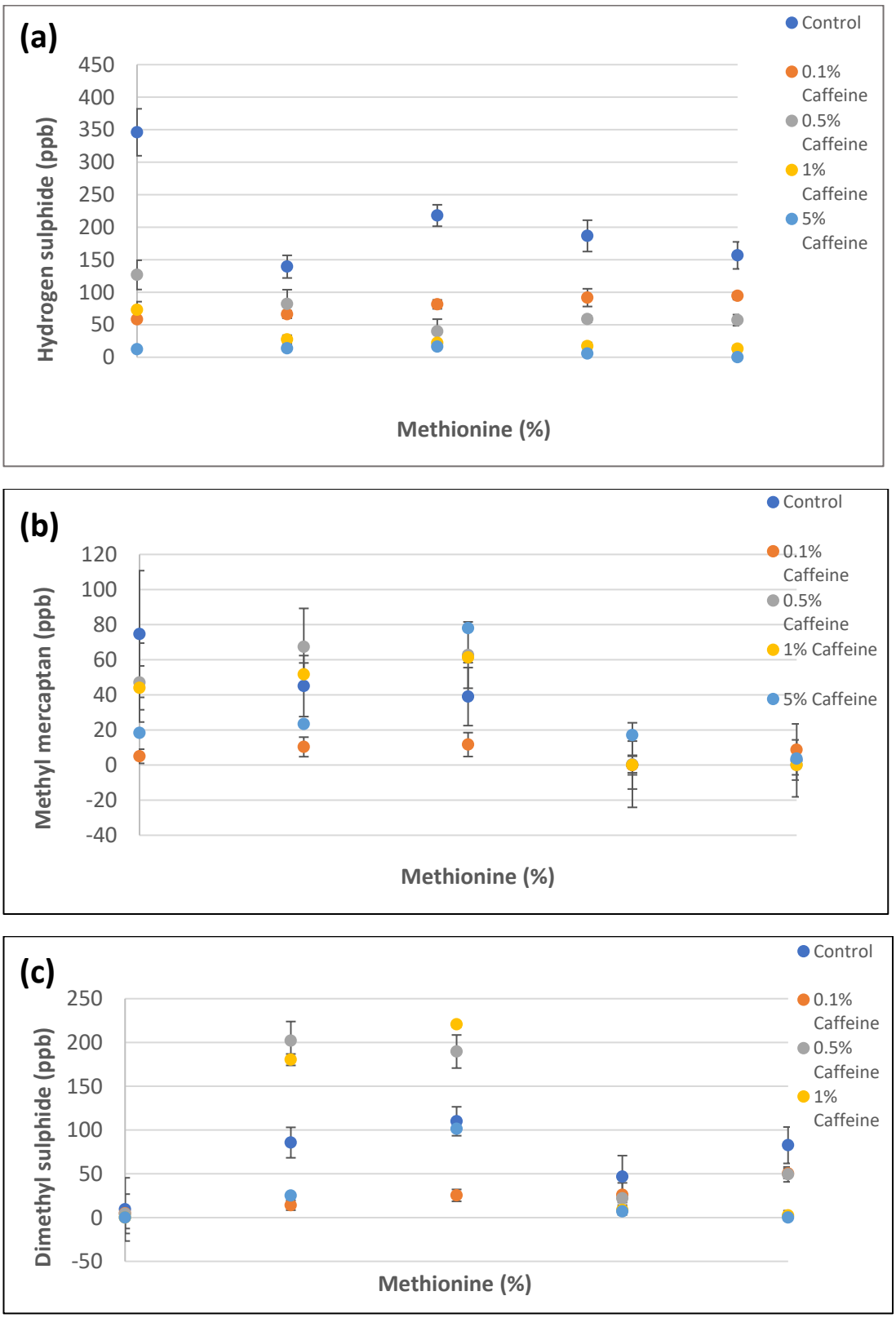

Figure 5.5 a, b, c. Concentrations of Caffeine tested on lysed bacteria with increasing concentrations of methionine (x axis) (Error bars represent ± SD)

Caffeine vs. Lysed bacteria- figure 5.5a (H_2S)

The control decreases from 346 ppb to under 150 ppb between 0.05% and 0.1% Methionine, this is not the expected trend with adding more substrate, this then increases by 79 ppb culminating at 218 ppb by 0.5% methionine but continues to decrease from here. 5% Caffeine added inhibits the production of hydrogen sulphide almost fully- highest at 0.5% methionine (16 ppb- which is not significant in terms of halitosis), 1% Caffeine follows this same trend but at lowest end of methionine added (0.05%) 1% Caffeine in solution produces 15 ppb more hydrogen sulphide than the addition of 0.1% caffeine. 0.5% at this concentration inhibits the least hydrogen sulphide (still 220 ppb less than control), 0.5% caffeine remains the least inhibitory solution until 1% methionine, where there is a trend wise gradient decrease in order of caffeine (%) in solution. This trend is sustained at 2% methionine.

Caffeine vs. Lysed bacteria- figure 5.5b (MM)

The results from this graph show that the control decreases with an increasing methionine concentration which is not the usual trend. Interestingly the solution containing 0.1% caffeine produced the least methyl mercaptan of all solutions including control of methionine+ lysed bacteria (with no caffeine). This is sustained until 1% methionine, where solutions with caffeine present are very similar levels to the control- with 5% caffeine producing the most methyl mercaptan. By 2% methionine all ppb readings for solutions, including the control are very similar between 0-8.66 ppb, the most methyl mercaptan produced is by 0.1% caffeine (with lysed bacteria and 2% methionine) at 8.667 ppb methyl mercaptan.

Caffeine vs. Lysed bacteria- figure 5.5c (DS)

At 0.05% methionine, all solutions (with and without caffeine) barely give a reading above 0 ppb. By 0.1% methionine, 0.5% and 1% caffeine show higher dimethyl sulphide concentrations than the control, but 0.1 and 5% caffeine solutions show concentrations 20-30 ppb lower than the control, this trend continues to the next methionine concentration (0.5%) but 5% produces more dimethyl sulphide with the increase of methionine (9 ppb less than control). By 1% methionine, all solutions containing caffeine fall under the 46 ppb

control with 5% inhibiting the most dimethyl sulphide; 7 ppb. As the concentration of methionine increases by another 1% (2% methionine) the trend remains the same with an increased control value, 5% and 1% caffeine inhibit dimethyl sulphide release completely whereas, 0.1 and 0.5% increase with the control and produce 33 ppb less than the control value of 82 ppb.

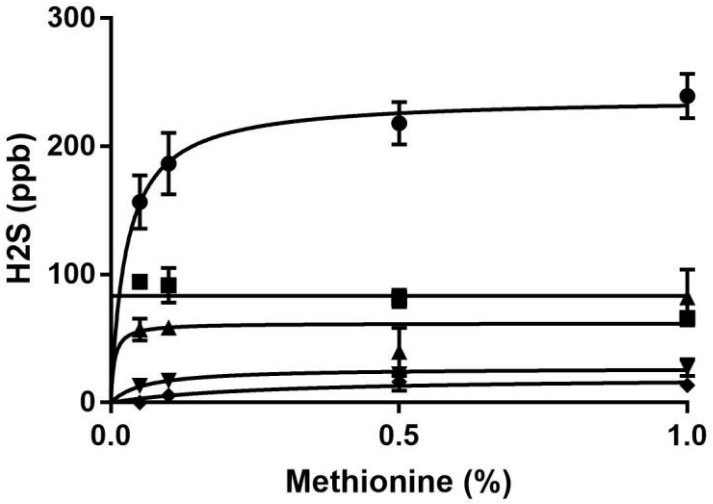

5.5 d. Michaelis-Menten plot showing caffeine's effect on hydrogen sulphide from methionine and lysed bacteria (Error bars represent ± SD)

There is a graduated decrease in hydrogen sulphide concentration with an increasing caffeine concentration. Solutions containing caffeine do not show any increase above 100 ppb, whilst control values of lysed bacteria and methionine displays a rise to over 200 ppb.

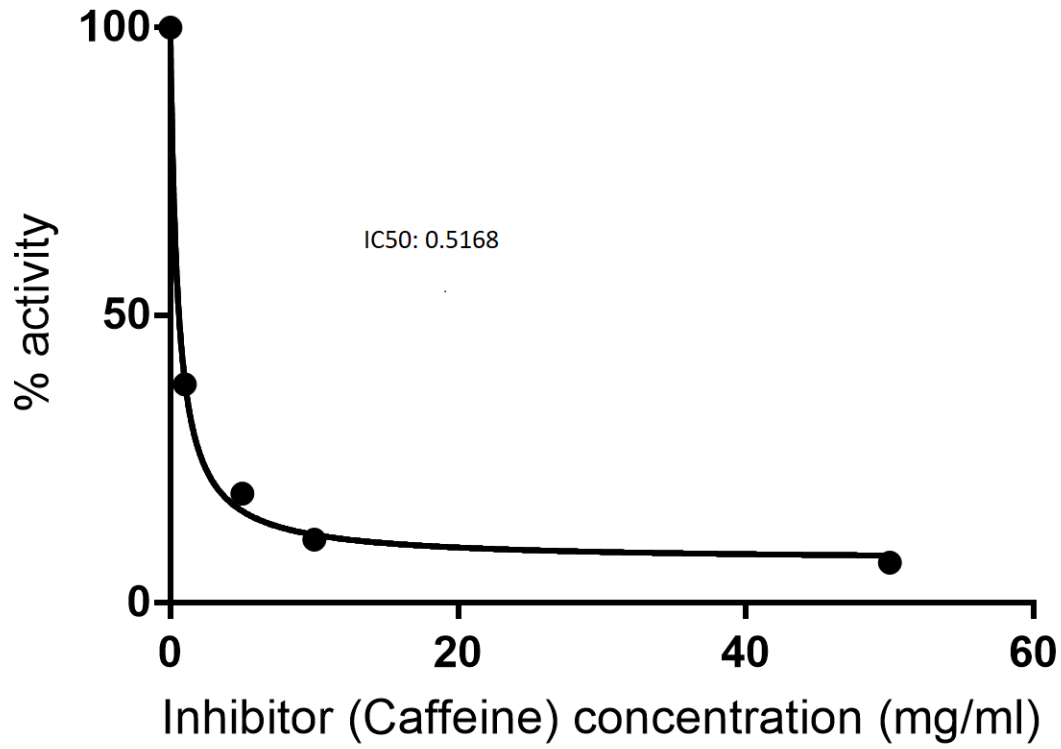

5.5 e. IC50 plot shows hydrogen sulphide producing activity (%) at 5 mg/ml methionine with caffeine increasing concentrations

Caffeine exhibits an IC50 of 0.52 mg/ml, rapidly decreasing methionine % activity to release hydrogen sulphide. However, the graph also shows a plateau at 10 mg/ml caffeine, not significantly decreasing hydrogen sulphide/ methionine % activity between 10 mg/ml and 50 mg/ml caffeine. Full inhibition can therefore not be seen with caffeine concentrations, which results in a less accurate IC50.

vi) Trigonelline

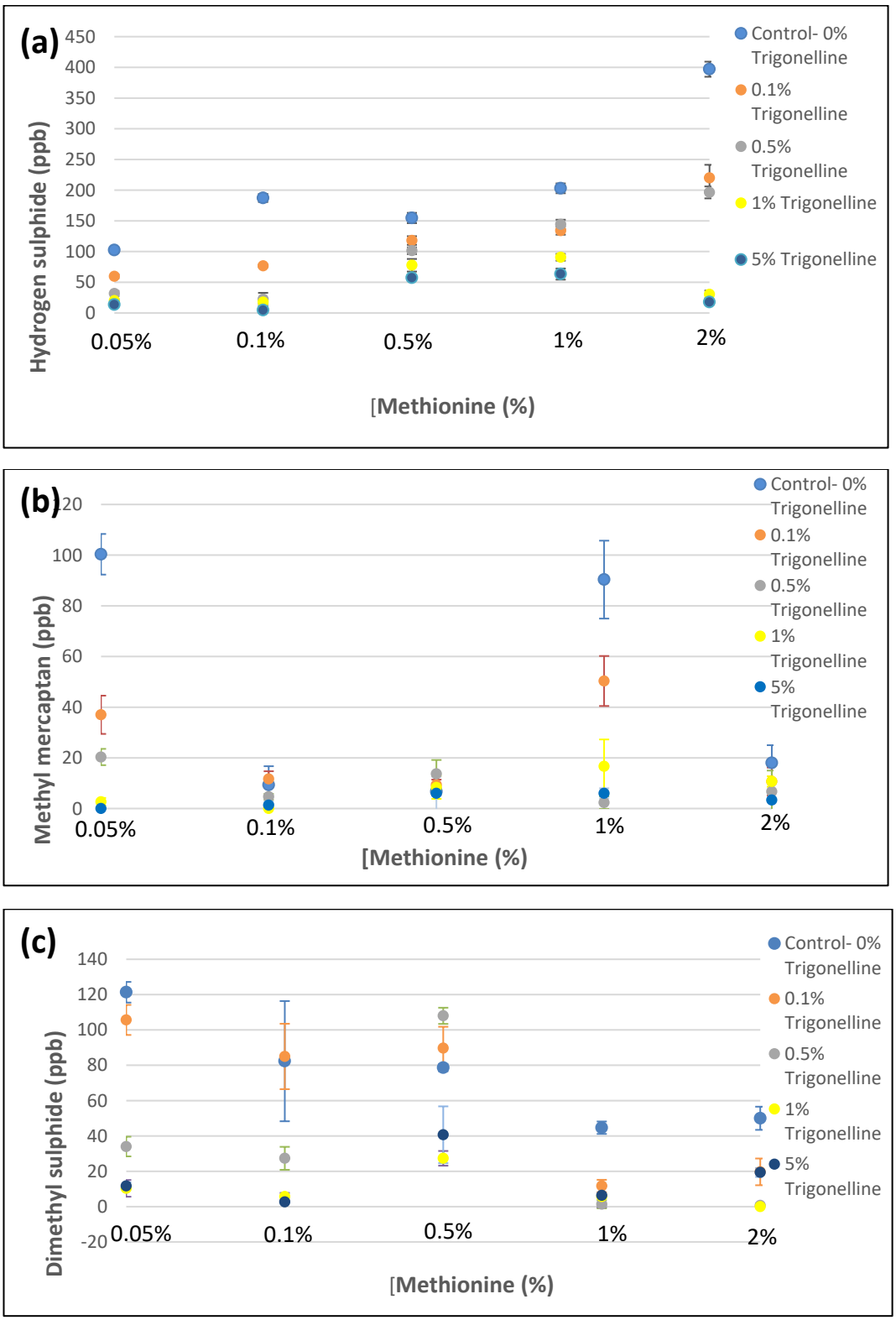

Figure 5.6 a, b, c. Concentrations of trigonelline tested on lysed bacteria with increasing concentrations of methionine (x axis) (Error bars represent ± SD)

Trigonelline vs. Lysed bacteria- figure 5.6a (H_2S)

The control of lysed bacteria with methionine rises according to methionine concentration (except for a minor decrease at 0.1 and 0.5% methionine). Solutions containing trigonelline also rise in the presence of increasing methionine, as the control does, but not above the control values. Throughout all methionine concentrations 0.1% inhibits the least hydrogen sulphide with 5% inhibiting the most representing a trend wise decrease of hydrogen sulphide. The exception being at 1% methionine, where 0.1% inhibits hydrogen sulphide by 10 ppb more than 0.5% trigonelline.

Trigonelline vs. Lysed bacteria- figure 5.6b (MM)

Results for methyl mercaptan are variable with the highest control value at 0.05% methionine (100.333 ppb) which shows inhibition by every trigonelline solution 0-37 ppb (0.1-5% trigonelline respectively). This control then decreases to under 20ppb by 0.1% methionine, along with all trigonelline containing solutions, this trend is seen at 0.1, 0.5 and 2% methionine. At 1% methionine, the control reaches 90 ppb, 0.1% trigonelline inhibits this rise the least (40 ppb lower), and 0.5% trigonelline inhibits even more than 5% (by 3.7 ppb).

Trigonelline vs. Lysed bacteria- figure 5.6c (DMS)

The control steadily decreases through increasing methionine concentrations, 0.1% trigonelline closely follows this trend increasing above the control at 0.1 and 0.5% methionine and decreases below the control inhibiting as much as 5% trigonelline at 1 and 2% methionine. 1% and 5% trigonelline values of dimethyl sulphide stay below 40 ppb through the experiment as does 0.5% trigonelline except for at 0.5% methionine where dimethyl concentrations of 0.5% trigonelline rises above the control (and 0.1% trigonelline)

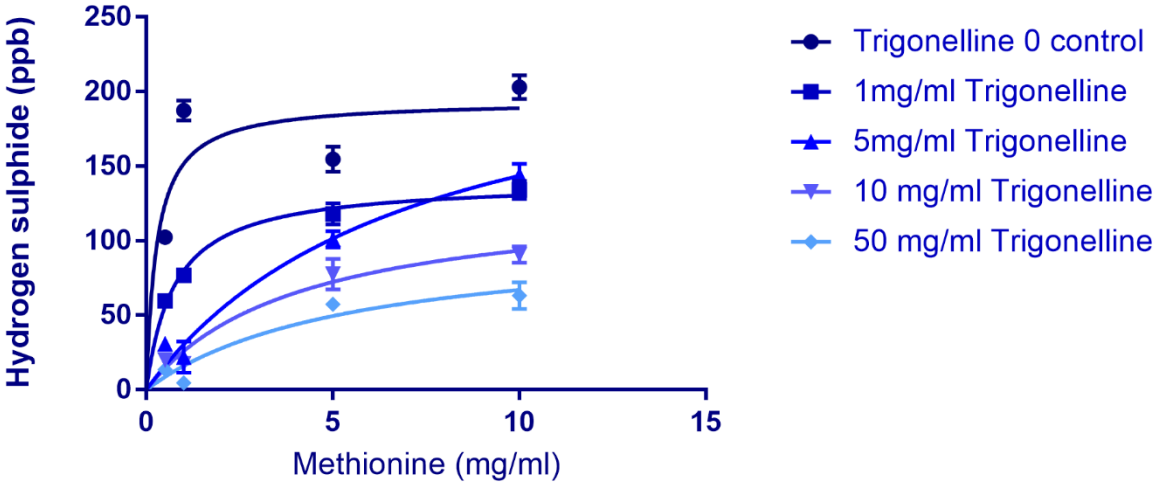

5.6 d Michaelis-Menten plot showing Trigonellines' effect on hydrogen sulphide from methionine and lysed bacteria (Error bars represent ± SD)

The trigonelline concentration of 5 mg/ml of starts having a normal trend, sitting between 10 mg/ml (with more of an inhibitory effect on hydrogen sulphide) and 1 mg/ml (less inhibitory), however, in the concentrations between 5 and 10 mg/ml of methionine, 5 mg/ml of trigonelline rises above 1 mg/ml to become less inhibitory to hydrogen sulphide concentrations. None of the solutions containing trigonelline reach 150 ppb, while the control (methionine and lysed bacteria) concentrations of hydrogen sulphide trend from 100 ppb to just under 200 ppb.

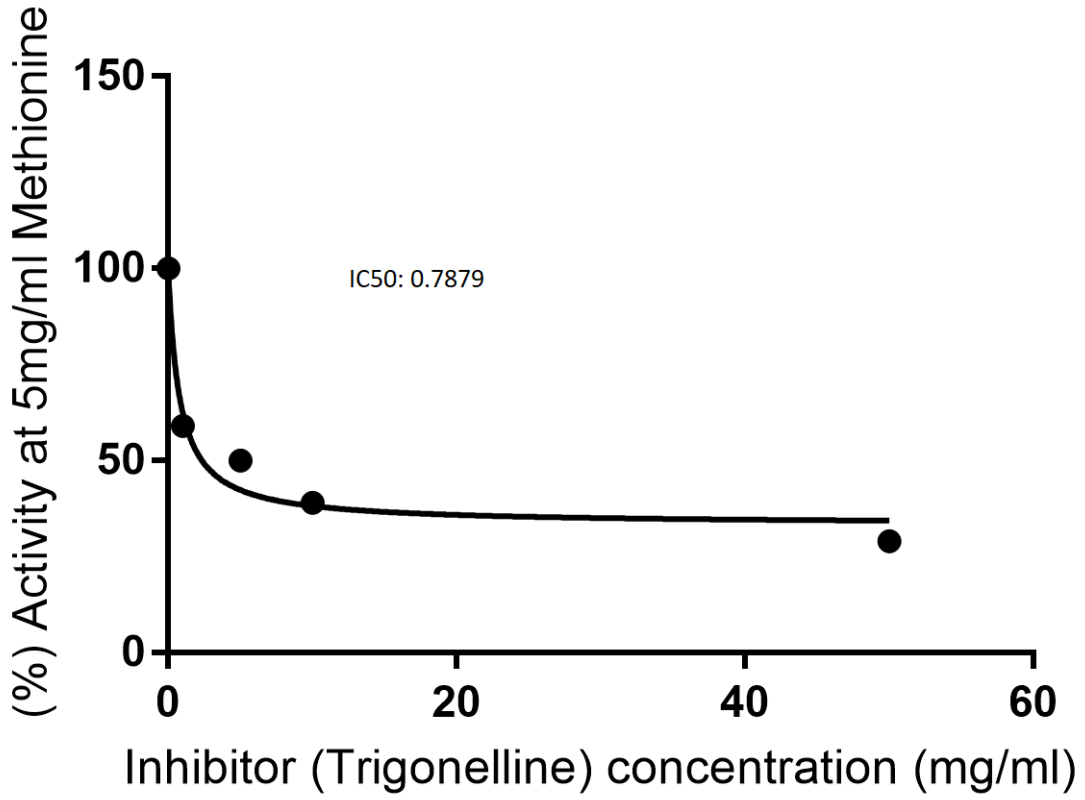

5.6 e IC50 plot shows hydrogen sulphide producing activity (%) at 5 mg/ml methionine with trigonelline at increasing concentrations

The IC50 for trigonelline is 0.79 mg/ml against the activity of methionine producing hydrogen sulphide. The line plateaus under 50% activity- indicating that trigonelline can only inhibit approx. 50% of the activity of methionine catalysis creating H_2S at all concentrations tested (up to 50 mg/ml trigonelline).

vii) Zinc citrate

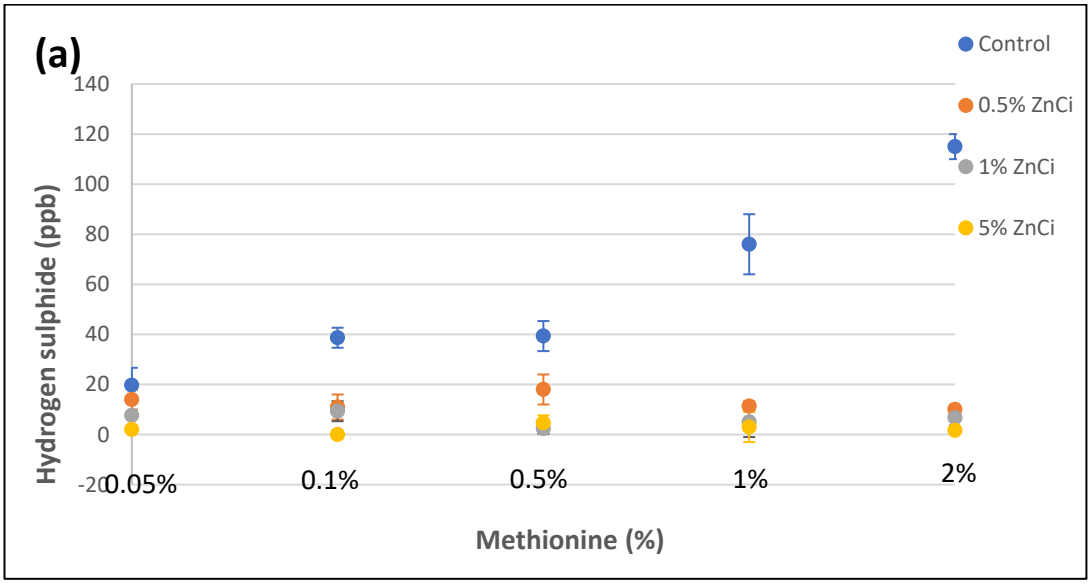

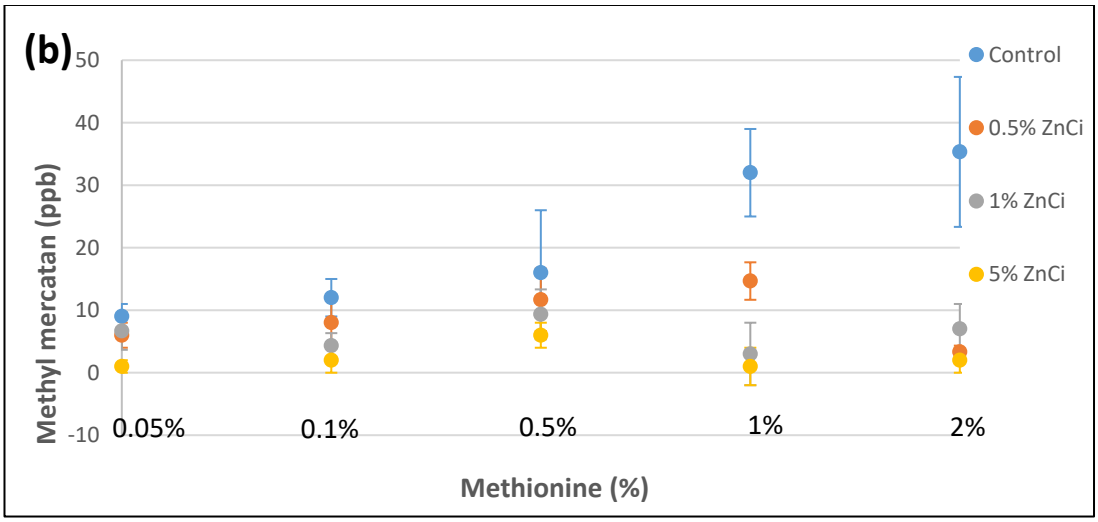

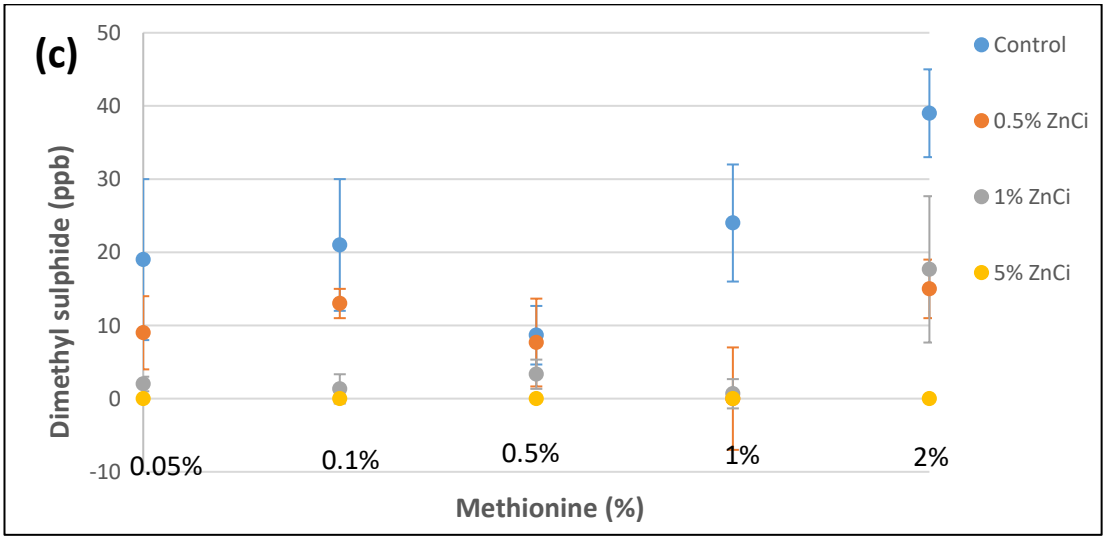

Figure 5.7 a, b, c. Concentrations of Zinc citrate tested on lysed bacteria with increasing concentrations of methionine (x axis) (Error bars represent ± SD)

Zinc citrate vs. Lysed bacteria- figure 5.7a (H_2S)

Methionine concentrations of 0.05% sees all solutions produce hydrogen sulphide under 20 ppb including the control (19.667) and decreases in order of Zinc citrate strength (conc.). This trend is followed but control concentrations continue to rise and solutions containing zinc citrate do not exceed 18 ppb (0.5% ZnCi at 0.5% methionine).

Zinc citrate vs. Lysed bacteria- figure 5.7b (MM)

Control methyl mercaptan concentrations rise as methionine concentrations increase to a peak of 37.3 ppb at 2% methionine. Solutions containing Zinc citrate increase with the control at all concentrations staying between 3-10 ppb of the control until 1% methionine where the control continues to rise, and inhibition from zinc citrate solutions increases, 5% zinc citrate inhibiting the most throughout all methionine concentrations (0 ppb at 2% methionine).

Zinc citrate vs. Lysed bacteria- figure 5.7c (DMS)

When adding 5% zinc citrate to lysed bacteria and methionine, no dimethyl sulphide is measurable. 0.5% Zinc citrate follows the trend of the control being just inhibitory even at 0.5% methionine where the control decreases to its lowest point (8.33 ppb). At 1% methionine the control increases again but all solutions containing zinc citrate inhibit dimethyl sulphide concentrations to below 1 ppb (although 0.5% ZnCi has bigger error bars). There is a notably strange switch at 2% methionine, where 1% Zinc citrate solution inhibits just less than 0.5%, however there are error bars showing that this is a variable result, and inconsistent over the triplicate.

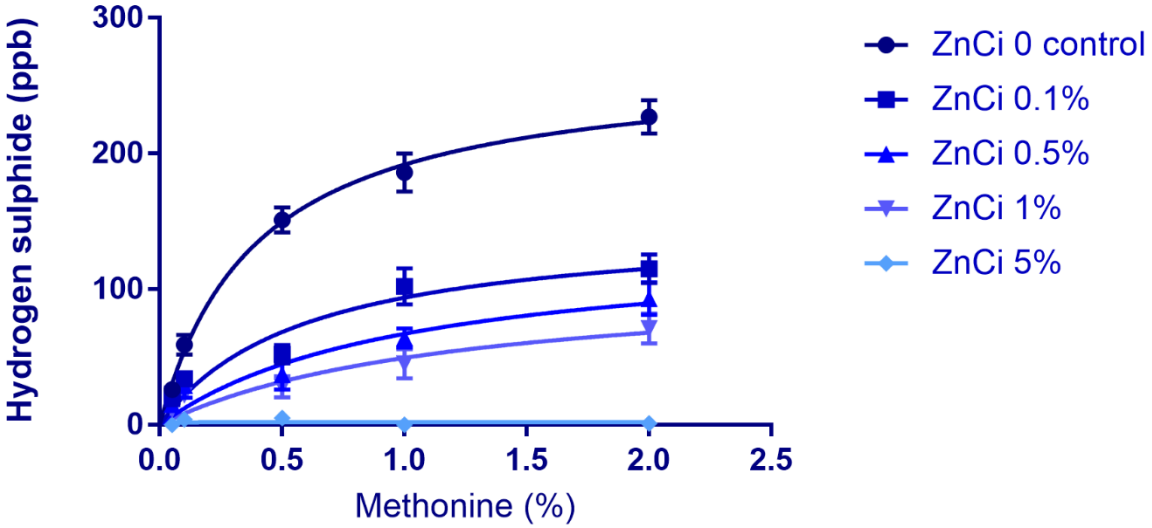

5.7 d. Michaelis-Menten plot for Zinc citrate effect on hydrogen sulphide

5% Zinc citrate is completely inhibitory on hydrogen sulphide concentrations at every increase in methionine concentration. All other concentrations decrease hydrogen sulphide output compared to the control by around 100 ppb at all methionine concentrations respectively. There is a trend wise increase in concentration (ppb) 5% zinc citrate exhibiting the most H_2S, and 0.1% ZnCi inhibiting the least H_2S.

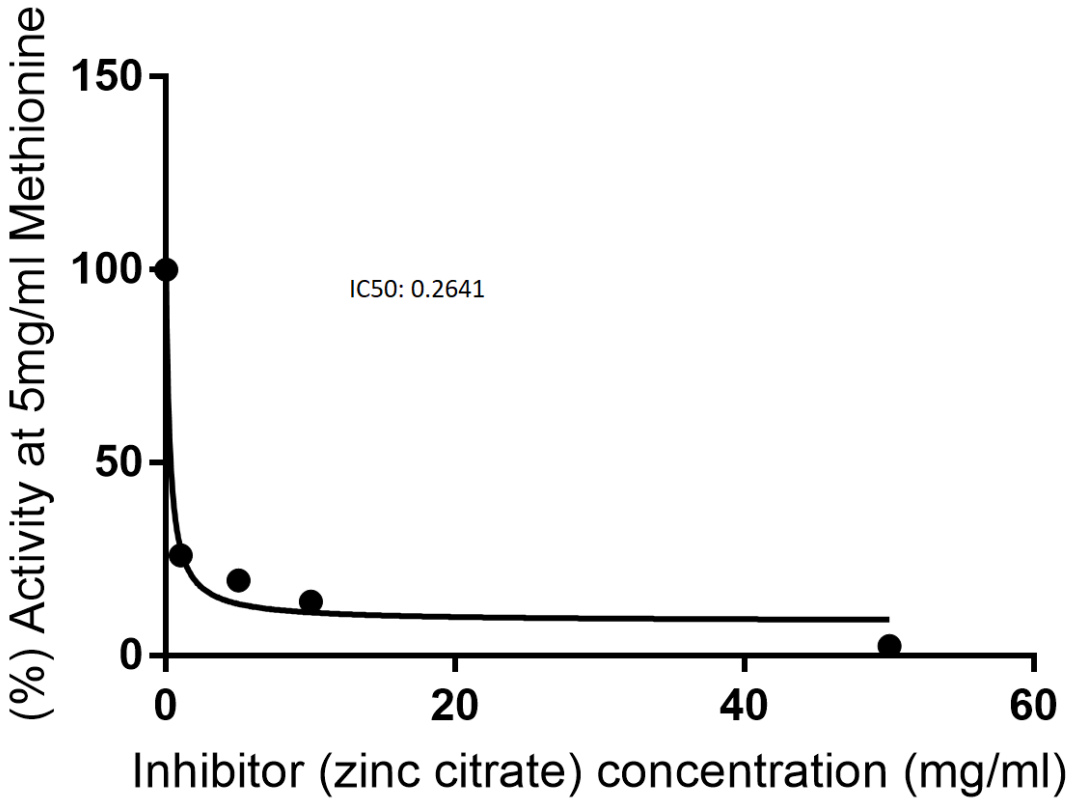

5.7e IC50 plot shows hydrogen sulphide producing activity (%) at 5 mg/ml methionine with zinc citrate at increasing concentrations

These graphs created depicting the rate and concentration at which the inhibitory panel can inhibit the bacterial production of hydrogen sulphide can be reviewed and compared to literature to uncover the mechanism of action (see discussion 5.4). Data showing the Km and Vmax values can be found in appendix 3 corresponding to the enzymatic rate of reaction. Below, are the results for the statistical analysis on the VSC reduction measured in graphs (5.1 -5.7 a, b and c).

Table 5.2. Table of Statistical tests done figures 5.1-5.7 a, b and c, on SPSS comparing the dependant and independent variables (ppb, concentrations of natural product/ substrate)

NP	**Caffeine**	**Gallic acid**	**Nicotinic acid**	**Trigonelline**	**ZnAc**	**ZnCi**
Pillais trace	1.95	2.58	2.138	2.685	2.062	1.156
F	(48,150) 5.833	(38,120) 20.646	(48,150) 7.764	(48,150) 26.668	(40,120) 7.327	(30,96) 2.228
P	<0.001	<0.001	<0.001	<0.001	<0.001	<0.001
Wilks λ	0.24	0.001	0.020	0.000	0.11	0.190
Partial ETA^2 (%) effective interaction	65%	86%	71%	89%	68%	38%

Pillais trace: The increase in this value indicates a larger contribution to effects in the chosen model, in this case, measuring gasses from the headspace model.

Wilks λ: This is a statistical test ranging 0-1, the lower the value for a natural product, the more it contributed to the effects of the headspace model.

F value: This F statistic compares the effect of all variables, interpreting this, along with the p value is crucial to rejecting the null hypothesis that there is no statistical significance within the data set.

P value: The p value is a measure of significance. If the p value is small (between 0-1) there is a stronger evidence for the significance between results. E.g. A p value of 0.001 means there is a 0.1% probability that the results are random (not due to headspace model parameters)

Partial ETA^2: This value is a percentage measure of the effective interaction (effect size). Larger effect sizes indicate significant differences.

A statistical analysis on data from graphs 5.1- 5.7 (a,b,c), is disclosed on table 5.2 this exposed the products in the chosen inhibitory panel that showed statistical effectiveness against VSC's. The largest pillais trace comes from trigonelline, followed by gallic acid and nicotinic acid, these are then followed by the zincs and caffeine. The increase in pillais trace indicates a larger contribution to the model. The inverse is true with wilks λ, a decrease indicates an impact on the model (0.000 from trigonelline reveals no variance). The same trend with these products is seen through all stats analysed. E.g. The largest effective interaction arises from trigonelline followed closely by gallic acid.

5.4 Discussion

5.4.1 Bacterial lysis

There are various methods of cell lysis that have been employed over the years for protein extraction including French- press, sonication and freeze thaw as well as the use of reagents. Extracting the protein this way has many applications such as western blot, immunoprecipitation and general protein extraction into lysate which can be used for enzyme assays, as the proteins become extracted into solution.

In this current study optimisation of lysis was initially tested using several different techniques, with the resulting supernatant spread on agar. If bacterial growth was present after overnight incubation this indicated a failure of lysis of the bacteria. Growth of bacteria appeared on samples that had been; sonicated, lysozyme solution and lysostaphin solution treated, as well as all three in combination. This demonstrated failure of these techniques to lyse the bacteria being used. The only technique which demonstrated lysis of the oral bacterial cell walls, with no growth on agar, was the Cellytic B ™ preparation (Sigma-Aldrich).

To test if the lysed bacteria with exposed protein in the supernatant had a higher rate of reaction with the methionine substrate than the whole bacteria, the lysate was tested against the same whole bacteria over 2 hours (result showed in table 5.1). An increase in all three gasses (hydrogen sulphide, methyl mercaptan and dimethyl sulphide) were observed in the lysed bacteria sample, this was viewed as successful and the lytic method was used in subsequent experimentation.

The lysed bacteria were preferred over whole cell, planktonic bacteria due to the nature of observing enzyme inhibition from the addition of products. Using lysed bacteria does not help differentiate between gas neutralisation or enzyme inhibitory properties under the headspace model. But it does allow for increased enzyme availability, resulting in a higher rate of reaction and binding, for a more accurate measure of the enzymatic parameters such as the IC50 (figure 5.1-5.7d) and Vmax (appendix). It also eliminated membrane bound enzymes from reacting with the substrate to produce the gasses.

Hydrogen sulphide was used as a measure for enzyme kinetic graphs as there is more of it produced compared to the other two gasses, this phenomenon is due to; 1. Enzymes that can catalyse the release of hydrogen sulphide from methionine and 2. Methionine and its products can be used as a precursor for cysteine, which releases hydrogen sulphide from enzyme activity.

5.4.2 Lysed bacteria vs. Natural products

i) Gallic acid

Gallic acid is present in tea, wine, coffee (initially used), fruits and other plants such as oak (gallnut) (Zhang *et al*., 2015; Dettweiler *et al*., 2019). It is a phenol which includes carboxylic acid and three hydroxyl groups, its antioxidant activity is well documented along with anti-cancer, anti-viral, anti-bacterial and anti-cholesterol effects (Badhani, Sharma and Kakkar, 2015). In the case of oral bacteria, gallic acid is effective, however, its mechanisms of action are by no means defined due to its diverse pharmacological effects. In current chapter (5), gallic acid at 0.1% had little effect on the production of hydrogen sulphide, however at 0.5% and 1% gallic acid were shown to be highly effective in reducing hydrogen sulphide production. In a study by Kang and colleagues (2008), gallic acid inhibited the growth of *S. mutans* biofilms as well as significantly decreasing the number of periodontal bacteria after 24 hours of incubation containing 1 mg/ml (0.1 % gallic acid), although the incubation period is one day, compared to 10 minutes in the current study. (fig 5.1 a, b and c) Both Kang *et al.,* (2008) and current chapter concludes that gallic acid is effective against periodontal bacteria and halitosis. In the same article it is shown that at 4 mg/ml gallic acid had a cytotoxic effect on KB (HeLa) cells decreasing their viability, therefore further research is warranted into the gallic acids effect on cell multiplication as well as metabolism. In a study by Borges and colleagues (2013), gallic acid increased the surface charge of pathogenic bacteria, which are normally very negatively charged, (*E. coli, S. aureus, P. aeruginosa*) and rupture the cell. This hypothesised mechanism of action is surface disruption of the bacteria with an affinity for the lipid bilayer, meaning a stronger affinity for disruption of Gram-negative bacterial membranes. However, in the current

study the cells are already lysed and gallic acid is still having an effect (to decrease VSC production) therefore it may have another mechanism of action, e.g. binding to bacterial enzymes inhibiting catalysis of amino acid (methionine) and production of VSCs. The Michaelis-Menten plot in the current study shows a normal dose response gradient and that at 0.5% methionine, gallic acid is a potent inhibitor of hydrogen sulphide produced from methionine activity 0.3198 mg/ml (fig 5.1e). This is 1000x higher than to 205µg ml -1 against *P. aeruginosa*, a Gram-negative bacterium reported by Cueva and colleagues (2012), however, this paper focused on inhibition of bacterial re-growth rather than inhibition of metabolic products analysed in the current thesis. Interestingly the IC50 was higher than *P. aeruginosa* for the Gram-positive bacterium *E. faecalis* (404mg ml -1), and higher still for streptococcus species, verifying that gallic acid has stronger affinity for gram negative bacteria (Cueva *et al.,* 2012).

ii) Zinc chloride

Zinc chloride exhibited the largest IC50 of 1.17 mg/ml, to the authors knowledge, no IC50 has been demonstrated with zinc chloride against periodontal bacteria). Zinc chloride displays an inhibitory action on the hydrogen sulphide, methyl mercaptan and dimethyl sulphide produced at all concentrations used. The control rises in an expected manner, with more substrate (methionine) put into the lysed mixed culture of bacteria, the greater concentration (ppb) of the VSCs produced. In figure 5.2b, methyl mercaptan levels for the control stayed low 36-44 ppb for 0.05% methionine to 1%, however when 2% methionine was added methyl mercaptan levels rose to 158 ppb. The addition of zinc chloride 9at all concentrations, had a small inhibitory effect on gas products. At 5% zinc chloride, the ppb levels of methyl mercaptan did not deviate much from 0 ppb with the highest value of 6.6 ppb at 0.5% methionine. A similar trend is observed from the graph showing hydrogen sulphide and dimethyl sulphide output (Fig 5.2a and c) which shows the inhibitory effect of the zinc chloride solution, decreasing ppb's in a gradual trend. In a study by Kang and colleagues (2017) zinc chloride exhibited a MIC of 0.0625–0.50%, against 8 orally relevant bacteria- a bacteriostatic effect was demonstrated; especially against *P. gingivalis*. However, the effects of VSC reduction in the current thesis cannot be attributed to a bacteriostatic mechanism due to use of lysates. Zinc chloride has also been shown to shut down glycolysis rate from oral microbes through measurement of pH, this effect is larger

in moderate concentrations of zinc chloride (0.2-0.3mM) rather than 1mM (which inhibits 80-90% glycolytic activity) (He, Pearce and Sissons, 2002). Zinc is a metal ion with low toxicity and does not cause dental staining like other metal ions eg. copper, which have an inhibitory effect on VSC production (Young *et al*., 2001). The metal has an affinity for sulphur, forming sulphides with low solubility, interacting with the metabolites (gasses) themselves to neutralise halitosis. The antibacterial effect is explained through other methods such as oxidising bacterial thiol groups and causing an inhibition of glycolytic enzymes. (Choi *et al*., 2010).

iii) Zinc acetate

In current studies, Zinc acetate was a very effective inhibitor of hydrogen sulphide over all concentrations of methionine used. The hydrogen sulphide levels increased to a maximum of 343.3 ppb as the control methionine concentrations increase. With the addition of zinc acetate, the hydrogen sulphide level recorded barely deviate from 0 ppb (highest from 1% ZnAc at 0.05% methionine: 22 ppb). This shows similarities to a study looking at the effects of metal chlorides and metal acetates against hydrogen sulphide, where zinc acetate (and zinc chloride) had a direct effect on gaseous hydrogen sulphide , explained through binding at a high affinity to the gaseous elements reducing hydrogen sulphide to 0 ppm (Young *et al.,* 2002). This mechanism of zinc binding sulphur from hydrogen sulphide has an effect on both the hydrogen sulphide gas itself and an antimicrobial activity on VSC producing bacteria (Suzuki *et al*., 2018). There is an overall inhibitory effect by zinc acetate on VSC output (except for 0.5% Zinc acetate vs. methyl mercaptan production at 0.05% Methionine – 6.7 ppb higher than control). All concentrations of zinc acetate inhibited hydrogen sulphide measurements, 5% is the most potent inhibitor for all three gasses and at the least inhibiting concentration of zinc acetate is 0.5% (the lowest concentration used) as expected. Due to the effective hydrogen sulphide inhibition, the IC50 for this presents a potent natural product for the inhibition of hydrogen sulphide at 0.5% Methionine (0.2mg/ml), however the mechanisms may be via gas neutralisation or antimicrobial effects rather than enzyme inhibition.

vii Zinc citrate

Zinc citrate already can be found within toothpaste formulations due to the safety of use, it can infer gas neutralisation and inhibition of bacterial glycolysis (Moran *et al*., 2001). This zinc combination is a low molecular weight form with basic anions and a high stability constant. Whilst the stability constant does not denote anti-VSC effect (as previously thought, in a paper by Young, Jonski and Rolla, 2002), in the same paper zinc citrate was proved less effective than zinc acetate at1, 2- and 3-hours post treatment at reducing VSC's. This contrasts with the findings in this study, where zinc citrate was shown to give a low IC_{50} (0.26 mg/ml), however the differing Km and Vmax values (see appendix) suggest a mixed mechanism of inhibition. There is a trend wise decrease in hydrogen sulphide concentrations with increasing zinc citrate concentrations, this is the reason behind a low IC50 value suggesting that gas neutralisation plays more of a role than enzyme inhibition, as described in previous chapters.

vi) Nicotinic acid

In current experiments, nicotinic acid was able to inhibit hydrogen sulphide released more than its effect on dimethyl sulphide or methyl mercaptan. It also presented a relatively low IC_{50} (0.5 mg/ml) displaying decreasing Vmax values (through increasing nicotinic acid %) indicating a lowered rate of reaction when increasing nicotinic acid concentrations, and Km's (enzyme affinity) are too low to accurately measure. No studies have yet directly test nicotinic acid on oral malodour; however, papers do use products which contain nicotinic acid with effectiveness. In a study by Naiktari and colleagues, (2014), Triphala was used (an herbal blend containing nicotinic acid) to combat halitosis and periodontitis comparing results to the use of chlorhexidine. The gingival and plaque index showed no significant differences between the two, showing that the herbal solution is as effective on plaque as the gold standard- chlorhexidine.

iv) Trigonelline

Trigonelline is an alkaloid and is formed as a methylation product of nicotinic acid (seen when arabica coffee is roasted (Trugo *et al*., 2003). This product shows antibacterial effect on the growth on enterobacteria, some of which contain the MGL gene (Almeida e*t al.,* 2006). In the current study, trigonelline was used as a powder natural product to be made

to a specific concentration, therefore not limited by the roasting degree of coffee beans. Trigonelline was shown to decrease the measured hydrogen sulphide measurement via the oralchroma, in a trend wise manner, 5% inhibiting the most hydrogen sulphide compared to the control throughout the experiment. An IC_{50} of 0.78 is the second highest in this group of results, however, exhibits the largest effect size as shown by partial ETA^2 of 89%. The addition of trigonelline to coffee extract increases the inhibition of bacterial growth by 14% compared to the aqueous solution of trigonelline alone measured via diameter of MIC zones of inhibition (Almeida *et al*., 2012). This MIC experiment shows initial antibacterial properties, additional anti-malodour properties has been attributed to coffee's antiadhesive properties on *Streptococcus mutans. (*Namboodiripad and Kori, 2009; Daglia *et al*., 2002). Although in the current chapter, the bacterial cell wall is removed. Therefore, the anti-malodour effect of trigonelline is credited to other mechanisms e.g. enzymatic inhibition, which is further investigated in the next chapter (Chapter 6).

v) Caffeine

Caffeine is one of the main constituents in coffee and therefore due to coffee's effect in the previous chapter (figure 4.9 a, b and c) caffeine was researched in the chapter for anti-VSC effectiveness. Caffeine has a trend wise effect against hydrogen sulphide concentrations. The IC_{50} shows a low concentration of 0.52mg/ml meaning it only takes this concentration to inhibit 50% of H_2S producing reaction. There is no current research implicating caffeine in the reduction of VSC's or inhibition of oral bacteria spp.

5.5 Conclusions

The kinetics completed in this chapter are based on the lysate results and measured through gas reduction using an oralchroma. Whilst the values give an idea of how effectively each natural product can reduce the VSCs output, there is no way to tell from this data if this is due to gas neutralisation or enzyme inhibition. Zinc + ligand's effect is attributed to a higher affinity for sulphide than its own bond, therefore chemically neutralising hydrogen sulphide before it is released. Some antibacterial claims have been made involving zinc-based products, but these are not comparable to current research that

used lysed bacteria, the cell walls are already disrupted, and antibacterial action cannot be quantified. The results for zincs seen in figure 5.2, 5.3 and 5.7 show effect against VSCs implying their control of gaseous products released by methionine catalysis by bacterial enzymes.

Gallic acid is thought to have an antibacterial mechanism of action particularly against Gram negative species of bacteria. The current results are not able to determine the antibacterial effect but shows an interference in enzyme reactions: IC50- 0.3198 mg/ml and a decrease in Vmax with increasing gallic acid (see appendix) implicates an inhibitory effect on enzymatic rate of reaction. Trigonelline binding to enzymes is also a possibility from these results but via a non-specific mechanism shown by high IC_{50} and the highest ETA^2 meaning that it potentially covers a broad range of bacterial enzyme binding.

The inhibitory potential of these products is further investigated in chapter 6.

Chapter 6 Exploring the inhibition of methionine gamma lyase from oral bacteria

6.1 Introduction

Methionine gamma lyase (MGL) is an enzyme contained within bacterial cells (not mammalian) as described in introduction 1.10.3, this enzyme predominantly catalyses the alpha, gamma elimination of methionine to produce methyl mercaptan, alpha-ketobutyrate and ammonia (Sato and Nozaki, 2009). It is also able to catalyse the alpha beta elimination of cysteine which produced hydrogen sulphide (Kudou *et al*., 2015). In this chapter the MGL enzyme was investigated for interactions with the inhibitory products chosen and rates of enzyme reactions using both product and substrate quantification.

There are many assays available for the quantification of volatile sulphur compounds. Classically this can be done for hydrogen sulphide using colorimetric assays, for example the methylene blue assay in which hydrogen sulphide directly converts N,N-dimethyl-p-phenylenediamine to methylene blue, the intensity of colour is measured at 670 nm and should directly correlate with concentrations of hydrogen sulphide in the solution. However, this assay has come under scrutiny due to its lack of specificity when using biological samples, and the sensitivity is relatively low. There are modifications of this assay (Kolluru *et al*., 2013), but they are for work on aqueous (water) samples. Other assays such as using chromatography techniques provide a sensitive and specific method for quantifying hydrogen sulphide in its gaseous form such as gas chromatography mass spectrometry (GC-MS) and high-performance liquid chromatography (HPLC). The OralChroma is a type of modified gas chromatography allowing the differentiation between sulphurous gasses (hydrogen sulphide, methyl mercaptan and dimethyl sulphide) and is relatively user friendly.

Quantifying the enzyme through its conversion of substrate into product, is the main route of kinetic analysis. This can be measured through gas production, as described above and conducted in this chapter, to achieve IC_{50} values. The MGL enzyme can also be analysed through colour changes from the direct production of alpha-ketobutyrate at around 315nm using methionine, and 3-methyl-2-benzothiazolinone hydrazone hydrochloride (MBTH)

(Yoshimura *et al*., 2000; Takakura *et al*., 2004). The derivatisation chemicals such as MBTH can bind to the P5P co-enzyme which could produce assay errors, therefore Foo *et al.,* (2016) developed an assay without the need for derivatisation measuring alpha keto-butyrate produced at 320nm continuously over 10 minutes- this assay was selected for this chapter. Measuring the substrate is the unconventional method of measuring enzyme activity. Substrate depletion (methionine) is quantified through HPLC with and without the enzyme, natural products are then added to look for an increase in substrate (in the presence of MGL) which would allude to competitive binding.

In this chapter, both lysed bacteria (used in chapter 5) and protein samples (methods 2.6 and 2.8) are used for analysis, these have both shown to contain multiple proteins. The data gathered in this chapter presents an interaction led approach to analyse the mechanism of action, including HPLC substrate depletion to predict type of binding, bioinformatic modelling to visually present potential interactions and IC_{50} values to assess concentrations of inhibitory action. Differential Scanning Fluorometry (DSF) assay was also used (fig 6.1) to unfold the protein and assess the thermodynamic nature of the enzyme (the conformation and temperatures increase ligand binding) however, this was unsuccessful compared to the reference plot (fig 6.2) which brought up the question of sample purity further investigated by gel electrophoresis (fig 6.3).

6.1.1 Aims

The aims in this chapter are to determine the effects of products chosen (zinc citrate, gallic acid, zinc chloride, caffeine and nicotinic acid) on the reaction involving methionine as a substrate and enzymes from oral bacteria (namely methionine gamma lyase- MGL). The enzyme kinetics and parameters are assessed from both sides of the reaction mechanism; the substrate depletion, and the product formation. The data from experiments conducted is manipulated to provide plots and values for example IC_{50} and full inhibitory plots (fig 6.13) building knowledge on the enzyme's reaction parameters (with chosen inhibitory products). The findings in this chapter are further supported with computer generated interactions (bioinformatics in figures 6.15 to 6.20) In combination, these exhibit the binding potentials of MGL, and products that can interfere with its reaction mechanism.

Initially it was chosen to determine rate of enzyme unfolding as a result of temperature (fig 6.1 a, b).

6.2 Methods

Making the enzyme solution- See method 2.8.1- 1.45 mg of 'pure' enzyme (Methionine gamma lyase- Sigma Aldrich) made to 0.08 units of enzyme.

Differential scanning fluorimetry (DSF)- Protein sample loaded with SYPRO orange dye and put into the DSF to read fluorescence intensity changes as a result of increasing temperature. See method 2.8.2.SDS page electrophoresis was performed- See method 2.8.3

High performance liquid chromatography (HPLC (350nm and 450nm excitation and emission wavelengths) was performed to quantify methionine alone with fluorescence (OPA) and then enzyme is added. This is then tested with a panel of inhibitors to determine concentration of free methionine left in solution. See method 2.9

IC_{50} determination was achieved using graphpad (prism 7), the function of the graphs created was: [Agonist] vs. normalised response to produce a variable slope with a nonlinear fit. The experiment measured volatile sulphur compounds from increasing concentrations of natural products up to 100 µM effect on 100 µM of methionine and converted into percentage inhibition. This graph extracts the IC_{50} value noted on graph.

Methionine gamma lyase (MGL) assay measured the reaction to produce alpha-ketobutyrate via colour intensity in a continuous spectrophotometer (BioTek, Synergy Mx). Measurements of colour intensity at 315nm (Corresponding to alpha keto butyrate formation) were read every minute for 10 minutes. This was achieved by adding MGL to methionine (0-40 mM) in a 96-well plate, this is repeated on 5 rows- controls are compared to wells with added inhibitor. See method 2.14

Bioinformatics- This section was completed using Autodock vino softwares, as well as, Pymol for visualisation. Bioedit/FASTA and chimera were used to investigate conservation of the MGL enzyme in differening bacterial species. On autodock multiple files containing the receptor and ligand co-ordinates were prepared into PDBQT files and collectively 'docked' in triplicate to give the best estimate of ligand positioning. This file was then transferred to Pymol to visualise the conformation and angstroms between the closest

amino acid residues to the ligand on the MGL receptor site- figures shown in results. See method 2.10.

6.3 Results

6.3.1 Dissociation and amplification on qpcr (DSF assay)- pilot study

The plots below are the real time unfolding information (dissociation and amplification curves) using SYPRO Orange as a fluorescent dye on Methionine gamma lyase (Sigma aldrich). The blue line represents the control protein sample of Methionine gamma lyase. From these plots it is seen that the protein did not undergo an unfolding process proven by the fluorescence readings through the cycle. The amplification plot only reaches highs of just over 200 (dR).

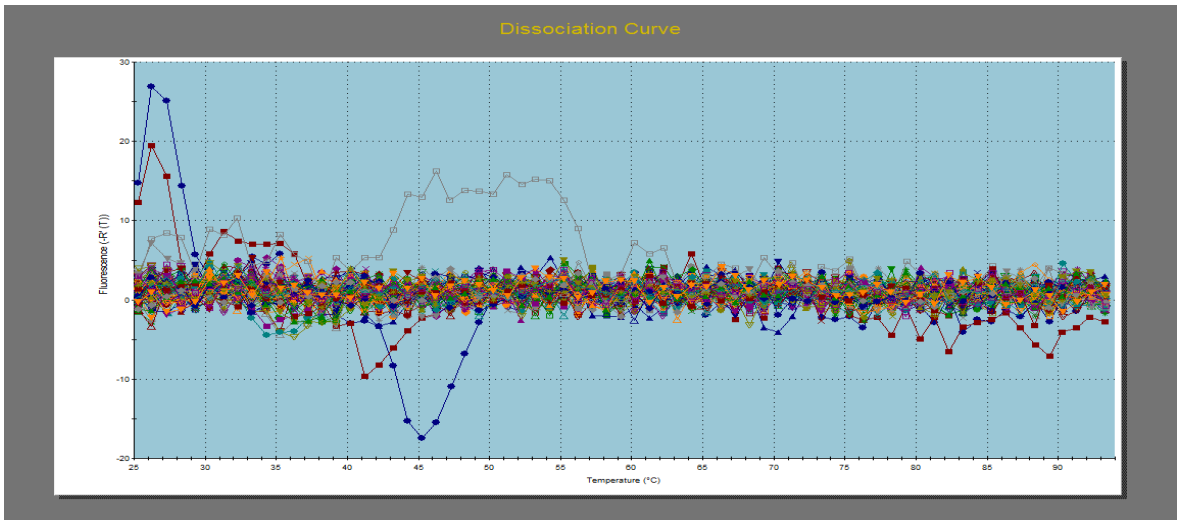

(a)

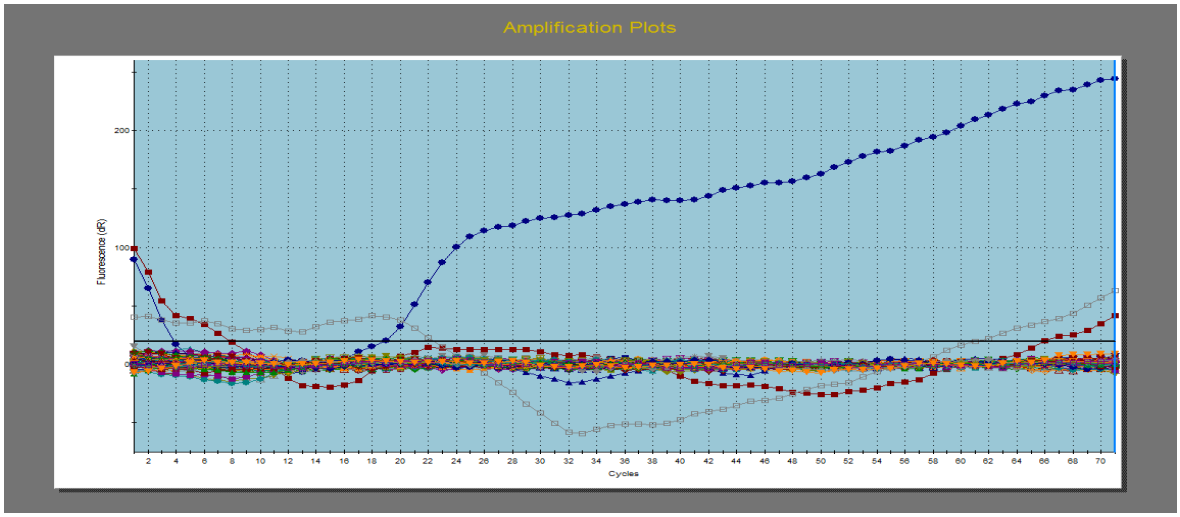

(b)

Figure 6.1 a and b Visualisation of fluorescence from QPCR (DSF assay) using SYPRO orange as fluorescent detector for the unfolding of methionine gamma lyase. The blue line (with circles) represents the neat MGL with buffer- the other lines represent dilutions from the pure MGL (see method 2.8.2)

The DSF assay should show the unfolding of a denatured protein through temperature dependant cycles. The melting point of the enzyme can be worked out using the minimum and maximum intensities and presented in graph form as a two- state transition. This would map the unfolding of the protein, on a temperature cycle, therefore the optimum temperature of enzyme unravelling. If the cycle (figure 6.1) showed the unravelling of a protein (MGL) over temperature, natural products would have been added to observe the areas of binding. This technique shows the binding activity in solution at increasing temperatures and used in the development of pharmaceuticals/active ingredients.

The results from the control were observed and compared to the reference figure 6.2. Comparing these figures, it was clear that the MGL protein in figure 6.1 did not unfold after a triplicate of attempts using the DSF assay. If a protein is pure, it would display some unfolding on the DSF assay, therefore the purity of the protein sample was questioned.

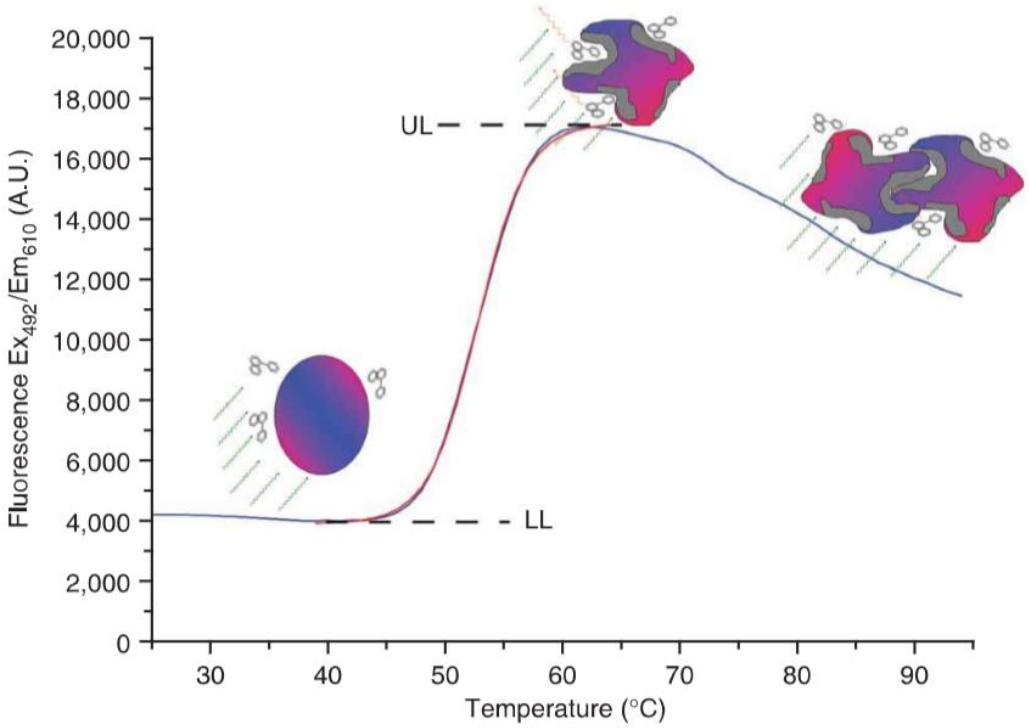

Figure 6.2 Extracted from Neisen, Burglund and Vedadi, (2007). This graph presents the reference plot, noting shape of the sigmoidal curve and values of fluorescence. The protein being unfolded is citrate synthase. LL represents minimum intensity and UL the maximum.

Grey regions on the protein show the exposed hydrophobic regions after unfolding. The maximum fluorescence value is 17,000 A.U. At this temperature (65 degrees C) the protein starts to denature shown by the downward curve. The differences between figure 6.1 and the reference (6.2) display that the protein in 4.1 did not sufficiently unfold or give an indication of denaturing temperature. As mentioned above, the next step was testing the purity of the purchased methionine gamma lyase. To get this result an SDS page gel electrophoresis was required to detect the protein and assess its purity (Fig 6.3)

6.3.2 SDS Page- Gel electrophoresis

In testing a single protein, there should be a single band marked at the corresponding molecular weight. This was expected from the methionine gamma lyase at 47kDa. However, results below (fig 6.3) show multiple bands of proteins.

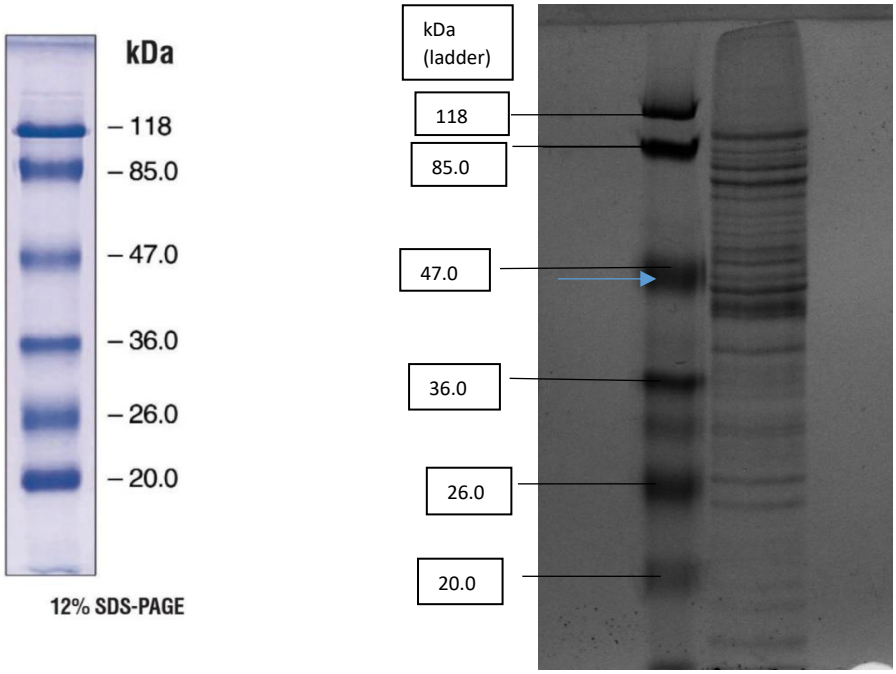

Figure 6.3 SDS page gel electrophoresis image from GelDocTM XR+ (BIO-RAD)- a molecular imager. The right image shows the tested enzyme (with multiple bands) and to the left of it is a reference ladder.

Figure 6.3 shows that enzyme was not 'pure' in a single band as expected. The image presents at least 25 protein bands (exceeding the ladder). After contacting the company (Sigma Aldrich), it was realised that the sample sent was the MGL gene inserted into a recombinant *E. coli*, which would explain the multiple bands seen. Some commercial enzymes may have several impurities as it is sold based of unit of activity per volume.

The commercially available sample expressed proteins from a bacterial genome vector. The protein of interest; MGL, is still expressed, seen by the darker band in the gel (fig 6.3) the blue arrow signals to the area. The molecular weight was calculated in (figure 6.4) the graph below. This extrapolates the kDa (molecular weight) of an unknown by using distance migrated (mm) and (log)molecular weight. The information is used to determine whether the larger band is in the right place for the correct kDa (corresponding to methionine gamma lyase), which would indicate that the enzyme is still able to bind and react with methionine, catalysing the replacement/elimination reactions, as it does in lysed bacteria.

.

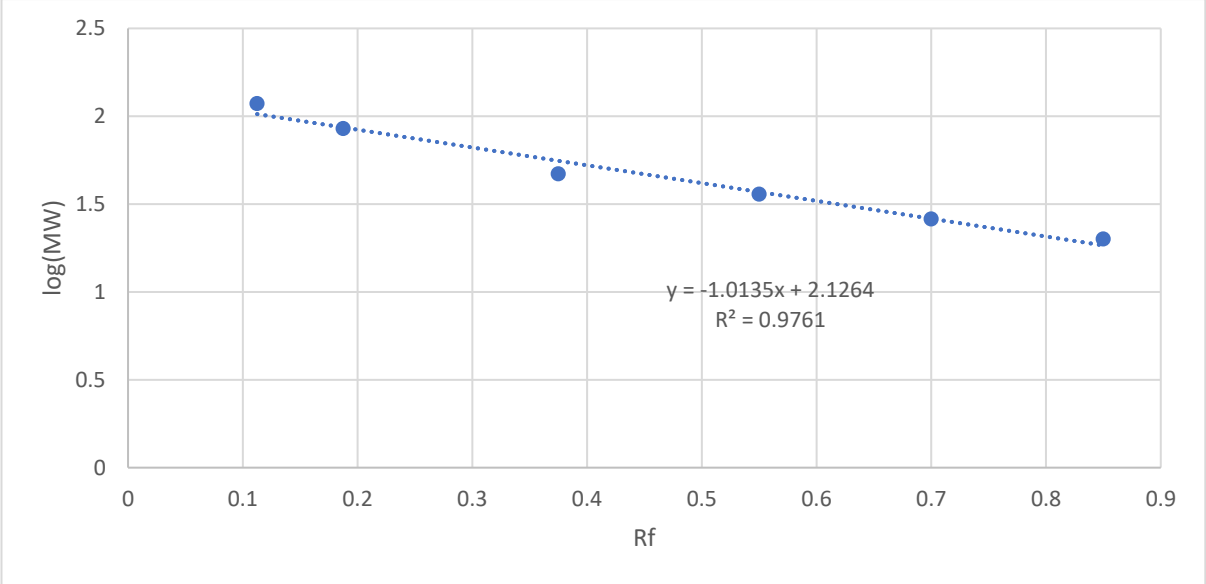

Fig 6.4 Determination of unknown molecular weight using Rf (distance migrated (mm) X dye front (mm)) against log molecular weight. This calibration curve/ equation can be used to extract log molecular weight of a known distance- unknowns 32-35 mm.

The ladder in image 6.3 shows a molecular weight of 47 kDa migrating 30 mm, however, on the graph the line of best fit suggests that this known band should have migrated further (seen by third point on figure 6.4- not sitting on the line of best fit). The error was calculated at 20%, therefore the unknowns (32 and 35mm migrated) will have an error and therefore a range of answers.

32 mm- 42-62 MW

35 mm- 38-57 MW

With the inverse relationship between distance migrated and molecular weight, the expected answer should be less than 47Kda, due to the bands in the test sample migrating further than 30mm which is indicative of 47Kda on the ladder.

From the literature, it is reasonable to estimate the molecular weight for a methionine gamma lyase unit as 45-47kDa, under denaturing conditions of the protein run with SDS page gel electrophoresis (El-Sayed, 2011; Hanniffy *et al*., 2009).

6.3.3 High performance liquid chromatography (HPLC)

High performance liquid chromatography was performed to determine methionine concentrations, these were measured at increasing concentrations to achieve a calibration curve. The methionine was then loaded with the enzyme for a concentration decrease reference (methionine used up and bound in the reaction). Products were added to this to assess potential binding sites (competitive binding would increase methionine concentration by inhibiting enzyme catalysis). Fig 6.5- 6.7 presents a sample of raw HPLC graphs, these are manipulated to produce a calibration curve (fig 6.8) and a bar chart showing methionine vs. methionine and enzyme vs. methionine, enzyme and product.

Methionine detection on HPLC

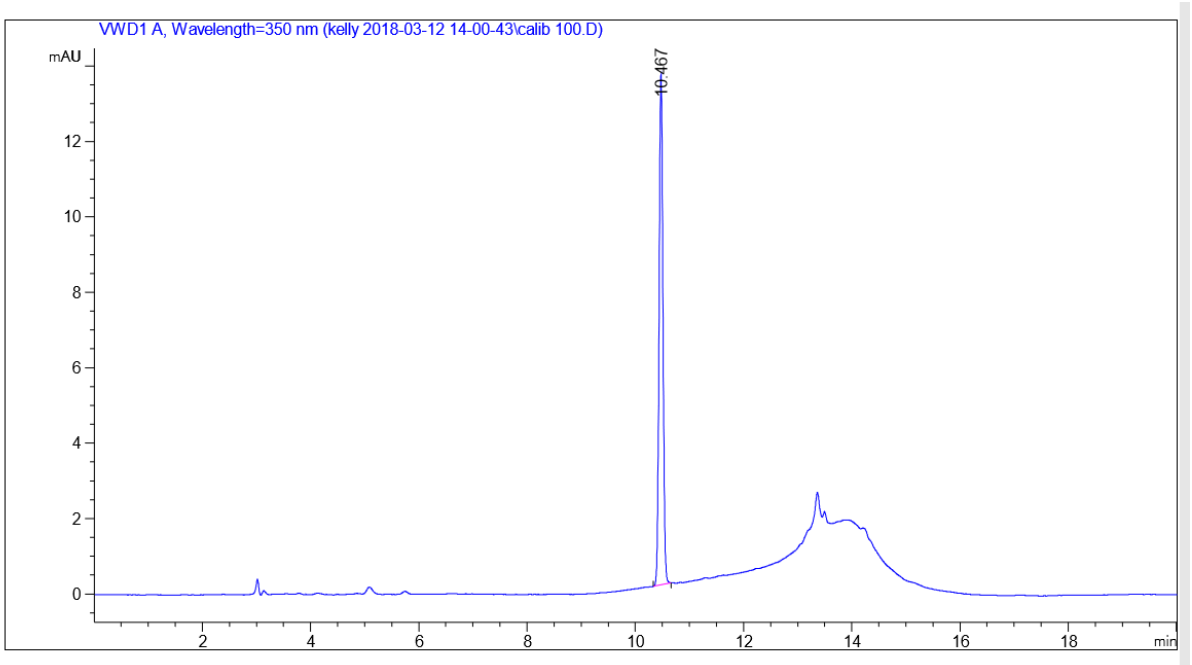

Figure 6.5 HPLC excitation of methionine in buffer (NaAc) with a fluorescent detector of methionine (OPA) Column information (Sigma- Aldrich 59555- SUPELCOSIL LC-18-DB HPLC Column)

Fig 6.5 illustrates the raw graph from HPLC machine presenting methionine derivatisation by OPA (sodium acetate buffer). Methionine is measured in the system with no enzyme, the excitation time is at 10.5-minute, this shows methionine concentrations as approximately 13mAU when eluted. This value is compared to methionine with additions described below.

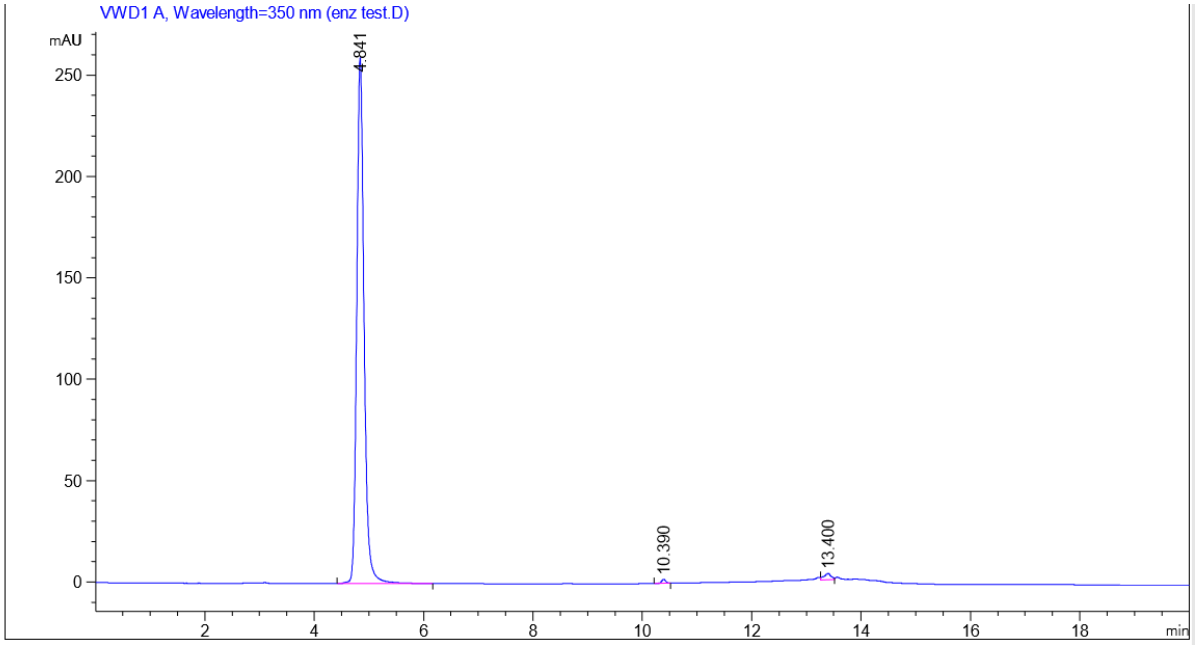

Figure 6.6 HPLC graph of enzyme tested with Methionine (analysed at the 10-minute mark- Methionine concentrations) (sodium acetate, OPA, Methionine, MGL) (Sigma- Aldrich 59555-SUPELCOSIL LC-18-DB HPLC Column)

Figure 6.6 represents the addition of the enzyme Methionine gamma lyase (MGL) which aids the catalysis of methionine into volatile sulphur compounds, ammonia and α keto-butyrate. Therefore, the decrease in methionine is a direct effect of the enzyme catalysis and only a fraction of the starting methionine remains to be measured (~7 mAU). The range of the graph (y axis: 250 mAU max) is larger than figures 6.5 and 6.7 however, this is accounted for in the calibration curve and bar chart adapted from the raw data (Fig 6.8 and 6.9). The higher elution at 4.8 minutes is theorised as the enzyme reacting with OPA to produce a peak.

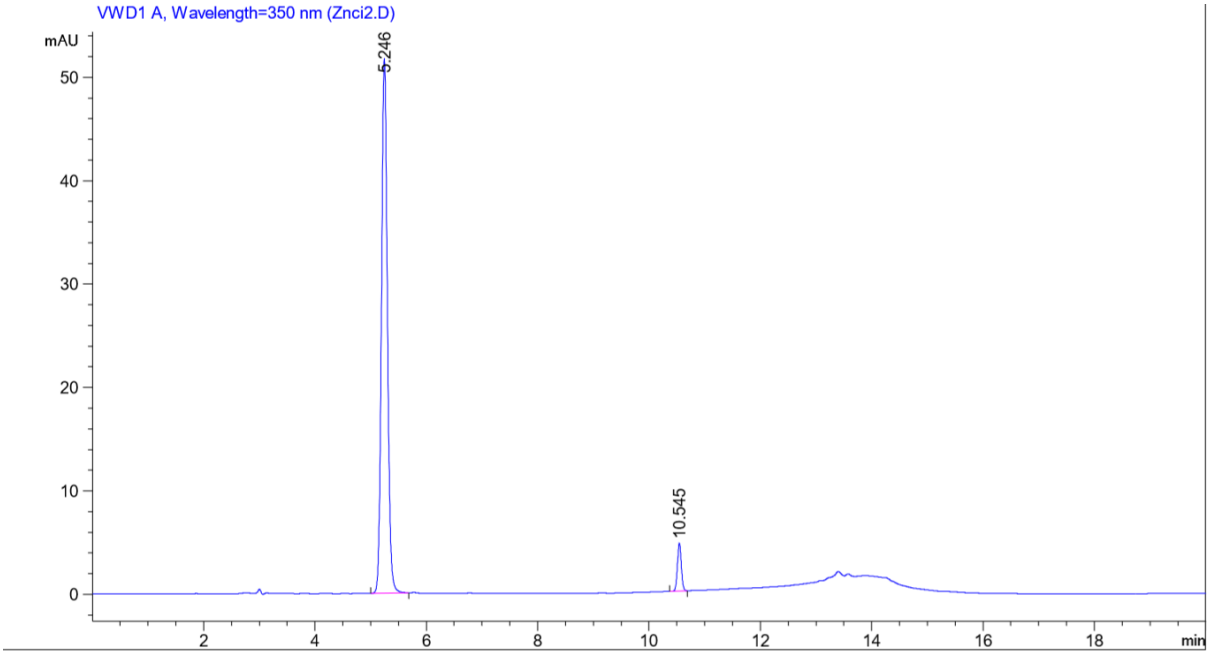

Figure 6.7 HPLC graph analysed with Methionine + MGL + Zinc citrate (NaAc and OPA) (Sigma-Aldrich 59555- SUPELCOSIL LC-18-DB HPLC Column)

This graph (fig 6.7) shows that there is more free methionine available to measure compared to the enzyme control but less than methionine alone, this eludes to a degree of inhibition by zinc citrate on the MGL to not let it carry out the binding of free methionine to full effect leaving a small amount free to be measured- the log absorbances for all products shown in fig 6.9 are calculated from the methionine calibration curve fig 6.8 below.

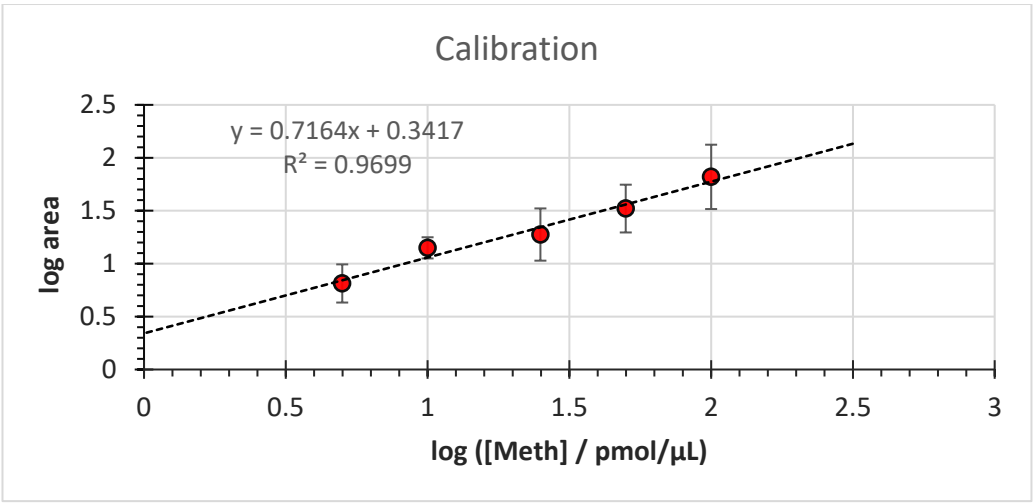

*Fig 6.8. Calibration curve using AUC mAU*S (Testing methionine concentrations (pmol/µl) in log)*

The calibration curve was made with a series of methionine concentrations, the x and y axis have been logged to normalise the result and achieve a log absorbance reading that can be read across and down. This graph (fig 6.8) helps convert readings from detection on HPLC to effective non-bound methionine concentrations.

Fig 6.9 shows a bar chart portraying this effect of natural products used on the enzymatic interaction between methionine and methionine gamma lyase and their efficiency in inhibiting substrate degradation.

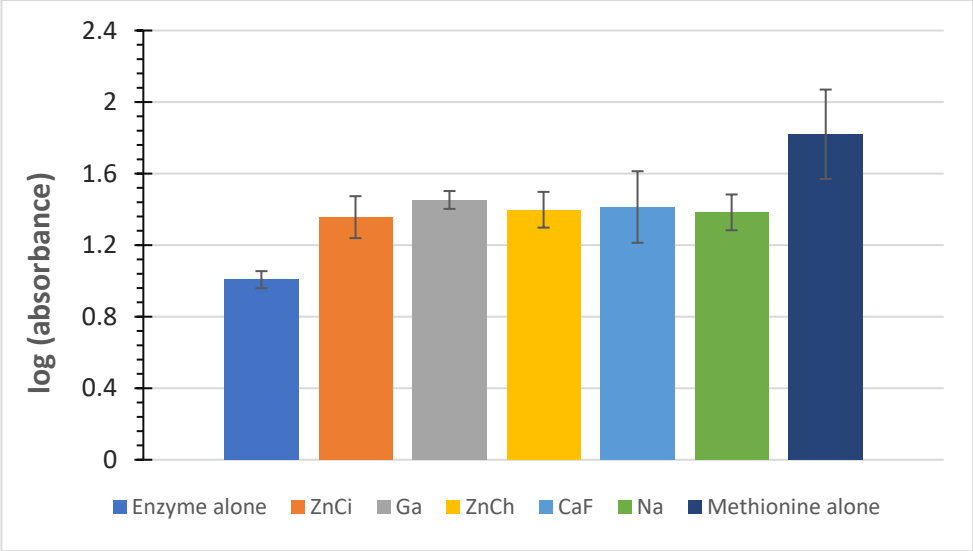

Fig 6.9. Methionine absorbance after addition of methionine gamma lyase and products for inhibition – methionine alone is the control absorbance (log) of free methionine. Enzyme alone (shows methionine and enzyme measured together), and everything in between exhibits the absorbance of natural product added to enzyme and methionine (ZnCi- zinc citrate, Ga- Gallic acid, ZnCl- zinc chloride, Trigonelline, Na- Nicotinic acid)

Catalysis of methionine by enzyme alone means there is less free methionine to measure. Therefore, the addition of natural products should in theory block the active site to some extent, shown by this bar chart (Fig 6.9)

The Methionine alone exhibits the highest absorbance with the fluorescent agent (OPA) and its absorbance value is proportional to methionine measured in solution (log 1.8), however, when adding enzyme, the methionine measured decreases as the enzyme is using the methionine converting it to the reaction metabolites. The addition of introduction of

chosen products increases the methionine elution, signifying natural product interference with the reaction producing VSCs, exhibiting enzyme interaction and/or inhibition of substrate catalysis.

The log absorbance readings signify how much methionine is left in the solutions with each natural product (and MGL). All the products leave more measurable methionine compared to enzyme, methionine with no product. This eludes to an inhibitory interaction, allowing more free methionine to be quantified. Free methionine measured at 2 pmole/µg exhibits a log absorbance 1.8. Gallic acid leaves the next most methionine with a log absorbance of 1.45 followed by caffeine at 1.41, then zinc chloride and nicotinic acid (1.39, 1.38 respectively) compared to methionine with enzyme reading at a log absorbance of 1.

This data shows some level of potential inhibition, to test this further, lysed bacteria and methionine were incubated together at lower concentrations than previously used in this thesis, to test natural products for an accurate % inhibition, to calculate the IC50.

6.3.4 Inhibition at 100 µM methionine with lysed bacteria

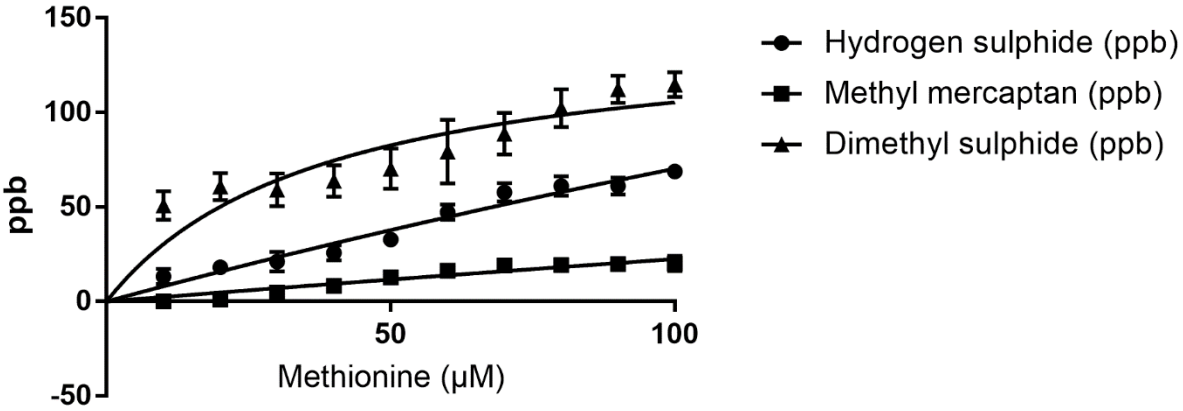

Figure 6.10 Using a concentration gradient of Methionine concentrations up to 100µM a Michaelis-Menten plot has been constructed

Using a lower concentration of methionine than previously in this thesis (100µM in fig 6.10-6.14 vs. 33mM in chapter 5 graphs 5.1 - 5.7 d and e, all using lysed bacteria), the methionine control releases the highest ppb through all concentrations of dimethyl sulphide. At 100µM methionine dimethyl sulphide levels are just above 100 ppb, hydrogen sulphide second

measuring just over 50 ppb and lastly methyl mercaptan that produces under 20 ppb at 100µM methionine.

The oral bacteria and methionine (Used in chapter 4) contains more enzymes and bacterial species present to catalyse the reaction, and a higher concentration of methionine is used, but the inhibitory product is not provided free access to the enzyme through the bacterial cell wall in figure 4.3 a, b and c – controls produce over 300 ppb hydrogen sulphide, 80 ppb methyl mercaptan and 20 ppb of dimethyl sulphide. A higher concentration of methionine (33mM) but with free access to the bacterial enzymes in figures 5.1-5.7 produces controls of H_2S- 350 ppb on average, MM- below 100 ppb and DS values are variable from 50 ppb to 700 ppb, this indicates different enzymes at play producing gasses at different concentrations.

Figure 6.10 shows lower ppb values than quoted above for previous chapters, however the reaction uses a smaller volume and concentration, along with transforming the data into percentage inhibition to witness trends when full inhibition (by inhibitory products) can be reached. Using lower concentrations, there is a more accurate measure of inhibition as there should be a full inhibitory effect from the natural products to accurately get an IC50 value. The graphs produced from Graphpad (prism 7) are under the parameters: [Agonist] vs. normalised response to produce a variable slope with a nonlinear fit. According to Ranaldi, Vanni and Giachetti (1999), the best method of evaluating the kinetic parameters is with a nonlinear regression. The double reciprocal plot should be avoided with a 150% difference between the kinetic results from a nonlinear regression. The graphs below, portray natural products increasing in concentration percentage inhibition of 100µM methionine. A percentage change equation was used to equate these graphs that follow (fig 6.11- 6.14).

Trigonelline

The graphs that follow show the addition of inhibitory panel to 100 µM methionine and lysed bacteria measured for VSC gaseous release on the oralchroma and the data manipulated on graphpad to achieve percentage inhibition vs log µM of inhibitory product.

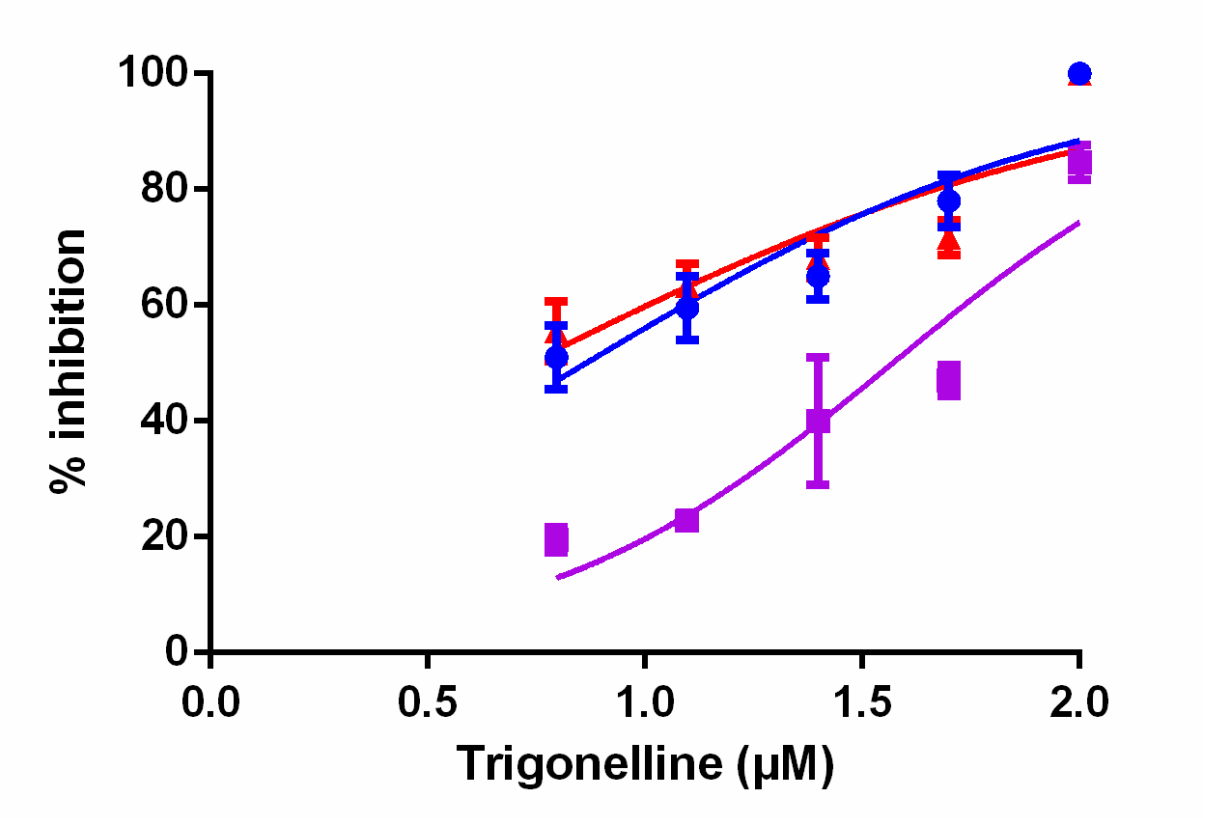

Figure 6.11 Trigonelline IC50 graph showing % inhibition against methionine at 100µM and lysed bacteria on a log scale (x axis) of all three gasses (hydrogen sulphide- blue circles, methyl mercaptan- red triangles, dimethyl sulphide- purple squares) (2.0 log = 100 µM)

At 100 µM methionine, dimethyl sulphide concentrations are inhibited by 80%, whilst methyl mercaptan and hydrogen sulphide are inhibited 100%. The inhibition of methyl mercaptan and hydrogen sulphide start at ~50% and at 2 µM trigonelline, 100% is inhibited, implying that a similar enzyme is targeted for inhibitory effect. Trigonelline also inhibits the release of dimethyl sulphide but to a lesser extent.

Gallic acid

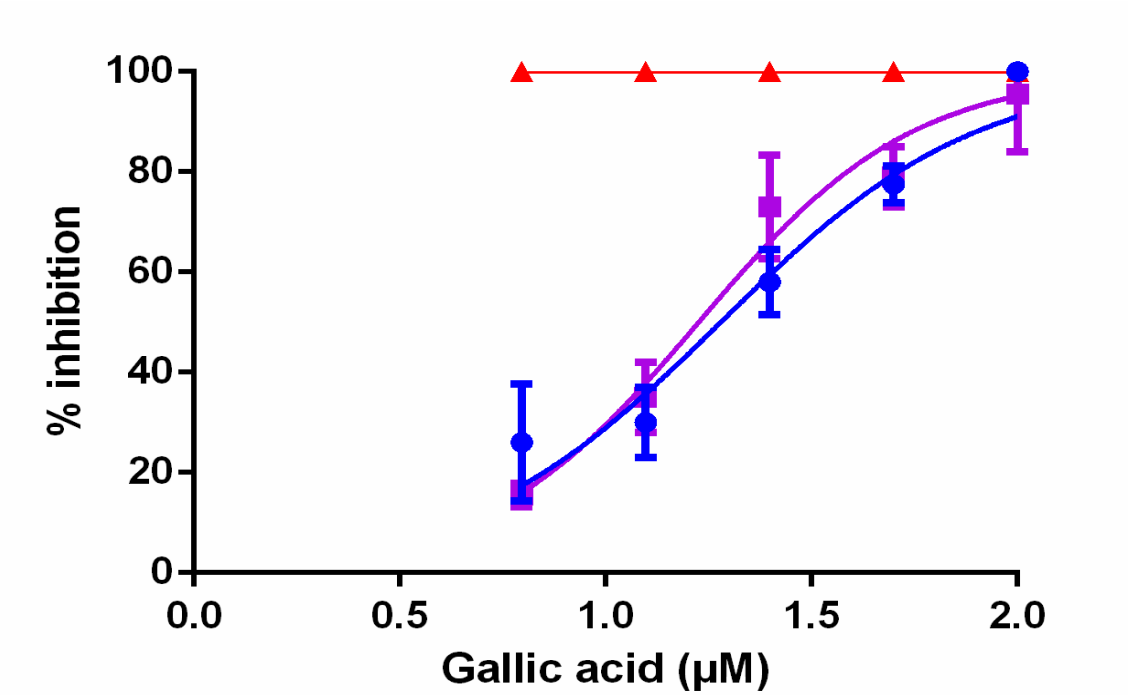

Figure 6.12 Gallic acid graph showing % inhibition on a log scale (x axis) of all three gasses (hydrogen sulphide- blue circles, methyl mercaptan- red triangles, dimethyl sulphide- purple squares) tested on 100µM methionine with oral bacteria

Gallic acid inhibits methyl mercaptan concentrations by 100% through all concentrations. Hydrogen sulphide and dimethyl sulphide are inhibited to the same trend by gallic acid as seen by the similar small sigmoid created by increasing gallic acid concentration. At 2 µM gallic acid, hydrogen sulphide and methyl mercaptan are inhibited 100%, with dimethyl sulphide inhibition finishing a fraction below this (99% inhibitory potential).

Zinc chloride

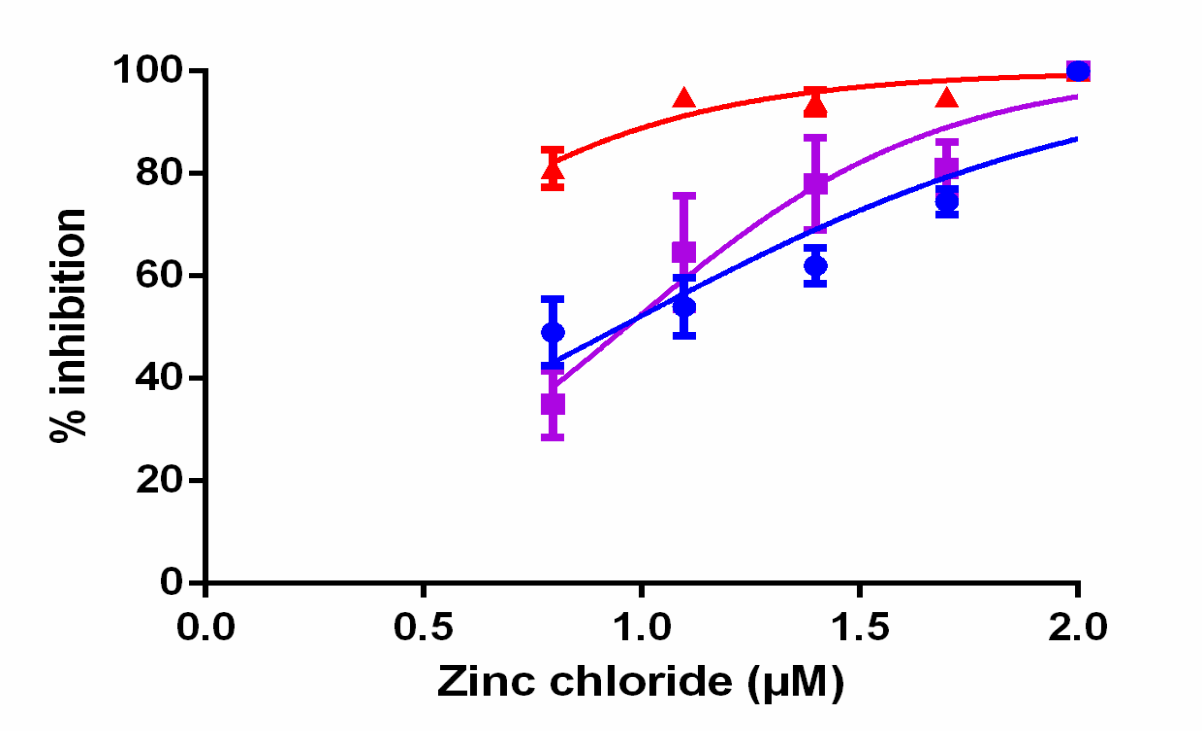

Figure 6.13 Zinc chloride graph showing % inhibition on a log scale (x axis) of all three gasses (hydrogen sulphide- blue circles, methyl mercaptan- red triangles, dimethyl sulphide- purple squares) tested on 100µM methionine with oral bacteria

The inhibition of methyl mercaptan by zinc chloride starts at 80% (at 6.25 µM zinc chloride). This inhibitory effect continues as the zinc chloride concentration increases to 100µM for which 100% inhibition of methyl mercaptan gas. At the highest zinc chloride concentration, hydrogen sulphide and dimethyl sulphide show full inhibition, their starting inhibitory potentials at 6.25 µM zinc chloride between 30-50% inhibition.

Zinc citrate

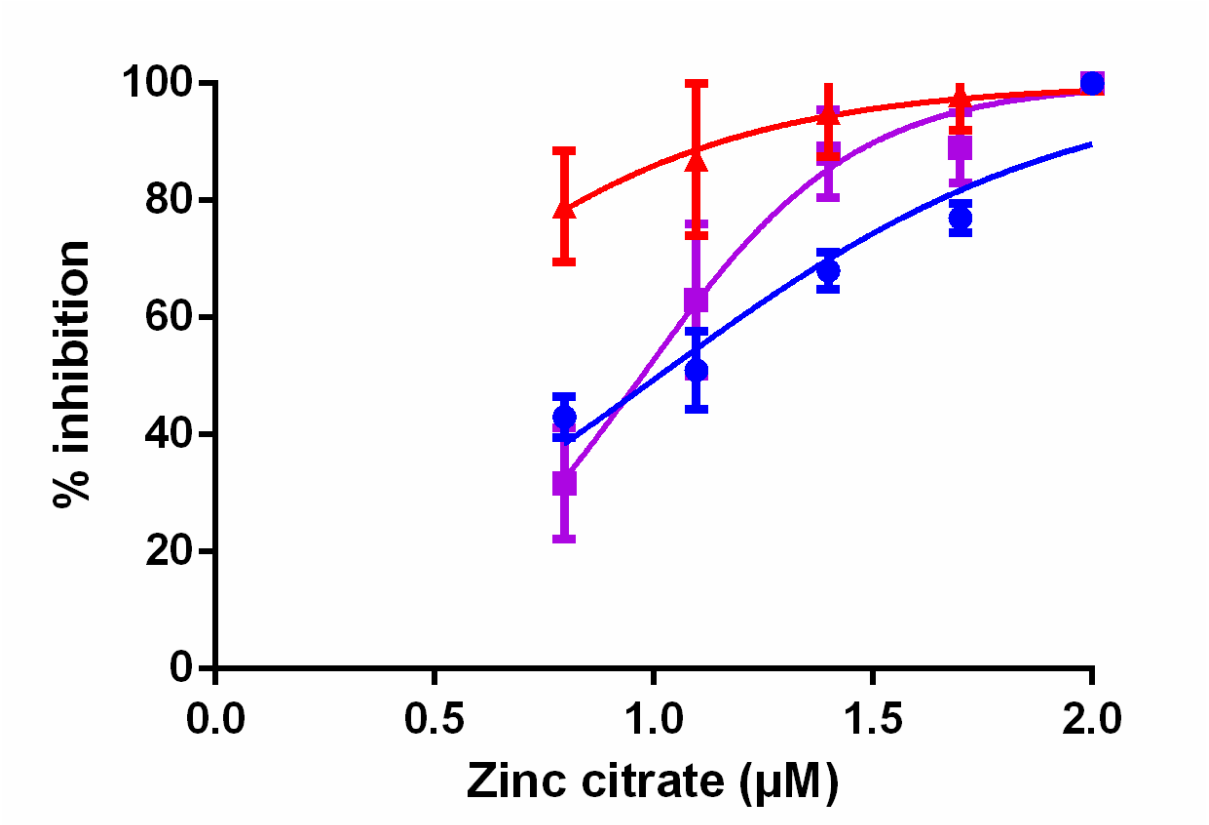

Figure 6.14 Zinc chloride graph showing % inhibition on a log scale (x axis) of all three gasses (hydrogen sulphide- blue circles, methyl mercaptan- red triangles, dimethyl sulphide- purple squares) tested on 100µM methionine with oral bacteria

In fig 6.14, 100µM Zinc citrate inhibits 100% of all three gasses. The starting inhibition at 6.25µM zinc chloride is just under 80% for methyl mercaptan which rises in small increments, comparable to the zinc citrate concentration increases (fig 6.13). Hydrogen sulphide starts at 40% inhibition and steadily rises through the doubling of Zinc citrate concentration. Dimethyl sulphide inhibition starts at 30% and rises rapidly and plateaus at 100% inhibition (100µM Zinc citrate).

Table 6.1 Log IC50 and IC50 determinations from graphpad according to graphs above.

Natural product	Log IC50 (hydrogen sulphide) (IC50)	Log IC50 (methyl mercaptan) (IC50)	Log IC50 (dimethyl sulphide) (IC50)
Zinc chloride	0.949 ± 0.07 (8.9)	0.235 ±0.138 (1.7)	0.963±0.04 (9.2)
Zinc citrate	1.01 ± 0.04 (10.25)	0.294± 0.25 (1.9)	0.973± 0.033 (9.4)
Gallic acid	1.28 ± 0.04 (19.0)	ND	1.226 ±0.03 (16.8)
Trigonelline	0.86 ± 0.07 (7.3)	0.73± 0.12 (5.4)	1.57± 0.04 (37.1)

IC_{50} definition- IC_{50} measurements are the inhibitory concentration at 50% of the active ingredients' efficacy (IC_{50}- **I**nhibitory **C**oncentration at 50%). The lower the value, the more potent the drug, however, this technique to view efficacy comes with limitations for example the value does not take hillslope or maximum effect into account, however for a preliminary drug efficacy *in vivo* the IC_{50} is the accepted enzymatic value.

The lowest IC50 for the inhibition of hydrogen sulphide production is trigonelline with a log IC_{50} of 7.3 µM (Table 6.1), for methyl mercaptan and dimethyl sulphide the most efficacious inhibitory product is Zinc chloride log IC50's 0.235, 0.963 µM respectively.

6.3.5 Bioinformatic modelling

In this section, potential binding capabilities of gallic acid and trigonelline to the MGL enzyme (from *Pseudomonas putida*) are examined via computational studies (bioinformatics). The method is explained in section 2.10. Briefly, documents containing the structures of ligand and substrate are inputted to the autodock vino software. This calculates the most likely distance and conformation of interactions (this process is run in triplicate for accuracy). The distance of the amino acids of the protein structures of ligand and substrate are shown in angstroms and described below.

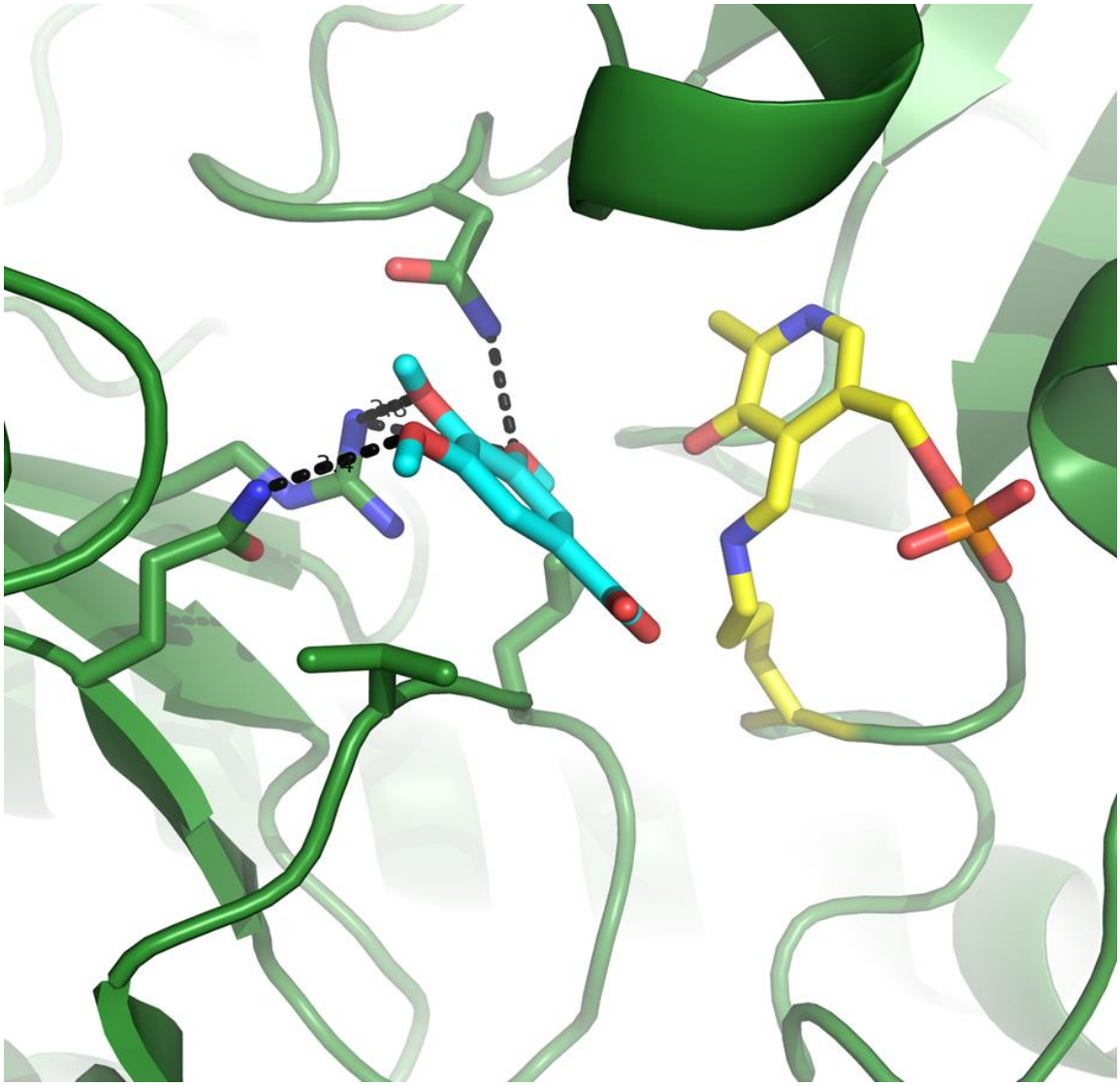

Fig 6.15. Docking (Autodock) 5x2v chain D with Gallic acid- images rendered in pymol

Gallic acid (in cyan) binds near the polar part of active site (2.8 angstroms from Arg 375, 3.3 angstroms from Glu 349, 3.3 angstroms from Asp 161) it is approximately 5 angstroms away from LLP (P5P cofactor- in yellow) (1 polar interaction). Serine shows a long-range H bond to carboxylate of ligand. The benzene ring forms potential hydrophobic interactions with valine 339 and leucine 341.

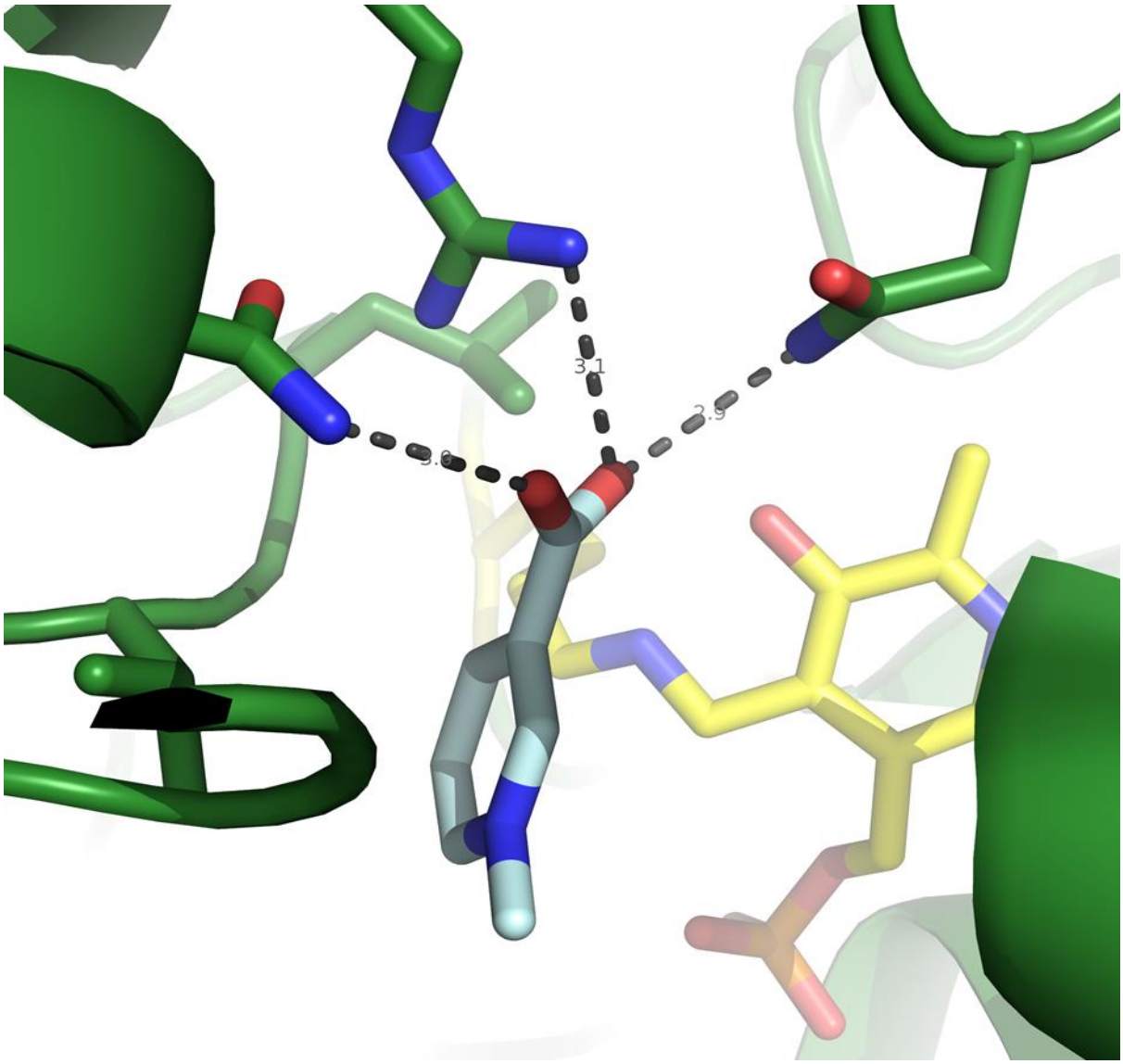

Fig 6.16. Docking (Autodock) 5x2v chain D with Trigonelline - images rendered in pymol

Trigonelline (in light blue) forms an ionic bond (salt bridge) with Arg 375 (positive charge) at 3.1 angstroms, 3 angstrom hydrogen bond with Glu 349 and 2.9 angstrom hydrogen bond with Asp 161- all hydrophilic short range interactions. This binding is located near the MGL active site and there are 2 potential hydrophobic interactions between leucine 341.

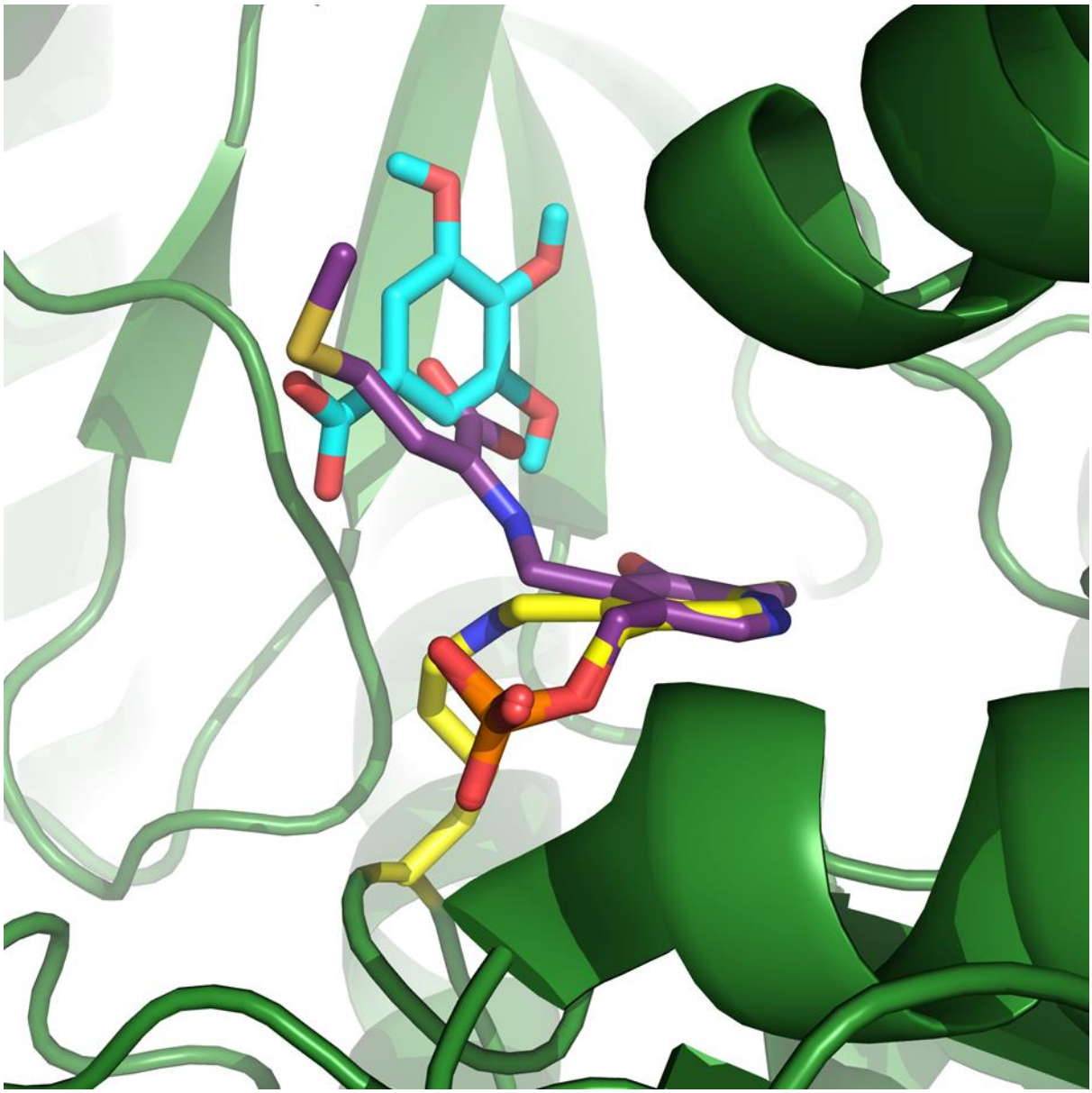

Fig 6.17. Gallic acid bound with methionine binding overlaid

This image shows the binding of gallic acid seen in figure 6.15 but overlaid with methionine (in purple) binding to the active site. From this, it is seen that the ligand (gallic acid) is further away from the P5P co-factor than the methionine, however, there is an overlap in methionine binding to the enzyme and gallic acid, suggesting that gallic acids effect mainly acts on the methionine binding mechanisms.

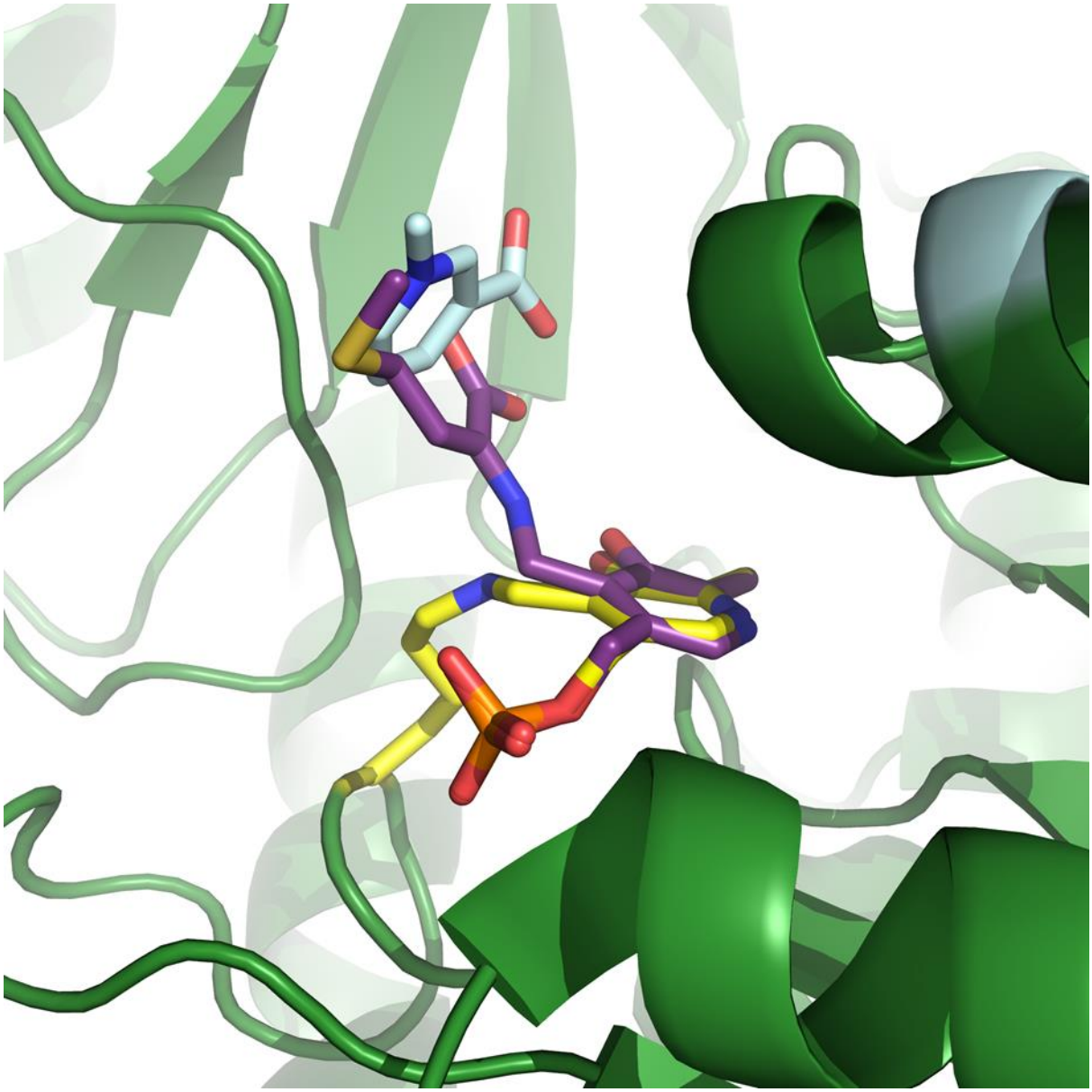

Fig 6.18. Trigonelline bound with methionine binding overlaid

Binding of trigonelline is seen in the same area whilst overlaid with methionine, in the protein active site, located near the P5P co-factor. This shows tight binding conformation of all structures, especially as the methionine wraps the trigonelline revealing the potential receptive conformation.

This prompted a comparison between the genes encoding the MGL enzyme in other oral bacteria of interest to test how comparable this enzyme, and therefore potential inhibitory action of gallic acid and trigonelline was to specific oral pathogens' MGL gene (figure 6.19).

Figure 6.19 BLAST(NCBI) to find sequence alignment and conservation between 5x2v (MGL from P.putida) and other bacteria (P.gingivalis, T.denticola, T.forsythia (37% identical, 55% similar) , V.ratti (57% identical, 74% similar) and F.nucleatum (55% identical, 75% similar)

Conservation on bioedit- the conserved region is viewed by dots under the reference strain of *P.putida*, all those that differ show a letter corresponding to the amino acid replacement

The amino acid at position 116 for *P.putida* MGL is cysteine 116, this is conserved by all the bacteria tested apart from *T.forsythia*. It is seen that *T.forsythia* has an added loop in the structure observed between amino acid 250-280, this explains why it is the least identical to the MGL from *P.putida.*

In terms of ligand binding sites of MGL, the points in the amino acid sequence where docking has shown the most likely placement for binding has been analysed in figure 6.15-6.20. Asparagine 161 and Arginine 375 where binding potentials are observed are completely conserved amino acid in the MGL protein for bacteria sp. analysed.

Valine 339 and Leucine 441 are conserved through all of the bacteria except *T.forsythia* where valine (non-polar amino acid) is replaced by threonine (polar amino acid) and leucine, by histidine.

Glutamine 349 is conserved by *P.putida, P.gingivalis, T.denticola* and *F.nucleatum* but not *T.forsythia* or *V.ratti*, replaced by leucine and glutamic acid respectively. These changes in the amino acid sequences may affect binding potentials of the MGL proteins in these organisms.

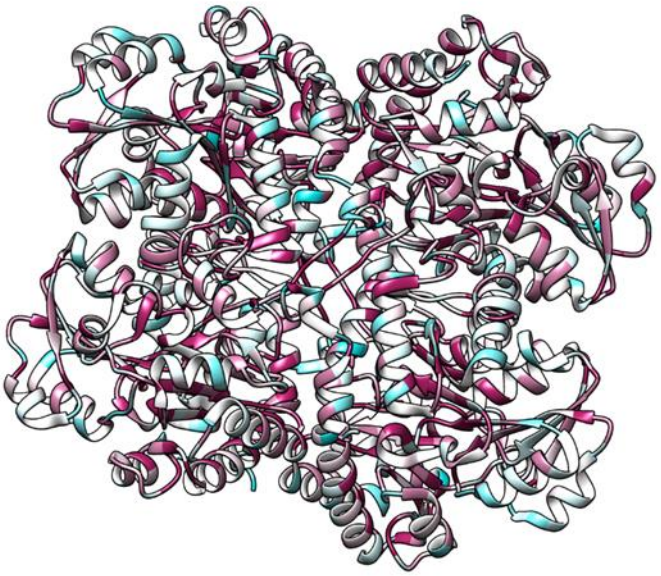

Figure 6.20. Visualisation of conserved and non-conserved regions of Methionine gamma lyase based on Bioedit results comapring P.putida (5X2V) to P.gingivalis, T.denticola, T.forsythia, V.ratti and F.nucleatum (Maroon- highly conserved, Cyan-non-conserved, white- mixed conservation)

The results in bioedit show alignment of protein amino acid across a range of bacteria, this shows that multiple bacteria found in the oral cavity have the protein sequence encoding methionine gamma lyase, therefore able to carry out the enzymatic pathways discussed in this chapter. A software called Chimera was applied to these results to construct the protein coloured to indicate conservation of proteins.

Maroon: The areas in maroon are the conserved amino acid in the sequence using the 6 mentioned bacteria in the figure legend. Most of the colouring shows maroon, representing a high degree of conservation.

White: All amino acids with a mixed conservation, meaning they could be either conserved or not, are shown in white. *T.forsythia* has the protein structure which differs the most from other bacterial proteins (MGL), this could partially explain the white areas in the protein structure.

Cyan: Cyan colouring on the protein structure shows non-conserved regions. There are fewer cyan regions than the other colours, however, there are still areas of 'non-conservation' dotted around the protein structure. These amino acids are not involved in the binding potentials seen in docking figures 6.15-6.18 and further shown in figure 6.19 e.g. amino acids 432-435 (Alanine vs. aspartic acid and glutamic acid).

6.3.6 Methionine gamma lyase (MGL) assay

This assay adapted from an article by Foo and colleagues, (2016), shows that the output of alpha-keto butyrate (a metabolite from bacterial enzyme (MGL) reacting with methionine) is detected at 315 nm without the need of a colour change reaction or fluorescent marker. The addition of the inhibitory products chosen to MGL enzyme allowed a 5-minute pre-treatment before adding methionine at increasing concentrations (Fig). This was measured over time (every minute for 10 minutes) in a 96 well plate reader. First the reaction was done with no inhibitor creating a dose response (figure 6.21), then the addition of inhibitor to 40 mM methionine (figure 6.22).

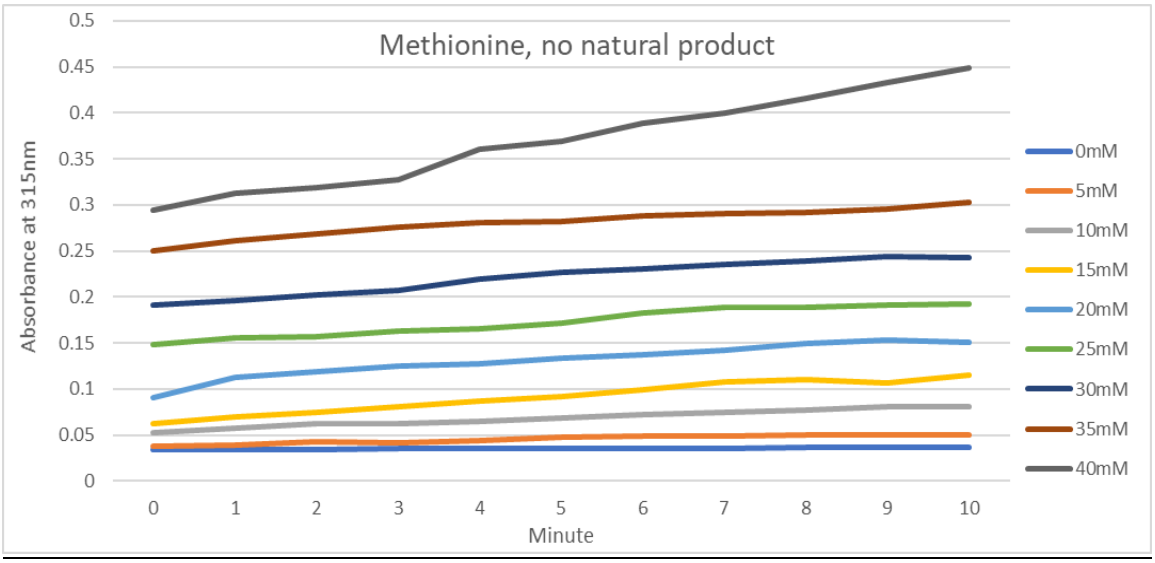

Figure 6.21 Using methionine concentrations with MGL enzyme to quantify alpha keto butyrate absorbance over 10 minutes (at minute intervals)

Figure 6.21 shows the calibration step using methionine in increasing concentration. This was used as a proof of concept that shows that adding a higher concentration of methionine to methionine gamma lyase will output a higher optical density at 315 nm corresponding to alpha keto butyrate. The addition of higher methionine mM increases the alpha keto butyrate but does not deviate much over 10 minutes (usually showing a slight rise e.g. 35 mM= 0.25 at 0 mins compared to 0.31 at 10 minutes). However, this trend changes with 40 mM methionine, which does show a time dependant increase of alpha keto butyrate at 315 nm between 0.29 and 0.45 presenting an overall rise of 0.16 in absorbance values.

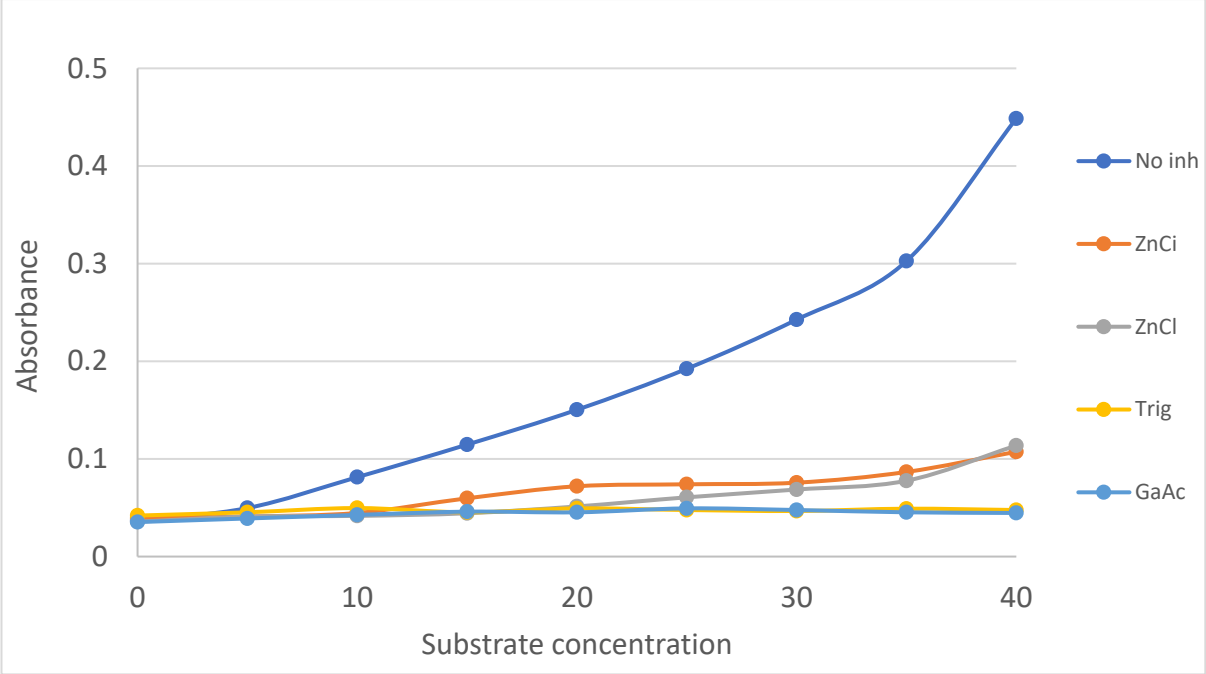

Figure 6.22 shows the addition of the inhibitory panel (at 15 mM) to increasing concentrations of methionine (and 0.08 units of MGL) to quantity metabolite production (alpha keto butyrate) after 10 minutes incubation at 37 ˚C

In this figure (6.22), the impact of the inhibitory panel on the production of alpha-keto butyrate is considered over substrate concentrations at the final 10-minute time point. There is a clear decrease from the control (no inhibitor) in alpha keto butyrate produced with the addition of zinc citrate, zinc chloride, gallic acid and trigonelline. At 10 mM substrate, the control values read 0.08 and the added inhibitors produce half this reading 0.04. Gallic acid and trigonelline produce a maximum of 0.05 absorbance over all substrate concentrations (methionine). Towards higher methionine concentrations (20-40 mM), the zinc products deviate from the others producing an optical density of just over 1.1. The control at 40 mM methionine provides 0.44 abs alpha keto butyrate. There is clearly an inhibitory effect with zinc being grouped together indicating a similar mechanism of action between zinc citrate and chloride.

6.4 Discussion

Methionine gamma lyase is a PLP (Pyridoxal 5 phosphate) dependant enzyme which catalyses the reactions of methionine and other sulphur containing amino acids- gamma replacement and gamma elimination of methionine, beta replacement and beta elimination in methionine, cysteine and analogues (Kandalam *et al.,* 2018). This enzyme is not present in mammalian cells which enhances its potential as a target for the inhibition of pathogenic activity. However, the catalysis of methionine in the oral cavity releases volatile thiols which contribute to oral malodour, as well as, increasing the permeability of the oral mucosa- attracting inflammatory cytokines, speeding the rate at which periodontitis progresses, and inducing the apoptosis of gingival fibroblasts. Methyl mercaptan in high concentrations can also cause damage to central nervous system. (Ratcliff and Johnson, 1999; Yaegaki *et al*., 2008). MGL has been identified in organisms such as *P.gingivalis, T.denticola, Bacteroids spp., C.freundii, P.putida* and some parasites such as *Entamoeba histolytica* and *Trichomonas vaginalis* (Sato *et al.,* 2008; (Sato *et al.,* 2017; Kandalam *et al.,* 2018). Methionine gamma lyase is a homotetramer, and its enzyme commission nomenclature is EC 4.4.1.11 (MGL).

Cancer cells have a high requirement of methionine for cell proliferation (Jeon *et al*., 2016) this means that the catalysis of methionine can have therapeutic effects on tumour proliferation. MGL is an ideal enzyme to target as it is not present in mammalian cells. This approach is therefore tumour specific, and can be administered within red blood cells, which extends the half-life to 9-12 days – compared to the <24h of pure enzyme. The effects of methionine depletion in cancer cells causes forced apoptosis (Gay *et al.,* 2017). Methionine gamma lyase, can therefore be used both as therapy and a target.

An MGL containing parasite *T. vaginalis* is a sexually transmitted infection which is also a co-factor in the transmission of HIV. *T. vaginalis* uses MGL to convert methionine via the gamma replacement mechanism producing methyl mercaptan, alpha-ketobutyrate and ammonia. The thiol, methyl mercaptan, can be used by cysteine synthase producing S-methylcysteine which results in lower intracellular levels of cysteine, revealed by ^{13}C labelling (Westrop *et al*., 2017). As described, there are many applications of studying methionine gamma lyase within cells, and they serve different functions depending on the

source and location. The below information represents the analysis of methionine gamma lyase in terms of oral bacterial origin, oral malodour and protein interaction with amino acid substrate (methionine) and the inhibitory panel used.

Differential scanning fluorometry (DSF) measures protein stability and unfolding through temperature cycles. In fig 6.1 the protein does not sufficiently unfold; this is a typical response of multiple proteins where the signal from the protein of interest (MGL) is lost within the sample 'noise'. This is usually due to the sample purity of methionine gamma lyase, which was further assessed.

SDS page was conducted to establish the purity of the purchased MGL, it was expected to see only one band against a ladder. However, as seen from figure 6.3 that the gel image contained many bands, representing proteins of different molecular weights. As explained in the results, the 'enzyme' sample sent was a mix of proteins from *E. coli*, which exhibits MGL activity converting 1 µM methionine to α-ketobutyrate per Unit of enzyme, at 37 °C, pH7. Determining the weight of the thickest band was done through measurements of distance of protein migrated through the gel/dye front. The log molecular weights are estimated based on the calibration graph (fig 6.4) (known molecular weights/distance migrated) to calculate the unknowns. This data had a 20% error as described in results (due to 0ne point on the line of best fit), therefore combined with the literature, an estimation of the molecular weight of the band was 45-47Kda representing methionine gamma lyase (MGL).

The lysed bacteria used in previous chapters was a mix of bacteria collected from the oral cavity that has been stored, grown and lysed using CelLytic™ B kit (Sigma-Aldrich). The lysed sample represents the enzymes present within oral bacteria, therefore would be representative of activity within the oral cavity rather than an MGL gene expressed in *E. coli*. The latter, however, is easier to quantify MGL within solution. Both enzyme mixes and lysed bacteria solutions were used within this chapter, and the whole thesis. MGL can degrade cysteine with a lower specificity than methionine (Hanniffy *et al.*, 2009). In the oral cavity, bacteria contain multiple enzymes, there is a connecting relationship between cysteine and methionine- using S-adenosylhomocysteine hydrolase (SAH) homocysteine can be converted into methionine by hydrolysis and back via re-methylation. Methionine/homocysteine are precursors for cysteine via the transulphuration pathway.

Cysteine is then catalysed and split to release hydrogen sulphide (Hoon *et al*., 2011). The convergence of more than one enzyme present in oral bacteria can produce both hydrogen sulphide and methyl mercaptan, the former being more widely produced from a range of substrates (Takeshita *et al*., 2012) . There is further evidence for multiple enzymes at work in the fact that IC50 values for hydrogen sulphide and methyl mercaptan differ (7.3 µM vs. 19.0 µM and 1.7 µM vs. 5.4 µM respectively) from each other signifying different enzymes and reaction mechanisms producing the gasses by various means described above. This is the expected result when using a lysed bacteria sample prepared from a solution of pooled oral bacteria, as MGL is expected to be present, which binds more readily to methionine and produce methyl mercaptan in the primary reaction.

…

High pressure liquid chromatography (HPLC) in reverse phase can measure primary amino acid concentrations, through reacting with amino groups to produce highly fluorescent products which can be measured on the fluorescent or UV HPLC (Jones and Gilligan, 1983). The quantification of substrate rather than products gives an alternate view to binding of methionine and the inhibition from the front side of the reaction rather than the inhibition of product formation/ or neutralisation of VSC's produced. In this experiment, enzyme (MGL) is used with the methionine (MET) to produce 'enzyme alone' which produced a (log)absorbance of 1, and methionine is measured with fluorescent OPA alone to give a (log) absorbance of 1.8. The products used shows some level binding to enzyme which could have occurred to leave some methionine to be quantified, resulting in (log)absorbance 1.4. This result suggests that there is an interaction between products and MGL which may block methionine binding to MGL (which would undergo catalysis). This is indicative of competitive inhibition, but there is not enough data in the literature to outright make this claim. However, the bioinformatics in this thesis, strengthens this theory given figures 6.15- 6.20 show overlapping predicted binding between methionine and gallic acid/ trigonelline when 'docked' onto MGL active site slowing the rate of the full reaction.

Interestingly the zinc products have low IC_{50} values for methyl mercaptan, this may be due to a direct reaction with MGL or gas neutralisation. The two mechanisms proposed for zinc's inhibitory action on oral malodour are direct gas inhibition and the suppression of bacterial growth (Suzuki *et al*., 2018). The former mechanism of gas inhibition relies on

zinc's dissociation and binding to another ligand, a proposed mechanism could result in citrate ligand reacting with H_2S forming an aldehyde, allowing zinc to create a bond with sulphur creating ZnS (reducing H_2S released from the oral cavity). Zinc salts have been investigated for their ability to bind sulphur ions from hydrogen sulphide and methyl mercaptan, the theory being a lower stability constant would readily provide free zinc ions with an affinity for sulphur, however Young, Jonski and Rolla, (2002), theorise that sulphur may provide a strong competing ligand for zincs bound to another ligand in order to release free zinc ions for interaction, and therefore the stability constants do not denote their anti-VSC effect. This is seen in figure 6.13 and 6.14, the zinc citrate and zinc chloride have a similar upwards curve for all VSC gasses tested, this denotes the dissociation and therefore the inhibition of volatile gas output. Zinc plays a crucial role in bodily biochemical functions, its binds to a large quantity of metal receptors and 70% zinc is bound to circulating albumin to be delivered to tissues (Roohani *et al*., 2013). The unspecific binding profile of zinc makes it a key biological mediator but also means it did not qualify for ligand docking experiments due to prolific binding leading to too large an error on docking potentials.

Gallic acid – Gallic acid has been linked with a multitude of phenolic effectiveness from bladder cancer- inhibiting migration and proliferation of cells through action on fatty acid synthase, to osteoarthritis, by reducing cartilage degradation (Wen *et al*., 2015; Liao *et al*., 2018). These mechanisms are mostly explained by the free radical scavenging activity- i.e. antioxidants. One report links gallic acid to the oral pathogen *F.nucleatum*, this bacteria adheres to cells and recruits inflammatory cytokines from oral epithelial cells such as IL-6 and IL-8. Whilst gallic acid shows no evidence in decreasing adhesion, it does have the capacity to inhibit the release of inflammatory cytokines and has shown bactericidal activity towards the *F.nucleatum*- MIC of 5mM (Kang *et al*., 2009). Current research shows that although gallic acid had a higher IC50 than zinc containing salts and trigonelline for hydrogen sulphide, it completely inhibited methyl mercaptan produced in the experimental procedure, this indicates a role directly on the MGL enzyme inhibiting the (alpha gamma elimination and gamma replacement) reaction. Further evidence for this is seen in figure 6.16 by a close proximity, 1 polar interaction from the MGL active site and overlapping the methionine substrate in figure 6.18.

Trigonelline- Potential for enzyme inhibition is, like gallic acid, is seen through multiple enzyme targets in for example glucose uptake inhibition in the intestine, and the stimulation of dopamine release (Zhou, Chan and Zhou, 2012). Trigonelline, unlike gallic acid, has antiadhesive properties against the sucrose dependant inhibition of *Streptococcus mutans* to hydroxyapatite surface, (Daglia *et al*., 2002) but does not seem to demonstrate antimicrobial activity against gram negative bacteria (Mueller *et al*., 2011). This suggest enzyme targets to slow and inhibit bacterial metabolic mechanisms. This is shown in table 6.1 which shows a low IC_{50} value (7.3µM) against H_2S, (lower than gallic acid and zinc chloride/citrate), possibly inhibiting the conversion of methionine to cysteine to inhibit H_2S production, or methyl mercaptan conversion to hydrogen sulphide via mechanisms explained in chapter 5 (5.4). An IC_{50} of 2.2 mg/ml was observed from trigonelline against *Salmonella sp.* in a study by (Almeida *et al*., 2006) This is much higher than in IC_{50}'s seen in the current study (7.3 µM) probably due to the barrier of a bacterial cell wall The differences in the IC_{50} from chapter 5 (fig 5.6e. IC_{50}- 0.789 mg/ml- trigonelline vs. H_2S with 0.5 mg/ml methionine) are seen due to the differences in concentrations of substrate used. The docking of trigonelline on MGL shown through bioinformatics seen on figures 6.16 and 6.18. Indicates, with the information in this paragraph, and HPLC results showing a lower methionine conversion when added, that trigonelline can bind to enzymes and inhibit the full rate of bacterial metabolism.

The active site from MGL based on PDB 3vK4 from *Pseudomonas putida* has a very conserved active site. Cys116, Lys240 and Asp241 the latter two from the second subunit of the dimer, forms a hydrogen bond network and this is the contributing factor to specificity to methionine. This information was gained through crystallography and thin layer chromatography analysis. C116 doesn't interact directly with the substrate, however, when substituted for histidine, the specificity to cysteine increases and decreases for methionine by 552-fold (Fukumoto *et al*., 2012). These amino acids mentioned above are completely conserved across the proteins from bacteria in figure 6.19 except *T.forsythia*. The binding shown in figure 6.15 gallic acid slots into MGL, 5 angstroms away from the co-factor and when methionine is overlaid in figure 6.17. This shows a link up with methionine which could change the confirmation decreasing the binding and therefore reaction rate

between methionine and MGL. Trigonelline has a similar effect in figure 6.16 forming short range hydrophilic interactions to Arg 375, Glu 349 and Asp 161, and overlaid with methionine shows an interaction in figure 6.18. This shows that the inhibitory products can interfere with the enzyme reaction, which is further evidence by figure 6.22 which exhibits a similar efficacy in reducing alpha keto butyrate measured from the addition of gallic acid and trigonelline. Zinc products (citrate and chloride) also exhibit similar trends not inhibiting to the same extent as the former two products indicating another mechanism such as gas neutralisation discussed in previous chapters.

In conclusion, zinc products show inhibitory action against the VSC's by chemically disrupting their structure to release sulphur (to bind to zinc) before they are released from the oral cavity. Gallic acid and trigonelline are seen to exhibit effect against VSC's released from the enzyme reaction as seen by figures 6.11 and 6.12, but also inhibiting the enzyme reaction that create the VSC's this is evidenced in HPLC data (fig 6.9) and assay inhibition in figure 6.22. This *in vitro* data in chapter 6 results, shows promising therapeutic potential of these natural products against the MGL enzyme from relevant oral bacteria, inhibiting the release of malodorous gasses.

Chapter 7 The effects of natural products on orally relevant biofilms

7.1 Introduction

The oral cavity contains a large quantity of bacteria, approximately 700 species (Kilian *et al*., 2016). The oral environment allows bacteria to attach to both hard and soft surfaces such as teeth and tongue (see chapter 1). This forms the base of a biofilm which are further built up through bonds and interactions (Fig 7.1) starting with weak physiochemical bonds which could be made stronger and more permanent by bacterial recognition of adhesins on the binding surfaces (Do, Devine and Marsh 2013). The biofilm is a self-regulating habitat containing bacteria, in the oral cavity, often referred to as plaque. This new biofilm environment is formed by many layers of bacteria co-aggregating making up a biofilm matrix and extracellular polymeric substances (EPS) (Bowen *et al*., 2018). These have key roles in the protection and longevity of the biofilm by increasing adhesion, stability and protection against antibiotic penetration compared to their planktonic state counterparts (Berger *et al*., 2018). Microbes in the dental biofilm can carry out genetic transfers and cell-cell signalling exhibiting co-operation and competition; with reactions such as hydrogen peroxide and bacteriocin production to eliminate other cells and compete for nutrients, such is the complexity of a mature biofilm (Marsh, 2017).

Interactions in the biofilm allow species to persist in the mouth that otherwise wouldn't be able to. Gram negative anaerobes are inevitable residents in the oral cavity, the makeup and location of the biofilm containing these potentially pathogenic (opportunistic) bacteria can determine diseases (periodontitis/halitosis). An increased proportion of these malodour causing bacteria such as *P. gingivalis*, *F. nucleatum* and *T. denticola* in a biofilm located in the gingival crevice are associated with inflammation leading to a diseased state (Avila, Ojcius and Yilmaz, 2009). These bacteria interact with the host immune system causing dysbiosis leading to gingivitis (Aas, 2005). The main prevention of plaque accumulation is adequate oral hygiene, which will help the mechanical removal of biofilms and improve the general health of an individual. Therefore, the control of malodour is essential from a cosmetic perspective and to prevent onset of oral diseases.

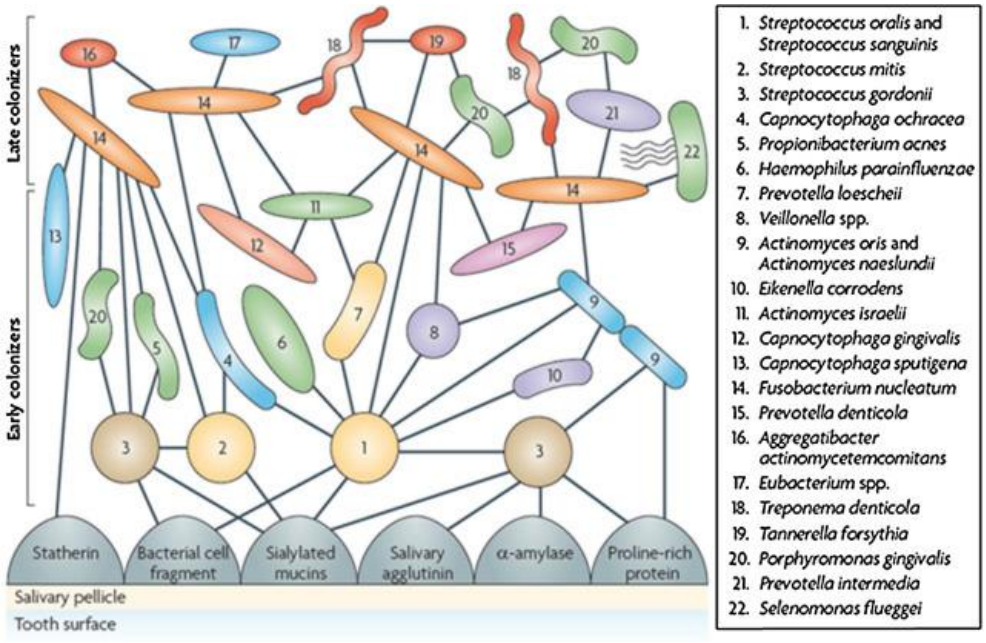

Figure 7.1 Development and bacterial aggregation in a biofilm. Image taken from a review article by Parashar et al., (2015)- shows the interspecies communications from early colonisers interactions and showing subsequent attachment and bonds created by late colonisers, creating an oral biofilm.

Actinomyces sp. (bacteria label 9 and 11 in fig 7.1) are often known as bridge bacteria, they can bind directly to proline-rich proteins on the pellicle surface as seen in image 7.1 or they can co-aggregate to late colonisers e.g. *Fusobacteria nucleatum* and *Porphyromonas gingivalis.* These bacteria contain the enzymes to catalyse salivary proteins and amino acids causing halitosis.

In previous studies, natural based inhibitors such as garlic extracts have been used to arrest the development of biofilms, the authors hypothesise an antagonistic effect on quorum sensing

(Cady *et al*., 2012). Testing products and inhibitors within and on a biofilm is key in tackling the larger issue of biofilm colonisation in diseases ranging from cystic fibrosis to wounds. The oral biofilm created the in current chapter looks at the penetration and overall bactericidal effect of the inhibitory panel chosen: gallic acid, trigonelline, zinc citrate and zinc chloride.

7.1.1 Aims and narrative

This chapter splits into two sections.

Part 1: Experimental biofilm growth in a chamber slide is conducted. This work aims to reveal the effects of the inhibitory panel (IP) on an oral biofilm by live/dead staining coupled with confocal laser scanning microscopy (CLSM) imaging.

The second aim was to test the growth of multiple experimental biofilms from pooled saliva samples (method 2.1), which are applicable for additional manipulation e.g. gas measurements and quantifying CFU/ml. An assessment can be made on the impact of the inhibitory panel used, on the viability of bacteria within the grown oral biofilms.

Part 2: This aims to outline current methods in the literature (and attempted) methods to grow a relevant oral biofilm such as the sorbarod method. This section also remarks on model systems and approaches to choosing biofilm methodologies. This ends with concluding remarks and future work.

7.2 Methods

Chamber slides see method 2.11.1. This process over 5 days allowed oral biofilms to grow on glass slides split into 8. Two of these were grown per experiment (one for imaging, one for CFU/ml analysis). In addition, headspace vials were incubated and prepared in the same way, for an airtight gas extraction inputted to the oralchroma. The initial establishment of these biofilms was checked by method 2.11.2, the crystal violet test for adhesion of bacterial cells to a surface.

The inhibitor panel included (1%) zinc citrate, zinc chloride, trigonelline and gallic acid, these were added to separate biofilms in the chamber for a 10 minutes exposure time. These were then stained- the live/dead procedure followed the baclight™ manufacturer's instructions (propidium iodide / SYTO 9 dyes) Method 2.11.1. Confocal scanning laser

microscopy was conducted on control and treated biofilms (Leica TCS SP2). Results are shown in fig 7.2- 7.6.

The Sorbarod model was trialled for the growth of a biofilm on a large surface area emulating the tongue's surface, the details in this chapter are based on its potential analysis and applications, this is due to technical errors when using the equipment, which did not yield sufficient data for discussion (method 2.13).

7.3 Results- confocal imaging

In this section, confocal images are viewed and analysed in terms of live/dead bacterial coverage. The images are of chamber slides with grown and dyed biofilms. A control image is taken, without the addition of any inhibitor product. The composition and colour differences are compared to addition of product.

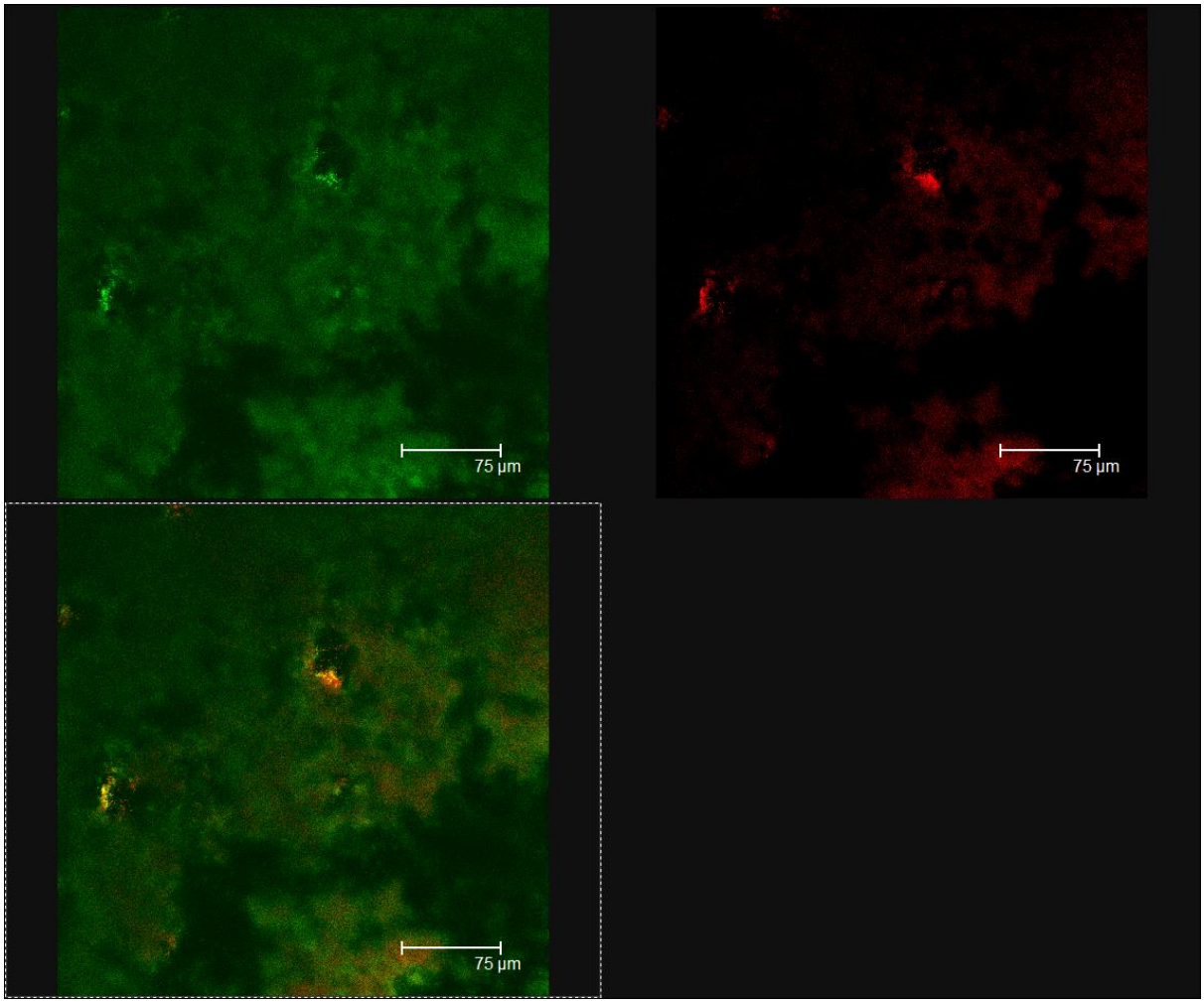

Fig 7.2 Confocal image showing the control growth of oral bacteria as a biofilm in the absence of any products. Stained with SYTO 9 and propidium iodine (representative of n=3)
(Top left pane)- showing 'live' bacteria fluoresced in green
(Top right pane)- showing 'dead' bacteria fluoresced in red
(Bottom left pane)- Live/Dead staining overlaid biofilm

In Figure 7.2 most bacteria are alive and viable seen by an intense green colour, especially when overlaid (bottom left image). The two points of intense fluorescence are the same area in the top two images, this shows that the area with the most intense bacterial growth consists of a mixture of live and dead cells- this is evident when overlaid in the bottom left pane, to produce a yellow colour.

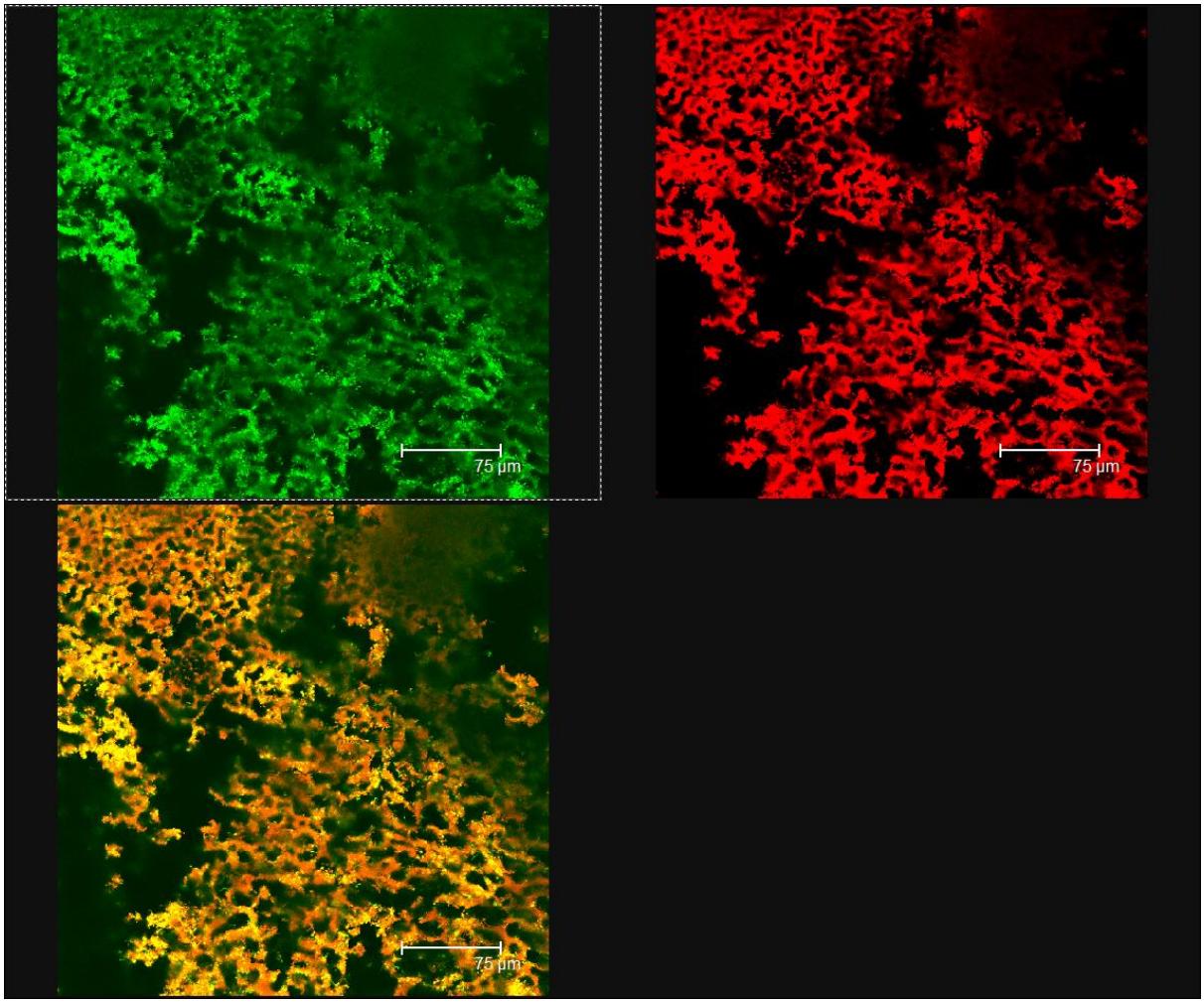

Fig 7.3 Confocal image showing trigonelline incubated with oral biofilms and stained with the Live/dead procedure
(Top left pane)- showing 'live' bacteria fluoresced in green
(Top right pane)- showing 'dead' bacteria fluoresced in red
(Bottom left pane)- Live/Dead staining overlaid biofilm

In this figure (7.3) the green staining is seen as much fainter than the control, the red fluorescence is much stronger but only in the areas of high-density bacterial growth. In the bottom left, overlaid image, there is a yellow/red appearance, the yellow represents both red dead cells and green live cells mixed.

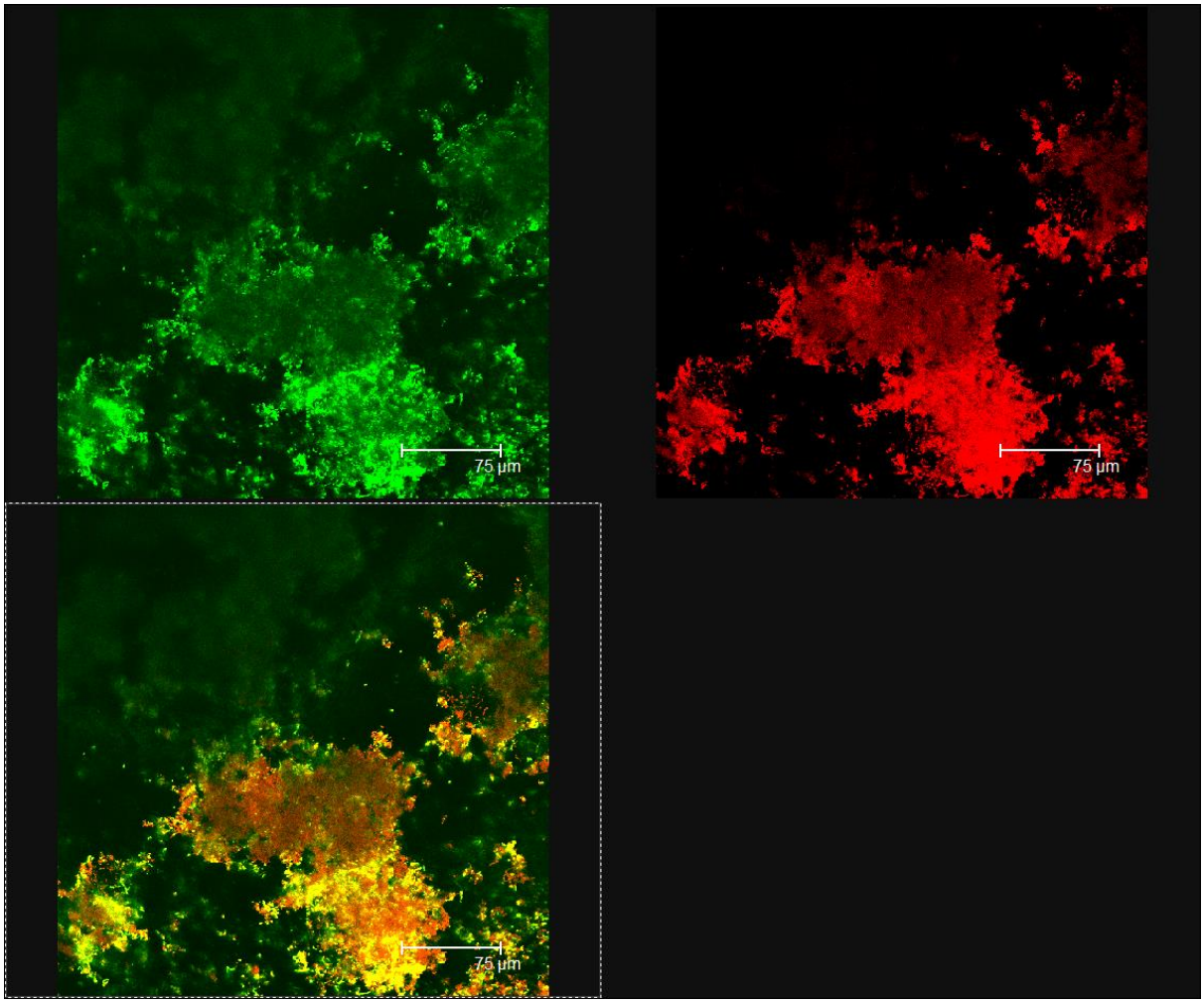

Fig 7.4 Confocal image showing Zinc citrate incubated with an oral biofilm and stained using Live/Dead procedure.
(Top left pane)- showing 'live' bacteria fluoresced in green
(Top right pane)- showing 'dead' bacteria fluoresced in red
(Bottom left pane)- Live/Dead staining overlaid biofilm

The top left of the top left (live) image shows the growth of live bacteria that doesn't fluoresce strongly and stays completely green when overlaid with the image of dead bacteria (red), followed down by a section of green viable bacteria that fluoresce slightly more and under that, a section of bacteria fluorescing green the most (bottom right of top left image) in a gradient of biofilm/ bacterial intensity. The dead (red) cells are prominent in the middle section of the bottom two bacterial sections of growth. The dead cells are integrated with the live cells, in the same areas of strong fluorescence, showing that with dense biofilm coverage there are more cells that take up propidium iodine displaying red colour under the CSLM.

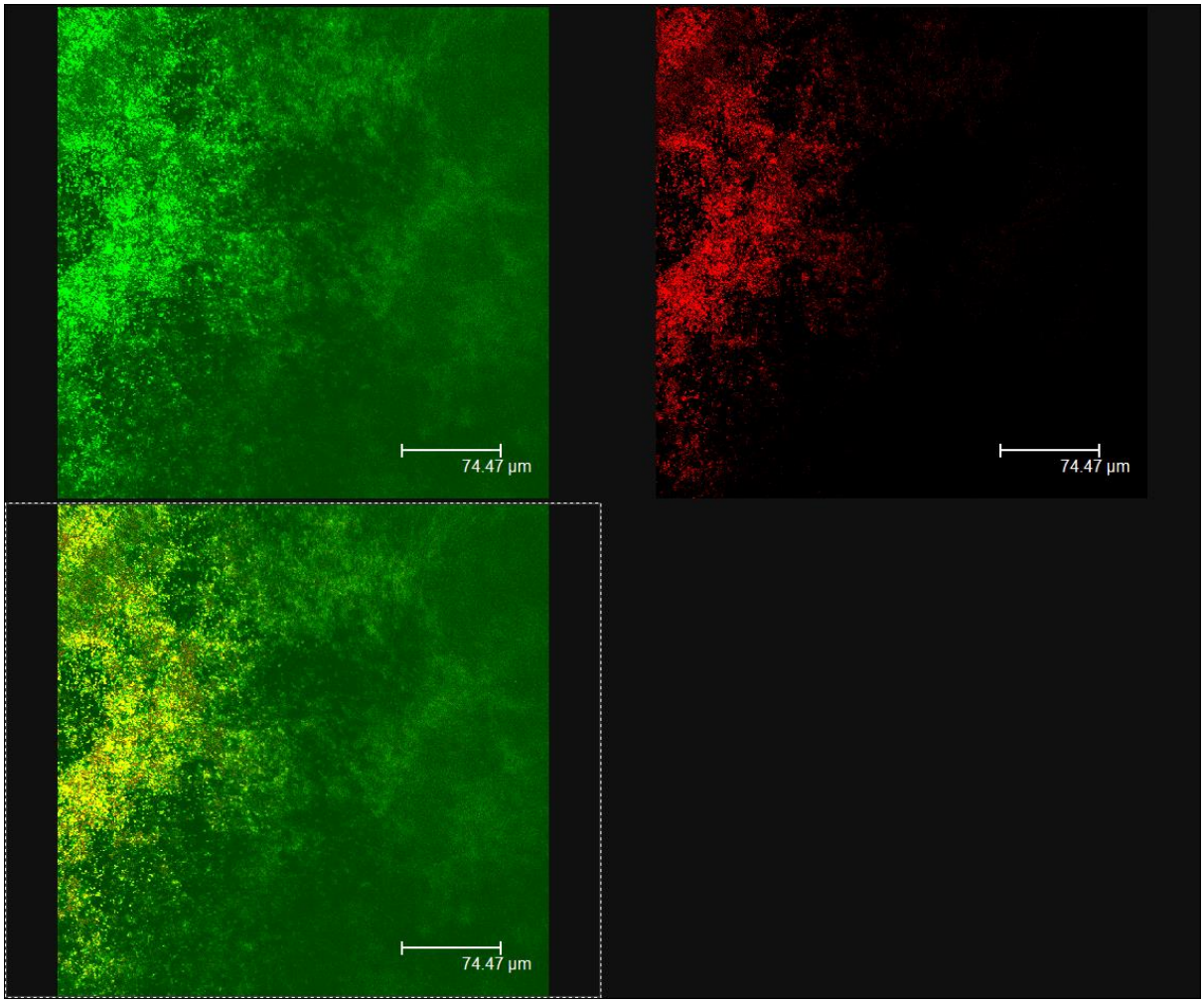

Fig 7.5 Confocal image showing Zinc chloride incubated with an oral biofilm and stained using Live/Dead procedure.
(Top left pane)- showing 'live' bacteria fluoresced in green
(Top right pane)- showing 'dead' bacteria fluoresced in red
(Bottom left pane)- Live/Dead staining overlaid biofilm

In this figure the live cells image (top left) shows dense bacterial growth spanning the captured image. The top right image presents a semi-circle of red cells protruding from the left-hand side. In the bottom left overlaid image, the red cells from the dead stain image, colours the green a slightly more yellow hue with dotted red cells, however, the green/ live cells are prominent in this case all over the image.

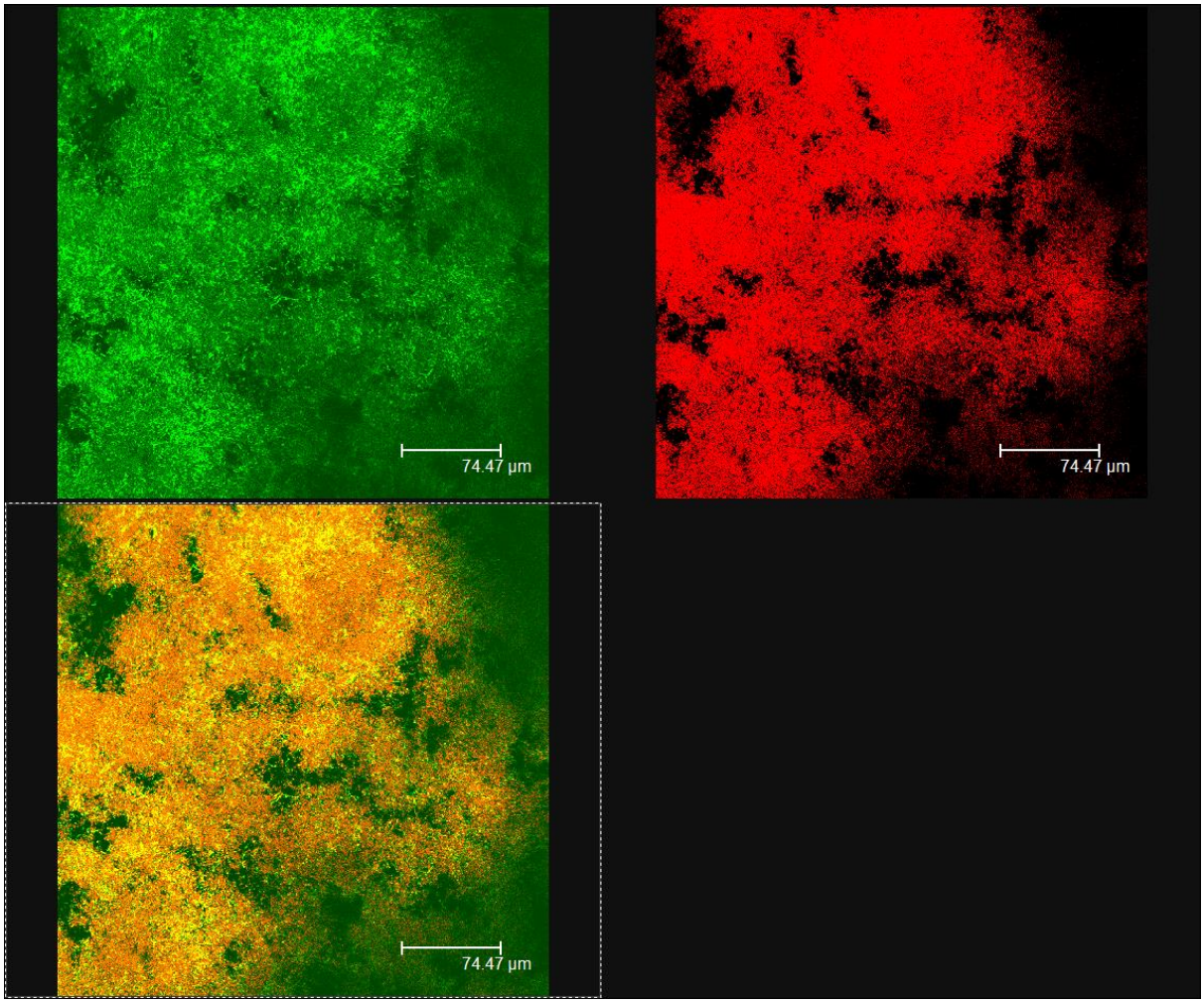

Fig 7.6 Confocal image showing Gallic acid incubated with an oral biofilm and stained using Live/Dead procedure.
(Top left pane)- Live bacteria fluoresced in green
(Top right pane)- Dead bacteria fluoresced in red
(Bottom left pane)- Live/Dead staining overlaid to obtain full image and intensities.

In the top left pane in figure 7.6, there is wash of green live cells, with more intense fluorescence emanating from a central column of cells coming from the bottom left and reaching the top of the image. This central column of cells are the ones affected by the product, staining red to display inviable cells. The overlay expresses a more intense red colour in the stained area resting on yellow cells (a mix of both live and dead), expanding into green live cells which are not damaged by gallic acid.

All chamber slides analysed and viewed in above images were grown in duplicate per experiment (n=3). In the adjacent chamber slides, biofilms were disrupted with 500 µl PBS, this was extracted, diluted and plated to achieve colony forming unit per ml (CFU/ml) count. Biofilms were also grown in the same way on glass bottomed headspace vials

(method 2.11.2). The headspace gas was extracted, and the hydrogen sulphide concentrations plotted on the chart below (figure 7.7).

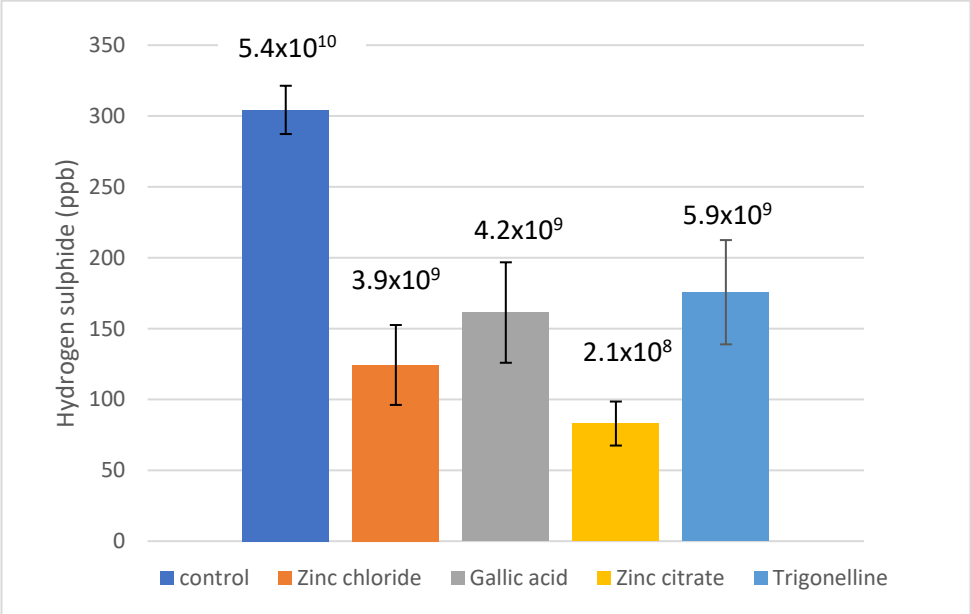

Fig 7.7 Hydrogen sulphide output from biofilms (pictured above), on top of each bar is the CFU/ml counted from the biofilm in the presence of the corresponding inhibitory product

This bar chart (fig 7.7) shows the hydrogen sulphide produced measured from the headspace containing biofilm on the oralchroma, and the colony forming units counted from biofilm dilutions (with and without natural product pre-incubation) spread onto Colombia blood agar.

The control presents the highest concentration of hydrogen sulphide (304 ppb). Zinc citrate incubated biofilm released the least hydrogen sulphide and a 2-log reduction compared to control in the colony forming units. This potentially indicate that the reduction in hydrogen sulphide produced is due a lower density of bacteria in this sample. Both gallic acid and trigonelline has a 1 log higher CFU/ml than the zinc citrate, and therefore more viable bacteria available to produce a slightly higher concentration of hydrogen sulphide. However, zinc chloride maintains the a similar CFU/ml to biofilm treated with gallic acid but produces 37 ppb less hydrogen sulphide. To the authors knowledge, this is first VSC gas assessment from static oral biofilm samples, and therefore provides the viability of using this model for future work.

7.4 Discussion

Chamber slides were used to grow the biofilm on a glass surface, supplemented BHI broth with 2% glucose was used and the chambers incubated for 5 days (see methods 2.11.1). The static growing conditions used is ideal for a mixed-model biofilm creating an *in vitro* biofilm for evaluation (Standar *et al*., 2010). This gave enough time for a visible biofilm to be grown in each chamber (verified with a crystal violet assay for adherence method 2.11.4). The solution was washed out carefully to remove planktonic debris and stained with live/dead stain (Baclight ™). This method of growing biofilms for manipulation and analysis was successful, as was the same method of growth on a glass bottom (in a headspace vial)- this method allowed the author to measure VSC gas concentrations released from a biofilm. Other methods of biofilm development trialled within current research were not successful such as the sorbarod method discussed in this chapter.

Biofilms are known to have an increased tolerance to antimicrobial agents due to increased protection from EPS, it can take up to 50 times the original MIC to eliminate a single species biofilm (Kavanaugh and Ribbeck, 2012). More reasons for increased tolerance of a biofilm include neighbouring cells offering group protection from antimicrobials, and decreased penetration limiting effectiveness. Therefore, imaging stains in a biofilm through CSLM can reveal the effect of an interfering substance, in this case the inhibitory panel discussed above are reviewed for their effect on the viability of bacteria within the biofilm.

STYO9/PI staining is classed as reliable staining technique to view the viability of bacteria, with a simple set up procedure, detectable and differentiable live and dead bacterial cells. Only 3 of the 10 staining combinations tested in this paper were deemed reliable (Tawakoli *et al.,* 2013). Draw backs include damaged cells (sub-lethally) will sometimes show up as dead/ stained red which eludes to more death than the true value. There is also the issue of non-culturable bacteria in the oral cavity which would not be accounted for during analysis. Non-culturable bacteria can be measured via PCR with no discrimination between live/dead cells, however Àlvarez *et al.,* (2013) paired qPCR with propidium monoazide to overcome this limitation and quantify viability, which could be the next step in further research to enhance the visual data in this chapter. The dyes work by penetration of the

membrane, PI only staining cells with high membrane permeability indicating damage or lysis.

The control confocal image of a biofilm uninterrupted by natural products (Fig 7.2) exhibits mostly green cover of bacteria indicating live viability, there are 2 very small pockets of red/dead cells but the overlay (bottom left pane)- yellow colouring, shows that this is minor and could be attributed to natural and complex killing mechanisms within the biofilm- these are protective mechanisms of the biofilm on the oral microbiome homeostasis e.g. *Streptococcus gordonii* production of hydrogen peroxide to compete with other bacteria of the same genus (*Streptococcus mutans)* in an oral biofilm (Kreth, Zhang and Herzberg, 2008).

The zinc products show a localised cell death where red cells dominate small areas, however, from the overlay of the live/dead images of the 2 individual zinc products, it is seen that zinc chloride has a greener output indicating more viable cells. This data is supported up by a larger hydrogen sulphide concentration from zinc chloride and a bacterial concentration of $39x10^8$ CFU/ml compared to zinc citrate with a concentration of $21x10^7$ CFU/ml (1 log lower than zinc chloride). Zinc citrate produces less hydrogen sulphide and the overlay of live/dead images shows a more predominant red colour, indicating a higher concentration of bacterial cell death.

Gallic acid and trigonelline shows a spread of red and green cells overlapping in areas of dense cell presence. These overlapping areas are mostly red with undertones of yellow showing that the top layers of bacteria are killed or damaged using gallic acid and trigonelline. The CFU/ml (10^8) is alike to zinc chloride which visually presents more viable bacteria from the CSLM (Fig 7.5) and less hydrogen sulphide (124 ppb compared to 165-175 ppb from gallic acid and trigonelline Fig 7.7). This could indicate other mechanisms of inhibiting hydrogen sulphide output whilst not damaging the bacterial cells- for example enzyme inhibition. Carvalho *et al.,* (2012) uses *S. mutans* biofilms to test the effect of clearfil protect bond containing 12-methacryloyloxydodecylpyridinium bromide (MDPB) as an antibacterial solution. A mix of viable and non-viable cells (green/red- yellow overlay) were observed over time. The antibacterial solution shows decreasing cell viability over 590s compared to the control- similar seen in current research (chapter 7), where after 10 minutes of incubation (600s), top layer cell death/ membrane disruption is observed (by

the red cells) compared to the control (Fig 7.2) indicating that the addition of inhibitors with no notable antibacterial effect, in an *In vitro* biofilm, will demonstrate a similar pattern of cell death to the addition of a membrane disrupting antimicrobial (MDPB).

However, biofilm disruption and activity is not only defined by the antimicrobial agents added. As detailed in this discussion section (*S.gordonii*), bacteria in the biofilm have the ability to kill cells to maintain its homeostasis, the biofilm also has the ability to auto repair, even when under stress. For example, Davey and Hexley, (2010) examined *Saccharomyces cerevisiae* uptake of propidium iodine: 7% of the species were able to self-repair, and therefore PI uptake does not always correspond to dead cells, it is the integrity and permeability of the membranes which allows dyes to stain cells. The transition of cell viability and the nature of irregular biofilm compositions makes it difficult to accurately quantify cells.

However, it is clear in this chapter that all products used (zinc chloride, zinc citrate, gallic acid and trigonelline) affected the cell membranes showing damage on the top layer of cells in all images. They also successfully decreased the hydrogen sulphide gas measured from the control (Fig 7.7). Although the least red seen in zinc chloride treated biofilms, which are similar to the control (visually), there is a 1-log reduction in CFU/ml. This shows that the cells are reducing in number/viability and decreasing H_2S gas production. But the CSLM images (representative from a triplicate) are only as reliable as the ever-changing composition of the oral biofilms.

Chapter 8 Oral biofilm methodologies and further research

8.1 Introduction- Approach to biofilm methodologies

The approach to producing biofilms comes in two veins. The first is controlling the environment and the maximum number of variables for reproducible biofilm establishment. However, reproducible is not a word usually associated with biofilms in nature. Holistic approaches retain 'real to life' scenarios but the reproducibility and therefore accuracy of data is depleted. Future techniques used in the oral health industry should take both approaches into consideration when choosing bacterial composition and methodology. The experimental outcomes should assist the experimental design. During the time of this thesis I have used multiple biofilm systems, each with advantages and disadvantages. Below, is a summary of these methodologies, some of which are emerging in this area of research within industry.

8.2 Biofilm models

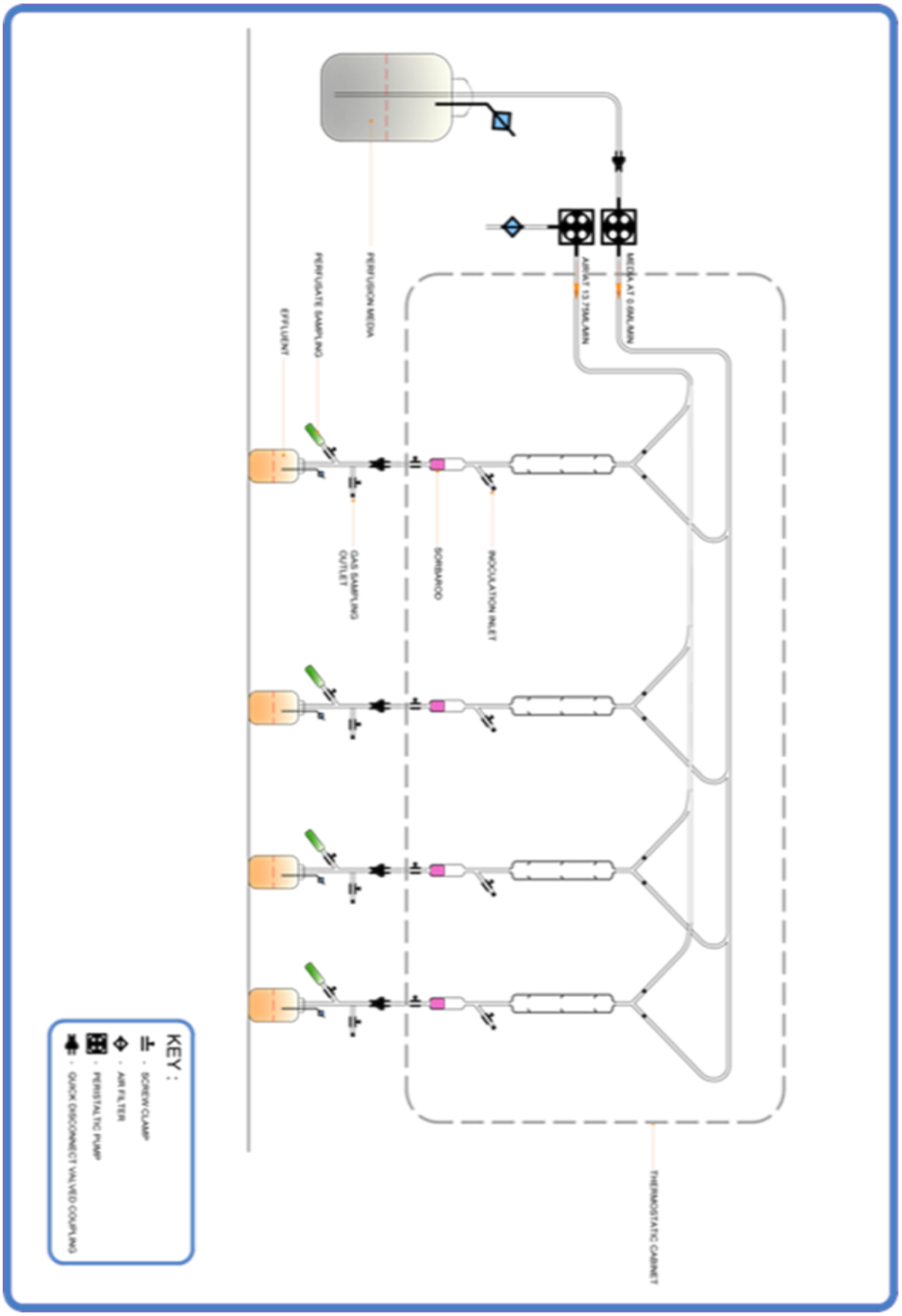

Figure 8.1 Adapted from Burnett and colleagues, (2011) and Maria Antonella sole (2014) (MSc project Kingston University). Demonstrates the sorbarod system set up.

The dotted line represents the isothermic cabinet, set at 37 °C. The sorbarod filter (made of cellulose fibres) was set up within silicon and marpene tubing. As seen in the image, above the sorbarod filter there is an inoculation inlet. Oral bacteria from tongue scrapings

samples were resuspended in 5 ml of specialised media 1ml was introduced to each filter via the inlet and allowed to establish for 48 hours. At the end of this initial incubation. Media and air are turned on to run through the tubing for an additional 18 hours. (Air at 13.75 mL/min) (media at 0.6 mL/min). Analysis of the samples included: gas extraction by syringe to be measured on the oralchroma resulting in VSC measurements from a biofilm representing the tongue surface. Effluent media was neutralised, diluted and swabbed onto Colombia blood agar, incubated and counted (CFU/ml). The sorbarod filter was cut up and stained (STYO9/ PI- Live/dead, baclight™) for confocal imaging. (Master's thesis of Maria Antonella Sola (Kingston university, 2014)

All parts of this experiment need to work in order to collate accurate data. The tubing rig- held together with connecters and cable ties was temperamental and broke apart often compromising the sterility within the tubes. The tubes are very small and would often result in the accumulation of water and pressure, this would burst the pipe connectors breaking the closed environment and letting water/media leak out onto the laboratory floor. The concept of testing a biofilm formed on fibres with a high surface area, pumping through air and media at a slow rate, emulates conditions in the oral cavity, this would be an ideal platform for further analytical steps described above, however, this did not work enough times to supply a triplicate of data in this thesis. The model currently is working within GSK oral healthcare, this has been down to new tubing, and new connectors, from a GSK supplier.

CDFF- The constant depth film fermenter (CDFF) is another method of growing biofilms. This method boasts rotating blades, delivering new inoculum and clearing some debris away at the same time. The mechanism of the CDFF is to keep all five biofilm plugs at a constant depth and therefore a reproducible biofilm for testing the effects of certain inhibitory agents. These plugs can be removed at any time, allowing the potential for immature biofilms as well as mature to be treated and evaluated (Pratten *et al*., 2007, Hope *et al*., 2012).

CDC- CDC biofilm reactor works by inserting rods into the biofilm reactor. Each rod contains three coupons of specified material. For oral biofilm growth, the coupon can be made of hydroxyapatite or an enamel surface. Within the reactor, a bulk of media/ artificial saliva (with bacterial inoculum) promotes the growth of a biofilm on the surface of the coupon.

This is under continuous shear flow due to a magnetic stirrer mixing the bulk providing consistent flow across all coupons. The coupons can be treated with a product of choice e.g. mouthwash, at any time in this process allowing the user to prepare an experimental design that suits the outcome e.g adherence inhibition data would require pre-treatment or data relating to penetration into the biofilm will require post-treatment. For the data output, these coupons are stained and scanned under the CSLM.

Flow cell- The flow cell technique allows the view of a developing biofilm. This is the only method available that permits set up under the confocal microscope (CSLM). There is an input and output flow which passes media/ artificial saliva through the cell (loaded with relevant substratum) and effluent media can be discarded. The strains of interest are subject to pre-staining, or GFP biofilm producing bacterial strains fluoresce green under the CSLM, this developmental analysis can be done in static conditions too. The inlet pipe (with peristatic pumps) can also deliver a product of interest to gage activity within the biofilm, or during its development.

Figure 8.2 Flow cell apparatus. Can be set up under a microscope and input and output tubes for media flow can be inserted into both ends.

Table 8.1 Advantages and disadvantages of biofilm model (Sorbarod)

Sorbarod pros	**Sorbarod cons**
Method suitability to test air/ media/ filter staining	Labour intensive/ fiddly and becomes non-sterile very quickly
5 biofilms tested with separate inlet tubes for 5 separate analysis at once	Cellulose fibres substratum hard to analyse- background staining
Orally relevant biofilm can be grown on sorbarod filter (high surface area)	Low throughput
	Biofilm of undefined size and composition
	Pressure build up/ leaking pipes
	Tubes set up from scratch every 5 autoclave runs
	Flow split between 5 pipes- inaccurate measure

Table 8.2 Advantages and disadvantages of biofilm model (CDC)

CDC pros	**CDC cons**
Coupons made of orally relevant material, (hydroxyapatite/ enamel)	Background staining of coupon
Potential gas analysis (unreported)	Low throughput
Consistent flow (rpm)- reproducible	No way to treat individual biofilms with product at flow (but can apply pre/post treatment to individual rods*)
Three coupons per rod, individual rods can be removed and multiple tested at once (with separate pre/post treatment*)	

Table 8.3 Advantages and disadvantages of biofilm model (CDFF)

CDFF pros	**CDFF cons**
Removable individual biofilm plugs- available to test at any time in growth (immature and mature)	Low throughput
Bacteria form biofilm at consistent flow rate (defined biofilm size)	No gas outlet, but could be made with Y shape connector
Visual analysis not subject to background staining	No individual inoculum inlet (for separate natural products to be added to each biofilm)
5 biofilms tested per pan	
Inoculum added over time (salivary flow rate)	

Table 8.4 Advantages and disadvantages of biofilm model (Flow cell)

Flow cell pros	**Flow cell cons**
Static or pressurised flow development of biofilm can be viewed under the microscope. (The only option that offers real time analysis)	Only one biofilm can be made and analysed and tested on at one time
Low background staining	as a GFP strain- green fluorescent protein)
Treatment can be introduced at any time during development	Organisms need to be pre-stained (or available

Although sorbarod seems to have the most cons, it is most holistic approach replicating tongue environment and it was chosen in regards to the additional testing available, however, with some alterations, additional information such as gas measurements and CFU/ml could be collated from other models that have a more stringent biofilm development system. The chamber slide model used in this thesis, is a fit for purpose static biofilm model with minimum background staining. The flow cell design is the closest to a shear flow model adapting the chamber slide model used to produce biofilm images (figures 7.2 to 7.6). The introduction of tubes into the chamber/cell means sterile delivery of inoculum and media, and less human variation replacing media every 24 hours.

8.2.1 Imaging techniques

Throughout this thesis the CSLM was used as the microscopic technique. This is a theme among the literature when working with biofilms, however other techniques of imaging a dental biofilm are available. Some of these include scanning electron microscopy (SEM) which provide a detailed view of the bacterial cells, shapes and adherence to a surface. Micro-computed tomography (Micro CT) allows a three- dimensional image to reveal bacterial binding and patterns within grooves. Pires and colleagues (2017), used dual-energy micro-CT to investigate dentin demineralisation and biofilm loads on, and in the tooth.

8.3 Thesis conclusion

The main aim of the thesis was to scope any enzymatic interactions between chosen and a protein responsible for catalysis of methionine in oral bacteria- Methionine gamma lyase. This analysis extended to bacteria in all forms: planktonic, lysed and biofilms as well as the enzyme studies. The crux of initial testing and a theme throughout was the oralchroma which provided hydrogen sulphide, methyl mercaptan and dimethyl sulphide measurements (VSC gasses) per sample injected and tested.

8.3.1 Summary – experimental chapters

The first step in achieving the aims of this thesis was the testing of an amino acid substrate that would provide a measurable interaction with oral bacteria to produce volatile sulphurous gasses. Cysteine, at all concentrations provided hydrogen sulphide levels which were too high to present a reliable negative control (Figures 3.2 and 3.3), reaching the limit of detection on the oralchroma when tested alone (dissolved in PBS) (figure 3.4). The theory behind these high controls was cysteine oxidation, allowing a release of hydrogen sulphide. Therefore, optimisation of cysteine followed by removing oxygen in a variety of ways. Methods included nitrogen and helium gasses pumped into an airtight system to remove the oxygen from the vial containing deionised water and cysteine powder (appendix 1). This did not stop the reaction of dissolved cysteine releasing high levels hydrogen sulphide detected by the oralchroma.

The oralchroma was tested for its ability to detect the correct concentration of hydrogen sulphide against known concentrations and the GC-MS, this verified that the oralchroma was within the correct limits to accurately detect hydrogen sulphide (table 3.2). After attempting to optimise cysteine, it was decided to move onto methionine as another sulphur containing amino acid, present in the oral cavity, metabolised by bacterial enzymes.

Enzymes in the oral bacteria can catalyse the metabolism of methionine and cysteine. The reactions from this produce hydrogen sulphide, methyl mercaptan and dimethyl sulphide (VSC's) and other metabolites including alpha-keto butyrate (figures 1.3 and 1.5). In addition, the research in chapter 4 and 5 points to an increased production of hydrogen

sulphide in multiple ways from bacterial enzymes (figure 4.13). This is further evidenced by differing IC_{50} values for the same inhibitory product for different gasses (table 6.1). The gasses released from methionine and whole bacterial cells (in solution) is displayed in chapter four; crude products were obtained, prepared and incubated with the above reaction/solution to determine which may have potential chemicals to achieve a decrease in VSC production. Initial assessments concluded that garlic inhibits gasses measured on the oralchroma compared to the control (fig 4.6), however odourless garlic capsules did not decrease gasses to the same degree (fig 4.7). Zinc citrate reduced hydrogen sulphide from the control by over 99% (table 4.3) however, only decreased hydrogen sulphide to this extent. It has been associated with the inhibition of plaque index when used in commercial toothpaste slurry (Moran *et al*., 2001). Green tea is also efficient at removing gasses measured with 100% inhibition over measured time points. Although red wine contains many active polyphenols it failed to inhibit the gasses released, hydrogen sulphide reached its limit of detection (max ppb) (figure 4.4a). Alcohol has reasons not to work- by cytotoxic action on bacteria cells/ or alternately providing ethanol for bacterial metabolism both causing dysbiosis (Fan *et al.,* 2018). De-alcoholised wine reduced by 50% its original liquid content, did not achieve the required inhibition to take forward either, the alcohol content was seemingly not the only issue. From this chapter, it is clear crude products can work inhibiting volatile sulphur compounds, the crude products contain many compounds which, when separated and tested for efficacy at specific concentrations can lead to the adoption into toothpaste formulation.

Methods of lysing the bacterial cells were attempted disussed in chapter 5– before cellytic B was chosen, which chemically lysed both gram positive and gram-negative cells (table 5.1). The importance of revealing the enzyme is to gain accurate kinetic parameters and in turn, analyse the mechanism of gaseous production and enzyme inhibitory processes. The whole cell analyte comparatively, provides a picture of the product penetration through the membrane over time. Using lysed bacteria is a theme throughout chapter 5 and 6, it is seen as a ‘happy medium’ containing all the exposed enzymes present in the supernatant with direct access for inhibitory products. The enzyme studies in current thesis, involves a mix of using the self-made cell lysate and a purchased oral enzyme- methionine gamma

lyase (MGL) (Sigma- Aldrich); however, the purity was equivalent to that of a single *spp*. lysate, containing the relevant enzyme of choice.

In chapter 5, gallic acid succeeded at decreasing all gasses measured from lysed bacteria and methionine. It has previously been reported to disrupt gram negative bacteria due to an affinity for the membrane (Kang *et al*., 2008), however, there was no membrane so the effect must extend beyond this. The reduction in H_2S occurs in a dose dependant way with a relatively low IC_{50}- 0.32 (figure 5.1e). Zinc chloride shows a trend wise decrease from the control on hydrogen sulphide, however, exhibits the largest IC_{50} value of all other products tested, in the literature it is noted for its bacteriostatic effect and inhibiting glycolysis by oxidising the thiol groups (Pearce and Sissons, 2002). Zinc acetate delivers the lowest IC_{50}, however, this could possibly be attributed to gas neutralisation. Zinc citrate is the most effective in theory with basic anions and a high stability constant, it is the most used zinc variation in current toothpaste formulations. The IC_{50} for zinc citrate in chapter 5 (figure 5.7e), is also very low showing rapid activity, but like zinc acetate, this is most likely the effect of neutralising the hydrogen sulphide before detection. Nicotinic acid shows a trend wise decrease in maximum velocity of the reaction (Vmax) as the concentration of nicotinic acid increased. Trigonelline decreased the hydrogen sulphide in a trend wise manner but not the other gasses. It had the second highest IC50 of 0.7 but also the largest effect size according to partial ETA^2 (89%) (table 5.2). From the results in this chapter, it is difficult to discern from gas ppb data whether the gasses are being neutralised or enzymes being inhibited, even with the addition of statistical and enzyme parameter analysis. Therefore, the aim of chapter 6 was to achieve enzymatic data and the inhibitory potentials of the inhibitory panel on the enzyme of choice- MGL.

Chapter 6 utilises experiments with both the cell lysate, but with a better suitability for enzyme analysis than chapter 5, and the purchased enzyme. Different IC_{50}'s for the same product on different gasses shows the mechanism of gas production involves various enzymes at play and inhibited within the supernatant of cell lysate. As described above, MGL is the main target and catalyses methionine being used as the substrate. The purchased enzyme that contained MGL, was used in experiments where other oral enzymes in the reaction would be detrimental to results obtained e.g HPLC and alpha-ketobutyrate assay (method 2.14).

HPLC used the enzyme and the reverse reaction was analysed, measuring methionine with and without the addition of the MGL enzyme, the enzyme notably decreased the methionine output with assumed catalysis transpiring. The inhibitory panel added to the HPLC vial increased methionine output compared to only enzyme (figure 6.9), inferring a link between MGL enzyme inhibiting methionine binding to its full potential reducing catalysis. The theory of this inhibition is strengthened by bioinformatic docking potentials, which indicate that gallic acid and trigonelline have a binding site on MGL overlapping that of methionine's. Gallic acid displays MGL inhibition by decreasing H_2S and methyl mercaptan (to a larger extent) the IC_{50} for gallic acid against methyl mercaptan could not be measured due to full inhibition through the whole experiment. Trigonelline results also indicate a type of inhibition, which mostly works on the production of hydrogen sulphide (0.8 IC50- the lowest of products tested). Trigonelline and gallic acid both inhibit MGL production of alpha-keto butyrate through methionine (substrate) increasing concentrations. From the effect on the small individual enzyme to the effect on the ecosystem of a biofilm seen in CSLM imaged biofilms in chapter 7. The gallic acid and trigonelline remain consistent in their ability to inhibit gas production, figures 7.3 and 7.6, only show a top layer cell 'death' with a 1-log kill compared to the control sample. This implies an enzyme-based mechanism at inhibiting halitosis. The zinc's (zinc citrate and zinc chloride) possess stable, comparable values for the decrease in concentrations of H_2S from biofilm samples, indicating they have a similar mechanism of action to each other. This is most likely bacteriostatic and gas neutralisation, see chapter 5, this theory is strengthened by their similar trend rise in figure 6.22, unable to inhibit MGL and methionine's production of alpha- keto butyrate as methionine concentrations rose. In addition to low levels of cell 'death' seen in figures 7.4 and 7.5. Both zinc products were ineligible for bioinformatic analysis due to documented prolific binding, which is incidentally the mechanism by which they bind sulphur from VSC's, to neutralise the gasses released from oral malodour.

8.3.2 Further research

The assessments carried out in the current thesis involve VSC reduction analysis, and further analytical techniques revealing the potential enzymatic activity through Km, Vmax

and IC50 values. The enzyme section of this thesis (chapter 6) describes tests done on a purchased enzyme which was not a pure sample, therefore the system is not as 'clean' as it could be, and lysed oral bacteria gives a more realistic perspective on what may occur in the oral cavity *in vivo.* The biofilm chapter shows a visual of the effect of natural product on cell viability through CSLM. There is also some bioinformatics giving theoretical data of pure enzyme and ligand binding which shows potential enzyme binding mechanisms. All the data gathered is *in vitro*. For further study on the enzymatic mechanisms and binding that could abate halitosis I would propose 1. Protein cloning, expression and purification 2. Toxicity studies on the effect of natural products at differing concentrations on oral cell lines and 3. Continue work with suitable biofilm model (described in chapter 8) to gain understanding of product efficacy in a biofilm and 4. *In vivo* testing/ clinical studies.

Protein cloning, expression and purification

This methodology from Morcos and colleagues (2015) describes a simple way to clone and purify the protein to use for in depth enzyme analytics. The DNA from MGL of *P.gingivalis* is amplified via PCR, the primers are designed to introduce NheI site before the start codon and EcoRI site after the stop codon and ligated into a pGEM-T vector. This was then sub-cloned by digestion of the inserted NheI and EcoRI sites and further ligated into pET28a vector (including N terminal His Tag) The vector was transformed into *E.coli* and grown in Luria broth supplemented with antibiotic in a shaking incubator at 37°C until mid-log phase. The cells were vortexed and resuspended in storage buffer. They can be frozen until needed for purification. (Raran-Kurussi *et al*., 2017)

A purification step is required to remove the tags, this is crucial to not interfere with structural studies, this can be performed with tobacco etch virus (TEV) protease a seven amino acid long protein where position of the amino acids is relatively relaxed but needs consideration pre-use. The TEV protease works by site- specific endoproteolysis to remove N-terminal His Tag. This is a 2-step process starting with His-tag removal by TEV protease and then conducting immobilised metal affinity chromatography (IMAC). The most common type of metal used is nickel for recombinant proteins which yields the most

sample. NaCl (250mM in the MGL case) should be used in the loading buffer to deter nickel bead electrostatic binding and glycerol to reduce hydrophobic interactions. (Waugh, 2011) (Bio-rad.com, 2019). The remaining proteins are then subject to SDS page to display the bands indicative of the cloned and purified protein.

APPLICATIONS: The purification of the enzyme allows further analysis into enzyme parameters such as structure, unfolding and binding information (at a range of temperatures, pH and concentrations). This information builds up an image of how the enzyme reacts and binds and dissociates to certain chemicals. Once this data is ascertained, it can be analysed alongside data in this thesis which determines enzyme parameters in the presence of the eluted cell contents. This information is applied in drug development. Enzymes are 're-useable' and speed up reactions, in this case the MGL enzyme is the target for halitosis management. Therefore, inhibitory data on all forms of this enzyme (pure, and within cell) are vital for *further in vitro* and *in vivo* investigations.

Toxicity studies on oral cell lines (with natural products at varying concentrations)

The oral cell lines that should be tested for cytotoxic effect of products/ drugs are human oral squamous cells and gingival fibroblasts, pulp cells, periodontal ligament fibroblast (Iida and colleagues, 2012).

MTT 3-(4,5 dimethylthiazole-2-yl)-2,5-diphenyltetrazolium bromide- The MTT test for cytotoxicity is designed to be colorimetric and measure cell viability. The formazan formed through the reduction of MTT by mitochondrial dehydrogenase gives a linear relationship between absorbance and cell metabolism. The rate of cell growth is directly expressed in the colour signal emitted. The cells are lysed, and crystals solubilised for measurements to be read at 570nm. This can be easily adapted into a high throughput method by using multi-well plates conducting many experiments at once (Chacon *et al*., 1997; Mahajan *et al*., 2012).

Lactate dehydrogenase- The LDH assay is a measure of how many dead or damaged cells are left in solution by the formation of formazan. Lactate dehydrogenase is released as the eukaryotic cell is damaged. In a second coupled reaction, NADH converts the tetrazolium

salt to a red colour, which can be measured at 492nm. The formazan released is proportional to the lactate dehydrogenase being released from cells (Kumar P, Nagarajan A, Uchil PD., 2018).

8.4 Conclusions

VSC reduction by using the chosen inhibitory products, shows real potential in eliminating odour. In chapters 3, 4, 5 and 6, the mechanism of VSC reduction in differing states of bacteria tested; whole cell, lysed cell, enzyme treatment can be attributed to inhibitory effects on the bacterial enzymes' rate of reaction and therefore decelerate metabolite formation. Interaction with specific bacterial enzyme (MGL) has been documented in chapter 6 through assays and computational bioinformatic modelling which eludes to an interaction between gallic acid/ trigonelline and MGL (especially when overlaid with methionine). Zinc products as described previously are prolific binding ions and therefore most likely neutralising VSC's. Chapter 7 reveals efficacy of the inhibitory panel on an oral biofilm which shows some promise and justifies further investigation to promote these products for commercial use in the control of oral malodour.

Appendix 1

Degassed cysteine quantified for VSC release. This includes methods of degassing (nitrogen supply tube, ultrasonic bath and helium bubbling) to eliminate the oxygen in solution, reported to oxidise cysteine and skew hydrogen sulphide results seen in chapter 3

2% Cysteine with degassed water (min)	**Hydrogen sulphide (ppb)**	**Methyl mercaptan (ppb)**	**Dimethyl sulphide (ppb)**	**2% methionine with degassed water (min)**	**Hydrogen sulphide (ppb)**	**Methyl mercaptan (ppb)**	**Dimethyl sulphide (ppb)**
0	2467	0	0	0	120	60	0
30	2376	0	0	30	102	0	0
60	2467	0	0	60	109	0	0
Degassing a different method (N2) (min)	**Hydrogen sulphide (ppb)**	**Methyl mercaptan (ppb)**	**Dimethyl sulphide (ppb)**	**Degassing a different method (N2) (min)**	**Hydrogen sulphide (ppb)**	**Methyl mercaptan (ppb)**	**Dimethyl sulphide (ppb)**
0	960	0	0	0	19	0	0
30	714	0	24	30	38	2	0
60	798	0	0	60	82	20	0
Degassing In ultrasonic bath and helium (min)	**Hydrogen sulphide (ppb)**	**Methyl mercaptan (ppb)**	**Dimethyl sulphide (ppb)**	**Degassing In ultrasonic bath and helium (min)**	**Hydrogen sulphide (ppb)**	**Methyl mercaptan (ppb)**	**Dimethyl sulphide (ppb)**
0	518	10	8	0	26	0	0
30	1275	0	0	30	13	8	0
60	2343	0	0	60	32	6	0

Appendix 2

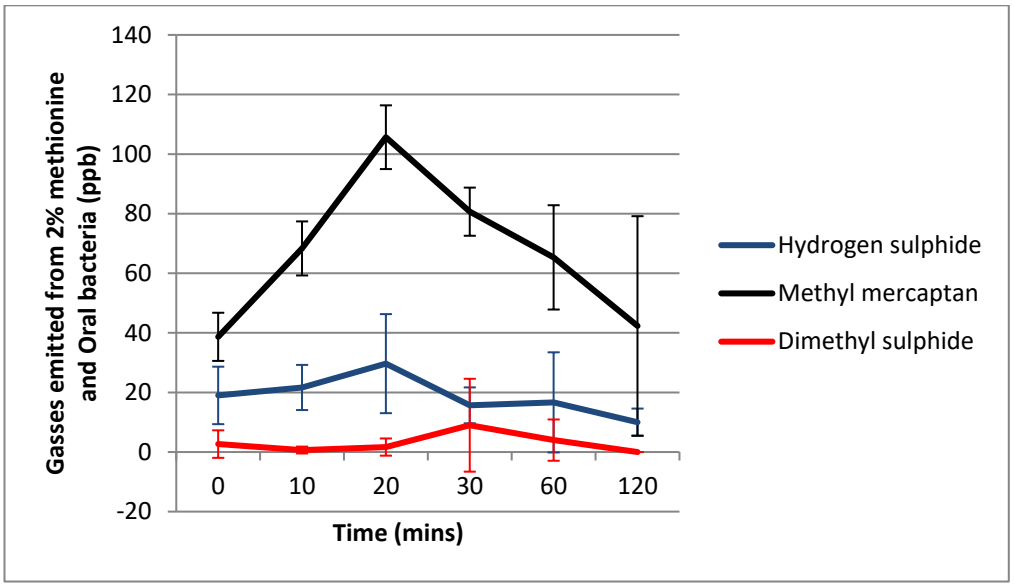

1% Methionine solution with oral bacteria at 0.6 OD. Based on a triplicate where gas measurements were taken at time intervals represented by the x axis of the graph and the data points exhibit the average result from the three and error bars display the standard deviation between the three experimental runs.

In this figure the bacteria were grown aerobically and the difference to microaerophilic growth of oral bacterial is clearly noticeable from the value achieved in fig 4.1.

Appendix 3

supplementary results to chapter 5

Vmax and Km values for gallic acid on hydrogen sulphide concentrations

Natural product	Vmax at 0.5% Methionine	Km at 0.5% Methionine
Gallic acid control	266.6 ± 13.1	0.25 ± 0.08
Gallic acid 0.1%	195.3 ± 9.4	0.19 ± 0.07
Gallic acid 0.5%	127.8 ± 4.9	N/A- 1.229e-016
Gallic acid 1%	86 ± 7.5	N/A- 2.137e-016
Gallic acid 5%	50 ± 5.3	N/A- 1.941e-016

Vmax and Km values for trigonelline on hydrogen sulphide concentrations

Natural product	Vmax at 0.5% Methionine	Km at 0.5% Methionine
Trigonelline control	194.2 ± 14.5	0.2819 ± 0.1
Trigonelline 0.1%	140.2 ± 3.5	0.7576 ± 0.07
Trigonelline 0.5%	245.5 ± 30.3	7.097 ± 2.3
Trigonelline 1%	131.3 ± 15.4	4.07 ± 1.2
Trigonelline 5%	103.7 ± 14.1	5.466 ± 2.8

Vmax and Km values for zinc citrate on hydrogen sulphide concentrations

Natural product	Vmax at 0.5% Methionine	Km at 0.5% Methionine
Zinc citrate control	267.5 ± 9.9	0.394 ± 0.04
Zinc citrate 0.1%	149 ± 19.1	0.5881 ± 0.02
Zinc citrate 0.5%	134.5 ± 28.4	1.001 ± 0.4
Zinc citrate 1%	109 ± 29.1	1.205 ± 0.4

Zinc citrate 5%	2.223 ± 0.9	0.01775 ± 0.06

Natural product	Vmax at 0.5% Methionine	Km at 0.5% Methionine
Nicotinic acid control	203.5 ± 26.78	0.382 ± 0.15
Nicotinic acid 0.1%	71.21 ± 12.54	N/A- 1.197e-016
Nicotinic acid 0.5%	38.42 ± 15.46	N/A- 2e-016
Nicotinic acid 1%	14.42 ± 5.36	N/A- 1.722e-016
Nicotinic acid 5%	7 ± 2.92	N/A- 2.151e-016

Vmax and Km values for nicotinic acid on hydrogen sulphide concentrations

Natural product	Vmax at 0.5% Methionine	Km at 0.5% Methionine
Caffeine control	238 ± 9.2	0.04 ± 0.006
Caffeine 0.1%	83.33 ± 6.1	N/A- 1.538e-016
Caffeine 0.5%	62.06 ± 9.3	0.005 ± 0.01
Caffeine 1%	26.95 ± 2.7	0.05776 ± 0.02
Caffeine 5%	19.98 ± 5.3	0.2645 ± 0.02

Vmax and Km values for caffeine on hydrogen sulphide concentrations

Natural product	Vmax at 0.5% Methionine	Km at 0.5% Methionine
Zinc chloride control	179.8 ± 5.7	0.0481 ± 0.007
Zinc chloride 0.1%	81.47 ± 10.8	N/A- 1.785e-016
Zinc chloride 0.5%	48.8 ± 7	N/A- 1.96e-016
Zinc chloride 1%	83.43 ± 11.9	2.33 ± 0.7
Zinc chloride 5%	48.82 ± 9.2	3.97 ± 2.3

Vmax and Km values for zinc chloride on hydrogen sulphide concentrations

Statistical tests done figures 5.1- 5.7 a, b and c on SPSS comparing the dependant and independent variables (ppb, concentrations of natural product/ substrate)

NP	Caffeine	Gallic acid	Nicotinic acid	Trigonelline	ZnAc	ZnCi
Pillais trace	1.95	2.58	2.138	2.685	2.062	1.156
F	(48,150) 5.833	(38,120) 20.646	(48,150) 7.764	(48,150) 26.668	(40,120) 7.327	(30,96) 2.228
P	<0.001	<0.001	<0.001	<0.001	<0.001	<0.001
Wilks λ	0.24	0.001	0.020	0.000	0.11	0.190
Partial ETA^2 (%) effective interaction	65%	86%	71%	89%	68%	38%

References

Adams, S., Theobald, A., Jones, N., Brading, M., Cox, T., Mendez, A., Chesters, D., Gillam, D., Hall, C. and Holt, J. (2003). The effect of a toothpaste containing 2% zinc citrate and 0.3% Triclosan on bacterial viability and plaque growth *in vivo* compared to a toothpaste containing 0.3% Triclosan and 2% copolymer. *International Dental Journal*, 53(S6P1), pp.398-403.

Adegboye, A., Christensen, L., Holm-Pedersen, P., Avlund, K., Boucher, B. and Heitmann, B. (2012). Intake of Dairy Products in Relation to Periodontitis in Older Danish Adults. *Nutrients*, 4(9), pp.1219-1229.

Al-Ahmad, A., Follo, M., Selzer, A., Hellwig, E., Hannig, M. and Hannig, C. (2009). Bacterial colonization of enamel in situ investigated using fluorescence in situ hybridization. *Journal of Medical Microbiology*, 58(10), pp.1359-1366.

Alcock, L., Perkins, M. and Chalker, J. (2018). *Chemical methods for mapping cysteine oxidation*.

Almeida, A., Farah, A., Silva, D., Nunan, E. and Glaria, M. (2006). Antibacterial Activity of Coffee Extracts and Selected Coffee Chemical Compounds against Enterobacteria. *Journal of Agricultural and Food Chemistry*, 54(23), pp.8738-8743.

Almeida, A., Naghetini, C., Santos, V., Antonio, A., Farah, A. and GlÃ³ria, M. (2012). Influence of natural coffee compounds, coffee extracts and increased levels of caffeine on the inhibition of Streptococcus mutans. *Food Research International*, 49(1), pp.459-461.

Alvarez, G., Gonzalez, M., Isabal, S., Blanc, V. and Lean, R. (2013). Method to quantify live and dead cells in multi-species oral biofilm by real-time PCR with propidium monoazide. *AMB Express*, 3(1), p.1.

Amou, T., Hinode, D., Yoshioka, M. and Grenier, D. (2013). Relationship between halitosis and periodontal disease - associated oral bacteria in tongue coatings. *International Journal of Dental Hygiene*, 12(2), pp.145-151.

Ankri, S. and Mirelman, D. (1999). Antimicrobial properties of allicin from garlic. *Microbes and Infection*, 1(2), pp.125-129.

Antonio, A., Morales, R., Perrone, D., Maia, L., Santos, K., Iario, N. and Farah, A. (2010). Species, roasting degree and decaffeination influence the antibacterial activity of coffee against *Streptococcus mutans*. *Food Chemistry*, 118(3), pp.782-788.

Arana, V., Medina, J., Alarcon, R., Moreno, E., Heintz, L., Schaefer, H. and Wist, J. (2015). Coffees country of origin determined by NMR: The Colombian case. *Food Chemistry*, 175, pp.500-506.

Avila, M., Ojcius, D. and Yilmaz, A–. (2009). The Oral Microbiota: Living with a Permanent Guest. *DNA and Cell Biology*, 28(8), pp.405-411.

Badhani, B., Sharma, N. and Kakkar, R. (2015). Gallic acid: a versatile antioxidant with promising therapeutic and industrial applications. *RSC Advances*, 5(35), pp.27540-27557.

Bakri, I. and Douglas, C. (2005). Inhibitory effect of garlic extract on oral bacteria. *Archives of Oral Biology*, 50(7), pp.645-651.

Bao, K., Belibasakis, G., Thurnheer, T., Aduse-Opoku, J., Curtis, M. and Bostanci, N. (2014). Role of *Porphyromonas gingivalis* gingipains in multi-species biofilm formation. *BMC Microbiology*, 14(1).

Basic, A., Blomqvist, S., Carlen, A. and Dahlen, G. (2015). Estimation of bacterial hydrogen sulfide production in vitro. *Journal of Oral Microbiology*, 7(1), p.28166.

Beder-Belkhiri, W., Zeghichi-Hamri, S., Kadri, N., Boulekbache-Makhlouf, L., Cardoso, S., Oukhmanou-Bensidhoum, S. and Madani, K. (2018). Hydroxycinnamic acids profiling, in vitro evaluation of total phenolic compounds, caffeine and antioxidant properties of coffee imported, roasted and consumed in Algeria. *Mediterranean Journal of Nutrition and Metabolism*, 11(1), pp.51-63.

Bertoldi, M., Cellini, B., D'Aguanno, S. and Voltattorni, C. (2003). Lysine 238 Is an Essential Residue for -Elimination Catalyzed by *Treponema denticola* Cystalysin. *Journal of Biological Chemistry*, 278(39), pp.37336-37343.

Bhouri, W., Boubaker, J., Skandrani, I., Ghedira, K. and Chekir Ghedira, L. (2012). Investigation of the apoptotic way induced by digallic acid in human lymphoblastoid TK6 cells. *Cancer Cell International*, 12(1), p.26.

Bhouri, W., Derbel, S., Skandrani, I., Boubaker, J., Bouhlel, I., Sghaier, M., Kilani, S., Mariotte, A., Dijoux-Franca, M., Ghedira, K. and Chekir-Ghedira, L. (2010). Study of genotoxic, antigenotoxic and antioxidant activities of the digallic acid isolated from *Pistacia lentiscus* fruits. *Toxicology in Vitro*, 24(2), pp.509-515.

Bingham, C. and Moni, M. (2013). Periodontal disease and rheumatoid arthritis. *Current Opinion in Rheumatology*, 25(3), pp.345-353.

Bio-rad.com. (2019). *Nickel Columns and Nickel Resin | Bio-Rad*. [online] Available at: http://www.bio-rad.com/featured/en/nickel-columns-nickel-resin.html

Bollen, C. and Beikler, T. (2012). Halitosis: the multidisciplinary approach. *International Journal of Oral Science*, 4(2), pp.55-63.

Borges, A., Ferreira, C., Saavedra, M. and SimÃµes, M. (2013). Antibacterial Activity and Mode of Action of Ferulic and Gallic Acids Against Pathogenic Bacteria. *Microbial Drug Resistance*, 19(4), pp.256-265.

Bowen, W., Burne, R., Wu, H. and Koo, H. (2018). Oral Biofilms: Pathogens, Matrix, and Polymicrobial Interactions in Microenvironments. *Trends in Microbiology*, 26(3), pp.229-242.

Brooks, J. and Jefferson, K. (2012). Staphylococcal Biofilms. *Advances in Applied Microbiology Volume 81*, pp.63-87.

Brosnan, J., Brosnan, M., Bertolo, R. and Brunton, J. (2007). Methionine: A metabolically unique amino acid. *Livestock Science*, 112(1-2), pp.2-7.

Budryn, G., Nebesny, E., PodsÄ™dek, A., Å»yÅ¼elewicz, D., Materska, M., Jankowski, S. and Janda, B. (2009). Effect of different extraction methods on the recovery of chlorogenic acids, caffeine and Maillard reaction products in coffee beans. *European Food Research and Technology*, 228(6), pp.913-922.

Buhlin, K., Gustafsson, A., Hakansson, J. and Klinge, B. (2002). Oral health and cardiovascular disease in Sweden. Results of a national questionnaire survey. *Journal of Clinical Periodontology*, 29(3), pp.254-259.

Burguera-Pascu, M., RodrÃ-guez-Archilla, A. and Baca, P. (2007). Substantivity of zinc salts used as rinsing solutions and their effect on the inhibition of Streptococcus mutans. *Journal of Trace Elements in Medicine and Biology*, 21(2), pp.92-101.

Burnett, G., Stephen, A., Pizzey, R. and Bradshaw, D. (2011). In vitro effects of novel toothpaste actives on components of oral malodour. *International Dental Journal*, 61, pp.67-73.

Bury, D., Jelen, P. and Kalab, M. (2001). Disruption of *Lactobacillus delbrueckii* spp. bulgaricus 11842 cells for lactose hydrolysis in dairy products: a comparison of sonication, high-pressure homogenization and bead milling. *Innovative Food Science & Emerging Technologies*, 2(1), pp.23-29.

Caballero, B., Trugo, L. and Finglas, P. (2003). *Encyclopedia of food sciences and nutrition*. San Diego, Academic, volume 8

Cammerer, B. and Kroh, L. (2006). Antioxidant activity of coffee brews. *European Food Research and Technology*, 223(4), pp.469-474.

Campisi, G., Musciotto, A., Di Fede, O., Di Marco, V. and Craxa, A. (2010). Halitosis: could it be more than mere bad breath? *Internal and Emergency Medicine*, 6(4), pp.315-319.

Cardenas, C., Quesada, A. and Medina, M. (2011). Correction: Anti-Angiogenic and Anti-Inflammatory Properties of Kahweol, a Coffee Diterpene. *PLoS ONE*, 6(11).

Carter, R. and Morton, N. (2015). Cysteine and hydrogen sulphide in the regulation of metabolism: insights from genetics and pharmacology. *The Journal of Pathology*, 238(2), pp.321-332.

Carvalho, F., Puppin-Rontani, R., Facio, S., Negrini, T., Carlo, H. and Garcia-Godoy, F. (2012). Analysis by confocal laser scanning microscopy of the MDPB bactericidal effect on S. mutans biofilm CLSM analysis of MDPB bactericidal effect on biofilm. *Journal of Applied Oral Science*, 20(5), pp.568-575.

Chacon E., and Lemasters J*., Primary Cultures of Cardiac Myocytes as In Vitro Models for Pharmacological and Toxicological* Assessments In Vitro Methods in Pharmaceutical Research, (1997) (4) Succinate dehydrogenase activity (MTT assay)

Chhibber-Goel, J., Singhal, V., Bhowmik, D., Vivek, R., Parakh, N., Bhargava, B. and Sharma, A. (2016). Linkages between oral commensal bacteria and atherosclerotic plaques in coronary artery disease patients. *npj Biofilms and Microbiomes*, 2(1).

Choi, E., Lee, H., Kang, M., Kim, B., Lim, H., Kim, S. and Kang, I. (2010). Potentiation of bacterial killing activity of zinc chloride by pyrrolidine dithiocarbamate. *The Journal of Microbiology*, 48(1), pp.40-43.

Cholet, O., Hanaut, A. and Bonnarme, P. (2007). Transcriptional analysis of L-methionine catabolism in Brevibacterium linens ATCC9175. *Applied Microbiology and Biotechnology*, 74(6), pp.1320-1332.

Christersson, L., Fransson, C., Dunford, R. and Zambon, J. (1992). Subgingival Distribution of Periodontal Pathogenic Microorganisms in Adult Periodontitis. *Journal of Periodontology*, 63(5), pp.418-425.

Chu, L., Ebersole, J., Kurzban, G. and Holt, S. (1999). Cystalysin, a 46 kDa L-Cysteine Desulfhydrase from *Treponema denticola*: Biochemical and Biophysical Characterization. *Clinical Infectious Diseases*, 28(3), pp.442-450.

Ciborowski, P. and Silberring, J. (2016). *Proteomic profiling and analytical chemistry*. Amsterdam, Netherland: Elsevier Science.

Codipilly, D. and Kleinberg, I. (2008). Generation of indole/skatole during malodor formation in the salivary sediment model system and initial examination of the oral bacteria involved. *Journal of Breath Research*, 2(1), p.017017.

Cohen, B. (2013). *Pediatric Dermatology*. 4th ed. Elsevier, pp.240-263.

Cueva, C., Mingo, S., Gonzalez, I., Bustos, I., Requena, T., del Campo, R., Alvarez, P., Bartoloma, B. and Moreno-Arribas, M. (2012). Antibacterial activity of wine phenolic compounds and oenological extracts against potential respiratory pathogens. *Letters in Applied Microbiology*, 54(6), pp.557-563.

Daglia, M., Papetti, A., Grisoli, P., Aceti, C., Dacarro, C. and Gazzani, G. (2007). Antibacterial Activity of Red and White Wine against Oral Streptococci. *Journal of Agricultural and Food Chemistry*, 55(13), pp.5038-5042.

Daglia, M., Tarsi, R., Papetti, A., Grisoli, P., Dacarro, C., Pruzzo, C. and Gazzani, G. (2002). Antiadhesive Effect of Green and Roasted Coffee onStreptococcus mutans' Adhesive Properties on Saliva-Coated Hydroxyapatite Beads. *Journal of Agricultural and Food Chemistry*, 50(5), pp.1225-1229.

Davey, H. and Hexley, P. (2010). Red but not dead? Membranes of stressed Saccharomyces cerevisiae are permeable to propidium iodide. *Environmental Microbiology*, 13(1), pp.163-171.

Deschepper, M., Waegeman, W., Eeckloo, K., Vogelaers, D. and Blot, S. (2018). Effects of chlorhexidine gluconate oral care on hospital mortality: a hospital-wide, observational cohort study. *Intensive Care Medicine*, 44(7), pp.1017-1026.

DeStefano, F., Anda, R., Kahn, H., Williamson, D. and Russell, C. (1993). Dental disease and risk of coronary heart disease and mortality. *BMJ*, 306(6879), pp.688-691.

Dettweiler, M., Lyles, J., Nelson, K., Dale, B., Reddinger, R., Zurawski, D. and Quave, C. (2019). American Civil War plant medicines inhibit growth, biofilm formation, and quorum sensing by multidrug-resistant bacteria. *Scientific Reports*, 9(1).

Dewhirst, F., Chen, T., Izard, J., Paster, B., Tanner, A., Yu, W., Lakshmanan, A. and Wade, W. (2010). The Human Oral Microbiome. *Journal of Bacteriology*, 192(19), pp.5002-5017.

Diebolt, M., Bucher, B. and Andriantsitohaina, R. (2001). Wine Polyphenols Decrease Blood Pressure, Improve NO Vasodilatation, and Induce Gene Expression. *Hypertension*, 38(2), pp.159-165.

Ditscheid, B., Fanfstack, R., Busch, M., Schubert, R., Gerth, J. and Jahreis, G. (2005). Effect of L-methionine supplementation on plasma homocysteine and other free amino acids: a placebo-controlled double-blind cross-over study. *European Journal of Clinical Nutrition*, 59(6), pp.768-775.

Dominy SS., Lynch C., Ermini F., Benedyk M., Marczyk A., Konradi A., Haditsch U., Raha D., Griffin C., Holsigner LJ., Aratsu-Kapur S., Kaba s., Lee A., Ryder MI, Potempa B., Mydel P., hellvard A., Adamowicz K., Hasturk H., Walker GD., Reynolds EC., Faull RLM., Curtis MA., Dragunow M., Potempa J., (2019) Porphyromonas gingivalis in Alzheimer's disease brains: Evidence for disease causation and treatment with small-molecule inhibitors. *Sci Adv,* 23;5(1)

Dong, J. and DeBusk, S. (2009). GC-MS Analysis of Hydrogen Sulfide, Carbonyl Sulfide, Methanethiol, Carbon Disulfide, Methyl Thiocyanate and Methyl Disulfide in Mainstream Vapor Phase Cigarette Smoke. *Chromatographia*, 71(3-4), pp.259-265.

Duve, C. (1975). Exploring cells with a centrifuge. *Science*, 189 (4198), pp.186-194.

Eberhardt, M., Dux, M., Namer, B., Miljkovic, J., Cordasic, N., Will, C., Kichko, T., de la Roche, J., Fischer, M., Suarez, S., Bikiel, D., Dorsch, K., Leffler, A., Babes, A., Lampert, A., Lennerz, J., Jacobi, J., MartÃ-, M., Doctorovich, F., Hagestaatt, E., Zygmunt, P., Ivanovic-Burmazovic, I., Messlinger, K., Reeh, P. and Filipovic, M. (2014). H2S and NO cooperatively regulate vascular tone by activating a neuroendocrine signaling pathway. *Nature Communications*, 5(1).

El-Sayed, A. (2011). Purification and characterization of a new L-methioninase from solid cultures of Aspergillus flavipes. *The Journal of Microbiology*, 49(1), pp.130-140.

Enberg, N., Alho, H., Loimaranta, V. and Lenander-Lumikari, M. (2001). Saliva flow rate, amylase activity, and protein and electrolyte concentrations in saliva after acute alcohol

consumption. *Oral Surgery, Oral Medicine, Oral Pathology, Oral Radiology, and Endodontology*, 92(3), pp.292-298.

Err-Cheng, C., Pi-Yueh, C., James T., W. and Tsu-Lan, W. (2005). Enzymatic Assay of Homocysteine on Microtiter Plates or a TECAN Analyzer Using Crude Lysate Containing Recombinant Methionine gamma-Lyase. *Ann Clin Lab Sci*, 35, pp.155-160.

Ewann, F. and Hoffman, P. (2006). Cysteine Metabolism in *Legionella pneumophila*: Characterization of an L-Cystine-Utilizing Mutant. *Applied and Environmental Microbiology*, 72(6), pp.3993-4000.

Fan, X., Peters, B.A., Jacobs, E., Gapstur S.M., Purdue, M.P., Freedman, N.D., Alekseyenko, A.V., Wu, J., Yang, L., Pei, Z., Hayes, R. & Ahn, J., (2018) Drinking alcohol is associated with variation in the human oral microbiome in a large study of American adults. *Microbiome*, 6 (59)

Faveri, M., Mayer, M., Feres, M., de Figueiredo, L., Dewhirst, F. and Paster, B. (2008). Microbiological diversity of generalized aggressive periodontitis by 16S rRNA clonal analysis. *Oral Microbiology and Immunology*, 23(2), pp.112-118.

Floege, J., Johnson, R. and Feehally, J. (2010). *Comprehensive clinical nephrology*. Philadelphia, PA: Saunders/Elsevier.

Foo, T., Terentis, A. and Venkatachalam, K. (2016). A continuous spectrophotometric assay and nonlinear kinetic analysis of methionine gamma-lyase catalysis. *Analytical Biochemistry*, 507, pp.21-26.

Fukamachi, H., Nakano, Y., Yoshimura, M. and Koga, T. (2002). Cloning and characterization of the l-cysteine desulfhydrase gene of *Fusobacterium nucleatum*. *FEMS Microbiology Letters*, 215(1), pp.75-80.

Fukumoto, M., Kudou, D., Murano, S., Shiba, T., SATO, D., Tamura, T., Harada, S. and Inagaki, K. (2012). The Role of Amino Acid Residues in the Active Site of L-Methionine gamma-lyase from Pseudomonas putida. *Bioscience, Biotechnology, and Biochemistry*, 76(7), pp.1275-1284.

Gay, F., Aguera, K., Sacnachal, K., Tainturier, A., Berlier, W., Maucort-Boulch, D., Honnorat, J., Horand, F., Godfrin, Y. and Bourgeaux, V. (2017). Methionine tumor starvation by erythrocyte-encapsulated methionine gamma-lyase activity controlled with per os vitamin B6. *Cancer Medicine*, 6(6), pp.1437-1452.

Gorman, M., Seers, C., Michell, B., Feil, S., Huq, N., Cross, K., Reynolds, E. and Parker, M. (2014). Structure of the lysine specific protease Kgp from *Porphyromonas gingivalis*, a target for improved oral health. *Protein Science*, 24(1), pp.162-166.

Gufran, K., Alasqah, M., Khan, S., Elqomsan, M., Kola, Z. and Hamza, M. (2016). Assessment of halitosis using the organoleptic method and volatile sulfur compounds monitoring. *Journal of Dental Research and Review*, 3(3), p.94.

Guo, L., McLean, J., Lux, R., He, X. and Shi, W. (2015). The well-coordinated linkage between acidogenicity and aciduricity via insoluble glucans on the surface of *Streptococcus mutans*. *Scientific Reports*, 5(1).

Hajishengallis, G., Abe, T., Maekawa, T., Hajishengallis, E. and Lambris, J. (2013). Role of complement in host microbe homeostasis of the periodontium. *Seminars in Immunology*, 25(1), pp.65-72.

Hajishengallis, G., Liang, S., Payne, M., Hashim, A., Jotwani, R., Eskan, M., McIntosh, M., Alsam, A., Kirkwood, K., Lambris, J., Darveau, R. and Curtis, M. (2011). Low-Abundance Biofilm Species Orchestrates Inflammatory Periodontal Disease through the Commensal Microbiota and Complement. *Cell Host & Microbe*, 10(5), pp.497-506.

Hammond, N., Wang, Y., Dimachkie, M. and Barohn, R. (2013). Nutritional Neuropathies. *Neurologic Clinics*, 31(2), pp.477-489.

Hanniffy, S., Philo, M., Pelaez, C., Gasson, M., Requena, T. and Martinez-Cuesta, M. (2009). Heterologous Production of Methionine-gamma -Lyase from Brevibacterium linens in Lactococcus lactis and Formation of Volatile Sulfur Compounds. *Applied and Environmental Microbiology*, 75(8), pp.2326-2332.

Hartle, M., Sommer, S., Dietrich, S. and Pluth, M. (2014). Chemically Reversible Reactions of Hydrogen Sulfide with Metal Phthalocyanines. *Inorganic Chemistry*, 53(15), pp.7800-7802.

Hartley, M., Elmaayta, M., McKenzie, C. and GREENMAN, J. (1996). The Tongue Microbiota of Low Odour and Malodorous Individuals. *Microbial Ecology in Health and Disease*, 9(5), pp.215-223.

Harvey-Woodworth, C. (2013). Dimethylsulphidemia: the significance of dimethyl sulphide in extra-oral, blood borne halitosis. *British Dental Journal*, 214(7)

He, G., Pearce, E. and Sissons, C. (2002). Inhibitory effect of ZnCl2 on glycolysis in human oral microbes. *Archives of Oral Biology*, 47(2), pp.117-129.

HIRAKAWA, N., OKAUCHI, R., MIURA, Y. and YAGASAKI, K. (2005). Anti-Invasive Activity of Niacin and Trigonelline against Cancer Cells. *Bioscience, Biotechnology, and Biochemistry*, 69(3), pp.653-658.

Hojo, K., Nagaoka, S., Ohshima, T. and Maeda, N. (2009). Bacterial Interactions in Dental Biofilm Development. *Journal of Dental Research*, 88(11), pp.982-990.

Holmstrup, P., Damgaard, C., Olsen, I., Klinge, B., Flyvbjerg, A., Nielsen, C. and Hansen, P. (2017). Comorbidity of periodontal disease: two sides of the same coin? An introduction for the clinician. *Journal of Oral Microbiology*, 9(1), p.1332710.

Hullo, M., Auger, S., Soutourina, O., Barzu, O., Yvon, M., Danchin, A. and Martin-Verstraete, I. (2006). Conversion of Methionine to Cysteine in Bacillus subtilis and Its Regulation. *Journal of Bacteriology*, 189(1), pp.187-197.

Hussain, M., Stover, C. and Dupont, A. (2015). P. gingivalis in Periodontal Disease and Atherosclerosis. Scenes of Action for Antimicrobial Peptides and Complement. *Frontiers in Immunology*, 6.

Iida S., Shimada J., Shakagami, H., (2012) Cytotoxicity Induced by Docetaxel in Human Oral Squamous Cell Carcinoma Cell Lines, *In vivo* (Athens, Greece) 27, 321-332

Janeway, C. (1999). *Immunobiology*. London: Harcourt Brace & Company.

Jeon, H., Kim, J., Lee, E., Jang, Y., Son, J., Kwon, J., Lim, T., Kim, S., Park, J., Kim, J. and Lee, K. (2016). Methionine deprivation suppresses triple-negative breast cancer metastasis *in vitro* and *in vivo*. *Oncotarget*, 7(41).

Johnson, P., Yaegaki, K. and Tonzetich, J. (1996). Effect of methyl mercaptan on synthesis and degradation of collagen. *Journal of Periodontal Research*, 31(5), pp.323-329.

Jones, B. and Gilligan, J. (1983). o-phthaldialdehyde precolumn derivatization and reversed-phase high-performance liquid chromatography of polypeptide hydrolysates and physiological fluids. *Journal of Chromatography A*, 266, pp.471-482.

Kamer, A., Craig, R., Dasanayake, A., Brys, M., Glodzik-Sobanska, L. and de Leon, M. (2008). Inflammation and Alzheimer's disease: Possible role of periodontal diseases. *Alzheimer's & Dementia*, 4(4), pp.242-250.

Kandalam, U., Ledra, N., Laubach, H. and Venkatachalam, K. (2018). Inhibition of methionine gamma lyase deaminase and the growth of *Porphyromonas gingivalis*: A therapeutic target for halitosis/periodontitis. *Archives of Oral Biology*, 90, pp.27-32.

Kang, J., Kim, D., Choi, B. and Park, J. (2017). Inhibition of malodorous gas formation by oral bacteria with cetylpyridinium and zinc chloride. *Archives of Oral Biology*, 84, pp.133-138.

Kang, M., Jang, H., Oh, J., Yang, K., Choi, N., Lim, H. and Kim, S. (2009). Effects of methyl gallate and gallic acid on the production of inflammatory mediators interleukin-6 and interleukin-8 by oral epithelial cells stimulated with *Fusobacterium nucleatum*. *The Journal of Microbiology*, 47(6), pp.760-767.

Kang, M., Oh, J., Kang, I., Hong, S. and Choi, C. (2008). Inhibitory effect of methyl gallate and gallic acid on oral bacteria. *The Journal of Microbiology*, 46(6), pp.744-750.

Kantorski, K., Souza, D., Yujra, V., Junqueira, J., Jorge, A. and Rocha, R. (2007). Effect of an alcoholic diet on dental caries and on Streptococcus of the mutans group: study in rats. *Brazilian Oral Research*, 21(2), pp.101-105.

Kilian, M., Chapple, I., Hannig, M., Marsh, P., Meuric, V., Pedersen, A., Tonetti, M., Wade, W. and Zaura, E. (2016). The oral microbiome- an update for oral healthcare professionals. *British Dental Journal*, 221(10), pp.657-666.

Kim, D., Lee, J., Kho, H., Chung, J., Park, H. and Kim, Y. (2009). A New Organoleptic Testing Method for Evaluating Halitosis. *Journal of Periodontology*, 80(1), pp.93-97.

Kim, H., Cha, G., Kim, H., Kwon, E., Lee, J., Choi, J. and Joo, J. (2018). Porphyromonas gingivalis accelerates atherosclerosis through oxidation of high-density lipoprotein. *Journal of Periodontal & Implant Science*, 48(1), p.60.

Kim, S., Jung, Y., An, H., Kim, D., Jang, E., Choi, Y., Moon, K., Park, M., Park, C., Chung, K., Bae, H., Choi, Y., Kim, N. and Chung, H. (2013). Anti-Wrinkle and Anti-Inflammatory Effects of Active Garlic Components and the Inhibition of MMPs via NF-Kb Signaling. *PLoS ONE*, 8(9), p.e73877.

Kimura, Y. and Kimura, H. (2004). Hydrogen sulfide protects neurons from oxidative stress. *The FASEB Journal*, 18(10), pp.1165-1167.

Kolenbrander, P., Andersen, R., Blehert, D., Egland, P., Foster, J. and Palmer, R. (2002). Communication among Oral Bacteria. *Microbiology and Molecular Biology Reviews*, 66(3), pp.486-505.

Kolluru, G., Shen, X., Bir, S. and Kevil, C. (2013). Hydrogen sulfide chemical biology: Pathophysiological roles and detection. *Nitric Oxide*, 35, pp.5-20.

Kreth, J., Zhang, Y. and Herzberg, M. (2008). Streptococcal Antagonism in Oral Biofilms: *Streptococcus sanguinis* and *Streptococcus gordonii* Interference with *Streptococcus mutans*. *Journal of Bacteriology*, 190(13), pp.4632-4640.

Kudou, D., Misaki, S., Yamashita, M., Tamura, T., Takakura, T., Yoshioka, T., Yagi, S., Hoffman, R., Takimoto, A., Esaki, N. and Inagaki, K. (2007). Structure of the Antitumour Enzyme L-Methionine gamma-Lyase from *Pseudomonas putida* at 1.8 A Resolution. *Journal of Biochemistry*, 141(4), pp.535-544.

Kudou, D., Yasuda, E., Hirai, Y., Tamura, T. and Inagaki, K. (2015). Molecular cloning and characterization of l-methionine gamma-lyase from *Streptomyces avermitilis*. *Journal of Bioscience and Bioengineering*, 120(4), pp.380-383.

Kumar P, Nagarajan A, Uchil PD. (2018) Analysis of Cell Viability by the Lactate Dehydrogenase Assay *Cold Spring Harb Protoc*. 1;2018(6)

Kumar Singh, S. and Patra, A. (2018). Evaluation of phenolic composition, antioxidant, anti-inflammatory and anticancer activities of *Polygonatum verticillatum* (L.). *Journal of Integrative Medicine*, 16(4), pp.273-282.

Kuznetsov, N., Faleev, N., Kuznetsova, A., Morozova, E., Revtovich, S., Anufrieva, N., Nikulin, A., Fedorova, O. and Demidkina, T. (2014). Pre-steady-state Kinetic and Structural Analysis of Interaction of Methionine gamma-Lyase from Citrobacter freundii with Inhibitors. *Journal of Biological Chemistry*, 290(1), pp.671-681.

Lachenmeier, D. (2008). Safety evaluation of topical applications of ethanol on the skin and inside the oral cavity. *Journal of Occupational Medicine and Toxicology*, 3(1), p.26.

Laleman, I., De Geest, S., Dekeyser, C., Teughels, W. and Quirynen, M. (2018). A new method of choice for organoleptic scoring: The negative-pressure technique. *Journal of Clinical Periodontology*, 45(11), pp.1319-1325.

Levitt, M., Furne, J., Springfield, J., Suarez, F. and DeMaster, E. (1999). Detoxification of hydrogen sulfide and methanethiol in the cecal mucosa. *Journal of Clinical Investigation*, 104(8), pp.1107-1114.

Liao, C., Chen, S., Huang, H. and Wang, C. (2018). Gallic acid inhibits bladder cancer cell proliferation and migration via regulating fatty acid synthase (FAS). *Journal of Food and Drug Analysis*, 26(2), pp.620-627.

Liu, Y. and Kitts, D. (2011). Confirmation that the Maillard reaction is the principle contributor to the antioxidant capacity of coffee brews. *Food Research International*, 44(8), pp.2418-2424.

Lu, Q., Chen, C., Zhao, S., Ge, F. and Liu, D. (2015). Investigation of the Interaction Between z and alpha-Amylase by Spectroscopy. *International Journal of Food Properties*, 19(11), pp.2481-2494.

Lynch, K. (2017). *Chapter 6 - Toxicology: liquid chromatography mass spectrometry*. Academic press, pp.109-130.

Magill, A. and Hunter, G. (2013). Hunter's tropical medicine and emerging infectious disease. London: Saunders, 9th Edition.

Mahajan, S.D, Schwartz S., *Nanomedicine,* Methods in Enzymology, (2012), 6.3 Cell viability measurement using an MTT (3-(4,5-dimethylthiazol-2-yl)-2,5-diphenyltetrazolium bromide, a tetrazole) assay.

Mamaeva, D., Morozova, E., Nikulin, A., Revtovich, S., Nikonov, S., Garber, M. and Demidkina, T. (2005). Structure of *Citrobacter freundii* L-methionine gamma-lyase. *Acta Crystallographica Section F Structural Biology and Crystallization Communications*, 61(6), pp.546-549.

Markoski, M., Garavaglia, J., Oliveira, A., Olivaes, J. and Marcadenti, A. (2016). Molecular Properties of Red Wine Compounds and Cardiometabolic Benefits. *Nutrition and Metabolic Insights*, 9, p.NMI.S32909.

Marsh, P. (2010). Microbiology of Dental Plaque Biofilms and Their Role in Oral Health and Caries. *Dental Clinics of North America*, 54(3), pp.441-454.

Matoba, Y., Yoshida, T., Izuhara-Kihara, H., Noda, M. and Sugiyama, M. (2017). Crystallographic and mutational analyses of cystathionine beta-synthase in the H_2S-synthetic gene cluster in Lactobacillus plantarum. *Protein Science*, 26(4), pp.763-783.

McBean, G. (2017). Cysteine, Glutathione, and Thiol Redox Balance in Astrocytes. *Antioxidants*, 6(3), p.62.

Miller, H., Eick, S., Moritz, A., Lussi, A. and Gruber, R. (2017). Cytotoxicity and Antimicrobial Activity of Oral Rinses In Vitro. *BioMed Research International*, 2017, pp.1-9.

Mishra, V., Shettar, L., Bajaj, M. and Math, A. (2016). Comparison of a commercially available herbal and 0.2% chlorhexidine mouthrinse for prevention of oral malodor: A clinical trial. *Journal of International Society of Preventive and Community Dentistry*, 6(7), p.6.

Mohamed Saleem, T. and Darbar Basha, S. (2010). Red wine: A drink to your heart. *Journal of Cardiovascular Disease Research*, 1(4), pp.171-176.

Mohd Arshad, Z., Amid, A. and Othman, M. (2015).Comparison of different cell disruption methods and cell extractant buffers for recombinant bromelain expressed in E.coli BL21-A1. *Jurnal Teknologi*, 77(24).

Mojica, B., Fong, L., Biju, D., Muharram, A., Davis, I., Vela, K., Rios, D., Osorio-Camacena, E., Kaur, B., Rojas, S. and Forester, S. (2018). The Impact of the Roast Levels of Coffee Extracts on their Potential Anticancer Activities. *Journal of Food Science*, 83(4), pp.1125-1130.

Moran, J., Addy, M., Corry, D., Newcombe, R. and Haywood, J. (2001). A study to assess the plaque inhibitory action of a new zinc citrate toothpaste formulation. *Journal of Clinical Periodontology*, 28(2), pp.157-161.

Morita, M. and Wang, H. (2001). Association between oral malodor and adult periodontitis: a review. *Journal of Clinical Periodontology*, 28(9), pp.813-819.

Motoshima, H., Inagaki, K., Kumasaka, T., Furuichi, M., Inoue, H., Tamura, T., Esaki, N., Soda, K., Tanaka, N., Yamamoto, M. and Tanaka, H. (2000). Crystal Structure of the Pyridoxal 5'-phosphate Dependent L-Methionine Â -Lyase from Pseudomonas putida. *Journal of Biochemistry*, 128(3), pp.349-354.

Mrizak, J., Ouali, U., Arous, A., Jouini, L., Zaouche, R., RebaÃ¯, A. and Zalila, H. (2018). Successful Treatment of Halitophobia with Cognitive Behavioural Therapy: A Case Study. *Journal of Contemporary Psychotherapy*.

Mueller, U., Sauer, T., Weigel, I., Pichner, R. and Pischetsrieder, M. (2011). Identification of H2O2 as a major antimicrobial component in coffee. *Food & Function*, 2(5), p.265.

Murata, T., Yaegaki, K., Qian, W., Herai, M., Calenic, B., Imai, T., Sato, T., Tanaka, T., Kamoda, T. and Ii, H. (2008). Hydrogen sulfide induces apoptosis in epithelial cells derived from human gingiva. *Journal of Breath Research*, 2(1), p.017007.

Naiktari, R., Gaonkar, P., Gurav, A. and Khiste, S. (2014). A randomized clinical trial to evaluate and compare the efficacy of triphala mouthwash with 0.2% chlorhexidine in hospitalized patients with periodontal diseases. *Journal of Periodontal & Implant Science*, 44(3), p.134.

Nair, H. and Clarke, W. (2017). *Mass spectrometry for the clinical laboratory, Chapter 6*. Amsterdam: Elsevier Ltd.

Namboodiripad, P. and Kori, S. (2009). Can coffee prevent caries? *Journal of Conservative Dentistry*, 12(1), p.17.

Nguyen, D., Seo, D., Lee, H., Kim, I., Kim, K., Park, R. and Jung, W. (2013). Antifungal activity of gallic acid purified from Terminalia nigrovenulosa bark against *Fusarium solani*. *Microbial Pathogenesis*, 56, pp.8-15.

Paju, S. and Scannapieco, F. (2007). Oral biofilms, periodontitis, and pulmonary infections. *Oral Diseases*, 13(6), pp.508-512.

Palmer Jr, R. (2013). Composition and development of oral bacterial communities. *Periodontology 2000*, 64(1), pp.20-39.

Parashar, A., Parashar, S., Zingade, A., Gupta, S. and Sanikop, S. (2015). Interspecies communication in oral biofilm: An ocean of information. *Oral Science International*, 12(2), pp.37-42.

Patil, S. (2013). Microbial Flora in Oral Diseases. *The Journal of Contemporary Dental Practice*, 14, pp.1202-1208.

Petti, S. and Scully, C. (2009). Polyphenols, oral health and disease: A review. *Journal of Dentistry*, 37(6), pp.413-423.

Pires P., dos Santos T., Fonseca-Gonçalvesa A., Melo Pithonc M., Tadeu Lopes R., Nevesa A., (2018) Dual energy micro-CT methodology for visualization and quantification of biofilm formation and dentin demineralization. *Archives of Oral Biology,* Volume 85, Pages 10-15

Plantinga, N., Wittekamp, B., Leleu, K., Depuydt, P., Van den Abeele, A., Brun-Buisson, C. and Bonten, M. (2016). Oral mucosal adverse events with chlorhexidine 2Â % mouthwash in ICU. *Intensive Care Medicine*, 42(4), pp.620-621.

Porter, S. (2006). Oral malodour (halitosis). *BMJ*, 333(7569), pp.632-635.

Porter, S. and Scully, C. (2006). Oral malodour (halitosis). *BMJ*, 333(7569), pp.632-635.

Raboni, S., Revtovich, S., Demitri, N., Giabbai, B., Storici, P., Cocconcelli, C., Faggiano, S., Rosini, E., Pollegioni, L., Galati, S., Buschini, A., Morozova, E., Kulikova, V., Nikulin, A., Gabellieri, E., Cioni, P., Demidkina, T. and Mozzarelli, A. (2018). Engineering methionine gamma-lyase from *Citrobacter freundii* for anticancer activity. *Biochimica et Biophysica Acta (BBA) - Proteins and Proteomics*, 1866(12), pp.1260-1270.

Ranaldi, F., Vanni, P. and Giachetti, E. (1999). What students must know about the determination of enzyme kinetic parameters. *Biochemical Education*, 27(2), pp.87-91.

Raran-Kurussi, S., Cherry, S., Zhang, D. and Waugh, D. (2017). Removal of Affinity Tags with TEV Protease. *Methods in Molecular Biology*, pp.221-230.

Rassameemasmaung, S., Phusudsawang, P. and Sangalungkarn, V. (2013). Effect of Green Tea Mouthwash on Oral Malodor. *ISRN Preventive Medicine*, 2013, pp.1-6.

Ratcliff, P. and Johnson, P. (1999). The Relationship Between Oral Malodor, Gingivitis, and Periodontitis. A Review. *Journal of Periodontology*, 70(5), pp.485-489.

Reis, S., Esparito Santo, A., Andrade, M. and Sadigursky, M. (2006). Cytologic alterations in the oral mucosa after chronic exposure to ethanol. *Brazilian Oral Research*, 20(2), pp.97-102.

Roohani, N., Hurrell, R., Kelishadi, R. and Schulin, R. (2013). Zinc and its importance for human health: An integrative review. *J Res Med Sci.*, 18(2), pp.144-157.

Salako, N. and Philip, L. (2011). Comparison of the Use of the Halimeter and the OralChroma in the Assessment of the Ability of Common Cultivable Oral Anaerobic Bacteria to Produce Malodorous Volatile Sulfur Compounds from Cysteine and Methionine. *Medical Principles and Practice*, 20(1), pp.75-79.

Salazar, O. and Asenjo, J. (2007). Enzymatic lysis of microbial cells. *Biotechnology Letters*, 29(7), pp.985-994.

Saosoong, K. and Ruangviriyachai, C. (2014). Antioxidant and Antimicrobial Activities of Methanolic Extract from Jatropha curcas Linn. Fruit. *Asian Journal of Chemistry*, 26(Supp.), pp.S225-S229.

Sato, D. and Nozaki, T. (2009). Methionine gamma-lyase: The unique reaction mechanism, physiological roles, and therapeutic applications against infectious diseases and cancers. *IUBMB Life*, 61(11), pp.1019-1028.

Sato, D. and Nozaki, T. (2009). Methionine gamma-lyase: The unique reaction mechanism, physiological roles, and therapeutic applications against infectious diseases and cancers. *IUBMB Life*, 61(11), pp.1019-1028.

Sato, D. and Nozaki, T. (2009). Methionine gamma-lyase: The unique reaction mechanism, physiological roles, and therapeutic applications against infectious diseases and cancers. *IUBMB Life*, 61(11), pp.1019-1028.

Sato, D., Shiba, T., Karaki, T., Yamagata, W., Nozaki, T., Nakazawa, T. and Harada, S. (2017). X-Ray snapshots of a pyridoxal enzyme: a catalytic mechanism involving concerted [1,5]-hydrogen sigmatropy in methionine gamma-lyase. *Scientific Reports*, 7(1).

Sato, D., Shiba, T., Yunoto, S., Furutani, K., Fukumoto, M., Kudou, D., Tamura, T., Inagaki, K. and Harada, S. (2017). Structural and mechanistic insights into homocysteine degradation by a mutant of methionine Î³-lyase based on substrate-assisted catalysis. *Protein Science*, 26(6), pp.1224-1230.

Sato, D., Yamagata, W., Harada, S. and Nozaki, T. (2008). Kinetic characterization of methionine Î³-lyases from the enteric protozoan parasite Entamoeba histolytica against physiological substrates and trifluoromethionine, a promising lead compound against amoebiasis. *FEBS Journal*, 275(3), pp.548-560.

Schlafer, S., Riep, B., Griffen, A., Petrich, A., HÃ¼bner, J., Berning, M., Friedmann, A., Gabel, U. and Moter, A. (2010). *Filifactor alocis* - involvement in periodontal biofilms. *BMC Microbiology*, 10(1), p.66.

Sen, N., Paul, B., Gadalla, M., Mustafa, A., Sen, T., Xu, R., Kim, S. and Snyder, S. (2012). Hydrogen Sulfide-Linked Sulfhydration of NF-Kb Mediates Its Antiapoptotic Actions. *Molecular Cell*, 45(1), pp.13-24.

Serra e Silva Filho, W., Casarin, R., Nicolela Junior, E., Passos, H., Sallum, A. and GonÃ§alves, R. (2014). Microbial Diversity Similarities in Periodontal Pockets and Atheromatous Plaques of Cardiovascular Disease Patients. *PLoS ONE*, 9(10), p.e109761.

Shehadul Islam, M., Aryasomayajula, A. and Selvaganapathy, P. (2017). A Review on Macroscale and Microscale Cell Lysis Methods. *Micromachines*, 8(3), p.83.

Sheiham, A. and James, W. (2015). Diet and Dental Caries. *Journal of Dental Research*, 94(10), pp.1341-1347.

Sheng, J., Nguyen, P. and Marquis, R. (2005). Multi-target antimicrobial actions of glycoagainst oral anaerobes. *Archives of Oral Biology*, 50(8), pp.747-757.

Shillitoe, E., Weinstock, R., Kim, T., Simon, H., Planer, J., Noonan, S. and Cooney, R. (2012). The oral microflora in obesity and type-2 diabetes. *Journal of Oral Microbiology*, 4(1), p.19013.

Singh, S., Padovani, D., Leslie, R., Chiku, T. and Banerjee, R. (2009). Relative Contributions of Cystathionine beta-Synthase and -Cystathionase to H_2S Biogenesis via Alternative Trans-sulfuration Reactions. *Journal of Biological Chemistry*, 284(33), pp.22457-22466.

Spencer, P., Greenman, J., McKenzie, C., Gafan, G., Spratt, D. and Flanagan, A. (2007). In vitro biofilm model for studying tongue flora and malodour. *Journal of Applied Microbiology*, p.0704200759140.

Standar, K., Kreikemeyer, B., Redanz, S., Manter, W., Laue, M. and Podbielski, A. (2010). Setup of an In Vitro Test System for Basic Studies on Biofilm Behavior of Mixed-Species Cultures with Dental and Periodontal Pathogens. *PLoS ONE*, 5(10), p.e13135.

Steegborn, C., Clausen, T., Sondermann, P., Jacob, U., Worbs, M., Marinkovic, S., Huber, R. and Wahl, M. (1999). Kinetics and Inhibition of Recombinant Human Cystathionine Î³-Lyase. *Journal of Biological Chemistry*, 274(18), pp.12675-12684.

Suarez, F., Furne, J., Springfield, J. and Levitt, M. (1998). Production and elimination of sulfur-containing gases in the rat colon. *American Journal of Physiology-Gastrointestinal and Liver Physiology*, 274(4), p. G727-G733.

Sun, B., Zhou, D., Tu, J. and Lu, Z. (2017). Evaluation of the Bacterial Diversity in the Human Tongue Coating Based on Genus-Specific Primers for 16S rRNA Sequencing. *BioMed Research International*, 2017, pp.1-12.

Suwabe, K., Yoshida, Y., Nagano, K. and Yoshimura, F. (2011). Identification of an L-methionine Â -lyase involved in the production of hydrogen sulfide from L-cysteine in Fusobacterium nucleatum subsp. nucleatum ATCC 25586. *Microbiology*, 157(10), pp.2992-3000.

Suzuki, N., Nakano, Y., Watanabe, T., Yoneda, M., Hirofuji, T. and Hanioka, T. (2018). Two mechanisms of oral malodor inhibition by zinc ions. *Journal of Applied Oral Science*, 26(0).

Suzuki, N., Yoneda, M. and Hirofuji, T. (2013). Mixed Red-Complex Bacterial Infection in Periodontitis. *International Journal of Dentistry*, 2013, pp.1-6.

Szabo, C. (2018). A timeline of hydrogen sulfide (H 2 S) research: From environmental toxin to biological mediator. *Biochemical Pharmacology*, 149, pp.5-19.

Takahashi, N. (2005). Microbial ecosystem in the oral cavity: Metabolic diversity in an ecological niche and its relationship with oral diseases. *International Congress Series*, 1284, pp.103-112.

Takakura, T., Mitsushima, K., Yagi, S., Inagaki, K., Tanaka, H., Esaki, N., Soda, K. and Takimoto, A. (2004). Assay method for antitumor l-methionine gamma-lyase: comprehensive kinetic analysis of the complex reaction with l-methionine. *Analytical Biochemistry*, 327(2), pp.233-240.

Takeshita, T., Suzuki, N., Nakano, Y., Yasui, M., Yoneda, M., Shimazaki, Y., Hirofuji, T. and Yamashita, Y. (2012). Discrimination of the oral microbiota associated with high hydrogen sulfide and methyl mercaptan production. *Scientific Reports*, 2(1).

Tang, Y. *et al*., (2015). *Molecular Medical Microbiology (Second Edition)*. Academic Press, pp.957-968.

Tangerman, A. (2009). Measurement and biological significance of the volatile sulfur compounds hydrogen sulfide, methanethiol and dimethyl sulfide in various biological matrices. *Journal of Chromatography B*, 877(28), pp.3366-3377.

Tangerman, A. and Winkel, E. (2008). The portable gas chromatograph OralChromaâ„¢: a method of choice to detect oral and extra-oral halitosis. *Journal of Breath Research*, 2(1), p.017010.

Tangerman, A. and Winkell, E. (2008). Intra- and extra-oral halitosis: finding of a new form of extra-oral blood-borne halitosis caused by dimethyl sulphide. *Primary Dental Care*, 15(2), pp.70-70.

Teodoro, G., Gontijo, A., Salvador, M., Tanaka, M., Brighenti, F., Delbem, A., Delbem, Ã. and Koga-Ito, C. (2018). Effects of acetone fraction from *Buchenavia tomentosa* Aqueous Extract and Gallic Acid on *Candida albicans* Biofilms and Virulence Factors. *Frontiers in Microbiology*, 9.

Tollefsbol, T. (2011). *Handbook of epigenetics*. Amsterdam: Elsevier/Academic Press, p.Metabolic Regulation of DNA Methylation in Mammals.

Tonzetich, J. (1977). Production and Origin of Oral Malodor: A Review of Mechanisms and Methods of Analysis. *Journal of Periodontology*, 48(1), pp.13-20.

Toue, S., Kodama, R., Amao, M., Kawamata, Y., Kimura, T. and Sakai, R. (2006). Screening of Toxicity Biomarkers for Methionine Excess in Rats. *The Journal of Nutrition*, 136(6), pp.1716S-1721S.

Vrolijk, M., Opperhuizen, A., Jansen, E., Hageman, G., Bast, A. and Haenen, G. (2017). The vitamin B6 paradox: Supplementation with high concentrations of pyridoxine leads to decreased vitamin B6 function. *Toxicology in Vitro*, 44, pp.206-212.

Wang, M., Krauss, J., Domon, H., Hosur, K., Liang, S., Magotti, P., Triantafilou, M., Triantafilou, K., Lambris, J. and Hajishengallis, G. (2010). Microbial Hijacking of Complement-Toll-Like Receptor Crosstalk. *Science Signaling*, 3(109), pp.ra11-ra11.

Wang, M., Shakhatreh, M., James, D., Liang, S., Nishiyama, S., Yoshimura, F., Demuth, D. and Hajishengallis, G. (2007). Fimbrial Proteins of *Porphyromonas gingivalis* Mediate In Vivo Virulence and Exploit TLR2 and Complement Receptor 3 to Persist in Macrophages. *The Journal of Immunology*, 179(4), pp.2349-2358.

Washio, J., Sato, T., Koseki, T. and Takahashi, N. (2005). *Hydrogen sulfide-producing bacteria in tongue biofilm and their relationship with oral malodour*.

Waugh, D. (2011). An overview of enzymatic reagents for the removal of affinity tags. *Protein Expression and Purification*, 80(2), pp.283-293.

Wei X., Zhao HQ., Ma C., Zhang AB., Feng H., Zhang D., (2019) The association between chronic periodontitis and oral *Helicobacter pylori*: A meta-analysis, *PLoS one*, 14(12)

Wen, L., Qu, T., Zhai, K., Ding, J., Hai, Y. and Zhou, J. (2015). Gallic acid can play a chondroprotective role against AGE-induced osteoarthritis progression. *Journal of Orthopaedic Science*, 20(4), pp.734-741.

Wendisch, V. (2007). *Amino acid biosynthesis*. Berlin: Springer, pp.195-218.

Westrop, G., Wang, L., Blackburn, G., Zhang, T., Zheng, L., Watson, D. and Coombs, G. (2017). Metabolomic profiling and stable isotope labelling of Trichomonas vaginalis and Tritrichomonas foetus reveal major differences in amino acid metabolism including the production of 2-hydroxyisocaproic acid, cystathionine and S-methylcysteine. *PLOS ONE*, 12(12), p.e0189072.

Wilson, M. (2009). *Food constituents and oral health*. Boca Raton, Fla: CRC Press.

Wolf, K. (2002). Measuring Î²-Galactosidase Activity in Bacteria: Cell Growth, Permeabilization, and Enzyme Assays in 96-Well Arrays. *Biochemical and Biophysical Research Communications*, 292(1), p.292.

Yaegaki, K. (2008). Oral malodorous compounds are periodontally pathogenic and carcinogenic. *Japanese Dental Science Review*, 44(2), pp.100-108.

Yaegaki, K., Qian, W., Murata, T., Imai, T., Sato, T., Tanaka, T. and Kamoda, T. (2008). Oral malodorous compound causes apoptosis and genomic DNA damage in human gingival fibroblasts. *Journal of Periodontal Research*, 43(4), pp.391-399.

Yang, G., Wu, L., Jiang, B., Yang, W., Qi, J., Cao, K., Meng, Q., Mustafa, A., Mu, W., Zhang, S., Snyder, S. and Wang, R. (2008). H2S as a Physiologic Vasorelaxant: Hypertension in Mice with Deletion of Cystathionine Â -Lyase. *Science*, 322(5901), pp.587-590.

Yoo, G. and Allred, C. (2016). The estrogenic effect of trigonelline and 3,3-diindolymethane on cell growth in non-malignant colonocytes. *Food and Chemical Toxicology*, 87, pp.23-30.

Yoshida, A., Yoshimura, M., Ohara, N., Yoshimura, S., Nagashima, S., Takehara, T. and Nakayama, K. (2009). Hydrogen Sulfide Production from Cysteine and Homocysteine by Periodontal and Oral Bacteria. *Journal of Periodontology*, 80(11), pp.1845-1851.

Yoshida, Y., Ito, S., Kamo, M., Kezuka, Y., Tamura, H., Kunimatsu, K. and Kato, H. (2010). Production of hydrogen sulfide by two enzymes associated with biosynthesis of homocysteine and lanthionine in *Fusobacterium nucleatum* subsp. nucleatum ATCC 25586. *Microbiology*, 156(7), pp.2260-2269.

Yoshida, Y., Suwabe, K., Nagano, K., Kezuka, Y., Kato, H. and Yoshimura, F. (2011). Identification and enzymic analysis of a novel protein associated with production of hydrogen sulfide and L-serine from L-cysteine in *Fusobacterium nucleatum* subsp. nucleatum ATCC 25586. *Microbiology*, 157(7), pp.2164-2171.

Yoshikawa, M., Yoshida, M., Mori, T., Hiraoka, A., Higa, C. and Tsuga, K. (2017). Change of Oral Conditions after Combined Use of a Tongue Brush and Toothbrush: A Pilot Study. *Journal of Dentistry and Oral Care*, 3(1), pp.1-4.

Yoshimura, M., Nakano, Y., Yamashita, Y., Oho, T., Saito, T. and Koga, T. (2000). Formation of Methyl Mercaptan from L-Methionine by *Porphyromonas gingivalis*. *Infection and Immunity*, 68(12), pp.6912-6916.

Young, A., Jonski, G. and Rolla, G. (2002). The oral anti-volatile sulphur compound effects of zinc salts and their stability constants. *European Journal of Oral Sciences*, 110(1), pp.31-34.

Young, A., Jonski, G., Rolla, G. and Waler, S. (2001). Effects of metal salts on the oral production of volatile sulfur-containing compounds (VSC). *Journal of Clinical Periodontology*, 28(8), pp.776-781.

Zanatta, F., Antoniazzi, R. and Rasing, C. (2010). Staining and calculus formation after 0.12% chlorhexidine rinses in plaque-free and plaque covered surfaces: a randomized trial. *Journal of Applied Oral Science*, 18(5), pp.515-521.

Zeigler, C., Persson, G., Wondimu, B., Marcus, C., Sobko, T. and ModÃ©er, T. (2011). Microbiota in the Oral Subgingival Biofilm Is Associated with Obesity in Adolescence. *Obesity*, 20(1), pp.157-164.

Zhang, B., Cai, J., Duan, C., Reeves, M. and He, F. (2015). A Review of Polyphenolics in Oak Woods. *International Journal of Molecular Sciences*, 16(12), pp.6978-7014.

Zhou, J., Chan, L. and Zhou, S. (2012). Trigonelline: A Plant Alkaloid with Therapeutic Potential for Diabetes and Central Nervous System Disease. *Current Medicinal Chemistry*, 19(21), pp.3523-3531.

Software references

Autodock vino- Autodock vina- O. Trott, A. J. Olson, AutoDock Vin: improving the speed and accuracy of docking with a new scoring function, efficient optimization and multithreading, *Journal of Computational Chemistry* 31 (2010) 455-461

Bioedit- BioEdit: A User-Friendly Biological Sequence Alignment Editor and Analysis Program for Windows 95/98/NT

BLAST/FASTA- NCBI (National Centre for Biotechnology Information)

Chimera: UCSF Chimera--a visualization system for exploratory research and analysis. Pettersen EF, Goddard TD, Huang CC, Couch GS, Greenblatt DM, Meng EC, Ferrin TE. J, *Comput Chem*. 2004 Oct;25(13):1605-12.

PyMOL Molecular Graphics System, Version 1.2r3pre, *Schrödinger*, LLC.